CRC Press
Taylor & Francis Group

Power Systems Analysis Illustrated with MATLAB® and ETAP®

Hemchandra Madhusudan Shertukde

Power Systems Analysis Illustrated with MATLAB® and ETAP®

Taylor & Francis
Taylor & Francis Group
http://taylorandfrancis.com

Power Systems Analysis Illustrated with MATLAB® and ETAP®

Hemchandra Madhusudan Shertukde

CRC Press
Taylor & Francis Group
Boca Raton London New York

CRC Press is an imprint of the
Taylor & Francis Group, an **informa** business

CRC Press
Taylor & Francis Group
6000 Broken Sound Parkway NW, Suite 300
Boca Raton, FL 33487-2742

Printed on acid-free paper

International Standard Book Number-13: 978-1-4987-9721-4 (Hardback)

Library of Congress Cataloging-in-Publication Data

Names: Madhusudan, Shertukde Hemchandra, author.
Title: Power systems analysis illustrated with MATLAB and ETAP / Shertukde Hemchandra Madhusudan.
Description: First edition. | Boca Raton, FL : CRC Press/Taylor & Francis Group, 2018. | Includes bibliographical references.
Identifiers: LCCN 2018034507| ISBN 9781498797214 (hardback : acid-free paper) | ISBN 9780429436925 (ebook).
Subjects: LCSH: Electric power systems--Design and construction. | Electric power systems--Computer simulation. | MATLAB.
Classification: LCC TK1001 .M268 2018 | DDC 621.310285/536--dc23
LC record available at https://lccn.loc.gov/2018034507

Visit the Taylor & Francis Web site at
http://www.taylorandfrancis.com

and the CRC Press Web site at
http://www.crcpress.com

This book is dedicated to the arrival of our first granddaughter:

Arya J Bhakta

And to my entire family:

Rekha, Amola, Karan, Rohan and Jignesh

Taylor & Francis
Taylor & Francis Group
http://taylorandfrancis.com

Contents

Foreword

Thomas Edison famously said, 'The doctor of the future will give no medicine, but will instruct his patient in the care of the human frame, in diet and in the cause and prevention of disease.'*

Power systems engineering is similar to the medical profession. Blood is a vital part of the human anatomy just as electricity is to modern civilization. We are most of the time unaware of the existence of either one of them; we rely on them for our daily functions and seldom pay attention to their importance until something goes wrong. Left unchecked, just as blood can carry the symptoms of a problem from the source to another point in the body, power systems issues originating in one area of the electrical network, such as power quality, coordination, arc flash, stability and so on, can manifest in areas least expected. Just like a doctor must diagnose a patient's health by analyzing bloodwork, it is crucial to diagnose the health of an electrical system by performing power systems analysis. Just as various bloodwork is necessary to understand the metrics in a body, power systems engineering has diverse analytical techniques and methods to pinpoint and understand the extent of the issue. A skilled engineer can then evaluate the impact of mitigation methods (medicine) prior to implementation, utilizing software tools such as ETAP to hone these diverse analytical methods. Power systems engineering has advanced such that Thomas Edison's famous quotation now holds true, where such software tools not only help us locate, diagnose, evaluate and mitigate the problems but also notify the power system's owner of imminent failure and recommend proactive action.

Most textbooks on power systems analysis discuss in great detail the techniques, methods, and theory and show the reader how analysis 'used' to be done. Power systems theory is indispensable, but knowledge on the application of that theory is essential in today's evolving power systems domain. Most students graduating learn this theory but fail to learn the application of the theory in a practical world. This book is exciting for me because Dr. Shertukde has delivered what power systems engineers and students of today need: the right balance between power systems theory and its engineering applications in the real world. Dr. Shertukde has successfully distilled 42 years of academic, industrial and leadership experience in the electrical engineering field in a clear, user-friendly yet focused manner. This is not another guidebook about power systems theory, as the use of ETAP and MATLAB® throughout the book, I am sure, will be refreshing and indispensable for the reader.

I feel honored and privileged to have this opportunity to write a foreword to Dr. Shertukde's book. I am sure it will find a wide audience and I cannot wait to add it as a vital reference book for power systems engineering and analysis.

Tanuj Khandelwal, CTO, ETAP
Irvine, California

* https://www.mindbodygreen.com/0-15699/why-functional-medicine-is-the-future-of-health.html.

Taylor & Francis
Taylor & Francis Group
http://taylorandfrancis.com

Preface

In the everyday life of individuals, electrical power is a necessary commodity for survival. In the present day, having the light in one's home remain on is an absolute necessity. The power provided to residential, commercial or industrial locations is harnessed and delivered using several energy sources, including coal, hydel, nuclear, solar, wind, fuel cells and so on. The generated power needs to be transmitted over long distances to support the load requirements of customers. In order for this generation, transmission and distribution of power to be efficient, one needs to understand the proper design and analysis of a power system. Power flow needs to be reliable, of good quality and above all fault free. The improper design and analysis of power systems will result in the 'light not remaining on', so to speak, for everyone worldwide and will eventually lead to 'brown out' locally and 'blackout' globally.

I have taught power systems analysis (PSA) at the University of Hartford, Connecticut, for more than two decades and feel that the current books available on the market mainly provide detailed but unrelated concepts of PSA, making the basic understanding of the finer nuances of PSA difficult for senior undergraduate or junior graduate students. With the advances in computing and canned software for different applications (PSA is not an exception), the normal principles of PSA can be supplemented with state-of-the-art software such as the Electrical Transient Analysis Program (ETAP®). Many authors have tried their level best to explain these intriguing concepts in PSA using mainly theory without supplementing it with present-day examples of software used by the industry. This effort will alleviate that handicap and make the material in PSA more understandable to students. My studies at the Indian Institute of Technology, Kharagpur, West Bengal, India, involved broad and rounded coverage of the current topics in electrical engineering from 1970 to 1975. These topics were in controls and power. My fourth monograph was on one of the former topics in digital controls. This will be my fifth monograph on topics related to electrical engineering and my third in the electrical power engineering arena. For this book I have collaborated with Mr. Tanuj Khandelwal, CTO of Operation Technology, Inc. (OTI), Irvine, California, to incorporate the ETAP software into the material covered in this book to illustrate certain aspects of PSA, such as load flow analysis, short-circuit analysis and so on.

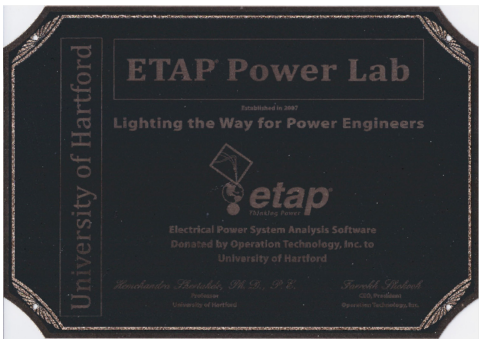

This is covered in the preamble to ETAP and is succinctly described in the foreword to this book by Mr. Khandelwal. I am grateful to him for providing this insight into the use of ETAP for PSA.

PSA has gone through many iterations, dealing with hand calculations, then aided by calculators, progressively evolving with the help of personal computers and now with miniaturized laptops and tablets with very high computing capabilities. My motivation to write a book on PSA started way back in 2006, when I received my first software grant ETAP from OTI to set up a power laboratory at the University of Hartford in 2007 (please see the preceding plaque). In 2007, OTI provided a software grant of 20 seats of ETAP to yours truly worth $265,000 with a continuing grant after 3 years of approximately $38,000 per year thereafter. This grant has continued to date and has been extremely useful in the instructions for the PSA course offered at the University of Hartford in the Samuel I. Ward Department of Electrical Engineering at the College of Engineering, Technology and Architecture (CETA).

Finally, I am grateful to Dr. Farrokh Shokooh, founder and CEO of OTI, for giving permission to incorporate ETAP into this book.

Acknowledgment

This is my third solo book in the field of electrical power engineering focused on power systems analysis. This effort truly reflects the rigor some of my professors at the Indian Institute of Technology (IIT) in Kharagpur, India, imbued in my study habits. I am grateful to all my professors in this area, namely Professor Mukhopadhyay, Professor Bandopadhyay and Professor Balaram Murthy. They taught me aspects of machine theory, switch gear and relays that form a complete core of pedagogy in the area of electrical power. As a professor myself I am proud to continue their legacy of lifelong teaching as I continue to complete my 31st year at the College of Engineering Technology and Architecture (CETA) in University of Hartford, West Hartford, Connecticut.

Taylor & Francis
Taylor & Francis Group
http://taylorandfrancis.com

Author Biography

Hemchandra M. Shertukde, PhD, PE, IEEE- SM'92, is a Professor of Electrical Engineering at the University of Hartford, Connecticut, since 1996 and President of Diagnostic Devices Inc. Since 2008 he has been the Chair of the Task Force (TF) on DPV Grid Transformers, for IEEE-TC. The work of the TF resulted in a position paper which was accepted to be presented at the next IEEE-ICEEOT Conference in Chennai, March 3–5, 2016. He has served as the Chair of the WG.C.57.159 since 2011, which has compiled the User's Guide for the Understanding and Application of DPV Grid Transformers in the electrical grid, and was recently published by IEEE-Standards Association. He has written four books, two of which are *Transformers: Theory, Design and Practice with Practical Applications,* published by Verlag-Dr. Mueller, in August of 2010, and *Distributed Photovoltaic Grid Transformers,* published by CRC Press in March of 2014. Dr. Shertukde has published several transaction papers in *IEEE Transactions of Controls and Signal Processing* and proceeding papers in several international conferences. He holds a B.Tech from the Indian Institute of Technology Kharagpur, as well as an MS and PhD in electrical engineering with a specialty in controls and systems engineering from the University of Connecticut, Storrs. Currently, he is professor of electrical and computer engineering for the College of Engineering, Technology, and Architecture (CETA) at University of Hartford, Connecticut. He is also senior lecturer at the Yale School of Engineering and Applied Sciences (SEAS), New Haven, Connecticut. Dr. Shertukde is the principal inventor of two commercialized patents, 6,178,386 and 7,291,111. In 2017, Dr. Shertukde was a recipient of three IEEE awards viz: IEEE-SA/EAB award for contribution to standard association work and incorporating it effectively in education; IEEE-PES CT Chapter Outstanding Engineer Award for 2017 and IEEE-PES Transformer Committee Working Group Chair Award for WG C.57.159 User's Guide for DPV Grid Generating Systems. The IEEE-SA/EAB Award was re-awarded by IEEE-TC at the 100-year anniversary celebrations in March of 2018 in Pittsburgh, Pennsylvania.

Taylor & Francis
Taylor & Francis Group
http://taylorandfrancis.com

Introduction to ETAP

ETAP is a full-spectrum analytical engineering software company specializing in the analysis, simulation, monitoring, control, optimization and automation of electrical power systems. ETAP software offers the best and most comprehensive suite of integrated power systems enterprise solutions, spanning modeling to operation.

- Offers a single connected platform with integrated applications
- Serves as an executable specification of the system under development
- Focuses on advanced power systems analytics
- Identifies root causes by the identification of operating problems
- Minimizes inadvertent outages caused by human error/equipment overload
- Offers optimization and business intelligence
- Provides design and operational insights
- Bridge the offline and online systems
- Reconstructs system conditions to check for user/operator actions
- Probes for alternative actions after the fact (*what-if analysis*)
- Facilities an ongoing learning process for the engineers and operators
- Enables data-driven decision-making and planning

ETAP is a fully graphical enterprise package that runs on the Microsoft® Windows® 2012, 2016, 7, 8, 8.1 and 10 operating systems. ETAP is the most comprehensive analysis tool available for the designing and testing of power systems. Using its standard offline simulation modules, ETAP can utilize real-time operating data for advanced monitoring, real-time simulation, optimization, energy management and high-speed intelligent load shedding.

ETAP has been designed and developed by OTI for engineers in Irvine to handle the diverse discipline of power systems for a broad spectrum of industries in one integrated package with multiple interface views, such as AC and DC networks, cable raceways, ground grid, geographic information systems (GISs), panels, arc flash, wind turbine generator (WTG), protective device coordination/selectivity and AC and DC control system diagrams.

ETAP allows you to easily create and edit graphical single-line diagrams (SLDs), underground cable raceway systems (UGSs), three-dimensional cable systems, advanced time-current coordination and selectivity plots, GIS schematics, as well as three-dimensional ground grid systems (GGSs). The program has been designed to incorporate the following four key concepts.

1. **Virtual Reality Operation**

   The program operation emulates real electrical system operation as closely as possible. For example, when you open or close a circuit breaker, place an element out of service or change the operating status of the motors, the de-energized elements and sub-systems are indicated on the SLD in gray. ETAP incorporates

innovative concepts for determining protective device coordination directly from the SLD.

2. **Total Integration of Data**

   ETAP combines the electrical, logical, mechanical and physical attributes of system elements in the same database. For example, a cable not only contains data representing its electrical properties and physical dimensions but also information indicating the raceways through which it is routed. Thus, the data for a single cable can be used for load flow or short-circuit analyses (which require electrical parameters and connections) as well as cable ampacity derating calculations (which require physical routing data). This integration of data provides consistency throughout the system and eliminates the need for multiple data entry for the same element, which can be a considerable time saver.

3. **Simplicity in Data Entry**

   ETAP keeps track of the detailed data for each electrical apparatus. Data editors can speed up the data entry process by requiring the minimum data for a particular study. In order to achieve this, we have structured the property editors in the most logical manner for entering data for different types of analysis or design.

4. **Quality Assurance**

   ETAP believes that a well-defined and effective quality assurance process that thrives on continuous improvement is the best vehicle to transform powerful ideas into powerful products. ETAP software meets the rigid standards for quality and safety established by U.S. and international standards bodies for nuclear facilities. In accordance with the ETAP Quality Assurance Program, all procedures and activities related to the quality of ETAP software are subject to audits. Qualified auditors periodically assess the program to detect any deviations from the complied standards and evaluate the effectiveness of the existing plans and procedures. Audit reports are properly documented and are subject to audits conducted by our nuclear clients and ISO 9001:2015 certification assessments. ETAP is on the supplier list of many nuclear facilities and Nuclear Procurement Issues Corporation (NUPIC) members. The ETAP Quality Assurance Program has undergone numerous audits since 1991. Our clients audit our program several times a year. For the past 2 years, the ETAP Quality Assurance Program has undergone audit assessments by the nuclear organizations.

   ETAP products comply with the U.S. Code of Federal Regulations as well as other quality assurance standards. The ETAP Quality Assurance Program strictly enforces policies and specific procedures that ensure the reliability of all ETAP software. For nuclear/high-impact facilities, all releases of ETAP go through an intensive verification and validation (V&V) process throughout the revision life cycle. Verification is the process of determining whether or not the products of a given phase of the revision life cycle fulfill the requirements established during the previous phase. Validation is the process of evaluating software at the end of the revision life cycle to ensure compliance with software requirements.

   The V&V method for ETAP is extensive, consisting of thousands of test cases that encompass each and every calculation module, user interface, persistence, reports, plots, library data and so on. The test cases include a comprehensive comparison of study results and system performance against hand calculations, field measurements, industry standards (ANSI/IEEE, IEC, UL, etc.) and other

established methods in order to ensure and verify the technical accuracy and performance stability of ETAP. The V&V process for the ETAP engineering libraries allows for 0% error in the library data based on published manufacturer data.

For further details of the different features available in the use of ETAP by Operations Technology Inc. for Power Systems Analysis are available at the URL: www.crcpress.com/9781498797214.

Benefits of Using ETAP for PSA

- Eliminate the man-hours and expense of internal software validation.
- Gain proof of software and libraries accuracy with minimal investment.
- Receive updated documentation on ongoing audits of ETAP.
- Operate your system with a virtual reality model concept.
- Gain more understanding of your system limitations.
- Manage system modifications in one integrated database.
- Have a team of experts for support.
- Avoid unnecessary system upgrade costs.

ETAP is a registered trademark of Operations Technology Inc.

Contact Information:

etap®
17 Goodyear
Irvine, CA 92618
United States of America

Taylor & Francis
Taylor & Francis Group
http://taylorandfrancis.com

1

Introduction to Power Systems Analysis

1. Single-line diagram (SLD)
2. Components of an SLD
3. Equipment in an SLD
4. Generation, transmission and distribution parts of an SLD

Single-Line Diagram

Every power system in the world is represented by a single-line diagram (SLD; also known as a one-line diagram) consisting of a generator, several transmission lines, many different kinds of transformers and a motor as a load. Each of these components is represented by a single-phase circuit, assuming all the phases are identical. In general, many systems have three phases, although some can have two or more.

To properly and accurately analyze the power flowing through an SLD, one has to represent these components as their respective equivalent circuit. Let us strive to find these equivalent circuits, starting with the transformer. Any transformer is represented by its equivalent leakage reactance in series with an ideal transformer, as shown in Figure 1.1.

The second most important component is the generator, which can be represented by a voltage source in series with the synchronous reactance of the machine, as shown in Figure 1.2.

The third most important component of an SLD is the transmission line, represented by a π-circuit, which is a combination of passive elements, as shown in Figure 1.3.

Finally, the remaining component of an SLD is the motor as a rotating load; its equivalent circuit is shown in Figure 1.4.

Sometimes, the load can be a purely resistive circuit as a stationary load, shown as pure resistance in Figure 1.5.

Combining all the preceding individual equivalent circuits representing the respective equipment or components, we can evolve a working representation of an SLD, as shown in Figure 1.6.

The SLD shown in Figure 1.6 helps to transfer electrical power from the generating end to the load end. In stable conditions, power is delivered to the load reliably and without delay. However, faults in the SLD cause reliability problems, generating several delays, which can be detrimental to the efficient working of the power system. In order to analyze this loss in the performance of a power system, we need to conduct an analysis generally called a *power systems analysis* (PSA). To conduct this analysis properly, we need to have proper representations of all the components shown in Figure 1.6. This entails that each and every component needs to be studied thoroughly and correctly. This will be done component-wise below.

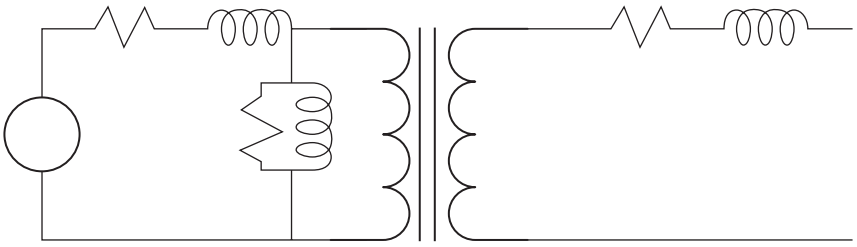

FIGURE 1.1
Equivalent circuit of a transformer.

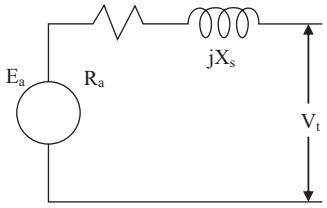

FIGURE 1.2
Equivalent circuit of a generator.

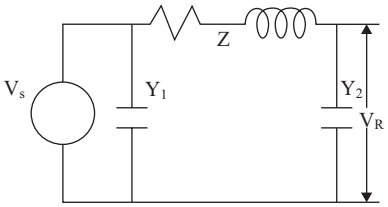

FIGURE 1.3
Equivalent circuit of a transmission line.

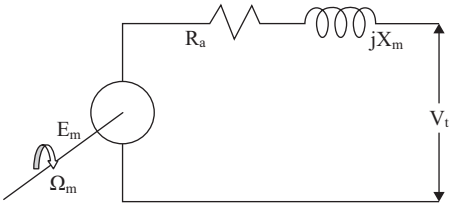

FIGURE 1.4
Equivalent circuit of a motor as a rotating load.

FIGURE 1.5
A pure resistive load.

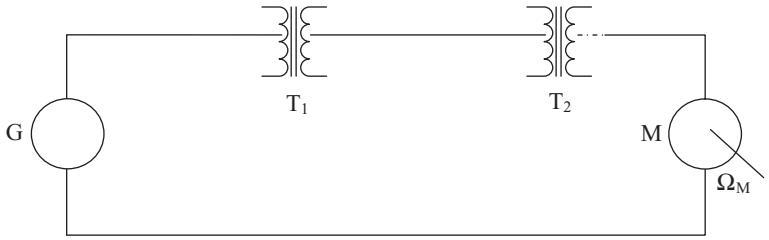

FIGURE 1.6
Working representation of an SLD.

Generation, Transmission, Distribution and Load Components of a Power System

Generation consists of a generator, which is generally a three-phase *synchronous machine*. This is a rotating electrical machine. The voltage rating of this component can reach as high as 33 kV.

Transmission consists of transmission lines, which are generally a set of three or four wires or conductors of a single strand or multiple strands. These are also along the way connected to different kinds and sets of transformers. The voltage rating of such components is very high. At present, they can reach 1500 kV.

Distribution consists of a set of three or four wires but at a lower voltage rating of up to 69 kV, reducing to 115 or 230 V single phase or 230 or 440 V three phase. In addition, it consists of either a rotating synchronous or asynchronous machine or a simple resistance connected at the load end to the distribution lines, along with suitably rated distribution transformers at the source end.

In addition to the these major components, the SLD has other components for the protection of the system, such as circuit breaker, switches, links and so on.

Example 1.1

A portion of the power system consists of two generators in parallel, as shown in Figure 1.7, connected to a step-up transformer that links them with a 230 kV transmission line. The detailed ratings for all components relevant to this example are as follows:

- Generator G_1: 10 MVA, with 12% reactance
- Generator G_2: 5 MVA, with 8% reactance
- Transformer T: 15 MVA, with 6% reactance
- Transmission line: $Z = (4 + j60)\ \Omega$, 230 kV

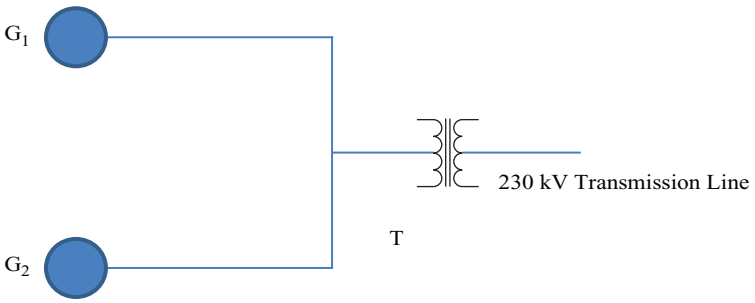

FIGURE 1.7
SLD of two generators connected to a transmission line via a transformer.

The percent reactances are computed on the basis of the individual ratings, respectively. Find the reactances and the impedance in percent with 15 MVA as the new base value.

SOLUTION 1.1

One needs to observe that the voltage is same for all the components in this example. Thus, the given and new voltage bases are the same. Using Equation A.38 as in Appendix A to obtain the pu values for all the components in the circuit, we have the following:

- Percent reactance of generator $G_1 = 12(15/10) = 18\%$
- Percent reactance of generator $G_2 = 8\ (15/5) = 24\%$
- Percent reactance of transformer $T = 6(15/15) = 6\%$

Now we proceed to evaluate the transmission line as follows:

$$\text{Percent impedance} = Z = \left(4 + j60\right)\left(15 \times 10^6\right) / \left(230 \times 10^3\right)^2 \times 100$$

$$= \left(0.113 + j1.7\right)\%$$

Example 1.2

This example illustrates a four-bus electric power system, as shown in Figure 1.8. This example will also be illustrated using the latest ETAP® version of the software provided by Operation Technology, Inc. (OTI), Irvine, California.

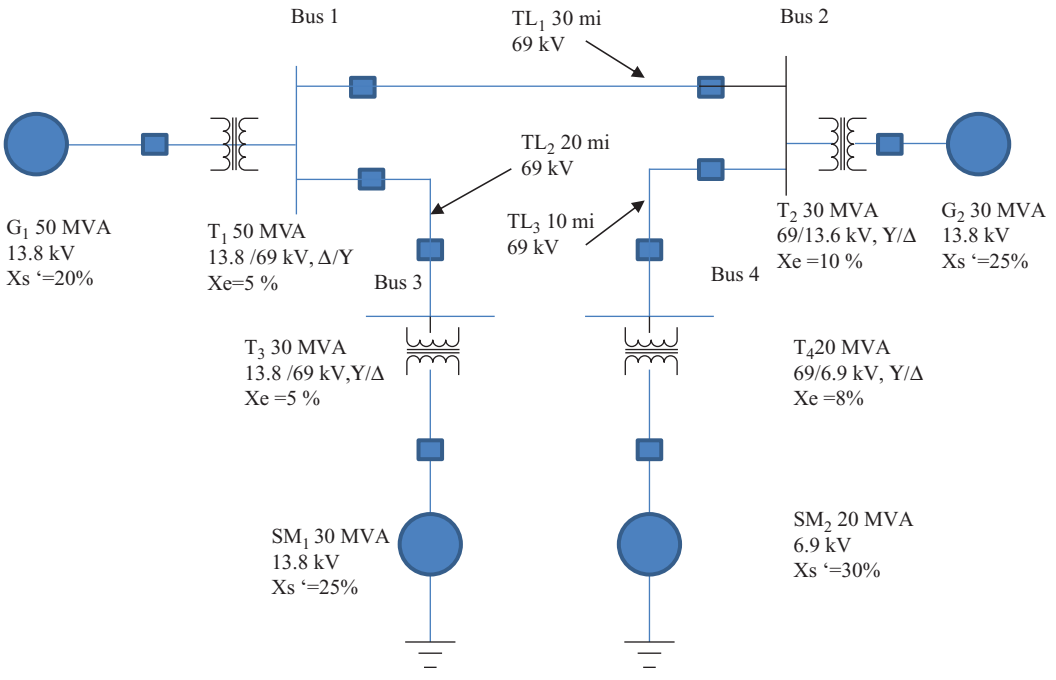

FIGURE 1.8
SLD of a four-bus electric power system.

1. Find the base impedance of the generator G_1 and determine the ohmic value of the transient reactance.
2. Find the base impedance of transformer T_4 at bus 4 referred to the low-voltage (LV) side of the transformer and evaluate the ohmic value of the leakage reactance on the LV side as the high-voltage (HV) side.

Generator G_1: 50 MVA, 13.8 kV, 20% transient reactance
Generator G_2: 30 MVA, 13.8 kV, 25% transient reactance
Transmission line MTL_1: 69 kV, 30 miles long
Transmission line TL_2: 69 kV, 20 miles long
Transmission line TL_3: 69 kV, 15 miles long
Synchronous machine SM_1: 30 MVA, 13.8 kV, 25% transient reactance
Synchronous machine SM_2: 20 MVA, 13.8 kV, 25% transient reactance
Transformer T_1: 50 MVA, 5% equivalent reactance, Delta/Wye, 13.8/69 kV
Transformer T_2: 30 MVA, 10% equivalent reactance, Wye/Delta, 69/13.8 kV
Transformer T_3: 30 MVA, 5% equivalent reactance, Wye/Delta, 69/13.8 kV
Transformer T_4: 20 MVA, 8% equivalent reactance, Wye/Delta, 69/6.9 kV
These components are configured in Figure 1.8.

SOLUTION 1.2

1. The base impedance of generator G_1 is given by

$$Z_{BG} = \frac{(13.8)^2}{50} = 3.81\Omega$$

Therefore,

$$X'_G = (\text{pu}X')Z_{BG} = \left(\frac{20}{100}\right)(3.81) = 0.762\Omega$$

2. On examining the circuit SLD, one realizes that the LV rating of transformer T_4 is 6.9 kV. Hence, the base impedance of T_4 on the LV side is given by

$$Z_{BL} = \frac{(6.9)^2}{20} = 2.381\Omega$$

Thus,

$$X_{eqLV} = (\text{pu}X_{eq})Z_{BL} = (0.08)(2.381) = 0.19\Omega$$

Knowing the turns ratio of transformer T_4 is $a = 10 = 69/6.9$, we have

$$X_{eq\text{HV}} = a^2 X_{eq\text{LV}} = \left(\frac{69}{6.9}\right)^2 (0.19) = 19\Omega$$

Example 1.3

Referring to Example 1.2 and the SLD in Figure 1.8, using all the same component details, determine the pu values of the reactances of generator G_1 and transformer T_4. Use a reference base as 100 MVA at 69 kV.

SOLUTION

In this case, referring to Figure 1.8, the reference voltage selection of 69 kV is the transmission line voltage. With this we can proceed with the evaluation of the pu values of the reactances posed in the problem statement as follows:

Generator G_1: If we examine the SLD in Figure 1.8, this generator is on the LV side of transformer T_1, so the reference voltage to be used for the conversion of the transient reactance of G_1 is 13.8 kV. Thus, using Equation A.38 in Appendix A, we have

$$\text{pu } X'_{\text{sr}} = \left(\frac{20}{100}\right)\left(\frac{13.8}{13.8}\right)^2\left(\frac{100}{50}\right) = 0.4$$

It is imperative to note here that this pu value is larger than the original or old value by a factor of 2. To recover the original or old value of this reactance, it is necessary to work with the reference base impedance on the LV side of G_1.

Thus,

$$Z_{BL} = \frac{(13.8)^2}{100} = 1.9\,\Omega$$

which yields $X'_s = (0.4)Z_{BL} = 0.762\,\Omega$, as before, and further yields the pu value of the equivalent reactance of T_4 as follows:

$$\text{pu } X_e = \left(\frac{8}{100}\right)\left(\frac{69}{69}\right)^2\left(\frac{100}{20}\right) = 0.4$$

As seen in Example 1.2 before.

2

Electrical Machines

2.1 Electrical Machines

These are the rotating machines that are part of the electrical machine domain.

2.1.1 Synchronous Machines

When a rotating machine speed is in synch with the power frequency of the applied signal, the appropriate speed of the shaft is given by the following equation:

$$n_s = \frac{120f}{p} \tag{2.1}$$

where:

- f is the frequency of the applied signal
- p is the number of poles of the machine initiating the magnetic flux
- n_s is the synchronous speed

The general Faraday's law is applied here as follows to the induced electromotive force (EMF) e, as in Equation 2.2 and illustrated in Figure 2.1.

$$e = \frac{d}{dt}(N\varphi)$$

$$= N\frac{d\varphi}{dt} + \varphi\frac{dN}{dt} \tag{2.2}$$

where:

- N is the number of turns in the rotor circuit
- Φ is the magnetic flux per pole created by the stator

As the rotor turns, the turns in the rotor circuit cut the spatially stationary magnetic flux, as shown in Figure 2.1 Thus, in Equation 2.2 for rotating machines, the first term is negligible, while the second term contributes to the effect caused by the rotating conductors and their cutting of the magnetic flux, thus resulting in the induced EMF. However, it is necessary for there to be an air gap between the stator's and rotor's magnetic circuits to cause the eventual rotating motion in the case of both the generator and motor actions of the synchronous machine, as is required of all rotating machines.

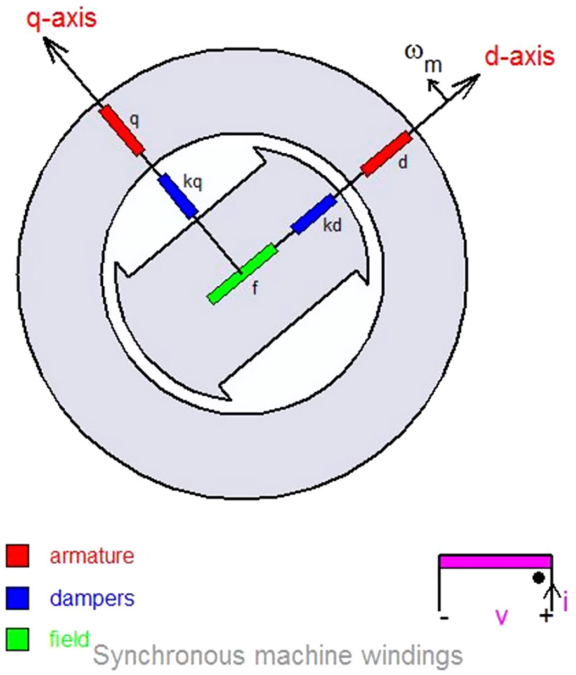

FIGURE 2.1
d-q model of the synchronous machine.

Because of the asymmetry of the synchronous machine created by rotor saliency and field excitation, the corresponding d-q model must use the rotor coordinates as a frame of reference. Details of the modeling are shown in Figure 2.1.

2.1.2 Asynchronous Machines

As discussed in Section 2.1.1, when the speed of an electrical machine is higher or lower than the synchronous speed, it is called an *asynchronous machine*. So, say we have a two-pole synchronous machine operating at a signal frequency of 60 c/s, with a synchronous speed of $n_s = 3600$ rpm, then an asynchronous machine operating at a slip s of 3%, will have a speed of $n = 3492$ rpm, as given by Equation 2.3.

$$n = n_s(1 - s) \tag{2.3}$$

where n_s is the synchronous speed as given by Equation 2.1.

This concept of *slip* (s) will be studied in detail in this chapter as an important factor that defines the operation of an asynchronous machine. It means that the rotor 'slips' behind or ahead of the rotating stator magnetic field when slip s is positive or negative, respectively. In the scope of this book, the main emphasis will be on asynchronous machines operating as motors—popularly called *induction motors* (IMs) or *squirrel cage* IMs. The squirrel cage is the shape of the rotor conductors short-circuited on themselves. This action is shown in Figure 2.2.

All the preceding actions are described succinctly in Chapter 4 on generalized machine theory using d-q axis modeling.

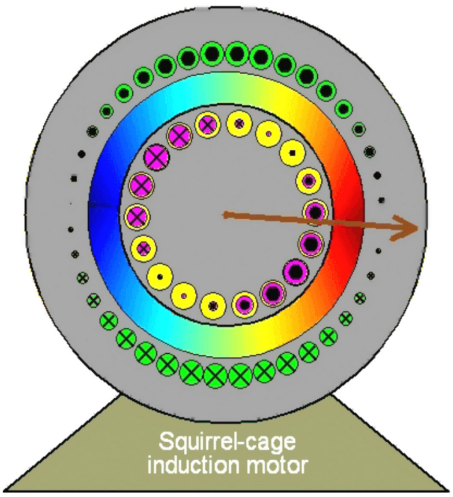

FIGURE 2.2
Squirrel cage IM.

2.1.3 Transformers

In Equation 2.2, when the first term is predominant and the second term is ignored since the machine components are stationary, the resulting machine with no air gap in the magnetic circuit is called a transformer.

Transformers are a vital part of power systems. Generally, seven to eight transformers are configured at strategically placed locations in the single-line diagram (SLD) of a power system, as follows:

- Generating point: generator step-up (GSU) transformer
- Receiving station point: receiving station (RS) transformer
- Substation point; substation transformer (ST)
- Distribution point: distribution station transformer (DST)
- Load point: where smaller-size transformers are connected to the load

Transformers thus form a major set of components in a single motor-generator system. This ratio of transformers to the motor-generator set is close to 10:1. The analysis of transformer theory can be easily understood by referring to [1]. The salient features of distributed photovoltaic grid transformers (DPV-GTs) are summarized in the following section.

2.2 Distributed Photovoltaic Grid Power Transformers [2]

2.2.1 Introduction

The increase in oil prices over the past few years has encouraged scientists, engineers and economists to look for alternative energy sources, one of which is the sun, whose abundant energy can be harnessed into reusable electric energy to supplement and

eventually be a major factor in overall energy generation, transmission and delivery to customers.

Wind energy, solar energy, and ocean wave energy have recently become notable players in this exchange. While penetration of alternate energy is the most important aspect of sustaining these alternative energies, considerable research and development work has been dedicated to the ancillary equipment needed for such energies to be efficiently delivered to the end user.

DPV-GTs, which convert solar energy, are gradually increasing in number in the field due to the recent focus on renewable energy sources. These transformers are primarily used as step-up transformers but can be used as step-down transformers as well. In the case of photovoltaic (PV) solar power, electrical power is generated by converting solar radiation into direct current (DC) electricity using semiconductors that exhibit the PV effect. PV power generation employs solar panels comprising a number of cells containing PV material.

The DC energy is then converted to one- or three-phase alternating current (AC) power using an inverter. The inverter is subsequently connected to a DPV-GT. This DPV-GT is further connected to a bus that can feed a suitable load. Figure 2.3 illustrates the process of converting energy from solar radiation into usable electrical power.

Currently, there are a variety of available industry standards that address many of these design, operation and maintenance aspects. Some of the key aspects to be considered are as follows.

2.2.2 Voltage Flicker and Variation [3]

Solar transformers operate at a steady voltage, with the rated voltage controlled by inverters. Therefore, voltage and load fluctuations are considerably reduced. The voltage variation is generally in the range of ±5% of the nominal voltage rating. Thus, standard design

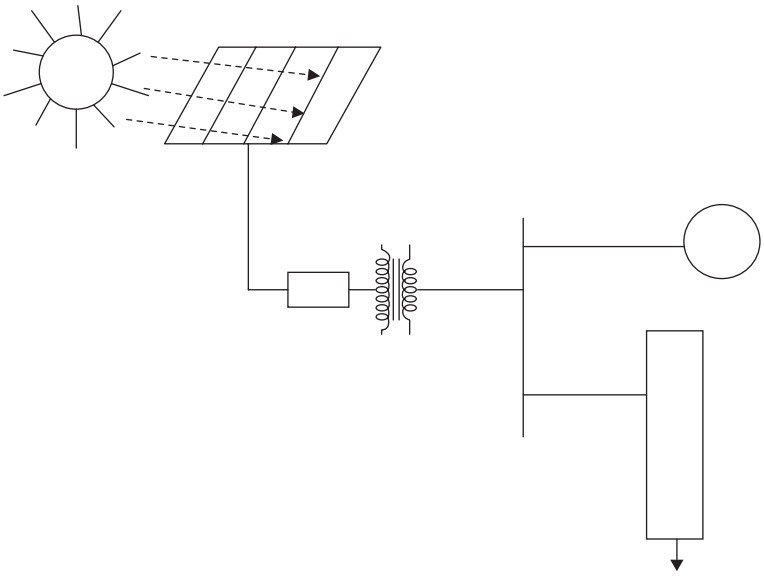

FIGURE 2.3
Typical one-line diagram with the solar panel connected to an inverter, which is in turn connected to a DPV-GT, a bus and further down to a load.

TABLE 2.1

Low-Voltage System Classification and Distortion Limits

	Special Applications[a]	General System	Dedicated System[b]
Notch Depth	10%	20%	50%
THD (Voltage)	3%	5%	10%
Notch Area (A_N)[c]	16,400	22,800	36,500

Source: Adapted and reprinted with permission from IEEE. © IEEE 1992. All rights reserved.
Note: The value A_N for other than 480 V systems should he multiplied by V/480.
[a] Special applications include hospitals and airports.
[b] A dedicated system is exclusively dedicated to the converter load.
[c] In volt-microseconds at rated voltage and current.

considerations for transformer windings are readily applied from experience. IEEE 519-92 [3] (Table 2.1) establishes limits for the allowable commutation notch depth introduced by power converters at critical points of the power system, normally coincident with transformer locations.

Load Tap Changer (LTC) control issues need to be addressed. Some LTCs are suitable to bidirectional power flow, but not all of them.

2.2.3 Harmonics and Waveform Distortion [3]

A solar inverter system's typical harmonic content is less than 5% (the threshold for normal service conditions), which has almost no impact on the system. The lower harmonic profile is because there are no generators or switching and protective controls such as those found on wind turbines.

IEEE C57.129 [4] sufficiently describes the requirements of the system designer to provide information on the harmonic content and the current waveform, including cases where there is more than one valve winding on a core leg.

IEEE C57.129 and C57.18.10 [5] use a definition of kVA rating based only on the fundamental frequency; additional losses due to the harmonic content are taken into account during the heat-run test.

IEEE 519-92 establishes limits for allowable harmonics levels in power systems. Table 2.2 shows the current distortion limits for general distribution systems (120–69,000 V) as a function of the short-circuit ratio and the harmonics order.

In case there is significant harmonic content in the DPV-GT, please refer to C57.110 [6], which is an IEEE Recommended Practice to establish a transformer's capability when supplying non-sinusoidal load current. Because of today's inverter practices, the harmonics generated from DC to AC conversion may be minimal, but they need to be included in the customer specifications so that transformer designers can take into account the additional losses due to harmonics in their transformer cooling designs.

2.2.4 Frequency Variation [7]

Since the frequency variation can come from the network only, there is no difference in design or manufacture from a 'standard' power transformer.

2.2.5 Power Factor (PF) Variation [7]

No significant differences from 'standard' power factor practices are expected.

TABLE 2.2

Current Distortion Limits for General Distribution Systems (120–69,000 V)

Maximum Harmonic Current Distortion in Percent of I_L						
	Individual Harmonic Order (Odd Harmonics)					
I_{sc}/I_L	<11	$11 \le h < 17$	$17 \le h < 23$	$23 \le h < 35$	$35 \le h$	TDD
< 20[a]	4.0	2.0	1.5	0.6	0.3	5.0
$20 < 50$	7.0	3.5	2.5	1.0	0.5	8.0
$50 < 100$	10.0	4.5	4.0	1.5	0.7	12.0
$100 < 1000$	12.0	5.5	5.0	2.0	1.0	15.0
> 1000	15.0	7.0	6.0	2.5	14	20.0

Source: Adapted and reprinted with permission from IEEE. © IEEE 1992. All rights reserved.
Notes: Even harmonics are limited to 25% of the odd harmonic limits.
Current distortions that result in a DC offset (e.g., half-wave converters) are not allowed.
[a] All power generation equipment is limited to these values of current distortion, regardless of actual I_{sc}/I_L, where I_{sc} = maximum short-circuit current at PCC and I_L = maximum demand load current (fundamental frequency component) at PCC.

IEEE C57.110 (§5.3 Power factor correction equipment): Power factor correction equipment is frequently installed to decrease utility costs. Care should be taken when this is done, since the current amplification in the circuit due to resonance at certain frequencies can be quite high. In addition, the inductance that is reduced in the circuit generally allows higher harmonic currents in the system. Harmonic heating effects from these conditions may be damaging to transformers and other equipment. The additional losses produced may also increase utility costs due to increased wattage requirements, even though the load power factor is improved.

2.2.6 Safety and Protection Related to the Public [7]

If residential and industrial (non-distributed) PV systems are addressed the specific safety requirements may be different from those power transformers, especially when it comes to residential applications.

IEEE C57.129: The converter transformer pollution aspects are extremely important and shall be accurately defined, so that proper external insulation (particularly bushings) may be provided.

2.2.7 Islanding [7]

In these conditions, when the system is functioning but not connected to a *high-inertia short-circuit capacity* network, then the system could be less stable and subject to frequency variations, but no significant differences from 'standard' transformers are expected.

2.2.8 Relay Protection [7]

The study of relay protection for DPV-GTs is extremely important given that such transformers operate with inverter circuits between the actual alternative energy source and the eventual connection to such transformers.

2.2.9 DC Bias [3]

IEEE C57.110 (§4.1.4 DC components of load current): Harmonic load currents are frequently accompanied by a DC component in the load current. The DC component of a load current will increase the transformer core loss slightly but will increase the magnetizing current and audible sound level more substantially. Relatively small DC components (up to the RMS magnitude of the transformer excitation current at the rated voltage) are expected to have no effect on the load-carrying capability of a transformer determined by this recommended practice. Higher DC load current components may adversely affect transformer capability and should be avoided.

Saturation of transformer core due to DC bias: One of the most important parameters to determine how much DC current will saturate the core is the core construction (three-phase three-limb, three-phase five-limb or single-phase cores). So, transformer manufacturers should gather data on possible DC bias currents before they finalize their designs. The saturation of the core is an important parameter to watch because of the possibility of ferro-resonance, in the case of cable-connected pad-mounted transformers, due to possible resonance between the non-linear self-inductance of the transformer and other capacitances connected in the system, such as the cable capacitance and filter capacitance of the inverter under saturation due to DC bias.

2.2.10 Thermocycling (Loading) [7]

In most geographical locations in the United States, solar power facilities experience steady-state loading when the inverters are operating. When the sun comes out, there is a dampened reaction process and the load on the transformer is more constant. The entire process is controlled by the insolation number in a particular location. The no-load operation of such transformers is completely controlled by a different set of parameters.

Nominal loading average: Solar power systems typically operate very close to their rated loads. Since the load variation from the rated value is appreciably low, the operation of transformers is not so adversely affected as to cause the deterioration of parameters that guide the insulation coordination of the core coil structure. Thus, forces experienced by the primary and secondary windings are not out of the ordinary, alleviating problems that may occur in the design of the mechanical structure.

Note on no-load operation: PV system transformers are subject to long-term no-load operation conditions, at least at night. This might have an impact on loss capitalization, which customers usually take into account, but also on the transformer design.

The storage battery's interaction with the transformer in a PV system may control the load consistency and alleviate the perceived problems.

The IEEE C57.129 standard requires a detailed thermal study if the transformer or some of the terminals operate above rated capacity. Standard power transformer loading tables *should not* be used for loading determination because of the effect of the harmonic currents and DC bias on the valve windings (for the high-voltage direct current (HVDC) converter transformers).

Even with the loss correction addressing the harmonic content during the heat run, the hot spot temperature may not be representative of the real conditions due to the nature of the harmonic current distribution in the winding and how it differs during the heat run. An 'extended load run with overload' is recommended by the CIGRE Joint Task Force 12/14.10-01 for HVDC converter transformers.

2.2.11 Power Quality [7]

Power quality aspects are generally addressed in other chapters of this book, although very clear emphasis is given to the preceding salient items.

2.2.12 Low-Voltage Fault Ride-Through

Fault ride-through has yet to be defined for solar power systems; this could be because it is easier to quickly turn solar power systems on and off.

2.2.13 Power Storage [7]

Battery storage impact will depend on the kind of system the DPV-GT is serving in a particular geographic environment.

2.2.14 Voltage Transients and Insulation Coordination [4]

Generator step-up duty: With solar transformers, step-up duty is required, but without the problems associated with over-voltages caused by unloaded generators. The inverter converts DC input from the PV array and provides AC voltage to the transformer, giving a steady and smooth transition, with no over-voltage caused by unloaded circuits. All general installations covered under this application pay much attention in their system considerations to over-voltage conditions. This problem is addressed by providing an *automatic gain control* scheme to the inverter circuit configuration.

The IEEE C57.129 standard provides specific recommendations on the insulation test levels for converter transformers. The development of a similar recommendation would be appropriate for the insulation test levels and procedures required to warrantee the reliability of the transformers in the PV application.

2.2.15 Magnetic Inrush Current [7]

Transformers experience a high current inrush when energized from a de-energized state. The inrush current is typically several times the rated current. The magnitude of the inrush current is determined by a variety of factors defined by the transformer design. The inrush current, when compared as a multiple of the rated current, is generally much higher when the energization takes place from the LV side. That is due to the fact that the LV winding is generally the winding that is closest to the core and therefore has a lower air-core reactance.

Since the inrush current is several times the rated current, each inrush event creates mechanical stresses within the transformer. Frequent energization from a de-energized state should be avoided since it wears down the transformer faster than normal. This should be a consideration for the operators of DPV step-up transformers, since they may wish to save energy by shutting down the transformers during the night. Such practices can shorten the transformer's life expectancy.

2.2.16 Eddy Current and Stray Losses [8]

Eddy currents and stray losses are present in every transformer. The primary stray and eddy losses are due to the 60 Hz fundamental frequency currents. These loss components

increase with the square of the frequency and the square of the magnitude of the eddy currents. If the inverter feeding the power into the step-up transformer is producing more than the standard level of harmonics, then the stray and eddy losses will increase. The effect of the increase in load loss on efficiency is not typically a concern. Of much greater concern is the increased hot spot temperature in the windings and hot spots in metallic parts that can reduce the transformer life. A special design transformer can compensate for the higher stray and eddy losses. Also, a larger than necessary kVA transformer can be selected to compensate for the higher operating temperatures. However, these concerns about increasing eddy current loss are generally mitigated since harmonics are less than 1%.

IEEE C57.129: The user shall clearly indicate the method to be used for evaluating the guaranteed load losses. The harmonic spectrum to be used for load loss evaluation shall be clearly identified. This spectrum may be different from the one specified for the temperature rise tests; the latter represents the worst-case operating conditions. A harmonic correction is added to the measured sinusoidal load losses as part of the calculation of the appropriate total loss value for the temperature rise test. The procedure to determine the total load losses is described in the standard.

2.2.17 Design Considerations: Inside/Outside Windings [4]

The design considerations for windings are dependent on the issues in the previous items, as shown in Figure 2.4. The design considerations to meet the special requirements depend on the manufacturer's construction, kVA size, voltage and other factors. Since inverter technology limits the size of the inverter, there may be multiple inverters at each solar station. Some users should consider having multiple LV windings in a single transformer, with each LV winding connected to an inverter. Design considerations such as impedance and short circuits cause multiple LV windings, creating a much more complex transformer. Additional complexity will increase cost and reduce the availability of the transformer. It is advisable to keep a transformer as simple as practical so that it can be mass produced and can be built by as many manufacturers as feasible.

In many cases, the limit of the kVA on the inverter circuits forces some of the designs to incorporate LV windings outside the HV windings. This enables easier connections to facilitate the paralleling of circuits to achieve a higher kVA rating for the entire transformer under consideration. This helps to alleviate some of the problems faced due to the constraints.

2.2.18 Special Test Considerations [4]

IEEE C57.129: Extended load run with overload; other power testing concepts and methodologies; specifics for the transformers used with voltage source converters. In addition to tests, a design review is recommended.

2.2.19 Special Design Considerations

Solar power systems use inverters to convert DC to AC. Since the largest practical inverter size to date is about 500 kVA, designers are building 1000 kVA transformers by placing two inverter-connected windings in one transformer. In this way the transformer has to have two separate windings to accept completely separate inputs. Design issues also stem from running cables long distances to convert from DC to AC.

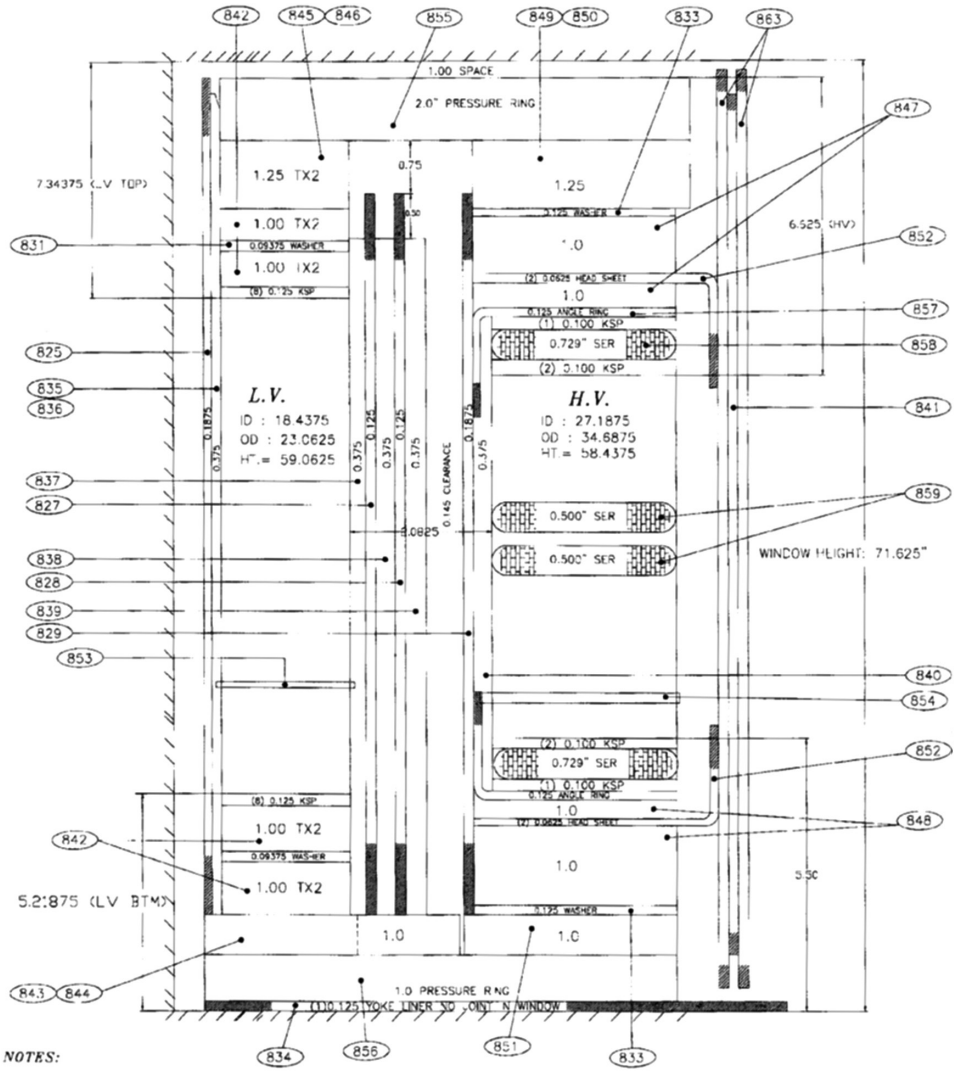

FIGURE 2.4
Core–coil–insulation coordination for a transformer.

2.2.20 Other Aspects

- Connection diagram: What are the standard connections of the PV application transformers?
- Shielding requirements (electrostatic shielding, protective shielding, harmonic filtration shielding).
- Inverter technology: Inverter technology has been slow to advance, because it is an electronic technology. It remains to be seen whether this comparative disadvantage will be a fatal flaw in the advancement of solar technology to the same level as wind farms in the renewable energy arena.

- Size of installation: The size of solar farms is limited by inverter technology, since inverters can currently only be built to about 500 kVA. This means that nearly all solar applications use pairs of 500 kVA inverters to drive the transformer and produce about 1000 kVA. Increasing the size by adding more inverters into one transformer box is extremely difficult, due to the complexities associated with the size of the box required and the practicalities of running cabling to convert from DC to AC.

Some of the core needs of DPV-GTs are

- Efficient heat management: The heat generated due to the uneven cooling of the coils leads to the creation of hot spots. This leads to the premature breakdown of the transformers.
- Lower harmonics and grid disturbances.
- The ability to withstand harsh weather conditions, temperatures, seismic levels and so on.

If necessary, DPV-GTs are designed and constructed to meet and exceed earthquake standards. Sometimes, DPV-GTs are rated for installation in the highest earthquake rating zones. In addition, it can incorporate a variety of fluids, including less flammable fluids required for enclosed applications.

DPV grid step-up transformers are especially designed to meet the solar industry's need for reliable service in remote locations and should offer advanced fault survivability/capability.

2.3 Relevant and Important Conclusions

DPV-GT solar converter step-up transformers are uniquely designed to connect solar farms to the electricity grid in large-scale solar power installations.

Step-up transformers are reliable and efficient engineered solutions with the necessary design flexibility needed for the solar industry. DPV-GTs are designed for the additional loading associated with the non-sinusoidal harmonic frequencies often found in inverter-driven transformers, and designs with multiple windings should be considered in case they can reduce transformer cost, minimize the transformer's footprint and provide the required functionality. Shell-type transformers can be also considered for this application.

The duty cycle seen in solar farms may not be as severe as those in wind farms, but solar power has its share of special considerations that affect transformer design. Those engaged in harnessing solar energy need to pay heed to these special needs to ensure that the solar installation is cost-effective and reliable.

References

1. Considerations for Power Transformers Applied in Distributed Photovoltaic (DPV): Grid Application, DPV-Grid Transformer Task Force Members, Power Transformers Subcommittee, IEEE-TC, Hemchandra M. Shertukde (chair), Mathieu Sauzay (vice chair), Aleksandr Levin (secretary), Enrique Betancourt, C. J. Kalra, Sanjib K. Som, Jane Verner, Subhash Tuli, Kiran Vedante, Steve Schroeder, Bill Chu, white paper in preparation for final presentation at the IEEE-TC conference in San Diego, CA, April 10–14, 2011.
2. C57.91: IEEE Guide for Loading Mineral-Oil-Immersed Transformers, 1995. Correction 1-2002.
3. Std. 519: Recommended Practices and Requirements for Harmonic Control in Electrical Power Systems, 1992.
4. C57.129: IEEE Standard for General Requirements and Test Code for Oil-Immersed HVDC Convertor Transformer, 1999 (2007 approved).
5. C57.18.10a: IEEE Standard Practices Requirements for Semiconductor Power Rectifier Transformers, 1998. Amended in 2008.
6. C57.110: IEEE Recommended Practice for Establishing Liquid-Filled and Dry-Type Power and Distribution Transformer Capability When Supplying Non-sinusoidal Load Current, 2008.
7. UL 1741: A Safety Standard for Distributed Generation, 2004.
8. Std. 1547.4: Draft Guide for Design, Operation and Integration of Distributed Resource Island Systems with Electric Power System, Only 1547.1 Is There, 2005.

3

Generalized Machine Theory and Reference Frame Formulation

3.1 Generalized Machine Theory and Reference Frame Formulation

Generalized machine theory (GMT) is developed on the hypothesis laid down by Park in 1926. This idea was then simplified by Kron and later further simplified by Gibbs using matrix algebra, to make the design and evaluation easily computable. The main consideration in this theory was to develop the equivalent circuit of rotating machines using the orthogonal direct and quadrature (*d*-*q*) axes as the basis vectors, as shown in Figure 3.1 for a salient two-pole synchronous machine.

The *d*-axis is in line with the magnetic north pole. θ is the angle between the *d*-axis and the reference axis. The *q*-axis is orthogonal to the *d*-axis. Generally, the three-phase equivalent circuits of rotating machines are developed using three-phase phasors of lines *a*, *b* and *c*, respectively. Thus, as shown in Chapter 2, we have the phasors for each phase as

$$V_{an}, V_{bn}, V_{cn} \tag{3.1}$$

where the second subscript of all variables in Equation 3.1 represents the neutral point of a four-wire system. The resulting line-to-line voltages would be

$$V_{ab}, V_{bc}, V_{ca} \tag{3.2}$$

Similarly, the phase currents and line-to-line currents are given by

$$I_{an}, I_{bn}, I_{cn} \tag{3.3}$$

$$I_{ab}, I_{bc}, I_{ca} \tag{3.4}$$

We now proceed to apply the theory of GMT to synchronous machines by conducting the *d*-*q* modeling as follows.

In addition to the *d*-*q* axes, we add one more axis, which is the reference zero axis colinear with the horizontal, such that it has a zero-phase shift. This converts the *d*-*q* axes to a *d*-*q*-0 transformation, as shown in Figure 3.2. It thus becomes a tensor that rotates the reference frame of a three-element vector or a similar 3×3 matrix in order to simplify the final analysis, as mentioned earlier. This *d*-*q*-0 transformation can be used in electrical engineering with a three-phase power system and applied to three-phase variables in Equations 3.1 through 3.4. The *d*-*q*-0 transform is used to rotate the reference frames of

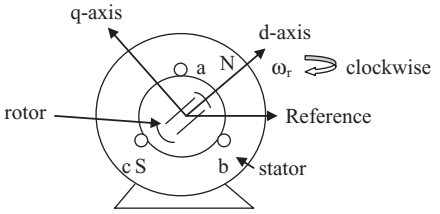

FIGURE 3.1
d-q axis of a salient two-pole synchronous machine.

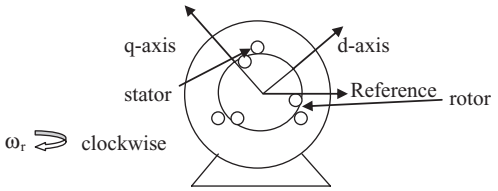

FIGURE 3.2
d-q-0 representation of polyphase IM.

the AC waveforms of variables in the above equations to align them such that the final alignment is necessarily visualized as DC transformation. Thus, if the analysis is applied to a three-phase synchronous machine, the *d-q*-0 transformation transforms the stator and rotor variables into a single-phase DC rotating frame to eliminate the effects of time-varying inductances. Another example is the use of the transform to calculate the control of three-phase inverters.

We will use subscripts *r* for rotor parameters and *s* for stator parameters and *q*, *d* and 0 for the corresponding *d-q*-0 transformations while relating with the *abc* three-phase parameters. Thus, for the stator it is

$$f_{qd0s} = K_s f_{abcs} \tag{3.5}$$

and for the rotor it is

$$f_{qd0r} = K_r f_{abcr} \tag{3.6}$$

where function *f* in Equations 3.5 and 3.6 represents any of the electrical parameters, as in Equation 3.7:

$$f = \text{voltage, current, flux linkage or charge} \tag{3.7}$$

and for a stator and a distributed rotor, respectively, as follows:

$$\left(f_{qd0s}\right)^T = \begin{bmatrix} f_{qs} & f_{ds} & f_{0s} \end{bmatrix} \tag{3.8}$$

$$\left(f_{qd0r}\right)^T = \begin{bmatrix} f_{qr} & f_{dr} & f_{0r} \end{bmatrix} \tag{3.9}$$

with the 3×3 transformation matrix K_s given by

$$K_s = \frac{2}{3}\begin{bmatrix} \cos\theta & \cos(\theta-120) & \cos(\theta+120) \\ \sin\theta & \sin(\theta-120) & \sin(\theta+120) \\ \frac{1}{2} & \frac{1}{2} & \frac{1}{2} \end{bmatrix} \tag{3.10}$$

and

$$(K_s)^{-1} = \begin{bmatrix} \cos\theta & \sin\theta & 1 \\ \cos(\theta-120) & \sin(\theta-120) & 1 \\ \cos(\theta+120) & \sin(\theta+120) & 1 \end{bmatrix} \tag{3.11}$$

with

$$\omega = \frac{d\theta}{dt} \tag{3.12}$$

The resulting three-phase electrical power in the stator of the synchronous machine is given by

$$P_{abcs} = V_{as}I_{as} + V_{bs}I_{bs} + V_{cs}I_{cs} \tag{3.13}$$

The resulting power in the *d*-*q*-0 transformation is as follows:

$$P_{dq0s} = \frac{2}{3}\left[V_{ds}I_{ds} + V_{dq}I_{qs} + V_{0s}I_{0s}\right] = P_{abcs} \tag{3.14}$$

Using this transformation, stationary circuit variables can be easily transformed to the arbitrary reference base frame. We can now generate the variables for a resistive circuit, assuming the stator winding has a realistic resistance R_s, as follows:

$$V_{abcs} = R_s I_{abcs} \tag{3.15}$$

Using Equations 3.10, 3.11, 3.13 and 3.14, the voltage in the stator winding resistance is given by

$$V_{dq0s} = K_s R_s \left[K_s\right]^{-1} I_{dq0s} \tag{3.16}$$

For a three-phase stator, R_s is the resistance matrix.

When the machine is symmetrical or balanced in all phases, R_s is a diagonal matrix and its non-zero elements along the diagonal are equal, which results in

$$K_s R_s \left[K_s\right]^{-1} = R_s \tag{3.17}$$

When the machine phases are unequal or unbalanced (i.e., asymmetrical), phase resistances are unequal; therefore, the *d*-*q*-0 variables contain sinusoidal functions of θ, except when $\omega = 0$.

We can now develop the transformation for the inductive elements in the stator winding by evaluating the time derivative of the flux linkage, as follows:

$$V_{abcs} = \frac{d}{dt}\left(\lambda_{abcs}\right) \tag{3.18}$$

Thus, the transformed voltage in the *d*-*q*-0 axes is

$$V_{dq0s} = K_s\left\{\frac{d}{dt}[K_s]^{-1}\left(\lambda_{dq0s}\right)\right\} \tag{3.19}$$

$$V_{dq0s} = K_s\left\{\frac{d}{dt}[K_s]^{-1}\right\}\left(\lambda_{dq0s}\right) + K_s K_s^{-1}\frac{d}{dt}\left(\lambda_{dqos}\right) \tag{3.20}$$

where:

$$\left\{\frac{d}{dt}[K_s]^{-1}\right\} = \omega\begin{bmatrix} -\sin\theta & \cos\theta & 0 \\ -\sin(\theta-120) & \cos(\theta-120) & 0 \\ -\sin(\theta+120) & \cos(\theta+120) & 0 \end{bmatrix} \tag{3.21}$$

which yields

$$K_s\left\{\frac{d}{dt}[K_s]^{-1}\right\} = \omega\begin{bmatrix} 0 & 1 & 0 \\ -1 & 0 & 0 \\ 0 & 0 & 0 \end{bmatrix} \tag{3.22}$$

Using Equation 3.22 in Equation 3.20 yields

$$V_{dq0s} = \omega\left(\lambda_{dq0s}\right) + \frac{d}{dt}\left(\lambda_{dqos}\right), \text{ where } \omega = \frac{d\theta}{dt} \tag{3.23}$$

which can be expanded as

$$V_{qs} = \omega\lambda_{ds} + \frac{d}{dt}\lambda_{qs} \tag{3.24}$$

$$V_{ds} = -\omega\lambda_{qs} + \frac{d}{dt}\lambda_{ds} \tag{3.25}$$

and

$$V_{0s} = \frac{d}{dt}\lambda_{0s} \tag{3.26}$$

All the preceding equations can be tabulated for several conditions, as follows.

1. Arbitrary reference frame

   In the arbitrary reference frame, the reference frame speed is ω and is generally not specified. The interpretation is related to stationary circuit variables referred to the stationary arbitrary reference frame. The variables involved are given by

$$\left(f_{dq0s}\right)^T = \begin{bmatrix} f_{ds} & f_{qs} & f_{0s} \end{bmatrix}, \quad \text{and} \quad K_s \tag{3.27}$$

2. Stationary reference frame

   In the stationary reference frame, the reference frame speed is zero and the stationary circuit variables referred to the stationary reference frame are specified as

$$\left(f^{s}_{dq0s}\right)^{T} = \left[f^{s}_{ds} \quad f^{s}_{qs} \quad f_{0s}\right], \quad \text{and} \quad K^{s}_{s} \tag{3.28}$$

3. Rotor reference frame

   In the rotor reference frame, the reference speed is ω_r and the stationary circuit variables referred to the reference frame are given by

$$\left(f^{r}_{dq0s}\right)^{T} = \left[f^{r}_{ds} \quad f^{r}_{qs} \quad f_{0s}\right], \quad \text{and} \quad K^{r}_{s} \tag{3.29}$$

4. Synchronously rotating reference frame

   In the synchronously rotating reference frame, the reference frame speed is ω_e and the variables referred to the reference frame are given by

$$\left(f^{e}_{dq0s}\right)^{T} = \left[f^{e}_{ds} \quad f^{e}_{qs} \quad f_{0s}\right], \quad \text{and} \quad K^{e}_{s} \tag{3.30}$$

In the preceding reference frames, the *s* subscript denotes variables and transformations associated with circuits that are stationary, as in a stator for an electrical machine, as opposed to the *r* subscript, which refers to rotor circuits, which generally rotate. The superscripts are related to *ds* and *qs* variables and transformations associated with a specific reference frame, as in the ones described previously, except in the arbitrary reference frame that carries no superscript index. This is because the 0*s* variables are independent of ω and thus not associated with a reference frame, and thus no superscript is assigned to f_{0s}. The transformation of variables associated with stationary circuits to a stationary reference frame was developed by E. Clarke, who used the notations

$$\left[f_{\alpha} \; f_{\beta} \; f_{0}\right] \text{ instead of } \left[f^{s}_{ds} \quad f^{s}_{qs} \quad f_{0s}\right] \tag{3.31}$$

In Park's transformations to the rotor reference, he used

$$\left[f_{d} \; f_{q} \; f_{0}\right] \text{ instead of } \left[f^{r}_{ds} \quad f^{r}_{qs} \quad f_{0s}\right] \tag{3.32}$$

which indicates no established notation for the variables in the synchronously rotating reference frame. The voltage equation for all reference frames can be obtained from those in the arbitrary reference frame. The transformations for a specific reference frame are obtained by substituting the appropriate reference frame speed for ω. In most cases, the initial or time-zero displacements can be selected equal to zero. However, there are situations where the initial displacement of the reference frame to which the variables are being transformed will not generally be zero.

In some derivations and further analysis, it is convenient to relate the variables of one reference to the variables of another reference frame directly, without involving the *abc* variables in the transformation. This can be achieved as follows.

Let *i* be the reference frame from which the variables are being transformed and *j* be the reference frame to which the variables are being transformed; then

$$f^{j}_{dq0s} = {}^{i}K^{j} f^{i}_{dq0s} \tag{3.33}$$

$$f^{i}_{dq0s} = K^{i}_{s} f_{abcs} \tag{3.34a}$$

Thus,

$$f^{j}_{dq0s} = {}^{i}K^{j} K^{i}_{s} f_{abcs} \tag{3.34b}$$

and

$$f^{j}_{dq0s} = K_{s}^{j} f_{abcs} \tag{3.35}$$

which yields

$${}^{i}K^{j} K^{i}_{s} = K_{s}^{j} \tag{3.36}$$

Thus,

$${}^{i}K^{j} = K_{s}^{j} (K_{s}^{i})^{-1} \tag{3.37}$$

and thus,

$${}^{i}K^{j} = \begin{bmatrix} \cos(\theta_j - \theta_x) & -\sin(\theta_j - \theta_x) & 0 \\ \sin(\theta_j - \theta_x) & \cos(\theta_j - \theta_x) & 0 \\ 0 & 0 & 1 \end{bmatrix} \tag{3.38}$$

We now proceed to apply this to generalized machines in electrical engineering.

3.2 Generalized Machine Model

All electrical machines can be represented by a generalized model, as proposed by Krone, and is basically a hypothetical machine. This idea is based on some assumptions, as follows:

1. As the distribution of the current along the air gap periphery and flux is repetitive in nature after every pole pair, a generalized machine is assumed to have one pole pair in order to avoid complicacy and to avoid the conversion of the electrical and mechanical angles.
2. For simplification, every generalized machine has a single coil.
3. As shown in Figure 3.1, the *d*-axis is co-linear with the magnetic axis (N–S pole). The *q*-axis is orthogonal to the *d*-axis.
4. The direction of the current and flux is governed by the right-hand thumb (RHT) rule. If the current is in the direction of the RHT, then the magnetic flux is in the direction of all other fingers curled around the direction of the thumb.

5. V and I represent the voltage externally impressed on the coil and the current, the magnitude and the direction of the current flowing in the coil. See assumption 4.
6. The machine is assumed to be rotating in the positive direction when rotating in the clockwise direction.
7. Subscripts s, r, d and q are used for stator, rotor, direct-axis and quadrature-axis, respectively.

Using the preceding assumptions, the voltage equations of the generalized machine shown in Figure 4.1 can be written as follows:

$$V_{ds} = \left(R_{ds} + L_{ds} \frac{d}{dt} \right) I_{ds} + M_d \frac{d}{dt} I_{dr} \tag{3.39}$$

$$V_{qs} = \left(R_{qs} + L_{qs} \frac{d}{dt} \right) I_{qs} + M_q \frac{d}{dt} I_{qr} \tag{3.40}$$

$$V_{dr} = M_d \frac{d}{dt} I_{ds} - M_q \omega_r I_{qs} + \left(R_{dr} + L_{dr} \frac{d}{dt} \right) I_{dr} - \omega_r L_{qr} I_{qr} \tag{3.41}$$

$$V_{qr} = M_d \omega_r \frac{d}{dt} I_{ds} + M_q \frac{d}{dt} I_{qs} + \left(R_{qr} + L_{qr} \frac{d}{dt} \right) I_{qr} + \omega_r L_{dr} I_{dr} \tag{3.42}$$

where:

$V_{ds}, V_{qs}, V_{dr}, V_{qr}$ are direct-axis and quadrature-axis voltages (3.43)

In a practical machine, these voltages can be transformed from the *abc* variables by using Equations 3.5 through 3.12.

$I_{ds}, I_{qs}, I_{dr}, I_{qr}$ are direct-axis and quadrature-axis currents (3.44)

In a practical machine these currents can be transformed from the *abc* variables by using Equations 3.5 through 3.12.

$r_{ds}, r_{qs}, r_{dr}, r_{qr}$ are direct-axis and quadrature-axis resistances (3.45)

$L_{ds}, L_{qs}, L_{dr}, L_{qr}$ are direct-axis and quadrature-axis self-inductances (3.46)

M_d, M_q are direct-axis and quadrature-axis mutual inductances (3.47)

The values of all the preceding parameters depend on the machine and the shape of the rotor: that is, salient or distributed in structure. Besides, all these parameters are assumed to be linear, time invariant and causal to be suitable for system analysis using generalized machine theory. This leads to a matrix-form representation, as follows:

$$\begin{vmatrix} V_{ds} \\ V_{qs} \\ V_{dr} \\ V_{qr} \end{vmatrix} = \begin{bmatrix} R_{ds} + L_{ds}\dfrac{d}{dt} & 0 & M_d\dfrac{d}{dt} & 0 \\ 0 & R_{qs} + L_{qs}\dfrac{d}{dt} & 0 & M_q\dfrac{d}{dt} \\ M_d\dfrac{d}{dt} & -M_q\omega_r & R_{dr} + L_{dr}\dfrac{d}{dt} & -\omega_r L_{qr} \\ M_d\omega_r & M_q\dfrac{d}{dt} & \omega_r L_{dr} & R_{qr} + L_{qr}\dfrac{d}{dt} \end{bmatrix} \begin{vmatrix} I_{ds} \\ I_{qs} \\ I_{dr} \\ I_{qr} \end{vmatrix} \tag{3.48}$$

which can be written in matrix form as $[V] = [Z][I]$,
where:

$$[Z] = \begin{bmatrix} R_{ds} + L_{ds}\dfrac{d}{dt} & 0 & M_d\dfrac{d}{dt} & 0 \\ 0 & R_{qs} + L_{qs}\dfrac{d}{dt} & 0 & M_q\dfrac{d}{dt} \\ M_d\dfrac{d}{dt} & -M_q\omega_r & R_{dr} + L_{dr}\dfrac{d}{dt} & -\omega_r L_{qr} \\ M_d\omega_r & M_q\dfrac{d}{dt} & \omega_r L_{dr} & R_{qr} + L_{qr}\dfrac{d}{dt} \end{bmatrix} \tag{3.50}$$

That is,

$$[Z] = [R] + [L]\frac{d}{dt} + [G]\omega_r$$

where the resistance matrix is

$$[R] = \begin{bmatrix} R_{ds} & 0 & 0 & 0 \\ 0 & R_{qs} & 0 & 0 \\ 0 & 0 & R_{dr} & 0 \\ 0 & 0 & 0 & R_{qr} \end{bmatrix} \tag{3.51}$$

The self-inductance matrix is

$$[L] = \begin{bmatrix} L_{ds} & 0 & M_d & 0 \\ 0 & L_{qs} & 0 & M_q \\ M_d & 0 & L_{dr} & 0 \\ 0 & M_q & 0 & L_{qr} \end{bmatrix} \tag{3.52}$$

and the speed-dependent component is

$$[G] = \begin{bmatrix} 0 & 0 & 0 & 0 \\ 0 & 0 & 0 & 0 \\ 0 & -M_q & 0 & -L_{qr} \\ 0 & 0 & L_{dr} & 0 \end{bmatrix} \tag{3.53}$$

We can now evaluate the real power, imaginary power and rotational power as part of the total power equation as follows:

$$\begin{aligned} P &= [I]^T [V] = V_{ds} I_{ds} + V_{qs} I_{qs} + V_{dr} I_{dr} + V_{qr} I_{qr} \\ &= \left[I \right]^T [R][I] + \left[I \right]^T [L] \frac{d}{dt} [I] + \omega_r [I]^T [G][I] \end{aligned} \tag{3.54}$$

where the copper loss is

$$P_{cu} = [I]^T [R][I] = I^2_{ds} R_{ds} + I^2_{qs} R_{qs} + I^2_{dr} R_{dr} + I^2_{qr} R_{qr} \tag{3.55}$$

the change in stored energy is

$$P_{se} = [I]^T [L] \frac{d}{dt} [I] \tag{3.56}$$

and the electrical power converted to mechanical power is

$$P_{\text{rot}} = \omega_r [I]^T [G][I] \tag{3.56}$$

resulting in the electrical torque, developed as

$$\tau_e = \frac{P_{\text{rot}}}{\omega_r} = [I]^T [G][I] \tag{3.57}$$

$$= I_{qr} M_d I_{ds} - M_q I_{dr} I_{qs} + \left(L_{dr} - L_{qr} \right) I_{qr} I_{dr} \tag{3.58}$$

In Equation 3.58, when the term $(L_{dr} - L_{qr})$ is zero, the third term goes to zero and is related to the reluctance torque, which is zero in the absence of salient poles and is achieved in distributed pole conditions. As we know, the difference between electrical torque and load torque generates the dynamics of the machine, as follows:

$$\tau_e - \tau_L = J \dot{\omega}_r \tag{3.59}$$

3.3 *d-q-0* Analysis of Three-Phase Induction Motor

We consider here a polyphase induction machine (IM), which necessitates that the *d-q-0* axes be fixed in the stator structure as shown in Figure 3.2.

The stator is shown offset from the rotor to highlight the slip action. The variable θ is the angle between the d-axis and the reference axis. As the three-phase stator windings are stationary (*a-b-c*) along with the *d-q-0* axes with respect to each other, the transformation matrix from (*a-b-c*) to (*d-q-0*) or vice a versa has constant coefficients. The transformation matrix is shown as

$$\begin{bmatrix} I_{ds} \\ I_{qs} \\ I_{0s} \end{bmatrix} = \frac{2}{3} \begin{bmatrix} \cos\theta & \cos(\theta - 120) & \cos(\theta + 120) \\ \sin\theta & \sin(\theta - 120) & \sin(\theta + 120) \\ \frac{1}{2} & \frac{1}{2} & \frac{1}{2} \end{bmatrix} \begin{bmatrix} I_a \\ I_b \\ I_c \end{bmatrix} \tag{3.60}$$

and

$$\begin{bmatrix} V_{ds} \\ V_{qs} \\ V_{0s} \end{bmatrix} = \frac{2}{3}\begin{bmatrix} \cos\theta & \cos(\theta-120) & \cos(\theta+120) \\ \sin\theta & \sin(\theta-120) & \sin(\theta+120) \\ \frac{1}{2} & \frac{1}{2} & \frac{1}{2} \end{bmatrix}\begin{bmatrix} V_a \\ V_b \\ V_c \end{bmatrix} \tag{3.61}$$

In Equations 3.60 and 3.61, the subscript *s* stands for the stator; the *d*-*q*-0 currents and voltages are with respect to the stator. Note that in reality the rotor is short-circuited on itself in an IM. The three-phase currents in the stator in the time domain are given by

$$I_A = I_m \cos(\omega t + \alpha) \tag{3.62}$$

$$I_B = I_m \cos(\omega t + \alpha + 120) \tag{3.63a}$$

$$I_C = I_m \cos(\omega t + \alpha - 120) \tag{3.63b}$$

where:

Peak value I_m is the $\sqrt{2}$ times the RMS value of the current

α is the phase angle of the respective phase current in the time domain origin

Thus, from Equations 3.60 and 3.61 we have

$$\begin{bmatrix} I_{ds} \\ I_{qs} \end{bmatrix} = \sqrt{\frac{2}{3}}\begin{bmatrix} I_m \cos(\omega t + \alpha) \\ I_m \sin(\omega t + \alpha) \end{bmatrix} \tag{3.64}$$

and

$$\begin{bmatrix} V_{ds} \\ VI_{qs} \end{bmatrix} = \sqrt{\frac{2}{3}}\begin{bmatrix} V_m \cos(\omega t + \alpha) \\ V_m \sin(\omega t + \alpha) \end{bmatrix} \tag{3.64}$$

From Equations 3.63 and 3.64 it is clear that the *d*-*q* axes currents as well as voltages are functions of time and are displaced by 90°, which shows that *d*-*q* currents constitute a two-phase system of currents having a frequency of the equivalent three-phase system. While this analysis is for a distributed rotor system of winding connections in a squirrel cage IM, the rotor is short-circuited on itself, which causes the voltages V_{dr} and V_{qr} to go to zero, resulting in the reversal of currents I_{dr} and I_{qr}, as shown in Equation 3.65:

$$\begin{vmatrix} V_{ds} \\ V_{qs} \\ 0 \\ 0 \end{vmatrix} = \begin{bmatrix} R_{ds} + L_{ds}\frac{d}{dt} & 0 & -M_d\frac{d}{dt} & 0 \\ 0 & R_{qs} + L_{qs}\frac{d}{dt} & 0 & -M_q\frac{d}{dt} \\ M_d\frac{d}{dt} & -M_q\omega_r & -\left(R_{dr} + L_{dr}\frac{d}{dt}\right) & \omega_r L_{qr} \\ M_d\omega_r & M_q\frac{d}{dt} & -\omega_r L_{dr} & -\left(R_{qr} + L_{qr}\frac{d}{dt}\right) \end{bmatrix} \begin{vmatrix} I_{ds} \\ I_{qs} \\ I_{dr} \\ I_{qs} \end{vmatrix} \tag{3.65}$$

Thus, from all the analysis shown in the previous sections it is understood that the GMT approach to synchronous machines and IMs is simpler than the coupled circuit approach, as long as matrix algebra is appropriately understood and applied. GMT makes use of simple concepts of electric circuits and provides a link between the three-phase system variables (*a-b-c*) and two-phase system variables (*d-q*). For further simplicity, a reference zero axis is added to obtain matrix algebra convenience in the manipulations of the *d-q*-0 axes system.

Problems

PROBLEM P.3.1

Under steady-state operating conditions, the armature of the salient-pole synchronous generator carries symmetrical sinusoidal three-phase currents.

$$i_a = \sqrt{2}\,|I_a|\sin(\theta_d - \theta_a)$$

$$i_b = \sqrt{2}\,|I_a|\sin(\theta_d - 120° - \theta_a)$$

$$i_c = \sqrt{2}\,|I_a|\sin(\theta_d - 240° - \theta_a)$$

where:

$$\theta_d = \omega t + \delta + 90°$$

Using the P-transformation matrix, find expressions for the corresponding *d-q*-0 currents of the armature.

PROBLEM P.3.2

DC current I_f is supplied to the filed winding of an unloaded salient-pole synchronous generator rotating with constant angular velocity ω. Find the form of the *oc* armature voltages and their *d-q*-0 components.

PROBLEM P.3.3

The armature of a three-phase salient pole generator carries the currents

$$i_a = \sqrt{2}\,|1000|\sin(\theta_d - \theta_a)\,A$$

$$i_b = \sqrt{2}\,|1000|\sin(\theta_d - 120° - \theta_a)\,A$$

$$i_c = \sqrt{2}\,|1000|\sin(\theta_d - 240° - \theta_a)\,A$$

1. Using the P-transformation matrix, find the direct axis current i_d and the quadrature axis current i_q.
2. What is the zero-sequence current i_0?
3. Suppose the armature currents are

$$i_a = \sqrt{2}\,|1000|\sin(\theta_d - \theta_a)\,A$$

$$i_b = i_c = 0$$

Find i_d, i_q and i_0.

4

Transmission Lines

4.1 Parameters

The three parameters of a transmission line that define its equivalent circuit are

1. Resistance
2. Inductance
3. Capacitance

There are several passive components in a single-line diagram (SLD) that are associated with many of the major components of a power system. One of the most important components is the resistance. The resistance of any electrical conductor is given by

$$R = \rho \frac{l}{A} \Omega \tag{4.1}$$

where:

- ρ is the resistivity of the material of the conductor
- l is its length in meters
- A is the area of the cross-section of the material

The resistivities of different materials are listed in Table 4.1.

The DC resistance of stranded conductors as calculated by Equation 4.1 is greater than its effective value, described in Equation 4.2:

$$R = \frac{P}{|I^2|} \Omega \tag{4.2}$$

where:

- P is the power loss in the conductor
- I is the current in the conductor

This effective DC resistance is different in stranded conductors due to the spiraling of the conductors. Spiraling causes some of the strands to be longer than the central core conductor. This increase is approximately 1% more for three-strand conductors and 2% for concentrically stranded conductors. In addition, the AC resistance of conductors is different due to the *skin effect*. With different frequencies of current flowing in the conductor, the current tends to flow more in the area of cross-section closer to the skin of the conductor.

TABLE 4.1

Material	ρ (Ω·m) at 20°C
Hard-drawn copper	1.77×10^{-8}
Aluminum	2.83×10^{-8}

Thus, the area of cross-section to be used in the denominator of Equation 4.1 is reduced, leading to an increase in the ohmic value. Besides, the resistance of metallic conductors varies with temperature, as shown in Figure 4.1. Temperature t is plotted on the vertical axis in degrees Celsius and resistance R on the horizontal axis in ohms. R_1 and R_2 are the resistances at temperatures t_1 and t_2, respectively. The extended line cuts the vertical axis, generating the value T. This value T is tabulated in Table 4.2 for different kinds of conductors and different materials.

$$\frac{R_2}{R_1} = \frac{T + t_2}{T + t_1} \tag{4.3}$$

or

$$R_2 = R_1\left[1 + \alpha\left(T_2 - T_1\right)\right] \tag{4.4}$$

where α is the temperature coefficient of resistance.

The resistivity of a material as given in Equation 4.1 is related to the conductivity σ of the material, as shown in Equation 4.5:

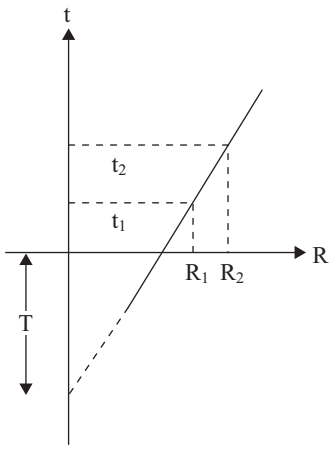

FIGURE 4.1
Variation of resistance of metallic conductors with temperature.

TABLE 4.2

Material	T
Annealed copper of 100% conductivity	234.5
Hard-drawn copper of 97.3% conductivity	241
Hard-drawn aluminum of 61% conductivity	228

TABLE 4.3

Material	Conductivity σ (S/m)	Resistivity ρ at 20°C (μΩ·cm)
Annealed copper of 100% conductivity	5.96×10^7	1.72
Hard-drawn copper of 97.3% conductivity	5.80×10^7	1.77
Hard-drawn aluminum of 61% conductivity	3.50×10^7	2.83

$$\sigma = \frac{1}{\rho} \tag{4.5}$$

This is shown in Table 4.3 for different materials.

The unit of conductivity is Siemens per meter, where Siemens (after the famous German scientist) is written as *mhos* (*mho* is the inverse of *ohm*).

4.2 Inductance *L* in Henry

The next important passive element that comprises a common and essential part of the SLD is the inductance *L* of a single-conductor coil, measured in units of henry (H). This is used to represent all components, including transmission lines, transformers and rotating machines both AC as well as DC. In general, inductance is given by Equation 4.6:

$$L = N^2 \wp = N^2 / \mathcal{R} \tag{4.6}$$

where:

- N is the number of turns of the coil
- $\wp$ is the permeance, which is the inverse of $\mathcal{R}$, as given in Equations 4.7 and 4.8, respectively:

$$\wp = \frac{1}{\mathcal{R}} \tag{4.7}$$

$$\mathcal{R} = \frac{l}{\mu A} \tag{4.8}$$

where:

- μ is the permeability of the magnetic medium
- l is the length of the magnetic circuit in meters (m)
- A is the area of cross-section in square meters (m^2)

In general, the inductance is evaluated by using Equation 4.9 for the constant permeability of the medium.

$$\lambda = N\Phi = LI \tag{4.9}$$

where:

- Φ is the magnetic flux permeating in the magnetic circuit
- $\lambda = N\Phi$ is the flux linkage
- I is the current in amperes carried by the coil with inductance L

Equation 4.5 can be derived from Equation 4.8 as follows:

$$LI = NBA = N\mu HA = \frac{N\mu NIA}{l}$$

$$L = \frac{N^2}{\mathcal{R}} = N^2\wp, \text{ as in Equations 4.6 and 4.7}$$

where:

B	is the magnetic flux density in tesla
H	is the magnetic field intensity in ampere-turns/meter
B and H	are related by Equation 4.10:

$$B = \mu H \tag{4.10}$$

μ is the permeability of the magnetic medium and is given by Equation 4.11 in terms of the absolute permeability of the air or free space, as follows:

$$\mu = \mu_r \mu_0 \tag{4.11}$$

where:

μ_r	is the relative permeability of the magnetic medium
μ_0	is the permeability of space or air given by $4\pi \times 10^{-7}$ H/m

The relative permeabilities of different media are given in Table 4.4.

Thus, if one has more than one conductor—that is, several strands of conductors, as in aluminum conductor steel-reinforced (ACSR) cable—then it is easy to find the flux linkage of the total magnetic circuit and divide this product by the current I to yield the inductance L.

To find the inductance of a transmission line, further care must be taken to account for the following:

1. Internal flux of the conductor
2. External flux associated with the conductor

This necessitates the use of Faraday's law:

$$e = \frac{d}{dt}(N\Phi) \tag{4.12}$$

TABLE 4.4

Material	Relative Permeability
Air	1
Silicon steel	6,000–8,000
Super-magnetic Mu material	75,000–100,000
Nickel	250
Cobalt	600

and Equation 4.9:

$$e = L\frac{di}{dt} \tag{4.13}$$

which yields

$$L = \frac{d(N\Phi)}{di} \tag{4.14}$$

Thus,

$$\Psi = LI \text{ Wb}\cdot\text{turn} \tag{4.15}$$

Once the current changes to AC, both the internal and external flux linkages are also sinusoidal and results in a phasor, as follows:

$$\Psi = LI \text{ Wb}\cdot\text{turn} \tag{4.16}$$

Ψ and I are in phase, and L results in a phasor voltage drop, as follows:

$$V = j\omega LI \text{ volts} \tag{4.17}$$

$$V = j\omega\Psi \text{ volts} \tag{4.18}$$

Besides the preceding kinds of fluxes, there is one more called the *mutual flux*, which results in the *mutual inductance*. This helps to analyze the influence of power lines on telephone lines as well as coupling between parallel lines. Mutual inductance is evaluated by finding the flux linkages of one circuit due to the current in the second circuit in the proximity or in the near or far field per ampere of current in the second circuit. Thus,

$$M_{12} = \frac{\Psi_{12}}{I_2}\text{H} \tag{4.19}$$

where Ψ_{12} is the mutual flux linkage, as described previously between the two circuits interacting magnetically with each other.

Then, the corresponding voltage in the first circuit is

$$V_1 = j\omega M_{12}I_2 = j\omega\Psi_{12} \text{ volts} \tag{4.20}$$

4.2.1 Inductance of a Conductor Due to Internal Flux

Let us now proceed to find the inductance of a conductor due to internal flux. Changing the lines of flux inside the conductors contributes to the induced voltage of the electrical circuit. This flux links only a fraction of the total current flowing through the conductor of the transmission line under consideration, as shown in Figure 4.2.

A conductor with radius r carries a current I out of the page. The flux caused by this current moves counterclockwise (CCW), as shown in Figure 4.2. This flux links only with a fraction of the total current I. The return path of the current I in the conductor is far away, so that the lines of flux are concentric around and inside the conductor and CCW with

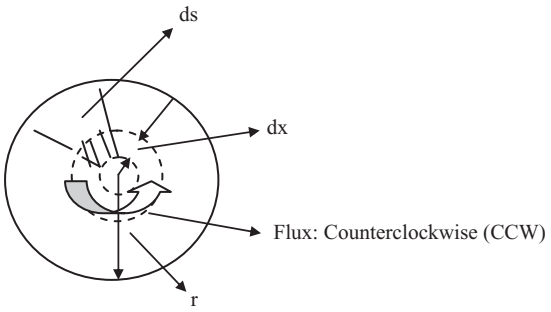

FIGURE 4.2
Conductor carrying current *I* out of the page; magnetic flux is CCW.

respect to the conductor. Using Ampere's integral law to calculate the magneto motive force (MMF) due to current *I* in the conductor, we have

$$MMF : I = \int J.da = \oint H.ds \;\; Wb.turn \tag{4.21}$$

where:

H	is the magnetic field intensity tangential to ds in At/m
S	is the distance along path, in meters
I	is the current A that is enclosed in the circuit
J	is the current density
A	is the area through which current density J exists along the path of the current.

To analyze this further, let H_x be the magnetic field intensity at a distance x from the center of the conductor and H_x is constant at all points equidistant from the center. Using Equation 4.21, we have the current at distance x as

$$\oint H_x ds = I_x \tag{4.22}$$

Conducting the closed-loop integral over the path at a distance x from the center yields

$$2\pi x H_x = I_x \tag{4.23}$$

For an uniform current density J in the conductor, we have

$$I_x = \frac{\pi x^2}{\pi r^2} I \tag{4.24}$$

where I is the total current in the conductor.

Then,

$$\begin{aligned} H_x &= \frac{I_x}{2\pi x} \\ &= \frac{\pi x^2 I}{\pi r^2 \cdot 2\pi x} \\ &= \frac{x \cdot I}{2\pi r^2} \;\; \text{At/m} \end{aligned} \tag{4.25}$$

The magnetic flux density x m from the center of the conductor is

$$B_x = \mu H_x = \mu \frac{x.I}{2\pi r^2} \quad \frac{\text{Wb}}{\text{m}^2} \tag{4.26}$$

Therefore, the flux per meter of the length of the conductor is

$$d\Phi = \frac{\mu x I}{2\pi r^2} dx \quad \frac{\text{Wb}}{\text{m}^2} \tag{4.27}$$

where the area of the cross-section of the conductor associated with this incremental magnetic flux at distance x from the center of the conductor is

$$A = dx.\ \text{axial length of the conductor} \tag{4.28}$$

yielding the flux linkage per meter of length of the conductor.

The linking fraction of the conductor turn of a radial element of thickness dx as a cylindrical element is as follows:

$$d\psi = \frac{\pi x^2}{\pi r^2} d\phi = \frac{\mu I x^3}{2\pi r^4} dx \text{ Wb.} \frac{\text{turn}}{\text{m}} \tag{4.29}$$

This results in the total flux linkage of a conductor due to internal flux, as follows:

$$\psi_{\text{int}} = \int_0^r \frac{\mu I x^3}{2\pi r^4} dx = \frac{\mu I}{8\pi} \tag{4.30}$$

For $\mu_r = 1$ and $\mu_0 = 4\pi \times 10^{-7}$ H/m:

$$\psi_{\text{int}} = \frac{I}{2} \times 10^{-7} \quad \text{Wb} - \frac{\text{turn}}{\text{m}}$$

which yields the inductance due to internal flux:

$$L_{\text{int}} = \frac{1}{2} \cdot 10^{-7} \quad \frac{\text{H}}{\text{m}} \tag{4.31}$$

We now proceed to find the inductance due to the external flux linkages caused by a current in a conductor. We start by assessing the flux linkages between two points external to an isolated current-carrying conductor. This is shown in Figure 4.3.

A circular conductor with radius r carries a current I out of the paper, as shown in Figure 4.3. According to Lenz's law, this creates a CCW magnetic flux, as shown within the radially thick dx concentric cylindrical tube along the length of the conductor assumed to be l m long. In this case as well, the return path is a far distance for mathematical analysis to conduct the overall MMF, as follows. For this analysis, two concentric circles at distances of D_1 and D_2 are shown in bold, where points P_1 and P_2 are shown and located. Dashed concentric circles are shown at a distance of x and $x + dx$ from the center of the conductor.

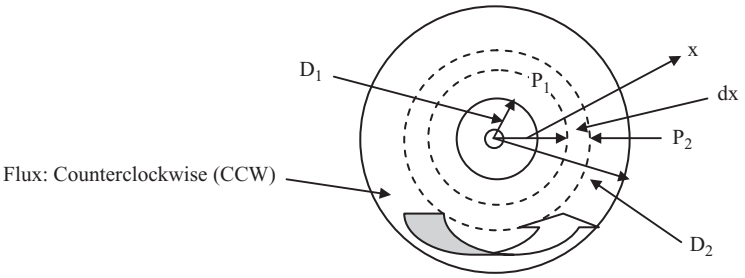

FIGURE 4.3
Single isolated conductor of radius *r* carrying current *I* out of the page and flux distribution around.

Thus, the total MMF at a distance x from the center of the conductor is given by

$$2\pi x H_x = I \tag{4.32}$$

where H_x is the magnetic field intensity at a distance x from the center of the conductor. This yields the magnetic flux density B_x, given by

$$B_x = \frac{\mu I}{2\pi x} \quad \frac{\text{Wb}}{\text{m}^2} \tag{4.33}$$

Therefore, the flux per meter of the length in the tubular element of thickness dx is given by

$$d\Phi = \frac{\mu I}{2\pi x} dx \quad \frac{\text{Wb}}{\text{m}} \tag{4.34}$$

where the area A through which the magnetic flux permeates is given by

$$A = dx\, x\, l \tag{4.35}$$

where l is the axial length of the conductor.

In the evaluation of the external flux linkage scenario it is imperative to observe that the flux linkages per meter are equal to the flux since all the flux external to the conductor links with all the current once (i.e., assuming there is only one single conductor accounting for the one single turn of the entire circuit) and the incremental flux linkage is now considered between the two points P_1 at distance D_1 and P_2 at distance D_2, respectively, from the center of the conductor due to current I in the conductor.

Thus,

$$\Psi_{12} = \int_{D_1}^{D_2} d\Psi = \int_{D_1}^{D_2} \frac{\mu I}{2\pi x} dx = \frac{\mu I}{2\pi} \ln \frac{D_2}{D_1} \quad \text{Wb} \cdot \frac{\text{turn}}{\text{m}} \tag{4.36}$$

Here, the permeability $\mu = \mu_r \mu_0$, where μ_r is the relative permeability of the medium in which the current carrying current I exists and μ_0 is the permeability of space given by $4\pi \times 10^{-7}$ H/m. Assuming $\mu_r = 1$, the mutual flux linkage is given as

$$\Psi_{12} = 2 \cdot 10^{-7} I \ln \frac{D_2}{D_1} \quad \text{Wb} \cdot \frac{\text{turn}}{\text{m}} \tag{4.37}$$

Thus the inductance only due to the flux included between the two points P_1 at distance D_1 and P_2 at distance D_2 respectively, is given by dividing Equation 4.37 by the current I carried by the conductor with radius r, as follows:

$$L_{12} = 2 \cdot 10^{-7} \ln \frac{D_2}{D_1} \quad \frac{\text{H}}{\text{m}} \tag{4.38}$$

We now extend this thought process to the following discussion to evaluate the *inductance of a single-phase two-wire transmission line*.

Figure 4.4 shows the two wires of the single-phase transmission line. Conductor *1* with radius r_1 carries current I out of the paper, resulting in a CCW magnetic flux. Conductor 2 with radius r_2 is the return circuit for the first conductor such that it carries a current into the paper. The back of the arrow ⊗ indicates the current entering the paper. For conductor 1, ○ indicates the direction of current coming out of the paper. In Figure 4.4, the dashed flux lines created by conductor 1 although are shown elliptically due to the paucity of space; these flux lines are actually concentric. The two conductors are separated by distance $D \gg r_1, r_2$.

One can now observe that

1. One conductor is the return circuit for the other. Thus, if conductor 1 carries a current of I, the second conductor 2 carries a current of $-I$.
2. A line of flux set up by the current in conductor 1 at a distance equal to or greater than $D + r_2$ from center of conductor 1 does not link the circuit and so cannot induce a voltage (using condition as in observation 1 above).
3. The fraction of the total current linked by a line of flux external to conductor 1 at a distance equal to or less than $D - r_2$ to $D + r_2$ the fraction changes from one to zero.
4. $D \gg r_1, r_2$.

Assuming that the external flux set up by the current in conductor 1 extending to the center of conductor 2 links all the current I and beyond the center of conductor 2 links none, as shown in Figure 4.4, this yields

$$L_{1,\text{ext}} = 2 \cdot 10^{-7} \ln \frac{D}{r_1} \quad \frac{\text{H}}{\text{m}} \tag{4.39}$$

and

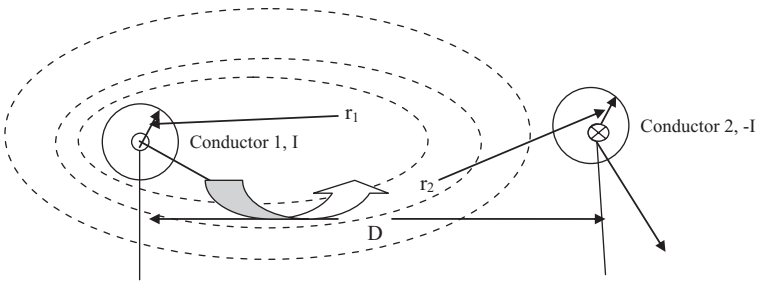

FIGURE 4.4
Single-phase two-wire line.

$$L_{1,\text{int}} = \frac{1}{2} \cdot 10^{-7} \quad \frac{\text{H}}{\text{m}} \tag{4.40}$$

which yields the total inductance of this circuit of a single-phase two-wire transmission line as follows.

Total inductance due to current in conductor 1:

$$L_1 = \left(\frac{1}{2} + 2 \ln \frac{D}{r_1} \right) \cdot 10^{-7} \quad \frac{\text{H}}{\text{m}} \tag{4.41}$$

$$L_1 = 2 \cdot 10^{-7} \left(\frac{1}{4} + \ln \frac{D}{r_1} \right) \quad \frac{\text{H}}{\text{m}} \tag{4.42}$$

$$\text{using } \ln e^{-1/4} = 1/4$$

yields

$$L_1 = 2 \cdot 10^{-7} \left(\ln \text{e}^{-1/4} + \ln \frac{D}{r_1} \right) \quad \frac{\text{H}}{\text{m}} \tag{4.43}$$

$$L_1 = 2 \cdot 10^{-7} \left(\ln \frac{D}{r_1 \text{e}^{-1/4}} \right) \quad \frac{\text{H}}{\text{m}} \tag{4.44}$$

$$L_1 = 2 \cdot 10^{-7} \left(\ln \frac{D}{r_1'} \right) \quad \frac{H}{m}, \text{ where } r_1' = r_1 \text{e}^{-1/4} = 0.778 r_1 \tag{4.45}$$

where r_1' is the radius of conductor 1 with no internal flux. The term 0.778 is the modification that yields the new equivalent radius with only external flux.

We can similarly find the conductance due to the current in conductor 2 of (–*I*) as follows:

$$L_2 = 2 \cdot 10^{-7} \left(\ln \frac{D}{r_2'} \right) \quad \frac{\text{H}}{\text{m}} \tag{4.46}$$

Thus, inductance *L* for the entire circuit of the single-phase two-wire transmission is given by the sum of Equations 4.45 and 4.46, which yields

$$L = L_1 + L_2 = 2 \cdot 10^{-7} \left(\ln \left(\frac{D^2}{r_1' r_2'} \right) \right)$$

$$L = 4 \cdot 10^{-7} \ln \left(\frac{D}{\sqrt{r_1' r_2'}} \right) \quad \frac{\text{H}}{\text{m}} \tag{4.47}$$

If $r_1' = r_2' = r'$ (i.e., both the conductors belong to the same single-phase two-wire system), then

$$L = 4 \cdot 10^{-7} \ln \left(\frac{D}{r'} \right) \quad \frac{\text{H}}{\text{m}} \tag{4.48}$$

resulting in an inductance per conductor of

$$2\times10^{-7}\ln\left(\frac{D}{r'}\right)\quad\frac{\text{H}}{\text{m}} \tag{4.49}$$

We now extend this to an evaluation of multiple conductors in a given circuit, for which we need to find the flux linkages of one conductor in a group, where the sum of the conductor currents is zero (Figure 4.5).

$$\sum_{j=1}^{n} I_j = 0,\ \text{for}\ n\ \text{conductors in the group}$$

We can now evaluate step by step the flux linkages of the n conductors at point P as follows:

1. Flux linkages of conductor 1, with radius r_1, due to current I_1, including the internal flux linkages in conductor 1 but excluding all the flux beyond point P at a distance D_{1P}, is given by

$$\Psi_{1P_1} = \left(\frac{I_1}{2} + 2I_1\ln\frac{D_{1P}}{r_1}\right)\cdot10^{-7}\quad \text{Wb}-\frac{\text{turn}}{\text{m}} \tag{4.50}$$

$$= 2\cdot10^{-7} I_1\ln\left(\frac{D_{1P}}{r_1'}\right)\quad \text{Wb}-\frac{\text{turn}}{\text{m}} \tag{4.51}$$

2. Flux linkages with conductor 1, with radius r_1, due to current I_2, including the internal flux linkages in conductor 1 but excluding all the flux beyond the point P (i.e., between distance D_{2P} and D_{1P}) is given by

$$\Psi_{1P_2} = \left(\frac{I_2}{2} + 2I_2\ln\frac{D_{2P}}{D_{12}}\right)\cdot10^{-7}\quad \text{Wb}-\frac{\text{turn}}{\text{m}} \tag{4.52}$$

$$= 2\cdot10^{-7} I_2\ln\left(\frac{D_{2P}}{D_{12}}\right)\quad \text{Wb}-\frac{\text{turn}}{\text{m}} \tag{4.53}$$

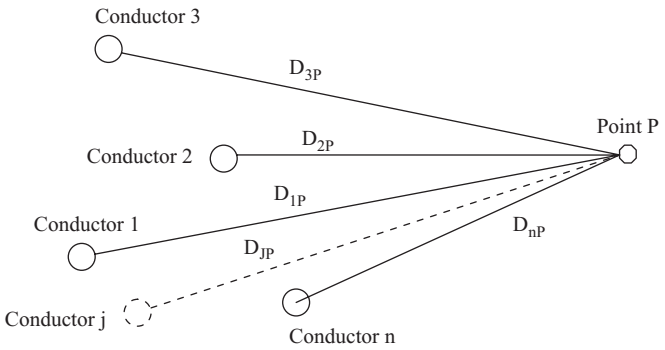

FIGURE 4.5
Circuit with multiple conductors located from point *P*.

3. Therefore, flux linkages Ψ_{1P} with conductor 1, with radius r_1, due to current I_j in all conductors in the group, including the internal flux linkages in conductor j but excluding all the flux beyond point P (i.e. between distance D_{jP} and D_{1P}), is given by

$$\Psi_{1P} = 2\cdot 10^{-7}\left\{I_1 \ln\left(\frac{D_{1P}}{r_1'}\right) + I_2 \ln\left(\frac{D_{2P}}{D_{12}}\right) + I_3 \ln\left(\frac{D_{3P}}{D_{13}}\right) + . + .I_n \ln\left(\frac{D_{nP}}{D_{1n}}\right)\right\} \text{ Wb} - \frac{\text{turn}}{\text{m}} \tag{4.53}$$

4. Using

$$\sum_{j=1}^{n} I_j = 0$$

we have

$$I_n = -\left(I_1 + I_2 + I_3 + \ldots I_{n-1}\right) \tag{4.54}$$

which yields

$$\Psi_{1P} = 2\cdot 10^{-7}\left\{\begin{array}{l} I_1 \ln\left(\frac{1}{r_1'}\right) + I_2 \ln\left(\frac{1}{D_{12}}\right) + I_3 \ln\left(\frac{1}{D_{13}}\right) + . + .I_n \ln\left(\frac{1}{D_{1n}}\right) + \\ \left\{\ln\left(\frac{D_{1P}}{D_{nP}}\right) + I_2 \ln\left(\frac{D_{2P}}{D_{nP}}\right) + I_3 \ln\left(\frac{D_{3P}}{D_{nP}}\right) + . + .I_{n-1} \ln\left(\frac{D_{(n-1)P}}{D_{nP}}\right)\right\} \end{array}\right\} \tag{4.55}$$

If we place point P at a far-field location that will assure all flux linkages due to conductor 1 with all other $(n-1)$ conductors, then

$$\frac{D_{1P}}{D_{nP}} = 1; \frac{D_{2P}}{D_{nP}} = 1; \ldots; \frac{D_{(n-1)P}}{D_{nP}} = 1 \tag{4.56}$$

And the factor within braces in Equation 4.55 reduces to zero as $\ln(1) = 0$, yielding

$$\Psi_1 = 2\cdot 10^{-7}\left\{I_1 \ln\left(\frac{1}{r_1'}\right) + I_2 \ln\left(\frac{1}{D_{12}}\right) + I_3 \ln\left(\frac{1}{D_{13}}\right) + . + . + I_n \ln\left(\frac{1}{D_{1n}}\right)\right\} \tag{4.57}$$

Then the corresponding inductance can be appropriately assessed. Thus, the result in Equation 4.57 can be used to obtain the following inductance for a composite conductor, especially of transmission lines with stranded conductors.

Conductor Y is the return path for conductor X in the transmission line circuit, as can be seen by the currents in each of their sub-parts or strands.

Applying Equation 4.57 to the circuit in Figure 4.6 yields the flux linkages of the strand a, as follows:

$$\Psi_a = 2\cdot 10^{-7}\frac{I}{n}\left\{\ln\left(\frac{1}{r_a'}\right) + \ln\left(\frac{1}{D_{ab}}\right) + \ln\left(\frac{1}{D_{ac}}\right) + \cdot + \cdot + \ln\left(\frac{1}{D_{an}}\right)\right\}$$

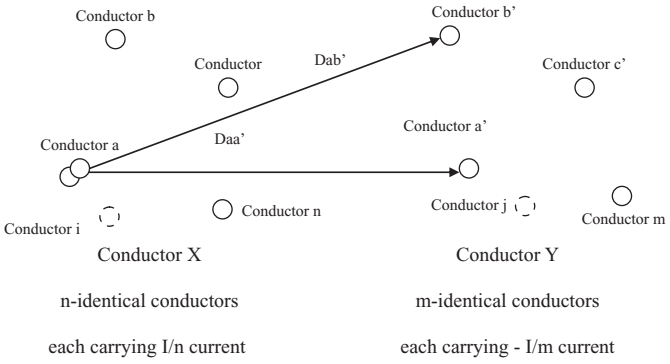

FIGURE 4.6
Transmission line with a composite conductor (stranded conductors).

$$-2\cdot 10^{-7}\,\frac{I}{m}\left\{\ln\left(\frac{1}{D_{aa'}}\right)+\ln\left(\frac{1}{D_{ab'}}\right)+\ln\left(\frac{1}{D_{ac'}}\right)+.+.+\ln\left(\frac{1}{D_{am}}\right)\right\} \tag{4.58}$$

Therefore,

$$\Psi_a = 2\cdot 10^{-7} I \ln\frac{\sqrt[m]{D_{aa'}\cdot D_{ab'}\cdot D_{ac'}\ldots.\cdot D_{am}}}{\sqrt[n]{r_a'\cdot D_{ab}\cdot D_{ac}\ldots.\cdot D_{an}}} \quad \text{Wb}-\frac{\text{turn}}{\text{m}} \tag{4.59}$$

which yields

$$L_a = \frac{\Psi_a}{I/n} = 2\cdot n\cdot 10^{-7}\cdot \ln\frac{\sqrt[m]{D_{aa'}\cdot D_{ab'}\cdot D_{ac'}\ldots.\cdot D_{am}}}{\sqrt[n]{r_a'\cdot D_{ab}\cdot D_{ac}\ldots.\cdot D_{an}}} \quad \frac{\text{H}}{\text{m}} \tag{4.60}$$

Similarly, for strand b of conductor X:

$$\Psi_b = 2\cdot 10^{-7} I \ln\frac{\sqrt[m]{D_{ba'}\cdot D_{bb'}\cdot D_{bc'}\ldots.\cdot D_{bm}}}{\sqrt[n]{D_{ba}\cdot r_b'\cdot D_{bc}\ldots.\cdot D_{bn}}} \quad \text{Wb}-\frac{\text{turn}}{\text{m}} \tag{4.61}$$

which yields

$$L_b = \frac{\Psi_b}{I/n} = 2\cdot 10^{-7}\cdot \ln\frac{\sqrt[m]{D_{ba'}\cdot D_{bb'}\cdot D_{bc'}\ldots.\cdot D_{bm}}}{\sqrt[n]{D_{ba}\cdot r_b'\cdot D_{bc}\ldots.\cdot D_{bn}}} \quad \frac{\text{H}}{\text{m}} \tag{4.62}$$

Therefore, the average inductance of the filaments (strands) of conductors X is given by

$$L_{\text{average of } X} = \frac{L_a + L_b + L_c + . + . + L_n}{n} \tag{4.63}$$

For n conductors in parallel:

$$L_X = \frac{L_{\text{average of X}}}{n} = \frac{L_a + L_b + L_c + . + . + L_n}{n\cdot n}$$

$$= 2\cdot 10^{-7}\cdot \ln\frac{\sqrt[mn]{\left(D_{aa'}\cdot D_{ab'}\cdot D_{ac'}\ldots.\cdot D_{am}\right)\left(D_{ba'}\cdot D_{bb'}\cdot D_{bc'}\ldots.\cdot D_{bm}\right)\cdot(\cdot)\cdot(\cdot)..\left(D_{na'}\cdot D_{nb'}\cdot D_{nc'}\ldots.\cdot D_{nm}\right)}}{\sqrt[n\cdot n]{\left(D_{aa}\cdot D_{ab}\cdot D_{ac}\ldots.\cdot D_{an}\right)\left(D_{ba}\cdot D_{bb}\cdot \mathbf{D}_{bc}\ldots.\cdot D_{bn}\right)\cdot(\cdot)\cdot(\cdot)..\left(D_{na}\cdot D_{nb}\cdot D_{nc}\ldots.\cdot D_{nn}\right)}} \quad \frac{\text{H}}{\text{m}} \tag{4.64}$$

We will define the parameters as follows:

D_m = numerator; (mn)th root of the $m \times n$ terms: mutual geometric mean distance (GMD) between two conductors

D_s = denominator; n^2 root of n^2 terms: self-GMD of conductor X.

Using these definitions in Equation 4.64 yields the inductance for conductor X:

$$L_X = 2 \cdot 10^{-7} \cdot \ln \frac{D_m}{D_s} \frac{\text{H}}{\text{m}} \tag{4.65}$$

which is almost equal to Equation 4.45:

$$L_1 = 2 \cdot 10^{-7} \left(\ln \frac{D}{r_1'} \right) \frac{\text{H}}{\text{m}}$$

Similarly, using these definitions in Equation 4.64 yields the inductance for conductor Y as follows:

$$L_Y = 2 \cdot 10^{-7} \cdot \ln \frac{D_m}{D_s} \frac{\text{H}}{\text{m}} \tag{4.66}$$

and the total inductance of the entire circuit consisting of stranded conductors X and Y, as follows:

$$L = L_X + L_Y$$

Example 4.1

Find the inductance of individual lines as the total inductance of the configuration of conductors A and B, as shown in Figure 4.7, with line B as the return circuit of line A.

SOLUTION 4.1

Note: Change all dimensions to the meter base. Using Equations 4.64 through 4.66 we have $m = n = 3$, and

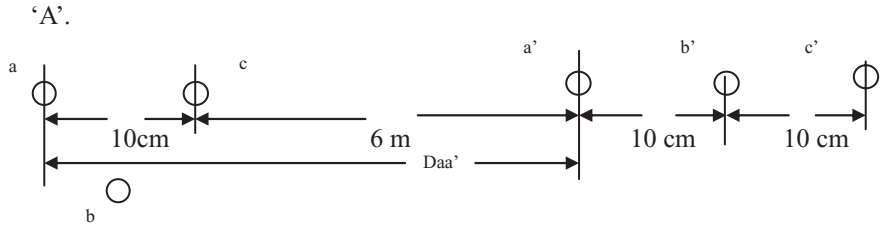

Line A	Line B
Conductors at the corner of an equilateral triangle	Conductors in a straight line;
of a side of 10 cm;	conductors are 10 cm apart.
Radius of conductor 2 cm	Radius of conductor 2 cm

FIGURE 4.7
Line with stranded conductors: line A and line B as a part of the composite single-phase two-wire transmission line.

$$D_m = \sqrt[9]{\left(D_{aa'} \cdot D_{ab'} \cdot D_{ac'}\right)\left(D_{ba'} \cdot D_{bb'} \cdot D_{bc'}\right)\left(D_{ca'} \cdot D_{cb'} \cdot D_{cc'}\right)}$$

with dimensions as given in Figure 4.7, where, for example, $D_{aa'}$ is the distance between conductor strands a and a', respectively.

$$D_{aa'} = D_{cb'} = 6.1\,\text{m};\ D_{ab'} = D_{cc'} = 6.2\,\text{m};$$

$$D_{ac'} = 6.3\,\text{m};\ D_{ca'} = 6\,\text{m};\ D_{ba'} = 6.05\,\text{m};\ D_{bb'} = 6.15\,\text{m};\ D_{bc'} = 6.25\,\text{m}$$

gives

$$D_m = 6.15\,\text{m}$$

$$D_s = \sqrt[9]{\left(D_{aa} \cdot D_{ab} \cdot D_{ac}\right)\left(D_{ab} \cdot D_{ab} \cdot D_{bc}\right)\left(D_{ca} \cdot D_{cb} \cdot D_{cc}\right)}$$

with dimensions as given in Figure 4.7.

$$D_{aa} = D_{bb} = D_{cc} = 0.02\,\text{m} \cdot 0.778 = r';\ D_{ab} = D_{ac} = D_{ba} = D_{bc} = D_{ca} = D_{cb} = 0.1\,\text{m}$$

gives

$$D_{ms} = 0.0538\,\text{m}$$

gives

$$L_A = 9.48 \cdot 10^{-7}\ \frac{\text{H}}{\text{m}}$$

for line B D_m is the same:

$$D_s = \sqrt[9]{\left(D_{a'a'} \cdot D_{a'b'} \cdot D_{a'c'}\right)\left(D_{a'b'} \cdot D_{a'b'} \cdot D_{b'c'}\right)\left(D_{c'a'} \cdot D_{c'b'} \cdot D_{c'c'}\right)}$$

with dimensions as given in Figure 4.7.

$$D_{a'a'} = D_{b'b'} = D_{c'c'} = 0.02\,\text{m} \cdot 0.778 = r'$$

$$D_{a'b'} = D_{b'c'} = D_{b'a'} = D_{b'c'} = 0.1\,\text{m};\ D_{a'c'} = D_{c'a'} = 0.2\,\text{m}$$

$$D_s = \sqrt[9]{(0.01556)^3 (0.1)^4 (0.2)^2} = 0.0628\,\text{m}$$

gives

$$L_B = 9.17 \cdot 10^{-7}\ \frac{\text{H}}{\text{m}}$$

Thus,

$$\text{Total } L = L_A + L_B = 18.65 \cdot 10^{-7}\ \frac{\text{H}}{\text{m}}$$

From the inductance of the reactance of the entire transmission line, the circuit comprising lines A and B can be found at a specific frequency f of 60 Hz as follows:

$$X_l = j\omega L = j2\pi fL = j \cdot 2 \cdot \pi \cdot 60 \cdot 18.65 \cdot 10^{-7} = j703.18 \text{ micro}\,\Omega/\text{m}$$

The values of the inductances at different frequencies can be also found from the library provided by ETAP® for different kinds of conductor sizes and configuration-like stranded conductors.

We now proceed to find the inductance of three-phase lines with symmetrical (equilateral) spacing without neutral, as shown in Figure 4.8.

Three conductors a, b and c of a three-phase line with a GMD of D_s, spaced equally at GMD = D, carry currents (without the fourth wire as neutral) as follows:

$$I_a + I_b + I_c = 0 \tag{4.67}$$

Using Equations 4.58 through 4.67, we have

$$\Psi_a = 2 \cdot 10^{-7} \left\{ I_a \ln\left(\frac{1}{D_s}\right) + I_b \ln\left(\frac{1}{D}\right) + I_c \ln\left(\frac{1}{D}\right) \right\} \quad \text{Wb} - \frac{\text{turn}}{\text{m}} \tag{4.68}$$

Using Equation 4.67 in Equation 4.68 yields

$$\Psi_a = 2 \cdot 10^{-7} \left\{ I_a \ln\left(\frac{1}{D_s}\right) - I_a \ln\left(\frac{1}{D}\right) \right\} \quad \text{Wb} - \frac{\text{turn}}{\text{m}} \tag{4.69}$$

which yields the inductance per phase of a three-phase line as

$$L_a = L_b = L_c = 2 \cdot 10^{-7} \left\{ \ln\left(\frac{D}{D_s}\right) \right\} \quad \frac{\text{H}}{\text{m}} \tag{4.70}$$

We now proceed to find the inductance of three-phase lines with unsymmetrical spacing without neutral, as shown in Figure 4.9.

1. Here, because of the unsymmetrical spacing between lines, as shown in Figure 4.9 with distances D_{12}, D_{23} and D_{31}, between conductors a and c, conductors c and b and conductors b and c, respectively, the flux linkages and inductance of each phase are not the same.
2. This unsymmetrical spacing leads to an unbalanced circuit from start to finish as the 'crow flies' in distance or the length of each conductor.

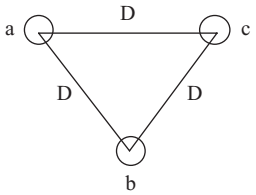

FIGURE 4.8
Three-phase line with equilateral spacing of distance D, without neutral.

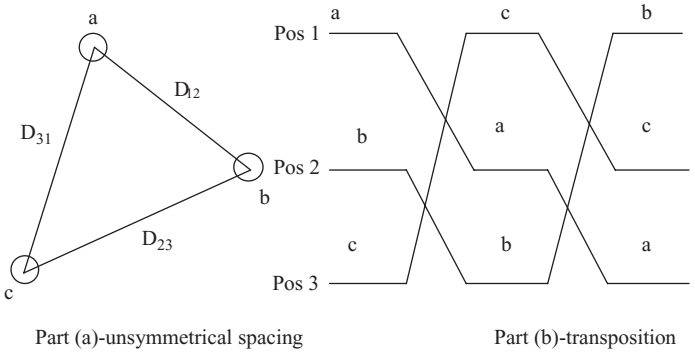

FIGURE 4.9
Three-phase transmission line with unsymmetrical spacing and transposition of conductor positions.

3. This imbalance is restored by exchanging or transposing the physical positions of the conductors at regular intervals over equal distances from start to finish, as shown in Figure 4.9b.
4. Thus, at different distances and positions, the average inductance of one conductor of a transposed line needs to be calculated as follows:

   Step 1:

   Conductor *a*: position 1; conductor *b*: position 2; conductor *c*: position 3

$$\Psi_{a1} = 2\cdot 10^{-7}\left\{I_a \ln\left(\frac{1}{D_s}\right) + I_b \ln\left(\frac{1}{D_{12}}\right) + \mathrm{I_c} \ln\left(\frac{1}{D_{31}}\right)\right\} \quad \mathrm{Wb} - \frac{\mathrm{turn}}{\mathrm{m}} \tag{4.71}$$

   Step 2:

   Conductor *a*: position 2; conductor *b*: position 3; conductor *c*: position 1

$$\Psi_{a2} = 2\cdot 10^{-7}\left\{I_a \ln\left(\frac{1}{D_s}\right) + I_b \ln\left(\frac{1}{D_{23}}\right) + \mathrm{I_c} \ln\left(\frac{1}{D_{12}}\right)\right\} \quad \mathrm{Wb} - \frac{\mathrm{turn}}{\mathrm{m}} \tag{4.72}$$

   Step 3:

   Conductor *a*: position 3; conductor *b*: position 1; conductor *c*: position 2

$$\Psi_{a3} = 2\cdot 10^{-7}\left\{I_a \ln\left(\frac{1}{D_s}\right) + I_b \ln\left(\frac{1}{D_{31}}\right) + \mathrm{I_c} \ln\left(\frac{1}{D_{23}}\right)\right\} \quad \mathrm{Wb} - \frac{\mathrm{turn}}{\mathrm{m}} \tag{4.73}$$

   This results in an average value of the total flux linkage for line *a* as follows:

$$\Psi_a = \frac{\Psi_{a1} + \Psi_{a2} + \Psi_{a3}}{3}$$

$$= 2\cdot 10^{-7}\left\{3I_a \ln\left(\frac{1}{D_s}\right) + I_b \ln\left(\frac{1}{D_{12}D_{23}D_{31}}\right) + \mathrm{I_c} \ln\left(\frac{1}{D_{31}D_{12}D_{23}}\right)\right\} \quad \mathrm{Wb} - \frac{\mathrm{turn}}{\mathrm{m}} \tag{4.74}$$

In Equation 4.74, notice the cyclic nature of the subscripts in the second and third terms in the denominators for the respective distances due to transposition $(1 \to 2 \to 3)$.

Because, as given in Equation 4.67,

$$I_a + I_b + I_c = 0$$

$$I_a = -I_b - I_c$$

which yields

$$\Psi_a = \frac{\Psi_{a1} + \Psi_{a2} + \Psi_{a3}}{3}$$

$$= 2 \cdot 10^{-7} \left\{ 3I_a \ln\left(\frac{1}{D_s}\right) - I_a \ln\left(\frac{1}{D_{12}D_{23}D_{31}}\right) \right\} \quad \text{Wb} - \frac{\text{turn}}{\text{m}}$$

$$\Psi_a = 2 \cdot 10^{-7} I_a \ln \frac{\sqrt[3]{D_{12}D_{23}D_{31}}}{D_s} \quad \text{Wb} - \frac{\text{turn}}{\text{m}} \tag{4.75}$$

Thus, the inductance of line a is given by dividing Equation 4.75 by I_a:

$$L_a = 2 \cdot 10^{-7} \ln \frac{\sqrt[3]{D_{12}D_{23}D_{31}}}{D_s} = 2 \cdot 10^{-7} \ln \frac{D_{eq}}{D_s} \frac{\text{H}}{\text{m}} \tag{4.76}$$

where

$$D_{eq} = \sqrt[3]{D_{12}D_{23}D_{31}} \tag{4.77}$$

and D_s is the geometric mean radius (GMR) of conductor a. If all the conductors are identical, their GMR is D_s.

Some of the EHV transmission lines are bundled besides being stranded.

1. 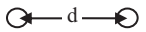

$$D_s^b = \sqrt{D_s \cdot d} \tag{4.78}$$

2. 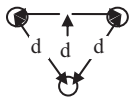

$$D_s^b = \sqrt[3]{D_s \cdot d^2} \tag{4.79}$$

3. 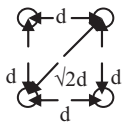

$$D_s^b = 1.09 \cdot \sqrt[4]{D_s \cdot d^3} \tag{4.80}$$

Similarly, the inductive reactance of the single-phase equivalent circuit for a parallel circuit three-phase transmission line can be found and is generally equal to one-half of that of each of the individual circuits.

So far we have not considered the effect of the fourth wire, which is generally the neutral line. We will now see the effect of the neutral conductor.

1. Neutral provides a path for the current flow when the system operates in unbalanced conditions.
2. Neutral also provides the transmission system with a shield to protect against lightning. The neutral wire is always connected to support towers and is thereby grounded.
3. In balanced conditions the neutral wires does not provide any role whatsoever.
4. In extremely unbalanced conditions when a line-to-line ground fault occurs, the neutral assumes a significant role.

A three-phase line in equilateral mode with an overhead line is shown in Figure 4.10.

The flux linkage of phase A when the current is simultaneously flowing in each of the other system conductors, including the neutral wire, with respect to point P in the field can be found as follows:

$$\Psi_a = 2\cdot 10^{-7}\left\{I_a \ln\left(\frac{D_P}{r_{a'}}\right) + I_b \ln\left(\frac{D_P}{D_{ab}}\right) + I_c \ln\left(\frac{D_P}{D_{ac}}\right) + I_n \ln\left(\frac{D_P}{D_{an}}\right)\right\} \tag{4.81}$$

$$= 2\cdot 10^{-7}\left\{\left(I_a + I_b + I_c + I_n\right)\ln D_P + I_a \ln\left(\frac{1}{r_{a'}}\right) + I_b \ln\left(\frac{1}{D_{ab}}\right) + I_c \ln\left(\frac{1}{D_{ac}}\right) + I_n \ln\left(\frac{1}{D_{an}}\right)\right\}$$

As $I_a + I_b + I_c + I_n = 0$ and $r_{a'} = r' = D_{aa}; D = D_{ab} = D_{ac}$.

$$\Psi_a = 2\cdot 10^{-7}\left\{I_a \ln\left(\frac{1}{r'}\right) + I_b \ln\left(\frac{1}{D}\right) + I_c \ln\left(\frac{1}{D}\right) + I_n \ln\left(\frac{1}{D_{an}}\right)\right\} \tag{4.82}$$

Eliminating or substituting $I_a + I_b + I_c = -I_n$ in Equation 4.82 yields the flux linkage for unbalanced conditions as follows:

$$\Psi_a = 2\cdot 10^{-7}\left\{I_a \ln\left(\frac{D_{an}}{r'}\right) + I_b \ln\left(\frac{D_{an}}{D}\right) + I_c \ln\left(\frac{D_{an}}{D}\right)\right\} \tag{4.83}$$

In a similar manner, the flux linkage of the neutral conductor are found as follows:

$$\Psi_n = 2\cdot 10^{-7}\left\{I_a \ln\left(\frac{D_P}{D_{na}}\right) + I_b \ln\left(\frac{D_P}{D_{nb}}\right) + I_c \ln\left(\frac{D_P}{D_{nc}}\right) + I_n \ln\left(\frac{D_P}{D_{nn}}\right)\right\}$$

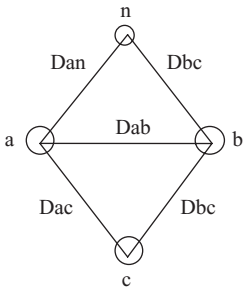

FIGURE 4.10
Three-phase line with neutral overhead.

which, on rearranging and using boundary condition $I_a + I_b + I_c = -I_n$, plus the representation of the modified radius of the neutral conductor $D_{nn} = r_n'$, yields

$$\Psi_n = 2\cdot 10^{-7}\left\{I_a \ln\left(\frac{1}{D_{na}}\right) + I_b \ln\left(\frac{1}{D_{nb}}\right) + I_c \ln\left(\frac{1}{D_{nc}}\right) + I_n \ln\left(\frac{1}{r_n'}\right)\right\} \tag{4.84}$$

PROBLEM 4.2

A single-phase transmission line with two conductors *a* and *b*, one being the return circuit for the other, is shown in Figure 4.11. Conductor *a* carries 150 A and conductor *b* carries –150 A as the return circuit. Below these is a two-wire communications circuit with conductors *c* and *d*; as always, the communications system takes advantage of the right of way (ROW) of the power system.

Find the voltage induced in the communications circuit by the two-wire power transmission line.

SOLUTION

Using Equations 4.51 through 4.54 we have

$$D_{ac} = \sqrt{1.8^2 + (1.25 - 0.5)^2} = 1.95\,\text{m};\ \Rightarrow D_1 \text{ for point } P_1 \tag{4.85}$$

$$D_{ad} = \sqrt{1.8^2 + (1.25 + 0.5)^2} = 2.51\,\text{m};\ \Rightarrow D_2 \text{ for point } P_2 \tag{4.86}$$

Therefore, the contribution flux linkage Ψ_{cd} = due to current I_a = 150 A.

$$\Psi cd\big|_{I_a} = 2\cdot 10^{-7}(150)\left(\ln\left(\frac{D_{ad}}{D_{ac}}\right)\right) = 2\cdot 10^{-7}(150)\left\{\ln\left(\frac{2.51}{1.95}\right)\right\} \tag{4.87}$$

Contribution flux linkage Ψ_{cd} = due to current $I_b = -I_a = -150$ A.

$$\Psi cd\big|_{I_b} = 2\cdot 10^{-7}(-150)\left(\ln\left(\frac{D_{ac}}{D_{ad}}\right)\right) = 2\cdot 10^{-7}(150)\left(\ln\left(\frac{D_{ad}}{D_{ac}}\right)\right) = 2\cdot 10^{-7}(150)\left\{\ln\left(\frac{2.51}{1.95}\right)\right\} \tag{4.88}$$

$$\text{Total } \Psi cd = 4\cdot 10^{-7}(150)\left\{\ln\left(\frac{2.51}{1.95}\right)\right\}$$

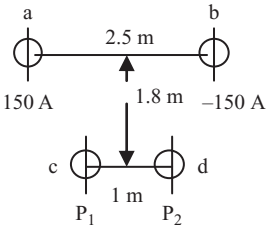

FIGURE 4.11
Power and communications circuits in proximity to each other.

Therefore,

$$M_{\text{cd}} = 4 \cdot 10^{-7} \left\{ \ln\left(\frac{2.51}{1.95} \right) \right\} = 1.01 \cdot 10^{-7} \ \frac{\text{H}}{\text{m}} \tag{4.89}$$

Thus, the total voltage coupling with the communications circuit is

$$\left| V_{cd} \right| = \omega \cdot M_{\text{cd}} \cdot I_a = 377 \cdot 1.01 \cdot 10^{-7} \cdot 150 = 5.71 \cdot 10^{-3} \frac{\text{V}}{\text{m}} = 5.71 \frac{\text{V}}{\text{m}} \tag{4.90}$$

4.3 Capacitance *C*

The third important passive element in power systems is capacitance *C*, measured in farads (F). A simple parallel plate capacitance is given by Equation 4.91:

$$C = \frac{A\varepsilon}{d} \tag{4.91}$$

where:

- A is the area of the cross-section of the two parallel plates
- d is the separation between the two plates
- ε is the permittivity of the insulation medium between the plates

The permittivity ε is given by Equation 4.92:

$$\varepsilon = \varepsilon_r \varepsilon_0 \tag{4.92}$$

where:

- ε_r is the relative permittivity of the medium between the parallel plates
- ε_0 is the absolute permittivity of space or air

The absolute permittivity ε_0 of space is 8.8542×10^{-12} F/m; the relativity for different media is given in Table 4.5.

TABLE 4.5

Dielectric Constants and Dielectric Strengths of Some Materials

Material	Dielectric Constant	Dielectric Strength (V/m)
Air	1.0	3×10^6
Mineral oil	2.3	15×10^6
Paper	2.0–4.0	15×10^6
Polystyrene	2.6	20×10^6
Rubber	2.3–4.0	25×10^6
Glass	4.0–10.0	30×10^6
Mica	6.0	200×10^6

As with inductance, the shape of the capacitance can be different—for example, a cylinder with single or multiple strands and a spherical capacitor. The evaluation of capacitances for such varied geometrical shapes is handled in the sequence.

The capacitance of transmission lines is a part of the shunt admittance (Y), consisting of conductance G and the corresponding susceptance of the capacitive part C. Generally, conductance G is negligible. For distances less than 50 miles (80 km), capacitance is negligible. In transmission lines, the flow of charge causes the current to flow, and the current thus caused by the alternate charging and discharging of the line due to the alternating voltage is called the *charging current* of the transmission line. The charging current flows in a line even when it is open-circuited. For all calculations of the capacitance of a transmission line, an evaluation of the electric field intensity is necessary. Thus, it is customary to find the electric field created by a long straight conductor at near field and far field surrounding it, mostly radially outward from the center of the conductor.

4.3.1 Electric Field of a Long Straight Conductor

The total electric flux due to the current-carrying conductor is numerically equal to the number of coulombs of charge on the conductor and is given by

$$D = \frac{\text{electric flux}}{\text{area}} = \frac{\text{coulombs of charge } q}{\text{m}^2} \quad \text{C/m}^2 \tag{4.93}$$

As indicated earlier, this flux is radially disposed with respect to the center of the conductor along the length of the conductor, resulting in equipotential points with equal flux density, as shown in Figure 4.12.

Thus, the electric flux density at radial distance x from the center of the conductor is given by

$$D = \frac{q}{2\pi x} \quad \text{C/m}^2 \tag{4.94}$$

This flux leaves per meter of the length of the conductor and is divided by the area of the surface in an axial length of 1 m of the conductor at a radial distance x from the conductor.

Further, *electric field intensity* is a measure of force on a charge q and is the negative of the potential gradient; that is,

$$E \triangleq -\nabla V = \frac{D}{\epsilon, \text{ permitivity of medium}} = \frac{q}{2\pi x \epsilon} \quad \frac{\text{V}}{\text{m}} \tag{4.95}$$

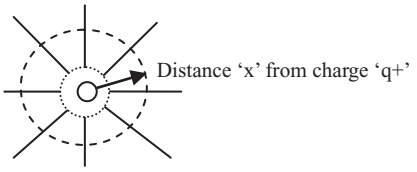

FIGURE 4.12
Radial flux distribution of a conductor with charge q^+.

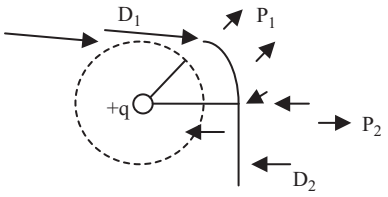

FIGURE 4.13
Wire carrying a charge with equipotential points P_1 and P_2 at distance D_1 and D_2, respectively.

We will now proceed to find the potential difference between two points due to charge q.

By definition, voltage in volts is the potential difference between two points in an electrical circuit and is also the work done in joules per coulomb to move a coulomb of charge between those two points in the given electrical circuit, as shown in Figure 4.13.

This circuit is a wire that carries a positive charge of q in coulombs per meter. Subsequently, if a separate positive charge is placed in the field of this wire, it will experience a repelling force. In addition, point P_1 is at a higher potential than point P_2. This potential difference, as defined earlier, is the work done on the positive charge q to move it from P_2 and P_1, as shown in Figure 4.13. However, this work done is independently of the specific path shown—that is, from P_1 to P_2 along the outer path or from P_2 to P_1 along the inner path. In other words, the voltage drop from P_1 to P_2 is the amount of energy expended in moving the charge between these two points, independent of the path taken to move this charge. Thus, from Equation 4.95, the instantaneous voltage drop between P_1 and P_2 is given by

$$v_{12} = \int_{D_1}^{D_2} E dx = \int_{D_1}^{D_2} \frac{q}{2\pi\epsilon x} dx = \frac{q}{2\pi\epsilon} \ln \frac{D_2}{D_1} \quad \text{volts} \tag{4.96}$$

Subsequently, by using the basic equation

$$q = CV \tag{4.97}$$

one can find the capacitance as follows:

$$C = \frac{q}{v} \frac{\text{F}}{\text{m}} \tag{4.98}$$

We will now proceed to find the *capacitance of a two-wire line*.

Again, we will use Equation 4.98, where q is the charge on the line in coulombs per meter; v is the potential difference between the conductors in volts (Figure 4.14).

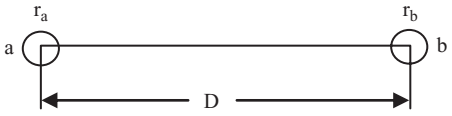

FIGURE 4.14
Capacitance of a two-wire line separated by a distance D with charges q_a and q_b at points a and b, respectively.

Voltage v_{ab} is now found by finding the potential difference between the two conductors of the line. We first find v_{ab} due to charge q_a and v_{ab} due to charge q_b.

Following the earlier derivation for the work done in moving a single charge from point P_1 to point P_2, as in Figure 4.13, we have the following for Figure 4.14:

For charge q_a: $D_2 \to D$; $D_1 \to r_a$
For charge q_b: $D_2 \to r_b$; $D_1 \to D$

Therefore, assuming all notations are as in phasor notations with q_a and q_b as complex numbers, we have the total voltage difference between points a and b as follows:

$$V_{ab} = \frac{q_a}{2\pi\varepsilon}\ln\frac{D}{r_a} + \frac{q_b}{2\pi\varepsilon}\ln\frac{r_b}{D} \quad \text{volts}$$

As in a two-wire line, one conductor is the return path of the other.

$$q_a = -q_b$$

$$V_{ab} = \frac{q_a}{2\pi\varepsilon}\left(\ln\frac{D}{r_a} - \ln\frac{r_b}{D}\right) \quad \text{volts}$$

$$V_{ab} = \frac{q_a}{2\pi\varepsilon}\ln\left(\frac{D^2}{r_a r_b}\right) \quad \text{volts} \tag{4.99}$$

Then, using Equation 4.98, the capacitance between the conductors of the two-wire line is

$$C_{ab} = \frac{q_a}{V_{ab}} = \frac{2\pi\varepsilon}{\ln\left(\frac{D^2}{r_a r_b}\right)} \quad \frac{\text{F}}{\text{m}} \tag{4.100}$$

If $r_a = r_b = r$, then (Figure 4.15)

$$C_{ab} = \frac{\pi\varepsilon}{\ln\left(\frac{D}{r}\right)} \quad \frac{\text{F}}{\text{m}} \tag{4.101}$$

We can then find the line to neutral capacitance as follows (Figure 4.16):

$$C_n = C_{an} = C_{bn} = 2C_{ab} = \frac{2\pi\varepsilon}{\ln\left(\frac{D}{r}\right)} \quad \frac{\text{F}}{\text{m}} \tag{4.102}$$

FIGURE 4.15
Capacitance of a two-wire line: line-to-line capacitance.

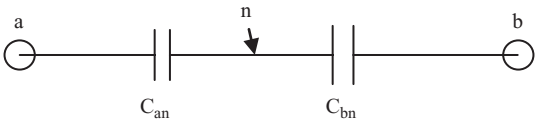

FIGURE 4.16
Two-wire line capacitance with a neutral point.

R is the actual radius of the conductor and not the GMR, and $\varepsilon = \varepsilon_0 \varepsilon_r$ with $\varepsilon_r = 1$ for space and $\varepsilon_0 = 8.8542 \times 10^{-12}$ F/m. This yields the capacitive reactance of a two-wire line as follows:

$$X_C = \frac{1}{2\pi f C} = \frac{2.862}{f} \cdot 10^9 \cdot \ln\left(\frac{D}{r}\right) \ \Omega \cdot \text{miles to neutral} \tag{4.103}$$

$$= \frac{1.779}{f} \cdot 10^6 \cdot \ln\left(\frac{D}{r}\right) \ \Omega \cdot \text{miles to neutral} \tag{4.104}$$

4.3.1.1 Capacitance of a Three-Phase Line with Equilateral Spacing

As shown in Figure 4.17, the three conductors of a three-phase delta-connected system are located at the corners of an equilateral triangle. The conductor radii are given as follows:

$$r = r_a = r_b = r_c \tag{4.105}$$

The sum of the charges on these three lines is equal to zero, as in Equation 4.106:

$$q_a + q_b + q_c = 0 \tag{4.106}$$

and the following boundary condition:

$$V_{ab} + V_{ac} = 3 \cdot V_{an} \tag{4.107}$$

We will now proceed to find the voltage between conductors *a* and *b*:

1. Due to the charges on conductors *a* and *b*
2. Due to only the charge on conductor *c*, assuming that the charge is concentrated at the center of conductor *c*

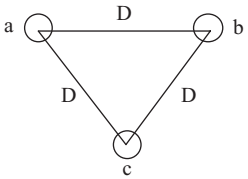

FIGURE 4.17
Three-phase line with equilateral spacing.

From the derivation of Equation 4.99, point 1 can be evaluated as follows:

$$V_{ab} = \frac{1}{2\pi\varepsilon}\left(q_a \ln\frac{D}{r_a} + q_b \ln\frac{r_b}{D}\right) \quad \text{volts} \tag{4.108}$$

Next, point 2 can be evaluated similarly, as follows:

$$V_{ab} = \frac{q_c}{2\pi\varepsilon}\left(\ln\frac{D}{D}\right) = 0 \quad \text{volts} \tag{4.109}$$

Point c is equidistant from both points a and b.
Therefore, the total potential difference between points a and b is given by

$$V_{ab} = \frac{1}{2\pi\varepsilon}\left(q_a \ln\frac{D}{r} + q_b \ln\frac{r}{D} + q_c\left(\ln\frac{D}{D}\right)\right) \quad \text{volts} \tag{4.110}$$

Similarly, the potential difference between points b and c is given by

$$V_{ac} = \frac{1}{2\pi\varepsilon}\left(q_a \ln\frac{D}{r} + q_c \ln\frac{r}{D} + q_b\left(\ln\frac{D}{D}\right)\right) \quad \text{volts} \tag{4.111}$$

and

$$V_{bc} = \frac{1}{2\pi\varepsilon}\left(q_a \ln\frac{D}{D} + q_b \ln\frac{D}{r} + q_c\left(\ln\frac{r}{D}\right)\right) \quad \text{volts} \tag{4.112}$$

Therefore,

$$V_{ab} + V_{ac} = \frac{1}{2\pi\varepsilon}\left(2q_a \ln\frac{D}{r} + (q_b + q_c)\ln\left(\frac{r}{D}\right)\right) \quad \text{volts} \tag{4.113}$$

$$V_{ab} + V_{ac} = \frac{3q_a}{2\pi\varepsilon}\ln\left(\frac{D}{r}\right) \quad \text{volts} \tag{4.114}$$

From Figure 4.18 we can see the phasor relationship that shows

$$V_{ab} + V_{ac} = 3V_{an}$$

which yields

$$V_{an} = \frac{q_a}{2\pi\varepsilon}\ln\left(\frac{D}{r}\right) \quad \text{volts} \tag{4.115}$$

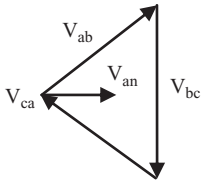

FIGURE 4.18
Phasor relationship.

$$C_{an} = C_n = \frac{q_a}{V_{an}} = 2\pi\varepsilon / \ln\left(\frac{D}{r}\right) \quad \frac{\text{F}}{\text{m}} \tag{4.116}$$

We now try to find the charging current we eluded to in the beginning, associated with the capacitance of a transmission line. For a single-phase circuit, this can be shown to be

$$I_{chg} = (\text{line to line voltage}) \cdot (\text{line-to line susceptance})$$

$$= V_{ab} \cdot (j\omega C_{ab}) = j\omega C_{ab} V_{ab} = j2\pi f C_{ab} V_{ab} \quad \text{A/mile} \tag{4.117}$$

Similarly, for a three-phase line:

$$I_{chg} = (\text{line to neutral voltage}) \cdot (\text{line-to neutral susceptance})$$

$$= V_{an} \cdot (j\omega C_n) = j\omega C_n V_{an} = j2\pi f C_n V_{an} \quad \text{A/mile} \tag{4.118}$$

4.3.2 Capacitance of a Three-Phase Line with Unsymmetrical Spacing

Generally, three-phase overhead lines of transmission systems are laid on towers of a certain shape, as in Figure 4.19. Three conductors are shown on the tower support: *a*, *b* and *c* (black, dark gray and light gray, respectively) with uneven separations (D_{12}, D_{23} and D_{31}, respectively).

Such asymmetrically spaced lines need transposition so that the overall length of each line is the same. As described earlier, we thus have three physical locations (1, 2 and 3, respectively) for each conductor at periodical distances along the total length of the transmission system. This is shown by the different shading.

If this transposition is not achieved or performed along the length of the conductors, it will lead to unequal capacitances of each phase to neutral. For a transposed line, the average capacitance to neutral of any phase for the completely transposed system is the same as the average capacitance to neutral of any other phase. Thus, as done earlier for the inductance calculations, we will find the average of three transpositions for the V_{ab} calculations as follows:

$$V_{ab} : a \text{ in position } 1;\ b \text{ in position } 2;\ c \text{ in position } 3$$

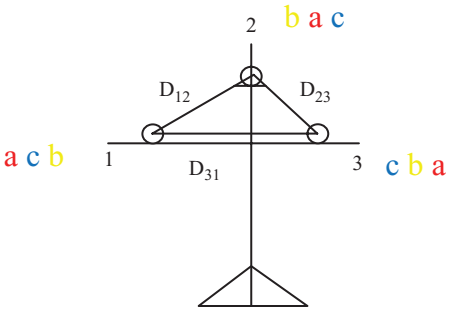

FIGURE 4.19
Transmission tower with a three-phase, three-wire line with unsymmetrical spacing.

$$V_{ab} = \frac{1}{2\pi\varepsilon}\left(q_a \ln\frac{D_{12}}{r} + q_b \ln\frac{r}{D_{12}} + q_c \ln\frac{D_{23}}{D_{31}}\right) \quad \text{volts} \tag{4.119}$$

Observe the pattern $1 \to 2 \to 3$ and the cyclic nature of the subscripts of the distances between conductors in Equation 4.119:

V_{ab} : a in position 2; b in position 3; c in position 1

$$V_{ab} = \frac{1}{2\pi\varepsilon}\left(q_a \ln\frac{D_{23}}{r} + q_b \ln\frac{r}{D_{23}} + q_c \ln\frac{D_{23}}{D_{31}}\right) \quad \text{volts} \tag{4.120}$$

V_{ab} : a in position 3; b in position 1; c in position 2

$$V_{ab} = \frac{1}{2\pi\varepsilon}\left(q_a \ln\frac{D_{31}}{r} + q_b \ln\frac{r}{D_{31}} + q_c \ln\frac{D_{12}}{D_{23}}\right) \quad \text{volts} \tag{4.121}$$

Therefore, the average V_{ab} is the sum total of Equations 4.119 through 4.121 divided by three.

$$V_{ab:\ \text{average}} = (|V_{ab}|_{a\,\text{in position}\,1} + |V_{ab}|_{a\,\text{in position}\,2} + |V_{ab}|_{a\,\text{in position}\,3})/3$$

$$V_{ab} = \frac{1}{6\pi\varepsilon}\left(q_a \ln\frac{D_{12}D_{23}D_{31}}{r^3} + q_b \ln\frac{r^3}{D_{12}D_{23}D_{31}} + q_c \ln\frac{D_{12}D_{23}D_{31}}{D_{12}D_{23}D_{31}}\right)$$

$$= \frac{1}{2\pi\varepsilon}\left(q_a \ln\frac{D_{eq}}{r} + q_b \ln\frac{r}{D_{eq}}\right), \text{ where } D_{eq} = \sqrt[3]{D_{12}D_{23}D_{31}} \quad \text{volts} \tag{4.122}$$

Similarly, the average voltage drop from conductor a to conductor c is as follows:

$$V_{ac} = \frac{1}{2\pi\varepsilon}\left(q_a \ln\frac{D_{eq}}{r} + q_c \ln\frac{r}{D_{eq}}\right), \text{ where } D_{eq} = \sqrt[3]{D_{12}D_{23}D_{31}} \quad \text{volts} \tag{4.123}$$

Further, using

$$3V_{an} = V_{ab} + V_{ac} \text{ and } q_a + q_b + q_c = 0 \tag{4.124}$$

we have

$$3V_{an} = \frac{1}{2\pi\varepsilon}\left(2q_a \ln\frac{D_{eq}}{r} + q_b \ln\frac{r}{D_{eq}} + q_c \ln\frac{r}{D_{eq}}\right)$$

$$= \frac{1}{2\pi\varepsilon}\left(3q_a \ln\frac{D_{eq}}{r}\right) \quad \text{volts} \tag{4.125}$$

$$V_{an} = \frac{1}{2\pi\varepsilon}\left(q_a \ln\frac{D_{eq}}{r}\right) \quad \text{volts} \tag{4.126}$$

Thus, the capacitance to neutral of a transposed three-phase line is

$$C_n = \frac{q_a}{V_{an}} = \frac{2\pi\varepsilon}{\ln\dfrac{D_{eq}}{r}} \quad \frac{\text{F}}{\text{m}} \tag{4.127}$$

Note: Equation 4.127 is similar to the earlier calculations for the inductance of a three-phase transposed line, as in Equation 4.76. We can now find the *capacitive reactance* using Equation 4.127:

$$X_c = \frac{1}{2\pi f C_n} = \frac{2.862}{f} \cdot 10^9 \ln\frac{D}{r} \quad \Omega \cdot \text{miles to neutral} \tag{4.128}$$

To obtain Ω·miles, divide Equation 4.128 by 1609; thus,

$$X_c = \frac{1}{2\pi f C_n} = \frac{1.779}{f} \cdot 10^6 \ln\frac{D}{r} \quad \Omega \cdot \text{miles to neutral} \tag{4.129}$$

$$= \frac{1.779}{f} \cdot 10^6 \ln\frac{1}{r} + \frac{1.779}{f} \cdot 10^6 \ln D \quad \Omega \cdot \text{miles to neutral} \tag{4.130}$$

The list of outside diameters for ACSR conductors; is available in a in ETAP. If D and r are in feet, then capacitive reactance $X_{a'}$ at 1 ft. spacing is the first term in Equation 4.130 and capacitive reactance with a spacing factor $X_{d'}$ is the second term. values available in ETAP Library

Many three-wire and four-wire transmission lines lying aboveground in transmission towers with suitable ROW need to consider the effect of earth on the capacitance, as evaluated earlier. This is shown in Figure 4.20 with distances between conductors at positions 1, 2 and 3 with charges q_a, q_b and q_c, respectively, shown with the shaded transposition a c b → b a c → c b a, also respectively, above the earth as an equipotential surface and with the reflection of charges and conductors at the opposite imaginary reflected side as an image below the earth line as an equipotential surface. The corresponding distances between the conductors are as follows:

- D_{12}, D_{23} and D_{31}, on the side above the earth and similar distances below the earth line
- H_1, H_2 and H_3 as distances between charges q_a and $-q_a$, q_b and $-q_b$, q_c and $-q_c$, respectively
- H_{12} between charges q_a and $-q_b$
- H_{21} between charges q_b and $-q_a$
- H_{13} between charges q_a and $-q_c$
- H_{31} between charges q_c and $-q_a$
- H_{23} between charges q_b and $-q_c$
- H_{32} between charges q_c and $-q_b$

The sum of charges is equal to zero; thus,

$$q_a + q_b + q_c = 0 \tag{4.131}$$

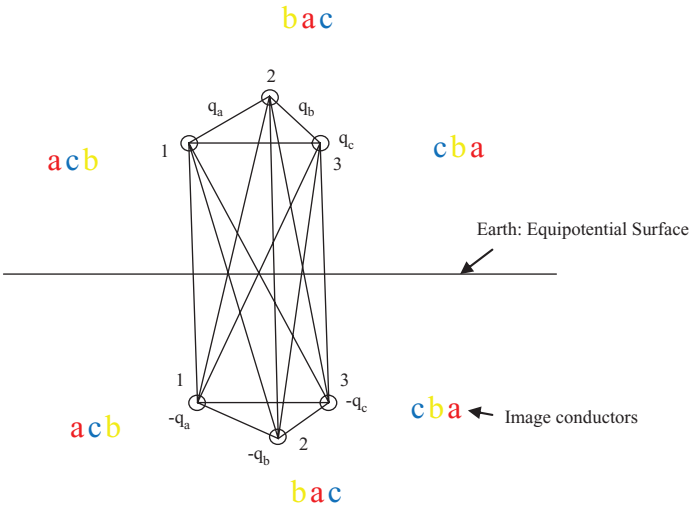

FIGURE 4.20
Three-phase transposed transmission line, three-wire equipotential line and its image about the earth.

and

$$-q_a - q_b - q_c = 0 \tag{4.132}$$

Applying the previously derived Equations 4.119 through 4.121 with the added consideration of the image charges and the equipotential earth line gives

$$V_{ab}: a \text{ in position 1, } b \text{ in position 2, } c \text{ in position 3}$$

$$V_{ab} = \frac{1}{2\pi\varepsilon}\left(q_a \left\{ \ln\frac{D_{12}}{r} - \ln\frac{H_{12}}{H_1} \right\} + q_b \left\{ \ln\frac{r}{D_{12}} - \ln\frac{H_2}{H_{12}} \right\} + q_c \left\{ \ln\frac{D_{23}}{D_{31}} - \ln\frac{H_{23}}{H_{31}} \right\} \right) \text{ volts} \tag{4.133}$$

Observe the pattern $1 \rightarrow 2 \rightarrow 3$ and the cyclic nature of the subscripts of the distances between conductors in the expression of Equation 4.133.

$$V_{ab}: a \text{ in position 2, } b \text{ in position 3, } c \text{ in position 1}$$

$$V_{ab} = \frac{1}{2\pi\varepsilon}\left(q_a \left\{ \ln\frac{D_{23}}{r} - \ln\frac{H_{23}}{H_2} \right\} + q_b \left\{ \ln\frac{r}{D_{23}} - \ln\frac{H_3}{H_{23}} \right\} + q_c \left\{ \ln\frac{D_{31}}{D_{12}} - \ln\frac{H_{31}}{H_{12}} \right\} \right) \text{ volts} \tag{4.134}$$

$$V_{ab}: a \text{ in position 3, } b \text{ in position 1, } c \text{ in position 2}$$

$$V_{ab} = \frac{1}{2\pi\varepsilon}\left(q_a \left\{ \ln\frac{D_{31}}{r} - \ln\frac{H_{31}}{H_3} \right\} + q_b \left\{ \ln\frac{r}{D_{31}} - \ln\frac{H_1}{H_{31}} \right\} + q_c \left\{ \ln\frac{D_{12}}{D_{23}} - \ln\frac{H_{12}}{H_{23}} \right\} \right) \text{ volts} \tag{4.135}$$

Therefore, the average V_{ab} with the effect of the image conductors and the equipotential earth line is the sum total of the Equations 4.133 through 4.135 divided by three.

$$V_{ab;\ \text{average}} = (|V_{ab}|_{a\ \text{in position 1}} + |V_{ab}|_{a\ \text{in position 2}} + |V_{ab}|_{a\ \text{in position 3}}) / 3$$

$$V_{ab} = \frac{1}{6\pi\varepsilon}\left(q_a \ln \frac{D_{12}D_{23}D_{31}}{r^3} + q_b \ln \frac{r^3}{D_{12}D_{23}D_{31}} + q_c \ln \frac{D_{12}D_{23}D_{31}}{D_{12}D_{23}D_{31}} \right.$$

$$\left. - q_a \ln \frac{H_{12}H_{23}H_{31}}{H_1H_2H_3} - q_b \ln \frac{H_1H_2H_3}{H_{12}H_{23}H_{31}} - q_c \ln \frac{H_{12}H_{23}H_{31}}{H_{12}H_{23}H_{31}} \right)$$

$$= \frac{1}{2\pi\varepsilon}\left(q_a \ln \frac{D_{eq}}{r} + q_b \ln \frac{r}{D_{eq}} - q_a \ln \frac{\sqrt[3]{H_{12}H_{23}H_{31}}}{\sqrt[3]{H_1H_2H_3}} - q_b \ln \frac{\sqrt[3]{H_1H_2H_3}}{\sqrt[3]{H_{12}H_{23}H_{31}}} \right) \quad \text{volts} \qquad (4.136)$$

Similarly, the average voltage drop from conductor *a* to conductor *c* is

$$V_{ac} = \frac{1}{2\pi\varepsilon}\left[\left(q_a \ln \frac{D_{eq}}{r} + q_c \ln \frac{r}{D_{eq}} \right) - q_a \ln \frac{\sqrt[3]{H_{12}H_{23}H_{31}}}{\sqrt[3]{H_1H_2H_3}} - q_c \ln \frac{\sqrt[3]{H_1H_2H_3}}{\sqrt[3]{H_{12}H_{23}H_{31}}} \right] \quad \text{volts} \quad (4.137)$$

Further, using

$$3V_{an} = V_{ab} + V_{ac} \qquad (4.138)$$

and

$$q_a + q_b + q_c = 0 \qquad (4.139)$$

and

$$-q_a - q_b - q_c = 0 \qquad (4.140)$$

we have

$$3V_{an} = \frac{1}{2\pi\varepsilon}\left[\left(3q_a \ln \frac{D_{eq}}{r} \right) - \left(3q_a \ln \frac{\sqrt[3]{H_{12}H_{23}H_{31}}}{\sqrt[3]{H_1H_2H_3}} \right) \right] \quad \text{volts} \qquad (4.141)$$

Thus,

$$C_n = \frac{q_a}{V_{an}} = \frac{2\pi\epsilon}{\ln \frac{D_{eq}}{r} - \ln \frac{\sqrt[3]{H_{12}H_{23}H_{31}}}{\sqrt[3]{H_1H_2H_3}}} \quad \frac{\text{F}}{\text{m}} \text{ to neutral} \qquad (4.142)$$

where

$$D_{eq} = \sqrt[3]{D_{12}D_{23}D_{31}} \qquad (4.143)$$

Equation 4.142 shows the effect of earth to increase the capacitance of line. Further, for very high conductors in extra-high-voltage (EHV) transmission lines, H_1, H_2, H_3 and H_{12}, H_{23}, H_{31} are nearly equal to each other, such that the second term in the denominator reduces to zero, yielding the same result as in Equation 4.127.

We can now proceed to find the capacitance of *bundled conductors*, as shown in Figure 4.21.

Figure 4.21 shows a three-phase line with bundled conductors (*a*-*a*′), (*b*-*b*′) and (*c*-*c*′) located in the same plane at locations 1, 2 and 3, separated by a distance of *d* between each other and between the bundles at locations 1, 2 and 3, shown as D_{12}, D_{23} and D_{31}. The conditions that underline this configuration of bundled conductors of a three-phase line as shown in Figure 4.21 are as follows:

1. Conductors of any one bundle are in parallel.
2. Charge per bundle divides equally between the individual conductors; that is, q_a: on conductor $a = q_a/2$ and on conductor $a' = q_a/2$
3. D_{12}, D_{23} and $D_{31} \gg d$

Using D_{12}, D_{23} and D_{31} as separation distances between the bundles of conductors, we have

$$V_{ab} = \frac{1}{2\pi\varepsilon}\left(q_a/2\left[\ln\frac{D_{12}}{r} + \ln\frac{D_{12}}{d}\right] + q_b/2\left[\ln\frac{r}{D_{12}} + \ln\frac{d}{D_{12}}\right] + \left(q_c/2\left[\ln\frac{D_{23}}{D_{31}} + \ln\frac{D_{23}}{D_{31}}\right]\right)\right)$$

Therefore,

$$V_{ab} = \frac{1}{2\pi\varepsilon}\left(q_a \ln\frac{D_{12}}{\sqrt{rd}} + q_b \ln\frac{\sqrt{rd}}{D_{12}} + q_c \ln\frac{D_{23}}{D_{31}}\right)$$

If the line is transposed, then find V_{ac} as before.

Then find V_{an}, and then it will yield

$$C_n = \frac{2\pi}{\ln\left(\dfrac{D_{eq}}{\sqrt{rd}}\right)} \quad \frac{\text{F}}{\text{m}} \text{ capacitance to neutral} \tag{4.144}$$

In Equation 4.144 we use *r* instead of D_s. This equation is similar to that of the inductance calculations derived earlier, and one can use this equation for bundled conductors as follows:

$$C_n = \frac{2\pi}{\ln\left(\dfrac{D_{eq}}{D_{sc}^{\,b}}\right)} \quad \frac{\text{F}}{\text{m}} \text{ capacitance to neutral} \tag{4.145}$$

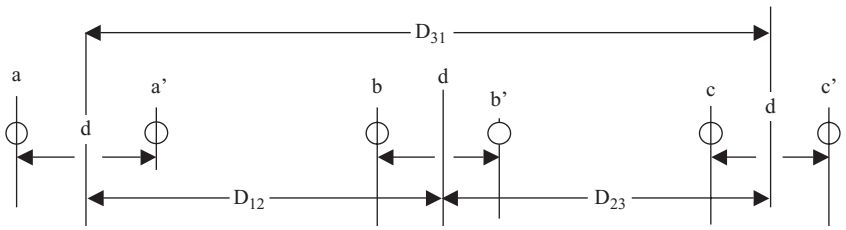

FIGURE 4.21
Three-phase line with bundled conductors.

where $D_{sc}{}^{b}$ is the modified GMR and can be shown to be

1. For a two-strand conductor:

$$D_{sc}{}^{b} = \sqrt[4]{(r \cdot d)^2} = \sqrt{rd} \tag{4.146}$$

2. For a three-strand conductor:

$$D_{sc}{}^{b} = \sqrt[9]{(r \cdot d \cdot d)^3} = \sqrt[3]{rd^2} \tag{4.147}$$

3. For a four-strand conductor:

$$D_{sc}{}^{b} = \sqrt[16]{(r \cdot d \cdot d \cdot d \cdot 2^{1/2})^4} = 1.09\sqrt[3]{r \cdot d^3} \tag{4.148}$$

Example 4.2

A bundled conductor and transposed three-phase transmission line has a conductor configuration as shown in Figure 4.22 at locations A, B and C with a radius r of the conductor as 0.74 cm.

Find

1. C_n in nano-F/km and nano-F/miles
2. Capacitive reactance of the line expressed in Ω.miles/phase
3. Capacitive reactance expressed in Ω/phase for a transmission line of length of 30 miles
4. Capacitive reactance expressed in Ω/phase for a transmission line of length of 100 miles

SOLUTION 4.2

1. Using Equation 4.146:

$$D_{sc}{}^{b} = \sqrt[4]{(r \cdot d)^2} = \sqrt{rd} = \sqrt{0.0074 \cdot 0.3} = 0.0471 \text{ miles}$$

Using Equation 4.143:

$$D_{eq} = \sqrt[3]{D_{12}D_{23}D_{31}} = \sqrt[3]{6^2 \cdot 12} = 7.56 \text{ miles}$$

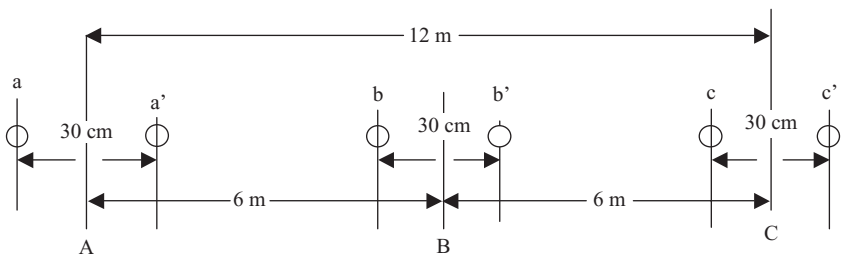

FIGURE 4.22
Three-phase transmission line with bundled conductors.

Then, the capacitance to neutral is using Equation 4.145:

$$C_n = \frac{2\pi}{\ln\left(\frac{D_{eq}}{D_{sc}{}^{b}}\right)} = \frac{2\pi \cdot 8.85 \cdot 10^{-12}}{\ln\left(\frac{7.56}{0.0471}\right)} = 10.85\frac{\text{nF}}{\text{km}} = 17.63 \text{ nF/miles}$$

2. $X_c = 29.63 \cdot 10^3 \ln\left(\frac{D_{eq}}{D_{sc}{}^{b}}\right) = 29.63 \cdot 10^3 \ln\left(\frac{7.56}{0.0471}\right) = 150{,}500 \ \Omega \cdot \text{miles}$

3. $X_c\,|_{30\,\text{miles}} = \frac{150{,}500}{30} = 5016.7 \ \Omega/\text{phase}$

4. $X_c\,|_{100\,\text{miles}} = \frac{150{,}500}{100} = 1505 \ \Omega/\text{phase}$

4.3.3 Capacitance of a Three-Phase Line with Unsymmetrical Spacing and Parallel Spacing in a Plane

Three conductors with radius r are shown in Figure 4.23.

The potential of point P for charges q_a, q_b and q_c residing on the line conductors is found using the log potentials given by

$$V_P = \frac{1}{2\pi\varepsilon}\left(q_a \ln\frac{1}{D_{aP}} + q_b \ln\frac{1}{D_{bP}} + q_c \ln\frac{1}{D_{cP}}\right) \quad \text{volts} \tag{4.149}$$

If point P is moved on to point a, then we can find the potential at point a as follows:

$$V_a = \frac{1}{2\pi\varepsilon}\left(q_a \ln\frac{1}{r} + q_b \ln\frac{1}{D} + q_c \ln\frac{1}{2D}\right) \quad \text{volts} \tag{4.150}$$

With the sum of charges

$$q_a + q_b + q_c = 0$$

$$V_a = \frac{1}{2\pi\varepsilon}\left(q_a \ln\frac{2D}{r} + q_b \ln 2\right) \quad \text{volts} \tag{4.151}$$

We repeat this for lines at b and c to obtain

$$V_b = \frac{1}{2\pi\varepsilon}\left(q_b \ln\frac{D}{r}\right) \quad \text{volts} \tag{4.152}$$

and

$$V_c = \frac{1}{2\pi\varepsilon}\left(q_b \ln 2 + q_c \ln\frac{2D}{r}\right) \quad \text{volts} \tag{4.153}$$

Transforming Equations 4.151 through 4.153 into matrix form we have

$$\begin{bmatrix} V_a \\ V_b \\ V_c \end{bmatrix} = \begin{bmatrix} \ln\frac{2D}{r} & \ln 2 & 0 \\ 0 & \ln\frac{D}{r} & 0 \\ 0 & \ln 2 & \ln\frac{2D}{r} \end{bmatrix} \begin{bmatrix} q_a \\ q_b \\ q_c \end{bmatrix} \text{ volts} \tag{4.154}$$

Note: If the conductors in Figure 4.23 are transposed, then matrix Equation 4.154 will be converted to diagonal form.

As a corollary to the inductance calculation of a similar setup of a three-phase line with unsymmetrical spacing and parallel spacing in a plane, we can have the following (three conductors with radius r) (Figure 4.24).

The flux linkage of a point P for currents I_a, I_b and I_c residing on the line conductors is found using the log linkages given by

$$\Psi_a = 2\cdot 10^{-7}\left(I_a \ln\frac{D_P}{r'_a} + I_b \ln\frac{D_P}{D} + I_c \ln\frac{D_P}{2D}\right) \text{ Wb}\cdot\text{turn} \tag{4.155}$$

Using

$$I_a + I_b + I_c = 0 \Rightarrow I_c = -I_a - I_b$$

gives

$$\Psi_a = 2\cdot 10^{-7}\left(I_a \ln\frac{2D}{r'_a} + I_b \ln 2\right) \text{ Wb}\cdot\text{turn} \tag{4.156}$$

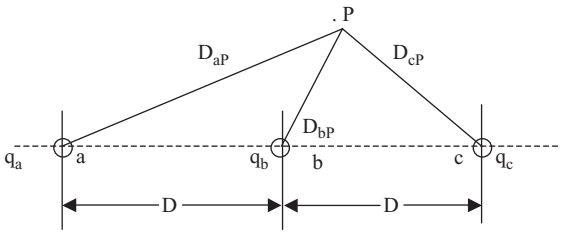

FIGURE 4.23
Three-phase line with unsymmetrical spacing.

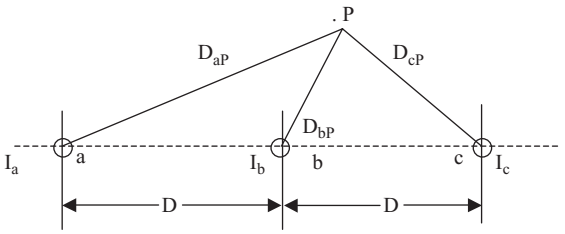

FIGURE 4.24
Three-phase line with unsymmetrical spacing.

We repeat this for lines at *b* and *c* to obtain

$$\Psi_b = 2\cdot 10^{-7}\left(I_b \ln\frac{D}{r_b'}\right)\ \text{Wb}\cdot\text{turn}$$

and

$$\Psi_c = 2\cdot 10^{-7}\left(I_b \ln 2 + I_c \ln\frac{2D}{r_c'}\right)\ \text{Wb}\cdot\text{turn}$$

Transforming Equations 4.156 through 1.158 in matrix form we have

$$\begin{bmatrix}\Psi_a\\ \Psi_b\\ \Psi_c\end{bmatrix} = \begin{bmatrix}\ln\frac{2D}{r'} & \ln 2 & 0\\ 0 & \ln\frac{D}{r'} & 0\\ 0 & \ln 2 & \ln\frac{2D}{r'}\end{bmatrix}\begin{bmatrix}I_a\\ I_b\\ I_c\end{bmatrix}\ \text{Wb}\cdot\text{turn}$$

Note: If the conductors in Figure 4.24 are transposed, then matrix Equation 4.159 will be converted to diagonal form.

Example 4.3

Figure 4.25 shows a three-phase, three-wire transposed transmission line with all the conductors in the same horizontal plane. This problem illustrates the effect of neutral on the value of capacitance.

Find the 60 Hz susceptance per mile per phase to neutral of the transposed three-phase line arranged as in Figure 4.25. Each conductor is a 715,500 circular-mil steel-reinforced aluminum cable, (54 + 7) strands with an outside diameter of 1.036 in. (0.0263 m). Conductors are separated with $D = 25$ ft. (7.61 m) and $h = 40$ ft. (12.18 m). Conductors *a*, *b* and *c* are located at locations 1, 2 and 3, respectively.

SOLUTION

$$H_{12} = \sqrt{(2h)^2 + D^2} = H_{23} = 25.52\,\text{m}$$

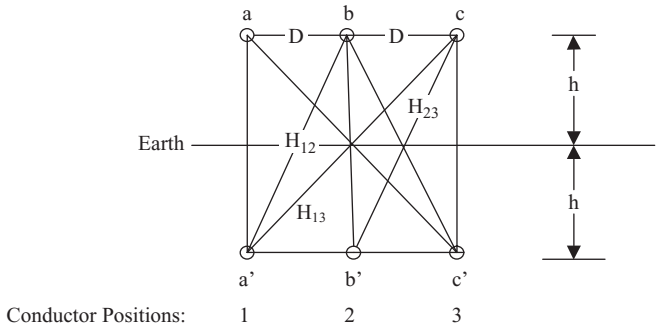

FIGURE 4.25
Three-phase, three-wire transposed transmission line with conductors in the same horizontal plane.

$$H_{31} = \sqrt{(2h)^2 + (2D)^2} = 28.72\,\text{m}$$

$$H_{ii} = H_i = 2h = 24.36\,\text{m};\ \forall i = 1,2,3$$

$$D_{eq} = \sqrt[3]{D^2 \cdot 2D} = 9.59\,\text{m}$$

$$C_n = \frac{2\pi\epsilon}{\ln\frac{D_{eq}}{r} - \ln\sqrt[3]{\frac{H_{12}H_{23}H_{31}}{H_1H_2H_3}}} = 1.380 \cdot 10^{-8}\ \frac{\text{F}}{\text{mile}}$$

$$Xcn = j\frac{1}{2\pi \cdot 60 \cdot 1.380 \cdot 10^{-8}} = j192{,}191\ \text{mhos/mile}$$

Exercise to check the effect of earth on C_n; ignore the effect of earth and evaluate C_n again!

Problems

PROBLEM P.4.1

Find the resistance of a 10 km-long solid cylindrical aluminum conductor with a diameter of 250 mil, at

1. 20°C
2. 120°C

PROBLEM P.4.2

A transmission line cable has 19 strands of identical copper conductor. Each conductor has a diameter of 1.5 mm. The length of the cable is 2 km, but because of the twist in the strands, the actual length of each conductor is increased by 5%.

1. Find the resistance of the cable for a resistivity of copper to be 1.72×10^{-8} Ω·m with a temperature coefficient α of 0.00382 C^{-1} at 20°C.
2. Find the resistance of the cable for a resistivity of copper to be 1.72×10^{-8} Ω·m with a temperature coefficient α of 0.00393 C^{-1} at 20°C.

PROBLEM P.4.3

A sample of copper wire has a resistance of 50 Ω at 10°C. What must be the maximum operating temperature of the wire if its resistance is to increase by at most 10%? Take the temperature coefficient α of 0.00409 C^{-1} at 10°C

PROBLEM P.4.4

The per-phase line loss in a 40 km-long transmission line is not to exceed 60 kW while it is delivering 100 A per phase. If the resistivity of the conductor material is 1.72×10^{-8} Ω·mi, find the required conductor diameter.

PROBLEM P.4.5

A coaxial cable has an inner conductor of radius r_1 and a hollow outer conductor of radius r_2, as shown in Figure P.4.5.

Find the inductance per unit length of the cable by finding the energy stored in the magnetic field of the cable and equating it to the energy stored in the cable inductance. Assume a uniform current density distribution over the conductor cross-section.

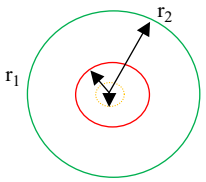

FIGURE P.4.5
Hollow coaxial cable.

PROBLEM P.4.6

A single-circuit, three-phase 60 Hz transmission line consists of three conductors arranged as shown in Figure P.4.6. The solid cylindrical aluminum conductors are with a diameter of 250 mil. What is the value of the reactance of this transmission line for a signal frequency of 60 Hz.

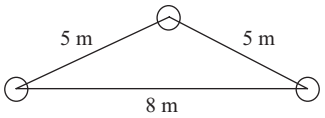

FIGURE P.4.6
Three conductors at the tip of a triangle.

PROBLEM P.4.7

A single-phase two-wire transmission line, 15 km long, is made up of round conductors 0.8 cm in diameter, separated from each other by 40 cm. Calculate the equivalent diameter of a fictitious hollow, thin-walled conductor having the same inductance as the original line. What is the value of this inductance?

PROBLEM P.4.8

Calculate the capacitance and capacitive reactance at 60 c/s of the transmission line in Problem P.4.7.

PROBLEM P.4.9

Find the capacitive reactance per kilometer of the three-phase transmission line in Problem P.4.7.

PROBLEM P.4.10

Calculate the inductance per unit length of the single-phase line shown in Figure P.4.10. Conductors *a*, *b* and *c* are 0.2 cm in radius, and conductors *d* and *e* are 0.4 cm in radius.

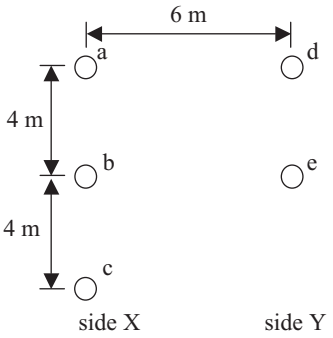

FIGURE P.4.10
Single-phase line.

PROBLEM P.4.11

Verify the result of Problem P.4.6 by applying the concept of GMR and GMD.

PROBLEM P.4.12

Calculate the capacitance per kilometer per phase of the single-circuit, two-bundle conductor shown in Figure P.4.12. The diameter of each conductor is 5 cm.

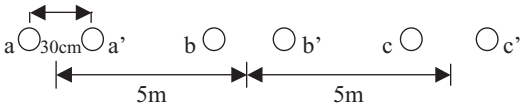

FIGURE P.4.12
Single-circuit two-bundle conductor transmission line.

Taylor & Francis
Taylor & Francis Group
http://taylorandfrancis.com

5

Line Representations

5.1 Introduction

The passive elements evaluated and calculated for the transmission line components resistance (R), inductance (L) and capacitance (C) are now used to represent them for different distances of lines. These parameters representing these lines are assumed to be parameters that are uniformly distributed along the length of the transmission line. A second thought is to represent the lines using lumped parameters. However, in both the cases, the parameters are used depending on the length (l) of the lines.

These lines are thus designated into three categories, depending on the length (l):

1. Short lines: $l <$ less than 80 km (50 mi.)
2. Medium lines: 80 km (50 mi.) $< l <$ 240 km (150 mi.)
3. Long lines: $l >$ 240 km (150 mi.)

Accordingly, the short lines and medium lines use lumped parameters in the representation. Besides, for short lines the shunt capacitance is assumed negligible and only series resistance (R) and series inductance (L) are considered as relevant parameters in the representation of the short line. Since no shunt capacitance is considered in the representation of a short line, lumped parameters or uniformly distributed parameters give almost the same results in the eventual calculations. Thus, a short line is represented as shown in Figure 5.1. A medium line with a single-phase representation is shown in Figure 5.2.

5.2 Short, Medium-Length and Long Lines

In order to evaluate the circuit in Figure 5.2, an important nomenclature needs to be defined as follows:

z = series impedance per unit length per phase

y = shunt admittance per unit length per phase to neutral

l = length of a line

$Z = z \times l$ = total series impedance per phase

$Y = y \times l$ = total shunt admittance per phase to neutral

So now we process the short, medium-length and long transmission lines as follows.

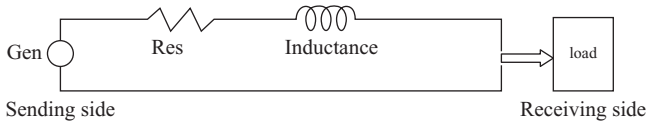

FIGURE 5.1
Short line.

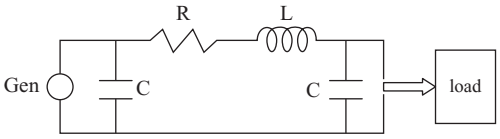

FIGURE 5.2
Single-phase equivalent of a power system with a transmission line that includes the capacitance to neutral for the entire length of the line divided between the two ends of the line.

5.2.1 Short Transmission Line: $l < 80$ km (50 mi.) (Figure 5.3)

R and L are values for the entire length of this transmission line. V_S is the voltage at the source or typically the sending end; V_R is the voltage at the load end or the receiving end. Let I_S be the current at the sending end and I_R the current at the receiving end. We now apply Kirchoff's Current Law (KCL) and Kirchoff's Voltage Law (KVL) to this circuit.

$$\text{KCL}: I_S = I_R \tag{5.1}$$

$$\text{KVL}: V_S = V_R + I_R \cdot Z \tag{5.2}$$

$$\text{Apparent power in the three-phase circuit: } S = 3 \cdot V_S \cdot I_S^* \tag{5.3}$$

We can now find the voltage regulation as a function of the power factor of the load component at the receiving end, as illustrated in the three cases shown in Figure 5.4.

We can now define the percentage of voltage regulation, using the magnitudes of the voltage at the receiving end at no load and full load, as follows:

$$\%\ \text{Voltage regulation} \triangleq \frac{|V_{R,NL}| - |V_{R,FL}|}{|V_{R,FL}|} \cdot 100\,|_{V_S = \text{constant}} \tag{5.4}$$

For the circuit in Figure 5.3, we have in Equation 5.4:

$$|V_{R,NL}| = |V_S|; \quad |V_{R,FL}| = |V_R| \tag{5.5}$$

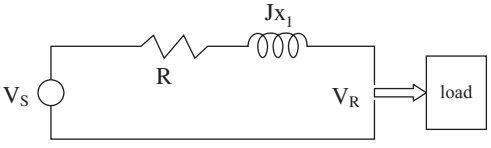

FIGURE 5.3
Equivalent circuit of a short transmission line.

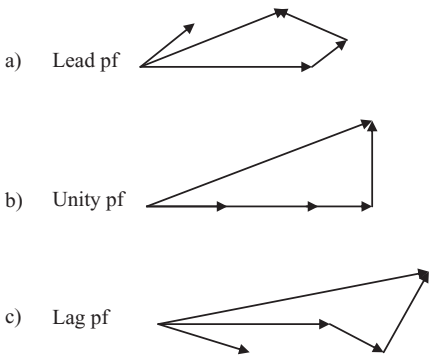

FIGURE 5.4
Different cases of power factor.

Thus, the maximum regulation occurs when $V_S = V_R$ are collinear. This takes place as shown in Figure 5.5 at a phase angle of load given by

$$\theta = \tan^{-1}\left(\frac{X_L}{R}\right) \tag{5.6}$$

5.2.2 Medium Transmission Line: 80 km (50 mi.) < *l* < 240 km (150 mi.)

In the case of a medium transmission line, the shunt admittance is comprised of pure capacitance, as the conductance of the circuit is ignored. With this assumption, the transmission line is best represented by an equivalent pi(π)-circuit employing lumped parameters. Thus, the total shunt admittance is divided into two equal parts placed at the sending and receiving ends of the line, respectively.

We now apply the KCL and KVL of the circuit in Figure 5.6 as follows:

KCL:

$$I_Z = I_R + I_{Y/2_S} = I_R + V_R \cdot \frac{Y}{2} \tag{5.7}$$

$$I_S = I_Z + I_{Y/2_R} = I_Z + V_S \cdot \frac{Y}{2} \tag{5.8}$$

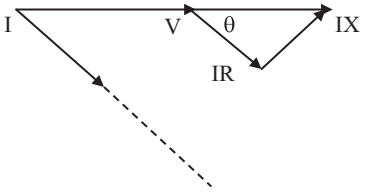

FIGURE 5.5
Maximum voltage regulation for a short transmission line.

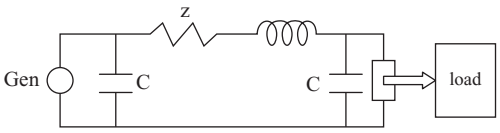

FIGURE 5.6
π-circuit of a medium transmission line.

KVL:

$$\begin{aligned} V_S &= I_Z \cdot Z + V_R \\ &= \left(I_R + V_R \cdot \frac{Y}{2} \right) Z + V_R \\ &= \left(1 + \frac{YZ}{2} \right) \cdot V_R + ZI_R \end{aligned} \tag{5.9}$$

From Equations 5.8 and 5.9,

$$\begin{aligned} I_S &= I_R + V_R \cdot \frac{Y}{2} + V_S \cdot \frac{Y}{2} \\ &= I_R + V_R \cdot \frac{Y}{2} + \left\{ \left(1 + \frac{YZ}{2} \right) \cdot V_R + ZI_R \right\} \cdot \frac{Y}{2} \\ &= I_R \left(1 + \frac{YZ}{2} \right) + V_R \cdot Y \left(1 + \frac{ZY}{4} \right) \\ &= V_R \cdot Y \left(1 + \frac{ZY}{4} \right) + I_R \left(1 + \frac{YZ}{2} \right) \end{aligned} \tag{5.10}$$

From Equations 5.9 and 5.10,

$$V_S = A \cdot V_R + B \cdot I_R \tag{5.11}$$

$$I_S = C \cdot V_R + D \cdot I_R \tag{5.12}$$

where:

$$A = 1 + \frac{YZ}{2} = D = 1 + Z \cdot \frac{Y}{2} \tag{5.13.a}$$

$$B = Z \tag{5.13.b}$$

$$C = Y \left(1 + \frac{ZY}{4} \right) = \left[Y + Z \cdot \frac{Y}{2} \cdot \frac{Y}{2} \right] \tag{5.13.c}$$

When $I_R = 0$ in Equation 5.11,

$$V_S = A \cdot V_R$$

$$A = \frac{V_S}{V_R}; V_R \mid_{I_R = 0} = \frac{V_S}{A}$$

resulting in a voltage regulation using Equation 5.4 as follows:

$$\%\ \text{Voltage regulation} \triangleq \frac{\left|\frac{V_S}{A}\right| - |V_{R,FL}|}{|V_{R,FL}|} \cdot 100\,|_{V_S=\text{constant}} \tag{5.14}$$

5.2.3 Long Transmission Line: >240 km (150 mi.)

Because of the length of the line, lumped parameters can introduce less accuracy in calculations of impedances. One can use uniformly distributed parameters along the length of the line, in which case, one needs a solution to a differential equation that involves the basic elemental change in length in dx that results in a change in the impedance values at different lengths of the line. The line is shown in Figure 5.7, starting from the generator side and terminating on the load. The generator side is the sending side, denoted by a subscript S, associated with each voltage and current parameter, and the load side is the receiving side, denoted by a subscript R, associated with each voltage and current parameter on the respective sides.

In Figure 5.7 we have a single-phase transmission line with a neutral return. Further, the following variables need to be defined to describe the different parameters in the circuit.

x = distance measured from the receiving end of the line to the small element of the line

Δx = length of the small element of the line

$z\Delta x$ = series impedance of the small element of the line

$y\Delta x$ = shunt admittance of the small element of the line

We now apply KVL to this small element as follows:

$$\Delta v = Iz\,\Delta x$$

$$\frac{\Delta v}{\Delta x} = Iz$$

$$\lim_{\Delta x \to 0} \frac{\Delta v}{\Delta x} = \frac{dv}{dx} = Iz \tag{5.15}$$

The differential current flowing in the shunt admittance of the small element of the line is given by

$$\Delta I = Vy\Delta x$$

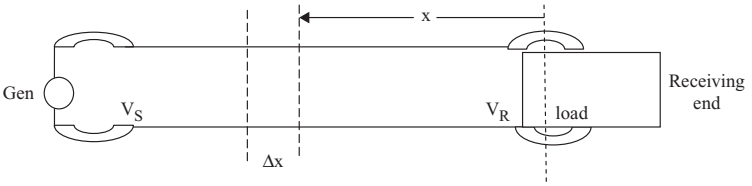

FIGURE 5.7
Long transmission line with uniformly distributed parameters.

Similarly:

$$\frac{dI}{dx} = Vy \tag{5.16}$$

Differentiating Equations 5.15 and 5.16 one more time w.r.t Δx yields

$$\frac{d^2v}{dx^2} = \frac{dI}{dx} \cdot z = y \cdot z \cdot V \tag{5.17}$$

and

$$\frac{d^2I}{dx^2} = \frac{dV}{dx} \cdot y = y \cdot z \cdot I \tag{5.18}$$

Equations 5.17 and 5.18 have a simple solution that has an exponential form as follows:

$$y = e^{ax} \tag{5.19}$$

We will differentiate Equation 5.19 w.r.t to x again yielding

$$\frac{dy}{dx} = a \cdot e^{ax} \tag{5.20}$$

Repeating this differentiation one more time yields

$$\frac{d^2y}{dx^2} = a^2 e^{ax} \tag{5.21}$$

This solution can be applied to Equations 5.16 and 5.17 and solved by trial and error as follows:

Let

$$V = A_1 e^{\sqrt{yz}x} + A_2 e^{-\sqrt{yz}x} \tag{5.22}$$

Following the mechanism of double differentiation yields

$$\frac{d^2V}{dx^2} = yz \cdot V \tag{5.23}$$

and

$$\frac{dV}{dx} = \sqrt{yz}\left[A_1 e^{\sqrt{yz}x} - A_2 e^{-\sqrt{yz}x}\right] \tag{5.24}$$

From Equations 5.15 and 5.24, we have

$$I = \frac{1}{z}\frac{dV}{dx} = \frac{1}{\sqrt{\frac{z}{y}}}\left[A_1 e^{\sqrt{yz}x} - A_2 e^{-\sqrt{yz}x}\right] \tag{5.25}$$

In Equations 5.24 and 5.25, A_1 and A_2 are found from boundary conditions from the values of V and I at different values of x, as follows.

For $x=0$, $V=V_R$ and $I=I_R$, which further yields

$$V_R = A_1 + A_2 \tag{5.26}$$

and

$$I_R = \frac{1}{\sqrt{\frac{z}{y}}}\left[A_1 - A_2\right] \tag{5.27}$$

We now define a commonly used term in circuits called *characteristic impedance*, given by

$$Z_c = \sqrt{\frac{z}{y}} \tag{5.28}$$

Using Equations 5.26, 5.27 and 5.28, we can solve A_1 and A_2 as follows:

$$A_1 = \frac{V_R + I_R Z_c}{2} \text{ and } A_2 = \frac{V_R - I_R Z_c}{2} \tag{5.29}$$

We now define another commonly used term, the *propagation constant*:

$$\gamma = \sqrt{zy} \tag{5.30}$$

Using Equations 5.28, 5.29 and 5.30 in Equations 5.21 and 5.25 for V and I respectively, yield a set of general equations, as follows:

$$V = \frac{V_R + I_R Z_c}{2} e^{\gamma x} + \frac{V_R - I_R Z_c}{2} e^{-\gamma x} \tag{5.31}$$

$$I = \frac{\frac{V_R}{Z_c} + I_R}{2} e^{\gamma x} - \frac{\frac{V_R}{Z_c} - I_R}{2} \cdot e^{-\gamma x} \tag{5.32}$$

In all the above equations, Z_c and γ are complex quantities; further:

$$\gamma = \alpha + j\beta \rightarrow e^{\gamma x} = e^{\alpha x} \cdot e^{j\beta x} = e^{\alpha x}\left\{\cos\beta x + j\sin\beta x\right\} \tag{5.33}$$

where the magnitude of the first term changes with x and the magnitude of the second term is always 1, and

Real term $\alpha \rightarrow$ neppers per unit length and is the attenuation constant

and

Imaginary term $\beta \rightarrow$ phase constant and is given in radians per unit length

Further, the first term of Equations 5.31 and 5.32 are the incident voltage and incident current, respectively, and the second term of Equations 5.31 and 5.32 are the reflected voltage and reflected current, respectively, for the line under consideration.

In addition, the important understanding of the characteristic impedance of a line is as follows: If a line is terminated in its characteristic impedance Z_c, then

$$V_R = I_R Z_C \rightarrow \text{no reflected wave is present in the line of } V \text{ or } I$$

Such a line is called a *flat line* or *infinite line*. Here, Z_c is also called the *surge impedance* and is a special type of lossless line, where the resistance and conductance of the line are zero and

$$Z_C = \sqrt{\frac{L}{C}} = \text{pure resistance} \tag{5.34}$$

5.3 Surge Impedance Loading (SIL)

The SIL of a line is the power delivered by a line to a pure resistive load equal to its surge impedance; that is,

$$|I_L| = \frac{|V_L|}{\sqrt{3} \cdot \sqrt{\frac{L}{C}}} \text{ in amperes} \tag{5.35}$$

Further, since the load is a pure resistance,

$$\text{SIL} = \sqrt{3}\,|V_L| \frac{|V_L|}{\sqrt{3} \cdot \sqrt{\frac{L}{C}}} \text{ in watts} \tag{5.36}$$

which yields

$$\text{SIL} = \frac{|V_L|^2}{\sqrt{\frac{L}{C}}} \text{ in megawatts with } V_L \text{ in kilovolts} \tag{5.37}$$

The loading of a transmission line is generally expressed as a fraction of SIL. SIL also provides a comparison of the load-carrying capabilities of all transmission lines in general.

Equations 5.31 and 5.32 appear to be hyperbolic functions as indicated by the general identities of hyperbolic functions given by

$$\sin h\theta = \frac{e^{\theta} - e^{-\theta}}{2} \tag{5.38}$$

$$\cos h\theta = \frac{e^{\theta} + e^{-\theta}}{2} \tag{5.39}$$

Thus, Equations 5.38 and 5.39 can be used to rewrite Equations 5.31 and 5.32 as follows:

$$V = V_R \cosh(\gamma x) + I_R Z_c \sinh(\gamma x) \tag{5.40}$$

$$I = I_R \cosh(\gamma x) + \frac{V_R}{Z_c} \sinh(\gamma x) \tag{5.41}$$

For $x = l$, at the sending end:

$$V_S = V_R \cosh(\gamma l) + I_R Z_c \sinh(\gamma l) \tag{5.42}$$

$$I_S = I_R \cosh(\gamma l) + \frac{V_R}{Z_c} \sinh(\gamma l) \tag{5.43}$$

Thus, rearranging the terms, we have at the receiving end:

Line-to-neutral voltage:

$$V_R = V_S \cosh(\gamma l) - I_S Z_c \sinh(\gamma l) \tag{5.44}$$

Line current:

$$I_R = I_S \cosh(\gamma l) - \frac{V_S}{Z_c} \sinh(\gamma l) \tag{5.45}$$

We now proceed to find the equivalent circuit of a long transmission line using lumped parameters (in π-circuit or T-circuit form).

We have shown in Figure 5.8 the parameters of a long line as lumped parameters Z' and $Y'/2$, and the sending and receiving end voltages and currents are given by

$$V_S = \left(Z' \frac{Y'}{2} + 1 \right) V_R + Z' I_R \tag{5.46}$$

and

$$I_S = I_R \left(1 + Z' \frac{Y'}{2} \right) + V_R Y' \left(1 + \frac{Y'Z'}{4} \right) \tag{5.47}$$

Comparing Equations 5.42 and 5.46, we have

$$Z' = Z_c \sinh(\gamma l) \tag{5.48}$$

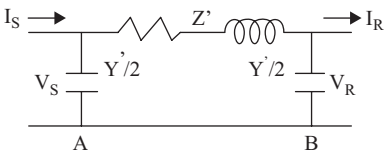

FIGURE 5.8
Representation of a long transmission line using lumped parameters.

$$= \sqrt{\frac{z}{y}} \sinh(\gamma l) = zl \frac{\sinh(\gamma l)}{\sqrt{zy} \cdot l}$$

$$Z' = Z \cdot \left(\frac{\sinh(\gamma l)}{\sqrt{zy} \cdot l} \right) = Z \cdot \left(\frac{\sinh(\gamma l)}{y \cdot l} \right) \tag{5.49}$$

and

$$Z' \frac{Y'}{2} + 1 = \cosh(\gamma l)$$

which yields

$$Z_c \sinh(\gamma l) \frac{Y'}{2} + 1 = \cosh(\gamma l) \tag{5.50}$$

using known identity for tangent hyperbolic for an angle as:

$$\tanh\left(\frac{\gamma l}{2} \right) = \frac{\cosh(\gamma l) - 1}{\sinh(\gamma l)}$$

$$\frac{Y'}{2} = \frac{\cosh(\gamma l) - 1}{Z_c \sinh(\gamma l)} = \tanh\left(\frac{\gamma l}{2} \right) \cdot \frac{1}{Z_c}$$

Thus,

$$\frac{Y'}{2} = \frac{\sqrt{y}}{\sqrt{z}} \tanh\left(\frac{\gamma l}{2} \right)$$

$$= \frac{\frac{\sqrt{y}\sqrt{y}l}{2}}{\frac{\sqrt{z}\sqrt{y}l}{2}} \cdot \tanh\left(\frac{\gamma l}{2} \right)$$

yielding

$$\frac{Y'}{2} = \frac{Y}{2} \left(\frac{\tanh\left(\frac{\gamma l}{2} \right)}{\frac{\gamma l}{2}} \right) \tag{5.51}$$

These yield the parameters of the long line with lumped parameters, as shown in Figure 5.8.

Equations 5.49, 5.50 and 5.51 are hyperbolic functions that can be plotted as shown in Figures 5.9 through 5.11, where the angle of sinh (θ)/θ versus the size of sinh (θ)/θ, the angle of cosh (θ) versus the size of cosh (θ) and the angle of tanh (θ/2) versus the size of tanh (θ/2) are plotted, respectively. Thus, problems about finding voltages and power at the sending and receiving ends of/in long transmission lines can be solved using the graphs shown in the following examples.

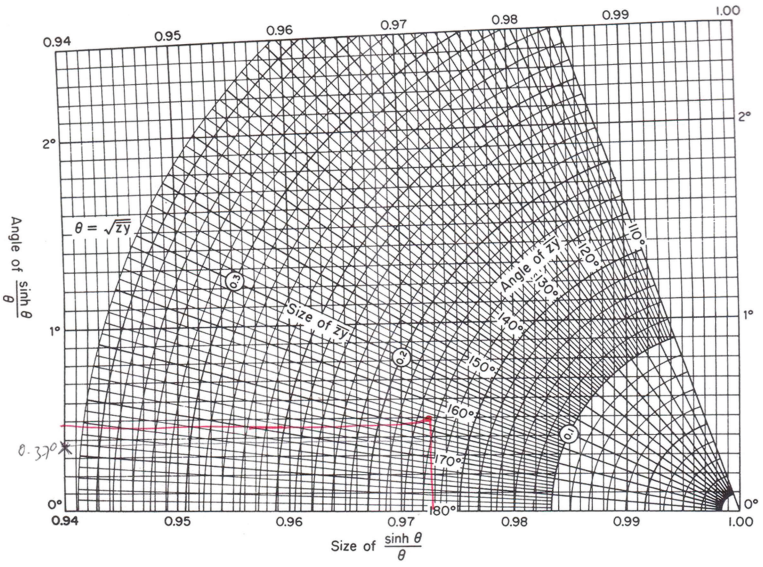

FIGURE 5.9
Angle of sinh (θ)/θ vs. size of sinh (θ)/θ.

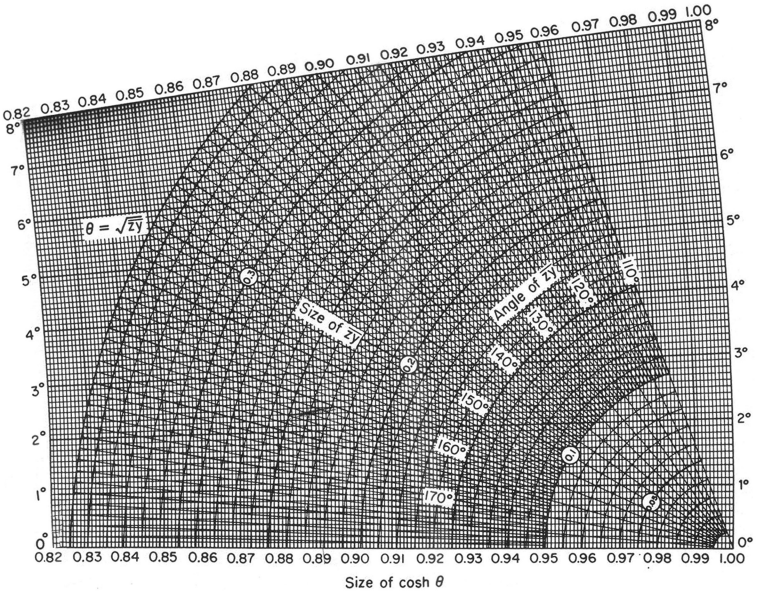

FIGURE 5.10
Angle of cosh (θ) vs. size of cosh (θ).

Example 5.1

A single-circuit 60 c/s transmission line is 370 km (230 mi.) long with Rook conductors that have a flat horizontal spacing of 2.5 m (23.8 in.) between conductors, as shown in Figure 5.12. The load on this long transmission line is 125 MW at 215 kV with unity power factor (upf).

Find V_S, I_S, the apparent power at the sending end ($S = V_S.I_S^*$) and the voltage regulation.

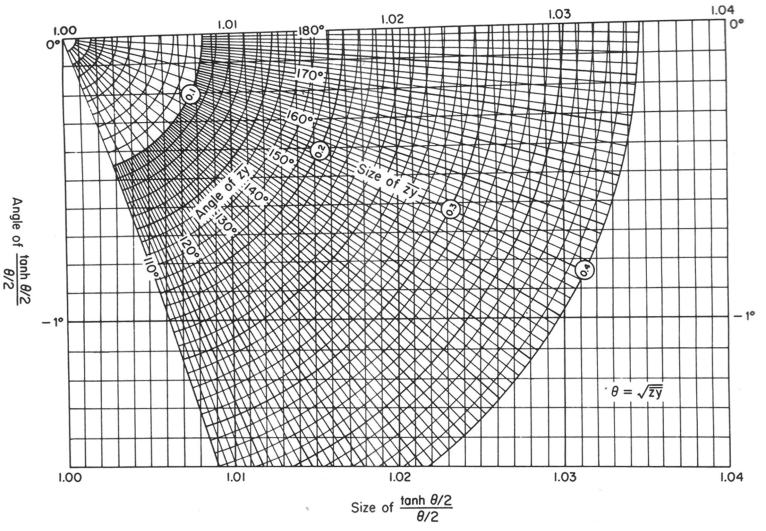

FIGURE 5.11
Angle of tanh (θ/2) vs. size of tanh (θ/2).

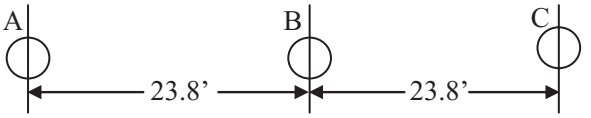

FIGURE 5.12
Flat, long transmission line of 370 km (230 mi.) length.

SOLUTION 5.1A

From Figure 5.12, we have

$$D_{eq} = \sqrt[3]{23.8 \cdot 23.8 \cdot 47.6} \cong 30.0'$$

For the Rook line, we have

$$z = 0.1603 + j\left(0.415 + X_d = \log D_{eq} \cdot 0.2794\right)$$

$$= 0.1603 + j\left(0.415 + 0.4127\right) = 0.8431\angle 79.04^\circ\ \Omega/\text{mi}.$$

and

$$y = j\left[\frac{1}{0.095 + 0.06831\log 30}\right] \times 10^{-6} = 5.105 \times 10^{-6}\angle 90^\circ\ \text{mhos/mi}.$$

$$\gamma l = \sqrt{yz} \cdot l = 230\sqrt{0.8431 \cdot 5.105 \times 10^{-6}}\angle \frac{(79.04 + 90)^\circ}{2}$$

$$= 0.4772\angle 89.52^\circ = 0.0456 + j0.4750$$

$$Z_c = \sqrt{\frac{z}{y}} = \sqrt{\frac{0.8431}{5.105 \times 10^{-6}}} \angle \frac{(79.04 + 90)^\circ}{2} = 406.4 \angle -5.48^\circ \Omega$$

$$V_R = \frac{215,000}{\sqrt{3}} = 124,130 \angle 0^\circ \text{ V; line-to-neutral voltage as reference}$$

At the receiving end:

$$S_R = P_R + jQ_R$$

where

$$P_R = 125 \text{ MW} = \sqrt{3} \cdot V_R I_R \cos\theta_R$$

$$\therefore I_R = \frac{125 \times 10^6}{\sqrt{3} \cdot 215,000} = 335.7 \angle 0^\circ \text{ with upf load}$$

Using Equations 5.40 and 5.41 for V_S and I_S, respectively, we have

$$V_S = V_R \cosh(\gamma l) + I_R Z_c \sinh(\gamma l)$$

$$= 124,130 \angle 0^\circ \times 0.8904 \angle 1.34^\circ + 335.7 \angle 0^\circ \times 406.4 \angle -5.48^\circ \times 0.4596 \angle 84.94^\circ$$

$$= 137,851 \angle 27.77^\circ \text{ V line to neutral}$$

and

$$I_S = I_R \cosh(\gamma l) + \frac{V_R}{Z_c} \sinh(\gamma l) = 335.7 \angle 0^\circ \times 0.8904 \angle 1.34^\circ + \frac{124,130 \angle 0^\circ}{406.4 \angle -5.48^\circ} \times 0.4596 \angle 84.94^\circ$$

$$= 332.27 \angle 26.33^\circ \text{ A}$$

$$S_S = 3 V_S I_S^*$$

$$= 3 \cdot 137,851 \angle 27.77^\circ \cdot 332.27 \angle 26.33^\circ$$

$$S_S = 137.411 \text{ MVA} \angle 1.5^\circ$$

$$P_S = 137.364 \text{ MW}$$

$$\text{Voltage regulation} = \frac{|V_{R_{NL}}| - |V_{R_{FL}}|}{|V_{R_{FL}}|}$$

At no load, $I_R = 0$:

$$V_S = V_R \cosh(\gamma l)$$

$$\therefore |V_{R_{NL}}| = \left|\frac{V_S}{\cosh(\gamma l)}\right| = \frac{137,851}{0.8904} = 154,272\,\text{V}$$

$$\%\ \text{Voltage regulation} = \frac{154,272 - 124,130}{124,130} = 24.3\%$$

Besides, we can find the propagation constant γ from Equation 5.31 as follows:

$$\gamma = \alpha + j\beta = 0.0456 + j0.4750$$

where β = 0.475°; therefore, β per mile = 0.475°/230 rad/mi.
Thus, λ = 2π/β = (2πx230)/0.475 = 3042.4 mi.
And velocity $v = f \times \lambda = 60 \times 3042.4 = 182,543$ mi./s
We now proceed to solve this problem using pu calculations.

SOLUTION 5.1B

We select an MVA base of 125 MVA and a voltage base of 215 kV (*L-L*) or 124.13 (*L-N*), which yields
Base impedance = $(\text{kV})^2/\text{MVA} = (215)^2/125 = 370\ \Omega$
Base current = $125 \times 10^6/(1.732 \times 215 \times 10^3) = 335.7$ A
Characteristic impedance Z_c is pu = 406.4/370 with an angle of −5.48° = 1.098 with an angle of −5.48°
$V_R = 1.0$ pu or 1.0 with an angle of 0°, which is a reference voltage.
Also, $I_R = 1.0$ with an angle of 0° for a load of upf.
This yields

$$V_S = 1.0\angle 0° \cdot 0.8904\angle 1.34° + 1\angle 0°\left(1.098\angle -5.48°\right) \cdot 0.4596\angle 84.94°$$

$$= 1.1102\angle 27.75° = 238.7\,\text{kV as before}$$

$$I_S = 1.0\angle 0° \cdot 0.8904\angle 1.34° + \frac{1\angle 0°}{1.098\angle -5.48°} \cdot 0.4596\angle 84.94°$$

$$= 0.99\angle 26.35° = 332.3\,\text{A as before}$$

Example 5.2

A three-phase, 60 Hz transmission line is constructed of ACSR conductors and is described as follows:
Aluminum area = 566,500 circular mils
Strands (Al/St): 26/7
Strand diameter = 0.1463 in.
Approximate current rating = 730 A
Resistance (Ω/mi.): DC @ 20°C = 0.1621; 60 Hz @ 20°C = 0.1663; 60 Hz @ 50°C = 0.1826
For the specific spacing used in the line construction, the per mile parameters are as follows:

$$z = r + j337L = 0.1826 + \frac{j0.784\,\dfrac{\Omega}{\text{mi.}}}{\text{phase}}$$

and

$$X_C = 185.5 \times 10^3 \angle -90° \ \Omega\text{-mi. per phase}$$

1. Find the total line impedance and admittance for a line length of 100 mi.
2. The load at the receiving end draws 200 MVA at a line-to-line voltage of 230 kV and upf. Determine V_S, I_S, P_S and Q_S.
3. Compute the voltage regulation.

SOLUTION 5.2

1. $Z = z \times l = 18.26 + j78.4 = 80.5$ with an angle of 76.8° Ω/phase

   $Y = 1/(X_C/l)$ with an angle of $90° = 1/(185.5 \times 10^3/100)$ with an angle of $90° = 0.5391 \times 10^{-3}$ with an angle of 90° S/phase
2. $I_R = (200 \times 10^6)/(\sqrt{3} \times 230 \times 10^3) = 502$ A with an angle of 0°.

   $V_R = (230 \times 10^3)/(\sqrt{3})$ with an angle of zero degrees = 132,800 with an angle of 0°.

   $I_Z = I_R + V_R$ (Y/2) = 502 with angle zero degrees + (132,800 with an angle of 0°) $(0.27 \times 10^{-3}$ with an angle of 90°)

   $= 502 + j35.86 = 503.3$ with an angle of 4.09°

   Sending end voltage:

$$V_S = V_R + I_Z \cdot Z$$

$$= 132.8\angle 0° + (0.5033\angle 4.09°)(80.5\angle 76.8°)\text{kV}$$

$$= 144.79\angle 16.04° \text{ kV}$$

Sending end voltage line to line:

$$|V_S| = \sqrt{3} \cdot 144.79 \text{ kV}$$

$$|V_S|_{L-L} = 250.784\text{kV}$$

$$I_S = I_Z + V_S \cdot \frac{Y}{2}$$

$$= 502 + j35.86 + (144.79\angle 16.04°)(0.27\angle 90°)$$

$$= 502 + j73 = 496.7\angle 8.5° \text{ A}$$

$$S = 3 \cdot V_S \cdot I_S^* = 3(144.79\angle 16.04°)(496496.7\angle -8.5°)$$

$$= (213.88 + j28.31)\text{ MVA} = P_S + jQ_S$$

$$\theta_S = 16.04° - 8.5° = 7.54°$$

3. $$\%\ \text{Regulation} = \frac{|V_S| - |V_R|}{|V_R|} \times 100 = \frac{144.49 - 132.8}{132.8} \times 100 = 9\%$$

Example 5.3: Solving problems using (1) equations and (2) hyperbolic graphs, as in Figures 5.9 through 5.11

The transmission line in Example 5.1 is extended to 200 mi.

1. Find V_S, I_S, P_S and Q_S.
2. Compute the voltage regulation assuming the conditions at the load are the same as in Example 5.1.

The method in (1) is illustrated earlier. Let us perform the latter (2).
From Example 5.1:

$$z = 0.1826 + j0.784 \frac{\Omega}{\text{mi.}} \text{ per phase}$$

$$y = \frac{1}{X_C \angle -90^\circ} = \frac{1}{185.5 \times 10^3} \angle 90^\circ = 5.391 \angle 90^\circ \frac{\text{S}}{\text{mi.}} / \text{ per phase}$$

Using $l = 200$ mi.:

$$\text{Z} = \text{z} \cdot \text{l} = 36.52 + j156.8 = 160.99 \angle 76.89^\circ$$

$$\text{Y} = y \cdot l = 1.078 \cdot 10^{-3} \angle 90^\circ$$

Now, to use the charts in Figures 5.9 through 5.11, we need the magnitude and phase of ZY.
As before:

$$Z \cdot Y = 160.99 \angle 76.89^\circ \cdot 1.078 \cdot 10^{-3} \angle 90^\circ = 0.1736 \angle 166.89^\circ$$

Using the preceding value for the magnitude and phase of ZY and the graphs in Figures 5.9 and 5.11, respectively, we have

$$\frac{\sinh(\gamma l)}{\gamma l} = 0.972 \angle 0.37^\circ \rightarrow Z' = Z \frac{\sinh(\gamma l)}{\gamma l} = 160.99 \angle 76.89^\circ \cdot 0.972 \angle 0.37^\circ$$

$$= 156.48 \angle 77.26^\circ$$

From Figure 5.11, we have

$$\frac{\tanh(\gamma l / 2)}{\gamma l / 2} = 1.0144 \angle -0.19^\circ \rightarrow Y / 2' = \frac{Y}{2} \left[\frac{\tanh\left(\frac{\gamma l}{2}\right)}{\frac{\gamma l}{2}} \right]$$

$$= 0.5476 \times 10^{-3} \angle 89.81^\circ$$

Using the lumped-parameter equivalent circuit for a long transmission line as in Figure 5.8,

$$I_{Z'} = I_R + V_R \frac{Y'}{2}$$

$$= 502\angle 0° + (132{,}800\angle 0°)\left(0.5476 \times 10^{-3}\angle 89.81°\right)$$

$$= 507.5\angle 8.24°$$

$$V_S = V_R + I_{Z'}Z'$$

$$= 132{,}800\angle 0° + 507.5\angle 8.24°\left(156.48\angle 77.26°\right)$$

$$= 160{,}835\angle 29.45°\,\text{V}$$

Also:

$$I_S = I_{Z'} + V_S \frac{Y'}{2}$$

$$= (502.24 + j72.72) + 160.855\left(0.5476 \times 10^{-3}\angle 29.49° + 89.81°\right)$$

$$= 482.93\angle 18.04°\,\text{A}$$

$$S = 3V_S I_S^*$$

$$= 3(160{,}835\angle 29.45°)(482.93\angle -18.04°) = (228.41 + j46.1)\,\text{MVA} = P_S + jQ_S$$

$$\text{Voltage regulation} = \frac{160.835 - 132.8}{132.8} \times 100 = 21.6\% \text{ as before}$$

We now proceed to find the *power flow* through a transmission line using

1. The A, B, C, D constants
2. The method needs to be applied to any two terminal pair network

Reiterating once again the items in point (1) from Equations 5.11, 5.12 and 5.13a,b, we have

$$V_S = AV_R + BI_R \tag{5.52}$$

Then,

$$I_R = \frac{V_S - AV_R}{B} \tag{5.53}$$

Equations 5.52 and 5.53 are both phasor equations, where:

$$A = |\text{A}|\angle\xi \text{ and } B = |\text{B}|\angle\eta \tag{5.54}$$

We will use the receiving end voltage as a reference, given by

$$V_R = |V_R|\angle 0° \tag{5.55}$$

and the sending end voltage, given by

$$V_S = |V_S| \angle \delta \tag{5.56}$$

which yields

$$I_R = \frac{|V_S|}{|B|} \angle(\delta - \eta) - \frac{|A||V_R|}{|B|} \angle(\xi - \eta) \tag{5.57}$$

We can now evaluate complex power received using Equations 5.56 and 5.57 as follows:

$$S_R = V_R \cdot I_R^* = P_R + jQ_R \tag{5.58}$$

which yields real power at the receiving end as follows:

$$P_R = \frac{|V_S||V_R|}{|B|} \cos(\eta - \delta) - \frac{|A||V_R|^2}{|B|} \cos(\eta - \xi) \tag{5.59}$$

and the reactive power at the receiving end as follows:

$$Q_R = \frac{|V_S||V_R|}{|B|} \sin(\eta - \delta) - \frac{|A||V_R|^2}{|B|} \sin(\eta - \xi) \tag{5.60}$$

The phasors of Equations 5.59 and 5.60 are plotted in the complex plane, as shown in Figure 5.12. These show the corresponding magnitudes and angles, respectively. If V_S and V_R are line-to-neutral voltages, then the resulting power is per phase. If these are line to line, then the power is for three phases (Figure 5.13).

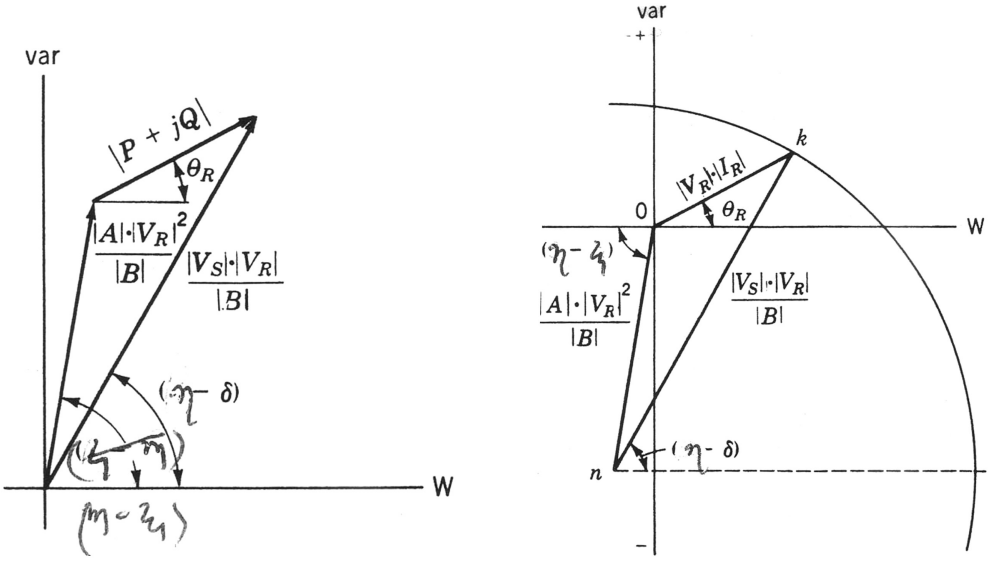

FIGURE 5.13
The resulting power diagram is obtained by shifting the origin of the coordinate axes of (a) and is shown in (b).

Points to note:

1. The location of point n does not depend on I_R and will not change as long as $|V_R|$ is constant.
2. The distance between points n and k remains constant for fixed $|V_R|$ and $|V_S|$.
3. The distance between points o and k changes with load, but a change in P_R requires a change in Q_R.

Power diagram (b) obtained by shifting the origin (a). Observe point n in this diagram and its relation to points k and o, respectively, distance-wise).

The same V_R but different V_S results in a new location for point n, resulting in a new power circle diagram, as shown in Figure 5.14.

As always, there is a limit to the power transmitted to the receiving end; thus,

$$P_{R_{\max}} = \frac{|V_S||V_R|}{|B|} - \frac{|A|\,|V_R|^2}{|B|}\cos(\eta - \xi) \tag{5.61}$$

That is, this occurs when point k moves along the circle until the angle (η-δ) is zero. Variations of $|V_S|$ and $|V_R|$ are used to study the addition of capacitor banks and the reactive power they draw; for example, if $|V_R|$ is kept constant and $|V_S|$ is reduced from $|V_{S4}|$ to $|V_{S3}|$, as in Figure 5.14, then the negative reactive power that must be drawn by capacitors added in parallel with the load is equivalent to distance *ab*, as shown in Figure 5.14.

5.4 Reactive Compensation of Transmission Lines

Reactive compensation provided to transmission lines improves the performance of medium and long lines using series or parallel compensation types. Figure 5.15 illustrates the reactive compensation of the series capacitor, as follows:

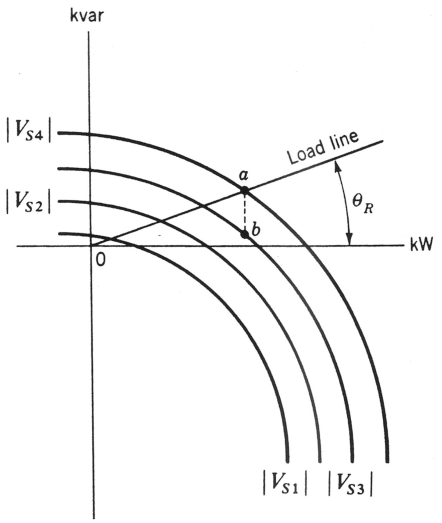

FIGURE 5.14
Receiving end power circles for various values of $|V_S|$ and $|V_R|$ respectively.

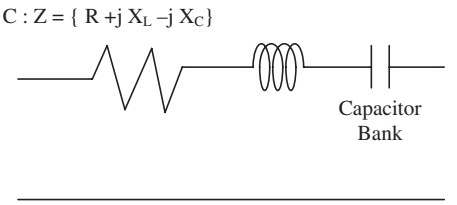

FIGURE 5.15
Series compensation using a capacitor.

$$Z = \{R + jX_L - jX_C\} \tag{5.62}$$

Such compensation using a series capacitor reduces the series impedance of the line for each line, as in Equation 5.62. The impedance in Equation 5.62 is the principal cause of voltage drop and is also the most important factor in determining the maximum power the line can transmit. This can be explained as follows:

$$B = Z \text{ for } \pi \text{ constants and equivalent } \pi \text{ constants: } Z\left(\frac{\sinh(\gamma l)}{\gamma l}\right)$$

The corresponding A, B, C and D are also likely to change, but such a change is generally small. The value of X_C can be found from the specific amount of the total X_L of the line by using the compensation factor X_C/X_L.

The second method is to provide shunt compensation, which is generally achieved by using a shunt reactor, as shown in Figure 5.16

Such shunt reactors are either air-core or gapped-core reactors [1], which partially or completely reduce the shunt susceptance of a high-voltage line, particularly at light loads when the receiving end voltage becomes very high. In this method, when the load on the transmission line is light or at no load, the charging current I_{chg} is important with the shunt reactor of susceptance B_L:

$$\begin{aligned} I_{chg} &= (B_C - B_L)|V| \\ &= B_C|V|\left(1 - \frac{B_L}{B_C}\right) \end{aligned} \tag{5.63}$$

where B_L/B_C is the shunt compensation factor.

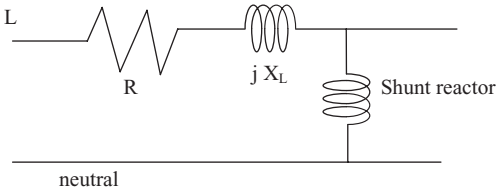

FIGURE 5.16
Reactive compensation using a shunt reactor on each line.

When shunt capacitance is neglected, $A = 1.0$. For medium and long lines, A is reduced. The reduction of shunt susceptance to $(B_C - B_L)$ can limit the rise of the no-load voltage at the receiving end of the line if shunt inductors are introduced as the load is removed.

5.5 Transmission Line Transients

Figure 5.17 shows a transmission line carrying a current I at distance x from the end. The voltage at distance x is v. This current increases to $i+(\partial i/\partial x)\Delta x$ and the voltage increases to $v+(\partial v/\partial x)\Delta x$ at a distance $(x+\Delta x)$. All distances are measured from the left end, which is the sending end.

1. When lightning strikes the ground, it causes an injection of current in the transmission line, which divides half the current flowing in one direction, say left to right, and the other half in the other direction from the point of contact on the transmission line. This current can be as high as 10,000 A.
2. When lightning hits the line directly, it can cause damage to the equipment, with voltages as high as 1 million V.
3. When lightning hits ground lines, it can also cause high-voltage surges on the power lines by electromagnetic induction. This requires an analysis of the transients that are caused as a result and necessitates the study of traveling waves in transmission lines.

5.6 Traveling Waves

1. We will consider only a lossless line analysis—that is, X_L and X_C, with resistance and conductance ignored.
2. As in Figure 5.17, the distance is measured as x from the sending end.
3. The series voltage drop along the elemental length of line is

$$i(R\Delta x) + L(\Delta x)\frac{\partial i}{\partial t} \tag{5.64}$$

Thus,

$$\frac{\partial v}{\partial x}\Delta x = -\left(Ri + L\frac{\partial i}{\partial t}\right)\Delta x \tag{5.65}$$

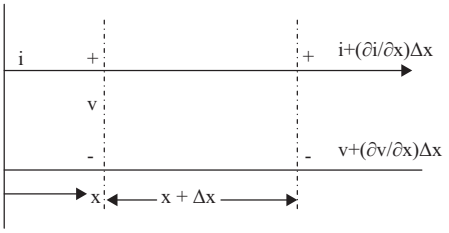

FIGURE 5.17
Transients in a transmission line.

The negative sign in Equation 5.65 is a result of

$$\left(v+\frac{\partial v}{\partial x}\Delta x\right)<v\ \forall \text{ positive values of } i \text{ and } \frac{\partial i}{\partial t}$$

Similarly,

$$\frac{\partial i}{\partial x}\Delta x=-\left(Gv+C\frac{\partial v}{\partial t}\right)\Delta x \tag{5.66}$$

If we now consider the values of R and G to be zero in Equations 5.65 and 5.66, we have

$$\frac{\partial v}{\partial x}=-\left(L\frac{\partial i}{\partial t}\right) \tag{5.67}$$

and

$$\frac{\partial i}{\partial x}=-\left(C\frac{\partial v}{\partial t}\right) \tag{5.68}$$

If we now differentiate Equation 5.67 with respect to x and Equation 5.68 with respect to t, we have

$$\frac{\partial^2 v}{\partial x^2}=-L\frac{\partial^2 i}{\partial x\partial t}\ \text{ and }\ \frac{\partial^2 i}{\partial x\partial t}=-C\frac{\partial^2 v}{\partial t^2} \tag{5.69}$$

$$\frac{1}{LC}\frac{\partial^2 v}{\partial x^2}=\frac{\partial^2 v}{\partial t^2} \tag{5.70}$$

This is the traveling wave equation of a lossless transmission line. This has a solution of the following form:

$$\text{Voltage: } u=v=f_1(x-vt) \tag{5.71}$$

where v is the velocity of the traveling wave in m/s for the forward-moving wave.

Equation 5.71 is a solution for Equation 5.70. Equation 5.71 is further explained as follows:

$$u=v=velocity=1/\sqrt{(LC)}\ \text{in m/s} \tag{5.72a}$$

Thus,

$$\frac{dx}{dt}=v=\frac{1}{\sqrt{LC}}\ \text{ in m/s} \tag{5.72b}$$

Equation 5.70 can also be solved as follows:

$$u=v=f_2(x+vt) \tag{5.73}$$

for a wave traveling in the opposite direction.

Thus, the total solution for Equation 5.70 is given by

$$v = f_1(x - vt) + f_2(x + vt) \tag{5.74}$$

$$v = v^+ + v^- \tag{5.75}$$

where

$$i^+ = \frac{1}{\sqrt{LC}} f_1(x - vt) \tag{5.76}$$

$$i^- = -\frac{1}{\sqrt{LC}} f_2(x + vt) \tag{5.77}$$

yielding

$$\text{Characteristic impedance } Z_C \text{ of line} \rightarrow \frac{v^+}{i^+} = \sqrt{\frac{L}{C}} \tag{5.78}$$

and

$$\text{Characteristic impedance } Z_C \text{ of line} \rightarrow \frac{v^-}{i^-} = -\sqrt{\frac{L}{C}} \tag{5.79}$$

5.7 Transient Analysis of Reflections

As shown in Figure 5.18, consider a line terminated in a pure resistance Z_R and a sending end voltage applied to it through a switch by a source v_s. The sending end current is i_s, and the corresponding receiving end voltage and current are v_R and i_R, respectively.

When the switch S is closed, a voltage wave v^+ accompanied by a current wave i^+ start to travel along the line, and at the receiving end,

$$\frac{v_R}{i_R} = Z_R \tag{5.80}$$

Also at the receiving end, one has v^- and i^- as reflected waves; therefore,

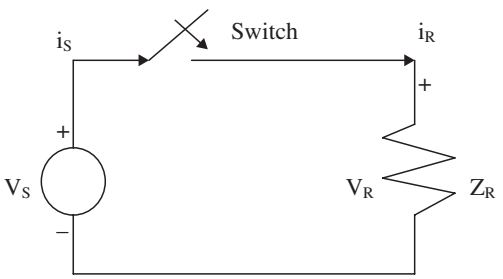

FIGURE 5.18
Transmission line terminated in pure resistance Z_R.

$$\frac{v_R}{i_R} = \frac{v_R^+ + v_R^-}{i_R^+ + i_R^-} = Z_R \tag{5.81}$$

Let the characteristic impedance

$$Z_C = \sqrt{\frac{L}{C}} \tag{5.82}$$

Then,

$$i_R^+ = \frac{v_R^+}{Z_C} \quad \text{and} \quad i_R^- = -\frac{v_R^-}{Z_C} \tag{5.83}$$

Using Equation 5.83 in 5.81 yields

$$\frac{v_R^+ + v_R^-}{i_R^+ + i_R^-} = \frac{v_R^+ + v_R^-}{\frac{v_R^+}{Z_C} - \frac{v_R^-}{Z_C}}$$

$$\rightarrow v_R^+ \left(1 - \frac{Z_R}{Z_C}\right) = -v_R^- \left(1 + \frac{Z_R}{Z_C}\right)$$

$$v_R^- = \left(\frac{-1 + \frac{Z_R}{Z_C}}{1 + \frac{Z_R}{Z_C}}\right) v_R^+ = \left(\frac{Z_R - Z_C}{Z_R + Z_C}\right) v_R^+ \tag{5.84}$$

$$\text{Voltage regulation coefficient } \rho_R = \frac{v_R^-}{v_R^+} = \frac{Z_R - Z_C}{Z_R + Z_C} \tag{5.85}$$

The reflection coefficient of the current is the negation of that of the voltage reflection coefficient.

$$\frac{i_R^+}{i_R^-} = -\frac{v_R^+}{v_R^-} \tag{5.86}$$

Thus, from Equation 5.85, if $Z_R = Z_C$ as termination, then

$$\rho_R = 0 \tag{5.87}$$

Meaning there is no reflected wave and the line is ∞ long.

If the termination is in a short circuit:

$$\rightarrow Z_R = 0 \rightarrow \rho_R = -1 \tag{5.88}$$

If the termination is in an open circuit:

$$\rightarrow Z_R = \infty \rightarrow \rho_R = +1$$

Note: Waves traveling back toward the sending end will cause new reflections, depending on

$$\rho_S = \frac{Z_S - Z_C}{Z_S + Z_C} \tag{5.89}$$

Example 5.4

As shown in Figure 5.19 at time $t = 0$, a 30 V battery with $R_S = 0$ is connected to a transmission line. Sketch the distribution of the voltage along the line for several instants of time. The velocity of the traveling wave is 200 m/μs. $R_C = 50\ \Omega$ and $R_R = 100\ \Omega$. The length of the transmission line is 400 m. The time taken by the traveling wave to travel along the transmission line is 2 μs.

SOLUTION 5.4

Thus, from the data given, and from Equations 5.85 and from 5.89, we have

$$\rho_R = \frac{R_R - R_C}{R_R + R_C} = \frac{100 - 50}{100 + 50} = \frac{1}{3}$$

$$\rho_S = \frac{R_S - R_C}{R_S + R_C} = \frac{0 - 50}{0 + 50} = -1$$

The traveling wave is thus shown at different instants at different distances from the sending end in Figures 5.20, 5.21, 5.22 and 5.23 at $t = 1$ μs, $t = 2.5$ μs, $t = 4.5$ μs and $t = 6.5$ μs, respectively.

At $t = 0$:

A 30 V pulse is sent down the line. The voltage is zero prior to the arrival of the pulse and 30 V after its departure.

At $t = 1$ μs, as shown in Figure 5.20:

The forward wave is at $x = 200$ meters as v^+.
The reflected wave is at $x = 600$ meters as v^-.

At $t = 2.5$ μs, as shown in Figure 5.21:

The pulse has already arrived at the load end.

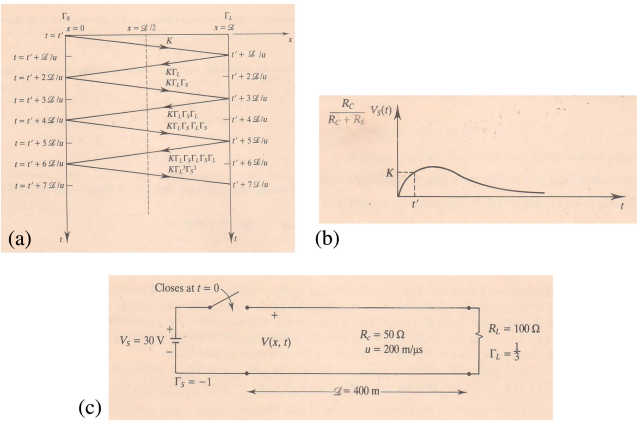

FIGURE 5.19
Transmission line with a dc supply of 30 volts

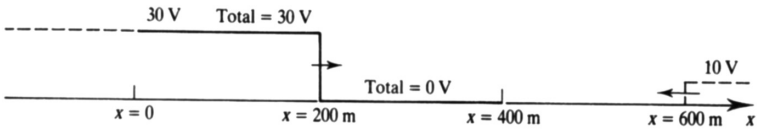

(*b*) $t = 1\ \mu s$

FIGURE 5.20
Traveling wave at $t = 1\ \mu s$.

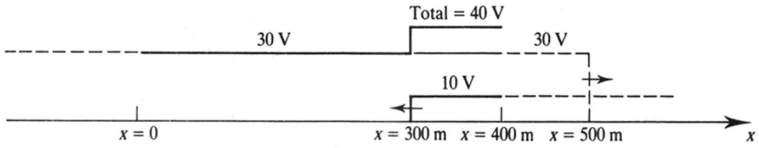

(*c*) $t = 2.5\ \mu s$

FIGURE 5.21
Traveling wave at $t = 2.5\ \mu s$.

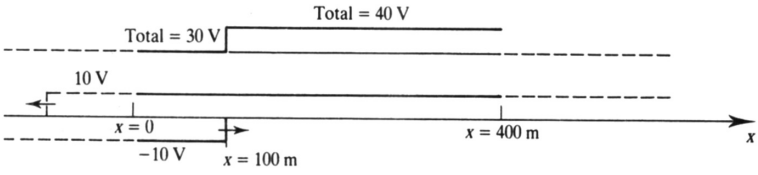

(*d*) $t = 4.5\ \mu s$

FIGURE 5.22
Traveling wave at $t = 4.5\ \mu s$.

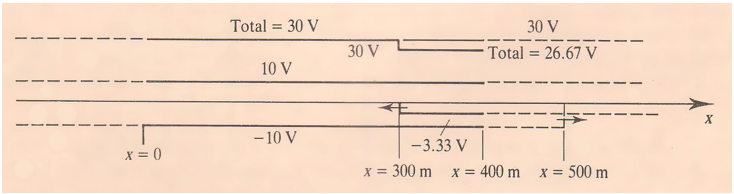

FIGURE 5.23
Travelling wave at $t = 6.5\ \mu s$.

A backward traveling pulse of magnitude $30 \times \rho_R = 10$ V is sent toward the source.

At $t = 4\ \mu s$:

A 10 V reflected pulse arrives at source
A pulse of -10 V $= 10$ V $\times \rho_S = -10$ V is sent back toward the load.

At $t = 4.5\ \mu s$:

The waves are shown in Figure 5.22.

At $t = 6\ \mu s$:

A –10 V pulse reaches the load.
A reflected wave of magnitude $\rho_R(-10\ V) = -10/3 = -3.33$ V is sent back to the source.

The final traveling wave is shown at $t = 6.5$ μs in Figure 5.23.

The time required to transit the line in one direction is 2 μs.

Problems

PROBLEM P.5.1

1. Draw the phasor diagram for the voltage and current phasors for a short transmission line, as shown in Figure P.5.1.
2. Evaluate the voltage regulation.
3. Relate regulation to the impedance angle or power factor (pf).

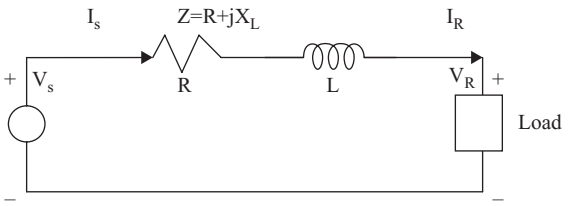

FIGURE P.5.1
Short transmission line.

PROBLEM P.5.2

A 60 Hz short transmission line has an R of 0.62 Ω per phase and L of 9.34 mH per phase. This transmission line supplies a three-phase, wye-connected 100 MW load of 0.9 pf lagging at 215 kV line-to-line voltage.

1. Calculate the sending.
2. Calculate the voltage regulation.
3. Find the power loss per phase.
4. Find the efficiency of the transmission of the transmission line.

PROBLEM P.5.3

A 10 km-long short transmission line has 0.5 with 60° Ω/km impedance. The line supplies a load at 316.8 kW at 0.8 pf lagging.

1. Find the voltage regulation if the receiving end voltage is 3.3 kV.
2. Find the efficiency of the transmission line.

PROBLEM P.5.4

Find the sending power for the short transmission line of Problem P.5.3 using

1. A loss calculation
2. The sending end voltage and power factor

PROBLEM P.5.5

A short transmission line has a per phase impedance of $(0.3+j0.4)\ \Omega$. The sending end line-to-line voltage is 3300 V, and the load at the receiving end is 300 kW per phase at 0.6 pf lagging.

1. Find the receiving end voltage.
2. Find the line current on a per-phase basis.

PROBLEM P.5.6

The per-phase parameters for a 60 c/s, 200 km-long transmission line are $R=2.07\ \Omega$, $L=310.8$ mH and $C=1.474\ \mu$F.

The line supplies a 100 MW, wye-connected load at 215 kV (line-to-line) and 0.9 pf lagging.

1. Find the sending end voltage, using the nominal π-circuit representation.
2. Find the sending end voltage, using the nominal T-circuit representation.
3. Use the *ABCD* constants to find the sending end voltage.

PROBLEM P.5.7

The pu length parameters of a 215 kV, 400 km, 60 Hz, three-phase long transmission line are

$$y = j3.2\times\frac{10^{-6}S}{\text{km}}$$

and

$$z=\left(0.1+j0.5\right)\Omega/\text{km}$$

The line supplies a 150 MW load at upf.

1. Find the voltage regulation.
2. The sending-end power.
3. Efficiency of transmission.

PROBLEM P.5.8

At time $t=0$, a 30 V battery with zero source resistance is connected to the transmission line, as shown in Figure P.5.8. Sketch the distribution of the voltage along the line for several instants of time.

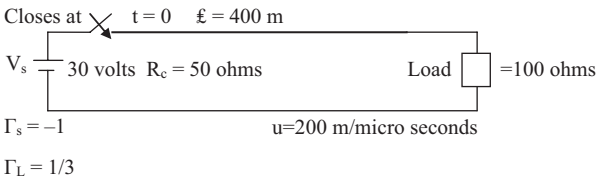

FIGURE P.5.8
30 V battery connected to a transmission line.

PROBLEM P.5.9

The transmission line of Problem P.5.8 terminates in a sc (i.e. $R_L = 0$) and is driven by a pulse source with an internal resistance of 150 Ω (i.e., $R_s = 150$ Ω). The source produces a pulse of magnitude 100 V and duration of 6 μs. Sketch the voltage $V(0,t)$ at the input to the line for the first 18 μs. The cable parameters are $C = 100$ pF/m and $L = 0.25$ μH/m.

PROBLEM P.5.10

A 300 MVA 20 kV three-phase generator has a subtransient reactance of 20%, as shown in Figure P.5.10. The generator supplies a number of synchronous motors over a 64 km short transmission line with transformers at both ends. The motors are all rated at 13.2 kV and are represented by just two equivalent motors. The neutral of one motor M_1 is grounded through a resistance. The neutral of the second motor M_2 is not connected to ground. Motors are rated at $M_1 = 200$ MVA and $M_2 = 100$ kVA, Both motors have a subtransient reactance of 20%. The three-phase transformer T_1 is rated at 350 MVA, 230/20 kV with leakage reactance of 10%. The transformer T_2 is comprised of three single-phase transformers, each rated 127/13.2 kV, 100 MVA with a leakage reactance of 10%. The series reactance of the transmission line is 0.5 Ω/km. Draw the reactance diagram with all reactances marked in pu. Select the generator rating as the base in the generator circuit.

FIGURE P.5.10
Two motors and a generator connected to a single generator via a short transmission line.

PROBLEM P.5.11

If the motors M_1 and M_2 in Problem P.5.10 have inputs of 120 MW and 60 MW, respectively, at 13.2 kV, and both operate at upf, find

1. The voltage at the terminals of the generator
2. The voltage regulation of the short line

PROBLEM P.5.12

A single-circuit 60 c/s transmission line is 370 km (230 mi.) long. The conductors are Rooks with flat spacing and 7.25 m (23.8 ft.) between them. The load on line is 125 MW at 215 kV at upf.

Find

1. The voltage, current and pf at the sending end and the voltage regulation of the line
2. The wavelength and velocity of the propagation of the line

PROBLEM P.5.13

A three-phase transmission line is 300 mi. long and serves a load of 400 MVA, with 0.8 pf lagging at 345 kV. The *ABCD* constants are

$$A = D = 0.8180\angle 1.3°$$

$$B = 172.2\angle 84.2° \ \Omega$$

$$C = 0.001933\angle 90.4° \text{S}$$

Find

1. The sending end line-to-neutral voltage
2. The sending end current
3. The percentage of voltage drop at full load
4. The receiving end line-to-neutral voltage at no load
5. The sending end current at no load
6. The voltage regulation

PROBLEM P.5.14

Solve Problem P.5.13 using the hyperbolic relations instead of the *ABCD* constants.

PROBLEM P.5.15

The shunt admittance of a 300 mi.-long transmission line is

$$y_c = 0 + j6.87 \times 10^{-6} \text{ S/mi.}$$

Find the *ABCD* constants of a shunt reactor that will compensate for 60% of the shunt admittance.

PROBLEM P.5.16

Construct a receiving end power circle diagram similar to Figure 5.14 for the line of Problem P.5.13. Locate the point corresponding to the load of Problem P.5.13 and locate the center of circles for various values of $|V_s|$ if $|V_R| = 220$ kV.

1. Draw the circle passing through the load point.

2. From the measured radius of the latter circle, determine $|V_S|$ and compare this value with the values calculated for Problem P.5.13.

PROBLEM P.5.17

A 250 MVAR, 345 kV shunt reactor whose admittance is $0.0021\angle -90°\,\text{S}$ is connected to the receiving end of the 300 mi. line of Problem P.5.13 at no load.

1. Find the equivalent *ABCD* constants of the line in series with the shunt reactor.
2. Recalculate Problem P.5.13b using these *ABCD* constants and the sending end voltage found in that problem.

PROBLEM P.5.18

A 60 c/s, three-phase CTC transmission line has the following total parameters:

$$Z = 13.114 + j52.952\ \Omega$$

$$Y = j0.311\times 10^{-3}$$

The sending end line-to-line voltage is 161 kV. The total receiving end load is represented by the load impedance:

$$Z_L = 143\angle 36.8°$$

1. Find receiving end line-to-line voltage.
2. Find the voltage regulation.
3. Calculate the sending end current.
4. Calculate the real and reactive power at the sending end.
5. Calculate the power delivered at the receiving end.
6. Find the transmission efficiency.

PROBLEM P.5.19

A 60 c/s, three-phase transmission line is 175 mi. long. It has a total series line impedance of $35 + j140\ \Omega$ and a shunt admittance of 930×10^{-6} S. The line delivers a power of 40 MW at 220 kV and 0.9 pf lagging.

Find the voltage of the sending end using the methodology of a long line.

PROBLEM P.5.20

A 60 c/s, three-phase transmission line is constructed of ACSR conductors and has the following parameters:

- Aluminum area (cmil) = 566,505
- Strands: (Al/St)=26/7

- Strand diameter = 0.1463 in.
- Approximate current rating = 730 A
- DC resistance (Ω/mil) = 0.1621
- 60 c/s resistance at 20°C = 0.1663
- 60 c/s resistance at 50°C = 0.1826

The line is 400 km long and is expected to receive a power of 150 MW at upf and a rated line-to-line voltage of 161 kV. Find

1. The sending end voltage
2. The sending end current
3. The sending end real power
4. The sending end imaginary power
5. The power loss in the line

PROBLEM P.5.21

A three-phase, 140 kV, 100 km transmission line consists of three conductors arranged as shown in Figure P.5.21.

Tests reveal the following parameters for the line:

- Resistance = 0.0910 Ω/km/phase
- Inductance = 1.34 mH/km/phase
- Capacitance = 8.55×10^{-9} farads/km/phase
- $D = 5$ m
- Diameter of conductors = 50 mm (~2 in.)

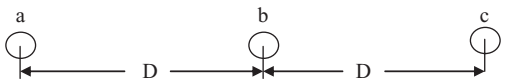

FIGURE P.5.21

Compute the sending end power if the receiving end voltage is $|V_2| - 140$ kV RMS and the receiving end power is $S_2 = 100 + j60$ (three-phase mega-values). Assume the line to be electrically short.

Reference

1. Buckmaster, D. E. and H. Shertukde, "Transformers for Wind Turbine Generators and Photovoltaic Applications", in J. H. Harlow (ed.), *Electric Power Transformer Engineering*. 3rd edition. CRC Press, Boca Raton, FL, 2012.

6

Network Calculations

6.1 Introduction

Having evaluated in the preceding chapters all the parameters of a single-line diagram (SLD) describing a power system, from the generator end to the load end, inclusive of generator(s), transformer(s), transmission line(s), motor(s) and load(s), we are now ready to start making the network calculations essential for a working power system to maintain reliability and stability in delivering power from one point to another in the SLD. To solve this problem we have to create *source equivalence* for the ease of network analysis. This entails the substitution of a source of constant current in parallel with an impedance for a constant electromagnetic force (EMF) source in series with an impedance, as shown in Figure 6.1.

From Figure 6.1a we have

$$V_L = E_g - I_L Z_g \tag{6.1}$$

And from Figure 6.1b we have

$$V_L = \left(I_S - I_L\right) Z_p = I_S Z_p - I_L Z_p \tag{6.2}$$

In both the cases, the voltage across the load and the current flowing through the load are equal and same. Further, if

$$E_g = I_S Z_p \text{ and } Z_g = Z_p \tag{6.3}$$

then

$$I_S = \frac{E_g}{Z_p} \tag{6.4}$$

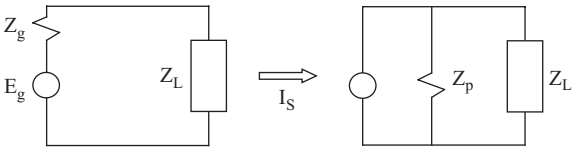

FIGURE 6.1
Series (a) and parallel (b) representation of a network.

Similar results can be obtained for load networks with active components of sources. This is regularly done by using the *superposition theorem*, where voltage sources are short-circuited and current sources are opened as usual.

6.2 Node Equations

We can now proceed to obtain the nodal equations while carefully defining the following with reference to Figure 6.2:

1. *R*, *L* or *C*, ideal voltage or current sources are defined as *elements.*
2. Junctions formed when two or more pure and passive elements *R*, *L* or *C*, ideal voltage or current sources are connected to each other are called *nodes*.
3. Nodes to which more than two elements are connected, as in (1), are called *major nodes* (Figure 6.3).

We will use KCL at all nodes in Figure 6.4 except the reference node 0 (zero). We will use single subscript notation and a three-phase circuit with a neutral; the neutral is the reference node 0.

Thus, at all nodes 1 through 4, respectively:

$$\begin{aligned} I_1 &= V_1 Y_a + (V_1 - V_3) Y_f + (V_1 - V_4) Y_d \\ I_1 &= V_1 (Y_a + Y_f + Y_d) - V_3 Y_f - V_4 Y_d \\ I_2 &= V_2 Y_b + (V_2 - V_3) Y_g + (V_2 - V_4) Y_h \end{aligned} \tag{6.5}$$

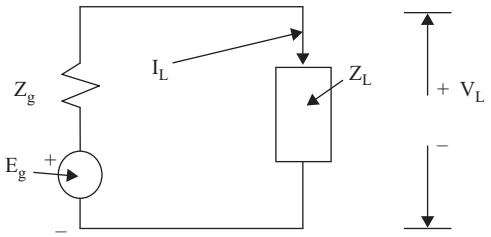

FIGURE 6.2
SLD of a power system with elements.

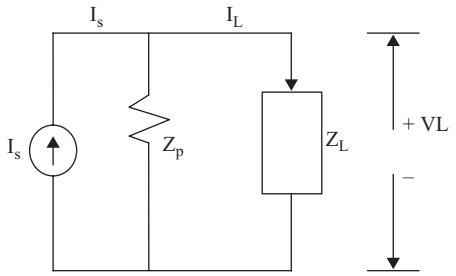

FIGURE 6.3
SLD of a power system with equivalent circuit representation of all elements as reactances and voltage sources.

$$I_2 = V_2\left(Y_b + Y_g + Y_h\right) - V_3 Y_g - V_4 Y_h \tag{6.6}$$

$$I_3 = V_3 Y_c + \left(V_3 - V_1\right) Y_f + \left(V_3 - V_2\right) Y_g + \left(V_3 - V_4\right) Y_e$$

$$I_3 = -\left(V_1\right) Y_f - V_2 V_g + V_3\left(Y_f + Y_g + Y_c + Y_e\right) - V_4 Y_e \tag{6.7}$$

$$0 = \left(V_4 - V_1\right) Y_d + \left(V_4 - V_2\right) Y_h + \left(V_4 - V_3\right) Y_e$$

$$0 = -V_1 Y_d - V_2 Y_h - V_3 Y_e + V_4\left(Y_d + Y_h + Y_e\right) \tag{6.8}$$

Notes:

1. The number of independent node equations is one less than the number of nodes; thus, in the example in Figure 6.4, there are $(4-1)=3$ independent node equations, as in Equations 6.5, 6.6 and 6.7, respectively.
2. At any node the current equation has on the right-hand side, one term is the voltage of the respective node times the sum of the admittances that terminate at that particular node. This is further evident by examining Equations 6.5 through 6.8, respectively. Further from Equations 6.5 through 6.8 we have

$$\begin{bmatrix} I_1 \\ I_2 \\ I_3 \\ I_4 \end{bmatrix} = \begin{bmatrix} Y_{11} & Y_{12} & Y_{13} & Y_{14} \\ Y_{21} & Y_{22} & Y_{23} & Y_{24} \\ Y_{31} & Y_{32} & Y_{33} & Y_{34} \\ Y_{41} & Y_{42} & Y_{43} & Y_{44} \end{bmatrix} \begin{bmatrix} V_1 \\ V_2 \\ V_3 \\ V_4 \end{bmatrix} \tag{6.9}$$

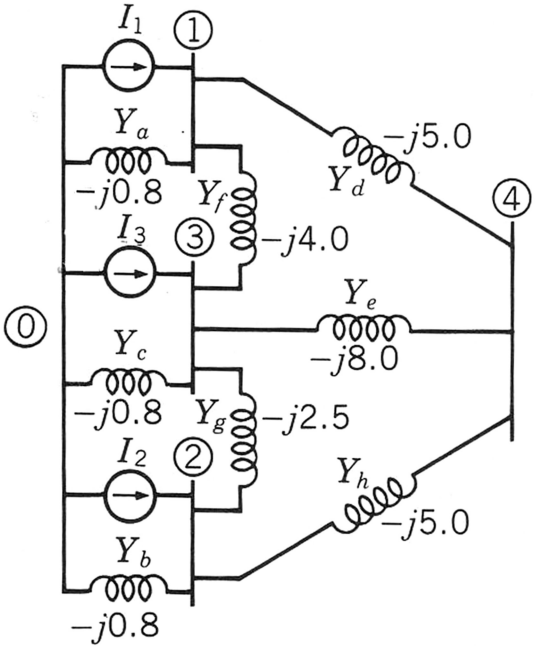

FIGURE 6.4
SLD of a power system with equivalent circuit representation of all elements as reactances and voltage sources replaced by current sources.

where:

$$Y_{11} = Y_a + Y_f + Y_d$$

$$Y_{12} = 0$$

$$Y_{13} = -Y_f$$

$$Y_{14} = -Y_d$$

$$Y_{21} = 0$$

$$Y_{22} = Y_b + Y_g + Y_h$$

$$Y_{23} = -Y_g$$

$$Y_{24} = -Y_h$$

$$Y_{31} = -Y_f$$

$$Y_{32} = -Y_g$$

$$Y_{33} = Y_f + Y_g + Y_c + Y_e$$

$$Y_{34} = -Y_e$$

$$Y_{41} = -Y_d$$

$$Y_{42} = -Y_h$$

$$Y_{43} = -Y_e$$

$$Y_{44} = Y_d + Y_h + Y_e$$

In matrix form, the preceding equations can be written as follows:

$$I = Y_{\text{bus}} \cdot V \rightarrow Y_{\text{bus}}{}^{-1} \quad I_{\text{bus}} = Z \cdot I = \left[\ddots\right] V_{\text{bus}}$$

where:

I	is an $[n \times 1]$ current column matrix
V	is an $[n \times 1]$ voltage column matrix
Y_{bus}	is an $[n \times n]$ admittance square matrix
[.]	is an [x n] identity matrix
Z_{bus}	is an $[n \times n]$ impedance matrix

As one can see, Y_{bus} is a symmetrical matrix, where Y_{ii} are called *self-admittances* and Y_{ij} are called *mutual admittances*.

$$Y_{\text{bus}} = [Yij];\ i = 1, 2, \ldots, n \ \text{ and } \ j = 1, 2, \ldots, n$$

Thus, the source current toward node k is

$$I_k = \sum_{n=1}^{N} Y_{kn} V_n, \text{ for an } N \text{ independent bus system} \tag{6.10}$$

Example 6.1

This example is related to Figure 6.1, where the values of the EMF sources are as follows:

$$E_a = 1.5\angle 0^\circ;\ E_b = 1.5\angle -36.87^\circ;\ E_c = 1.5\angle 0^\circ, \text{ all in pu}$$

The values of the different impedances are as follows:

$$Z_a = j1.25 = Z_c;\ Z_b = j1.25$$

Thus,

$$I_1 = \frac{E_a}{Z_a} = \frac{1.5\angle 0^\circ}{j1.25} = 1.2\angle -90^\circ = I_3 = 0 - j1.2 \text{ in pu}$$

$$I_2 = \frac{I_b}{Z_b} = \frac{1.5\angle -36.87^\circ}{j1.25} = 1.2\angle -126.87^\circ = -0.72 - j0.96 \text{ in pu}$$

The nodal equations from Equation 6.9 are

$$\begin{bmatrix} I_1 \\ I_2 \\ I_3 \\ I_4 \end{bmatrix} = \begin{bmatrix} Y_{11} & Y_{12} & Y_{13} & Y_{14} \\ Y_{21} & Y_{22} & Y_{23} & Y_{24} \\ Y_{31} & Y_{32} & Y_{33} & Y_{34} \\ Y_{41} & Y_{42} & Y_{43} & Y_{44} \end{bmatrix} \begin{bmatrix} V_1 \\ V_2 \\ V_3 \\ V_4 \end{bmatrix}$$

$$\begin{bmatrix} 0 - j1.2 \\ -.72 - j0.96 \\ 0 - j1.2 \\ 0 \end{bmatrix} = \begin{bmatrix} -j9.8 & j0.0 & j4.0 & j5.0 \\ j0.0 & -j8.3 & j2.5 & j5.0 \\ j4.0 & j2.5 & -j15.3 & j8.0 \\ j5.0 & j5.0 & j8.0 & -j18.0 \end{bmatrix} \begin{bmatrix} V_1 \\ V_2 \\ V_3 \\ V_4 \end{bmatrix}$$

yielding the voltage using MATLAB® as follows:

$$\begin{bmatrix} V_1 \\ V_2 \\ V_3 \\ V_4 \end{bmatrix} = \begin{bmatrix} 1.436\angle -10.71^0 \\ 1.427\angle -14.24^0 \\ 1.434\angle -11.36^0 \\ 1.432\angle -11.47^0 \end{bmatrix} \text{ all in pu}$$

6.3 Matrix Partitioning

Matrix partitioning is a necessary tool for solving problems with dependent node equations in a given power system SLD. We will tackle this method as follows.

Say A is a 3×3 square matrix, as shown in Equation 6.11, and is partitioned as shown by the dashed lines to form the submatrices D, E, F and G, as in Equation 6.11

$$A=\begin{bmatrix} a_{11} & a_{12} & a_{13} \\ a_{21} & a_{22} & a_{23} \\ a_{31} & a_{32} & a_{33} \end{bmatrix}=\begin{bmatrix} D & E \\ F & G \end{bmatrix} \tag{6.11}$$

Let B be a column matrix partitioned with the dashed line as follows:

$$B=\begin{bmatrix} b_{11} \\ b_{21} \\ b_{31} \end{bmatrix}=\begin{bmatrix} H \\ J \end{bmatrix} \tag{6.12}$$

Say matrix C is the product of matrices A and B, as follows:

$$C=A\cdot B=\begin{bmatrix} D & E \\ F & G \end{bmatrix}\cdot\begin{bmatrix} H \\ J \end{bmatrix}=\begin{bmatrix} DH & + & EJ \\ FH & + & GJ \end{bmatrix}=\begin{bmatrix} M \\ N \end{bmatrix}$$

$$s.t\ M=DH+EJ \text{ and } N=FH+GJ \tag{6.13}$$

The preceding mechanics are used for node elimination using matrix algebra, as in the case of Equation 6.9, recreated here as Equation 6.14:

$$I=Y_{\text{bus}}V \tag{6.14}$$

To apply the preceding partitioning to the solution, the nodes to be eliminated are reduced from Equation 6.14 by rearranging the node equations associated with such nodes at the bottom of the Y_{bus} matrix, as follows:

$$I=\begin{bmatrix} I_A \\ I_x \end{bmatrix}=\begin{bmatrix} K & L \\ L^T & M \end{bmatrix}\begin{bmatrix} V_A \\ V_x \end{bmatrix} \tag{6.15}$$

where:

- I_x is the submatrix of currents entering the nodes to be eliminated (elements of this submatrix should be zero to be eliminated)
- V_x is a submatrix composed of voltages of nodes to be eliminated
- I_A is the submatrix of currents to be retained
- V_A is the submatrix of voltages to be retained

Thus, applying the result of Equation 6.13 to Equation 6.15 yields

$$I_A=KV_A+LV_x \tag{6.16}$$

and

$$I_x = L^T V_A + M V_x \tag{6.17}$$

Because $I_x = 0$, we have

$$-L^T V_A = M V_x$$

$$\therefore V_x = -M^{-1} L^T V_A$$

$$\therefore I_A = K V_A - L M^{-1} L^T V_A = \left[K - L M^{-1} L^T \right] V_A \tag{6.17}$$

Applying this to Equation 6.14 yields the new admittance matrix with unwanted nodes eliminated, as follows:

$$Y_{\text{bus}} = \left[K - L M^{-1} L^T \right] \tag{6.18}$$

6.4 Node Elimination One at a Time

We now proceed to eliminate one node at a time by handling the original Y_{bus} matrix as shown in Equation 6.19, in which the top $(n-1)$ rows represent the submatrix L, and the first $(n-1)$ columns represent the submatrix L^T.

$$Y_{\text{busoriginal}} = \begin{bmatrix} Y_{11} & . & Y_{1j}.. & Y_{1n} \\ . & . & . & . \\ Y_{k1} & . & Y_{kj} & Y_{kn} \\ . & . & . & . \\ Y_{n1} & . & Y_{nj} & Y_{nn} \end{bmatrix} \tag{6.19}$$

The left nn element represents the submatrix M. The reduced $(n-1)\times(n-1)$ matrix is given by

$$Y_{\text{bus}} = \begin{bmatrix} Y_{11} & . & Y_{1j}.. & . \\ . & . & . & . \\ Y_{k1} & . & Y_{kj} & . \\ . & . & . & . \\ . & . & . & . \end{bmatrix} - \frac{1}{Y_{\text{nn}}} \begin{bmatrix} Y_{1\text{n}} \\ . \\ Y_{\text{kn}} \\ . \end{bmatrix} \begin{bmatrix} Y_{\text{n1}} & . & Y_{\text{nj}} & . \end{bmatrix} \tag{6.20}$$

where the $(n-1)\times(n-1)$ matrix has the kjth element, as follows:

$$Y_{kj}(\text{new}) = Y_{kj}(\text{original}) - \frac{Y_{kn} Y_{nj}}{Y_{nn}} \tag{6.21}$$

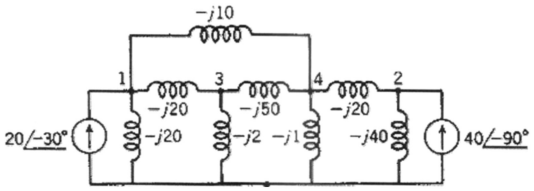

FIGURE 6.5
SLD of a simple power system for Example 6.2.

Example 6.2

An SLD of a Power System is shown in Figure 6.5. Solve the inversion of the original voltage matrix without eliminating nodes 3 and 4 and the inversion of the modified node voltage matrix after the elimination of nodes 3 and 4 using the MATLAB software.

Example 6.3

An example of a computer assignment with four buses and EMF sources connected to only two buses has a Y_{bus} matrix as follows:

$$Y_{\text{bus}} = \begin{bmatrix} -j10.5 & j0.0 & j5.0 & j5.0 \\ j0.0 & -j8.0 & j2.5 & j5.0 \\ j5.0 & j2.5 & -j18.0 & j10.0 \\ j5.0 & j5.0 & j10.0 & -j20.0 \end{bmatrix}$$

We eliminate nodes 3 and 4 (which have no EMF connected to them; i.e., the current into the node is zero) from the network. The Y_{bus} matrix is partitioned by the dashed lines such that the submatrices are as follows:

$$K = \begin{bmatrix} -j10.5 & j0.0 \\ j0.0 & -j8.0 \end{bmatrix}$$

$$L = \begin{bmatrix} j5.0 & j5.0 \\ j2.5 & j5.0 \end{bmatrix}$$

$$L^T = \begin{bmatrix} j5.0 & j5.0 \\ j2.5 & j5.0 \end{bmatrix}$$

$$M = \begin{bmatrix} -j18.0 & j10.0 \\ j10.0 & -j20.0 \end{bmatrix}$$

which yields

$$M^{-1} = -\frac{1}{260}\begin{bmatrix} -j20.0 & j10.0 \\ j10.0 & -j18.0 \end{bmatrix} = \begin{bmatrix} j0.0769 & j0.0385 \\ j0.0385 & j0.0692 \end{bmatrix}$$

$$LM^{-1}L^T = \begin{bmatrix} j5.0 & j5.0 \\ j2.5 & j5.0 \end{bmatrix}\begin{bmatrix} j0.0769 & j0.0385 \\ j0.0385 & j0.0692 \end{bmatrix}\begin{bmatrix} j5.0 & j5.0 \\ j2.5 & j5.0 \end{bmatrix}$$

$$LM^{-1}L^T = \begin{bmatrix} -j5.575 & -j4.135 \\ -j4.135 & -j3.173 \end{bmatrix}$$

$$\left[K - LM^{-1}L^T\right] = \begin{bmatrix} j5.0 & j5.0 \\ j2.5 & j5.0 \end{bmatrix} - \begin{bmatrix} -j5.575 & -j4.135 \\ -j4.135 & -j3.173 \end{bmatrix}$$

$$Y_{\text{busnew}} = \begin{bmatrix} -j4.975 & j4.135 \\ j4.135 & -j4.827 \end{bmatrix}$$

(*Note:* This example will also be verified using MATLAB® and ETAP© in Chapter 13.)

6.5 Modification of an Existing Bus Impedance Matrix

Let $Z_{\text{bus}} = Z_{\text{original}}$ as an xn matrix. It is known and is given by the following equation in matrix form:

$$V = Z_{\text{bus}} \cdot I \tag{6.22}$$

There are three cases that will be discussed that find place in real-time applications in a given power system.

Case 1: Adding Z_b from a new bus p to the reference bus, as shown in Figure 6.5.

1. Without connection to any other buses in the given power system SLD, the voltages at other buses are unaltered.
2. $V_p = Z_b \cdot I_P$, where I_P is the current injected at the new bus p.

Then, as shown by the dashed lines, the new form of Equation 6.22 becomes

$$\begin{bmatrix} V_1 \\ V_2 \\ . \\ . \\ V_n \\ V_p \end{bmatrix} = \begin{bmatrix} Z_{11} & . & Z_{1n} & 0 \\ . & . & . & . \\ Z_{n1} & . & Z_{nn} & 0 \\ 0 & . & 0 & Z_b \end{bmatrix} \begin{bmatrix} I_1 \\ I_2 \\ . \\ . \\ I_n \\ I_p \end{bmatrix} \tag{6.23}$$

The physical connection of the introduction of a new bus p is shown in Figure 6.6.

Case 2: Adding Z_b from a new bus p to an existing bus k, as shown in Figure 6.7.

1. Injecting I_p at bus p will cause the current entering the original network at bus k to change to

$$I_k + I_p \tag{6.24}$$

$$\therefore V_{k(\text{new})} = V_{k\ (\text{original})} + I_p Z_{kk} \tag{6.25}$$

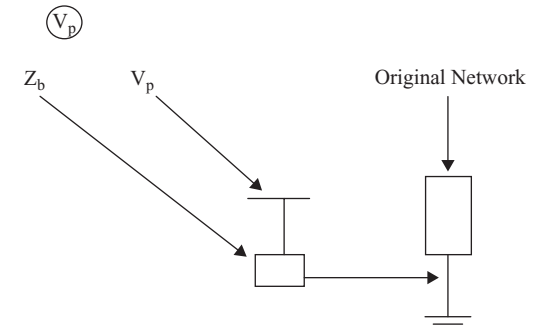

FIGURE 6.6
SLD for Case 1.

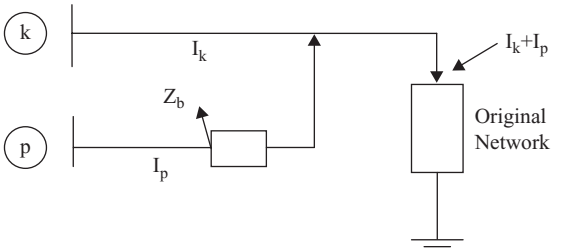

FIGURE 6.7
SLD for Case 2.

and

$$V_p = V_{k(\text{original})} + I_p Z_{kk} + I_p Z_b$$
$$= I_1 Z_{k1} + I_2 Z_{k2} + \ldots I_n Z_{kn} + I_p \left(Z_{kk} + Z_b \right) \tag{6.26}$$

Thus,

$$\begin{bmatrix} V_1 \\ V_2 \\ . \\ . \\ V_n \\ V_p \end{bmatrix} = \begin{bmatrix} Z_{11} & . & Z_{1n} & Z_{1k} \\ Z_{21} & . & . & Z_{2k} \\ . & . & . & . \\ Z_{n1} & . & Z_{nn} & Z_{nk} \\ Z_{k1} & . & Z_{kn} & Z_{kk} + Z_b \end{bmatrix} \begin{bmatrix} I_1 \\ I_2 \\ . \\ . \\ I_n \\ I_p \end{bmatrix} \tag{6.27}$$

Case 3: Adding Z_b from an existing bus k to the reference bus.

This problem can be solved using the solution in Case 2 by making bus p in Case 3 go to zero potential (i.e., $V_p = 0$), then proceeding to eliminate the $(n+1)$ row and $(n+1)$ column by node elimination, as seen at the beginning of the chapter.

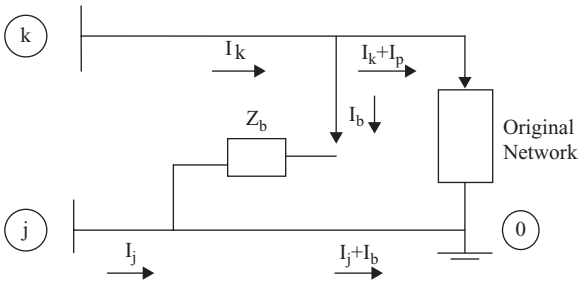

FIGURE 6.8
SLD for Case 4.

Then, Z_{new} has each element, given by

$$Z_{hi(\text{new})} = Z_{hi(\text{original})} - \frac{Z_{h(n+1)}Z_{(n+1)i}}{Z_{kk}+Z_b}, \text{ where } Z_{kk}+Z_b = Z_{n+1,n+1} \tag{6.28}$$

Case 4: Adding *Zb* between two existing buses *j* and *k*, as shown in Figure 6.8.

$$V_j = Z_{j1}I_1 + \ldots + Z_{jj}\left(I_j + I_b\right) + Z_{jk}\left(I_k - I_b\right)$$

$$= Z_{j1}I_1 + \ldots + Z_{jj}I_j + Z_{jk}I_k + I_b\left(Z_{jj} - Z_{jk}\right)$$

Similarly,

$$V_k = Z_{k1}I_1 + \ldots. + Z_{kj}I_j + Z_{kk}I_k + I_b\left(Z_{kj} - Z_{kk}\right)$$

$$I_b = \frac{V_k - V_j}{Z_b} \rightarrow V_k - V_j = I_b \cdot Z_b \rightarrow I_b \cdot Z_b - V_k + V_j = 0$$

$$0 = I_b \cdot Z_b + \left(Z_{j1} - Z_{k1}\right)I_1 + \ldots + \left(Z_{jj} - Z_{kj}\right)I_j + \left(Z_{jk} - Z_{kk}\right)I_k + \left(Z_{jj} + Z_{kk} - Z_{jk} - Z_{kj}\right)I_b$$

$$Z_{bb} = Z_b + Z_{jj} + Z_{kk} - 2Z_{jk} \tag{6.29}$$

Then, the new Z_{bus} is given by

$$\begin{bmatrix} V_1 \\ V_2 \\ . \\ . \\ V_n \\ 0 \end{bmatrix} = \begin{bmatrix} Z_{11} & . & Z_{1n} & Z_{1j} - Z_{1k} \\ Z_{21} & . & . & Z_{2j} - Z_{2k} \\ . & . & . & . \\ Z_{n1} & . & Z_{nn} & Z_{kj} - Z_{kn} \\ Z_{j1} - Z_{k1} & . & Z_{kj} - Z_{kn} & Z_{bb} \end{bmatrix} \begin{bmatrix} I_1 \\ I_2 \\ . \\ . \\ I_n \\ I_b \end{bmatrix} \tag{6.30}$$

Problems

PROBLEM P.6.1

1. From the results of Example 6.2, find the pu impedance between buses 1 and 2 of the circuit with nodes 3 and 4 eliminated.
2. Also determine the admittance between buses 1 and 2 and the reference bus.

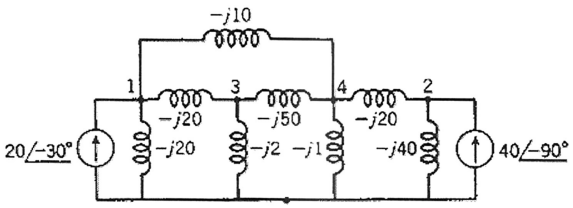

FIGURE P.6.1
Four-bus power system network.

PROBLEM P.6.2

1. Draw an equivalent circuit with the given current sources and admittances and with nodes 3 and 4 eliminated.
2. Redraw the equivalent circuit with voltage sources and impedances and with nodes 3 and 4 eliminated.

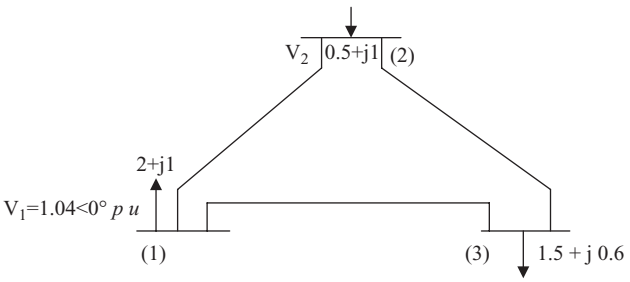

FIGURE P.6.2
SLD for Problem P.6.4.

PROBLEM P.6.3

Solve the problem shown in Figure 6.P.1 and find the Y_{bus}. Solve the required inversion of the original node voltage matrix without eliminating nodes 3 and 4 and the inversion of the modified node voltage matrix after eliminating nodes 3 and 4 using

1. Hand calculations
2. MATLAB software
3. ETAP software

PROBLEM P.6.4

A power system network is shown in Figure 6.P.2.

The Y_{bus} for the network is given by

$$Y_{bus} = \begin{bmatrix} 24.23\angle -79.95° & 12.13\angle 104.04° & 12.13\angle 104.04° \\ 12.13\angle 104.04° & 24.23\angle -75.95° & 12.13\angle 104.04° \\ 12.13\angle 104.04° & 12.13\angle 104.04° & 24.23\angle -75.95° \end{bmatrix}$$

Using the pu values for the voltages and power shown, find V_2 using the Newton–aphson method.

PROBLEM P.6.5

The SLD of a system is given in Figure P.6.5. The desired values are as follows:

$$|V_1| = |V_2| = 1\,\text{pu}$$

The loads are shown as

$$S_1 = 6 + j10\,\text{pu}$$

$$S_2 = 14 + j8\,\text{pu}$$

If the real power at each bus is 10 pu,

1. Find the power at the two bus ends.
2. Find the pfs at the two bus ends.

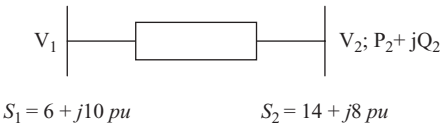

FIGURE P.6.5
SLD of a two-bus system.

PROBLEM P.6.6

As shown in Figure P.6.6,

$$V_1 = 1\angle 0°\ \text{pu}$$

$$Z_l = 0.05 + j0.02\,\text{pu}$$

$$P_2 + jQ_2 = 1.0 + j0.6\,\text{pu}$$

1. Find V_2.
2. Find $P_1 + j\,Q_1$.

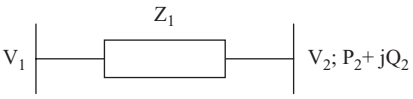

FIGURE P.6.6
Two-bus system.

PROBLEM P.6.7

It is necessary to have $|V_1| = |V_2| = 1.0$ pu by supplying reactive power at bus 2. Find the reactive power to be supplied at bus 2.

PROBLEM P.6.8

Two buses are interconnected by a transmission line of a given impedance of

$$Z = (0.3 + j1.2)\,\text{pu}$$

The voltage on one bus is given by $V_1 = 1\angle 0°$ and the load on the other bus is $(1 + j0.4)$ pu.

1. Find the pu voltage on the second bus.
2. Calculate the pu real and imaginary power on the first bus.

PROBLEM P.6.9

The pu impedance of a short transmission line is $j0.06$. The pu load on the line is $(1 + j0.6)$ pu at a receiving end voltage of $Z = (0.3 + j1.2)\,\text{p}\mu$.

1. Find the average imaginary power flow over the line.
2. Calculate the voltage regulation at the receiving end.

7

Load Flow Analysis

7.1 Load Flow Solutions and Control

In Chapter 6, we learned how to analyze power system networks via single-line diagrams (SLDs) and solutions to linear sets of equations for an n-bus system. We now proceed to find load flow solutions and the eventual control using two major methods:

1. **Newton–Raphson method**
2. **Gauss–Seidel method**

The Newton–Raphson method is a fast-converging method and an iterative process where the solution to the problem is achieved in two or three iterations, while the Gauss–Seidel method is simpler and less demanding of computer capability, besides having short comings, as it converges very slowly toward a solution for systems with a large number of buses. Both these methods are used to solve non-linear systems of equations that define an SLD.

Let n be the number of buses, of which n_g are generator buses. With this in mind, we develop our first equation, concerning the number of unknowns in a n-bus system, as follows:

$$\#\text{ of unknowns} = 2(n-1) - n_g \tag{7.1}$$

7.2 Newton–Raphson Method

Case 1: One unknown variable.

The solution is in two steps:

1. Making a good initial guess of the solution
2. Using Taylor series expansion

Let $p(y)$ be a non-linear function in a single variable y. We then solve for y

$$p(y) = 0 \tag{7.2}$$

Following the preceding steps we make an initial guess y^0 at iteration #1 and use a Taylor series on Equation 7.2 about the value y^0, as follows:

$$p(y) = p(y^0) + \left(\frac{dp}{dy}\right)^0 (y - y^0) + \frac{1}{2!}\left(\frac{d^2p}{dy^2}\right)^1 (y - y^0)^2 + \ldots \tag{7.3}$$

Assuming y^0 is a good guess and the higher-order terms (HOTs) (i.e., the third term in Equation 7.3 and beyond) can be ignored, then Equation 7.2 reduces to

$$p(y) = p(y^0) + \left(\frac{dp}{dy}\right)^0 (y - y^0) = 0 \tag{7.4}$$

yielding

$$(y - y^0) = -\frac{p(y^0)}{\left(\frac{dp}{dy}\right)^0} \cong -\Delta y^0 \tag{7.5}$$

It is imperative to make a note at this point to help understand some of the superscripts related to variables and functions such as

$$y^0; \Delta y^0; \left(\frac{dp}{dy}\right)^0; \left(\frac{d^2p}{dy^2}\right)^1$$

and so on.

These superscripts denote the iteration number in the iterative solution process using the Newton–Raphson method.

Thus, if $\Delta y^0 = 0 \rightarrow$ stop further iteration

If $\Delta y^0 \neq 0$, then,

using Equation 7.5, guess iteration #2 as follows:

$$y^1 = y^0 - \Delta y^0 = y^0 - \frac{p(y^0)}{\left(\frac{dp}{dy}\right)^0} \tag{7.6}$$

Thus, in general, at the kth iteration the solution y^k is given by

$$y^k = y^{k-1} - \Delta y^{k-1} = y^{k-1} - \frac{p(y^{k-1})}{\left(\frac{dp}{dy}\right)^{k-1}} \tag{7.7}$$

Equation 7.7 is called the kth iteration solution or the recursion formula for the non-linear problem in Equation 7.2.

Example 7.1

Say

$$p(y) = (y\sin y + 4) \tag{7.8}$$

Note: Equation 7.8 contains terms that are often found in power flow equations (e.g., those representing the imaginary power).

SOLUTION

Following the earlier formulations in Equations 7.1 through 7.7, choose

- Iteration #0 first guess:

$$y^0 = 4 \text{ radians}$$

where sin(4) = –0.7568, which is not far from unity.
Thus,

$$p\left(y^0\right) = p(4) = 4\sin(4) + 4$$

$$= -3.027 + 4 = 0.9728 \neq 0 \rightarrow \text{continue iteration}$$

- Iteration #1 second guess using Equation 7.7 with $k = 1$:

$$y^1 = y^0 - \Delta y^0 = y^0 - \frac{p\left(y^0\right)}{\left(\frac{dp}{dy}\right)^0} = 4 - \frac{0.9728}{-3.3714} = 4.289$$

where

$$\left(\frac{dp}{dy}\right)^0 = p'\left(y^0\right) = y\cos(y) + \sin(y) = 4(-0.6536) + (-0.7568) = -3.3714$$

$$\therefore p\left(y^1\right) = p(4.289) = 0.0807 \neq 0 \rightarrow \text{continue iteration}$$

- Iteration #2 third guess using Equation 7.7 with $k = 2$:

$$y^2 = y^1 - \Delta y^1 = y^1 - \frac{p\left(y^1\right)}{\left(\frac{dp}{dy}\right)^1} = 4.289 - \frac{0.0897}{-2.674} = 4.3225$$

$$\therefore p\left(y^2\right) = p(4.3225) = 0.0019 \neq 0 \rightarrow \text{continue iteration}$$

- Iteration #3 fourth guess using Equation 7.7 with $k=3$:

$$y^3 = y^2 - \Delta y^2 = y^2 - \frac{p\left(y^2\right)}{\left(\frac{dp}{dy}\right)^2} = 4.3225 + 0.00074 = 4.32324$$

$$\therefore p\left(y^3\right) = p\left(4.32324\right) = 0.000001 \to 0$$

Here we stop iterations, as the value of the function p(y^3) has now reached close to zero; thus the estimate of the solution for y is given by

$$\hat{y} = y^3 = 4.32324 \text{ radians}$$

It is imperative to note that at the end of the third iteration, we set a stopping criterion when the value of the function tends to zero. To aid the computerized calculations, this is generally set to 10^{-6}.

7.3 Case of Two Unknown Variables

Here we have two unknowns and two simultaneous equations: namely,

$$p\left(y,z\right) \text{ and } q\left(y,z\right) \to \text{non-linear in } y \text{ and } z \tag{7.9}$$

We will find the values of the variables that permit the functions to take on specific values, as follows:

Say

$$P = p\left(y,z\right) \text{ as in a real power equation} \tag{7.10}$$

and

$$Q = q\left(y,z\right) \text{ as in an imaginary power equation} \tag{7.11}$$

As earlier, we apply the Taylor series expansion to the right-hand side of Equations 7.10 and 7.11, ignoring HOTs, as follows:

$$p\left(y,z\right) = p\left(y^0,z^0\right) + \frac{1}{1!}\left(\frac{\partial p}{\partial y}\right)^0 + \frac{1}{1!}\left(\frac{\partial p}{\partial z}\right)^0 \tag{7.12}$$

$$q\left(y,z\right) = q\left(y^0,z^0\right) + \frac{1}{1!}\left(\frac{\partial q}{\partial y}\right)^0 + \frac{1}{1!}\left(\frac{\partial q}{\partial z}\right)^0 \tag{7.13}$$

Further, we use:

$$\Delta y^0 = y - y^0 \text{ or } y = y^0 + \Delta y^0 \tag{7.14}$$

$$\Delta z^0 = z - z^0 \text{ or } z = z^0 + \Delta z^0 \tag{7.15}$$

Using Equations 7.10, 7.11, 7.14 and 7.15 in Equations 7.12 and 7.13 and rearranging yields

$$P - p\left(y^0, z^0\right) = \frac{1}{1!}\left(\frac{\partial p}{\partial y}\right)^0 \Delta y^0 + \frac{1}{1!}\left(\frac{\partial p}{\partial z}\right)^0 \Delta z^0 \tag{7.16}$$

$$Q - q\left(y^0, z^0\right) = \frac{1}{1!}\left(\frac{\partial q}{\partial y}\right)^0 \Delta y^0 + \frac{1}{1!}\left(\frac{\partial q}{\partial z}\right)^0 \Delta z^0 \tag{7.17}$$

Further, using incremental notation as done earlier, we have

$$\Delta p^0 = P - p\left(y^0, z^0\right) \tag{7.18}$$

and

$$\Delta q^0 = Q - q\left(y^0, z^0\right) \tag{7.19}$$

Note: Equations 7.18 and 7.19 are called *residues*.

Then, from Equations 7.16 and 7.17, we have

$$\Delta p^0 = \left(\frac{\partial p}{\partial y}\right)^0 \Delta y^0 + \left(\frac{\partial p}{\partial z}\right)^0 \Delta z^0 \tag{7.20}$$

$$\Delta p^0 = \left(\frac{\partial q}{\partial y}\right)^0 \Delta y^0 + \left(\frac{\partial q}{\partial z}\right)^0 \Delta z^0 \tag{7.21}$$

resulting in

$$\begin{bmatrix}\Delta p^0 \\ \Delta q^0\end{bmatrix} = \begin{bmatrix}\frac{\partial p}{\partial y} & \frac{\partial p}{\partial z} \\ \frac{\partial q}{\partial y} & \frac{\partial q}{\partial z}\end{bmatrix}^0 \begin{bmatrix}\Delta y \\ \Delta z\end{bmatrix}^0 = \left[J^0\right]\begin{bmatrix}\Delta y \\ \Delta z\end{bmatrix}^0 \tag{7.22}$$

where

$$\begin{bmatrix}\Delta y \\ \Delta z\end{bmatrix}^0 = \left[J^{-1}\right]^0 \begin{bmatrix}\Delta p^0 \\ \Delta q^0\end{bmatrix} \tag{7.23}$$

is used as a correction term for the system state vector for the next iteration update values, as follows:

$$y^1 = y^0 + \Delta y^0 \tag{7.24}$$

$$z^1 = z^0 + \Delta z^0 \tag{7.25}$$

Thus, at the kth iteration we have

$$\begin{bmatrix} \Delta y \\ \Delta z \end{bmatrix}^{k-1} = \left[J^{-1} \right]^{k-1} \begin{bmatrix} \Delta p \\ \Delta q \end{bmatrix}^{k-1} \tag{7.26}$$

and

$$y^k = y^{k-1} + \Delta y^{k-1} \tag{7.27}$$

$$z^k = z^{k-1} + \Delta z^{k-1} \tag{7.28}$$

As required, update the end of the kth iteration for the state vector components. If Equation 7.26 tends to zero or close to zero (i.e., 10^{-6}), stop iteration.

Example 7.2: Set of Two Non-linear Equations in Two Unknowns

$$y^2 + 2z^2 - 4 = 0$$

$$y^2 - z^2 - 2 = 0$$

This solution can be obtained in the following using MATLAB® code. It is interesting to observe that the preceding equations may represent the real and imaginary powers as in a power flow problem, as seen in the following section.

7.4 Application of Newton–Raphson Method to Power Flow for *n*-Buses

Conditions:

1. In an electric power system most of the buses are load buses with a real power p and imaginary power q, respectively associated with each of these load buses.
2. A transmission network with n buses will have $2n$ simultaneous equations and $2n$ variables: namely, bus voltage magnitudes and the corresponding phase angles.
3. At the voltage-controlled buses there are only the related p equation and the phase angle as the corresponding unknowns.
4. For simplicity, the generator buses are treated as load buses.
5. At the *slack bus* (generally bus 1) the following condition is imposed: $V_1 = 1$ with a phase angle of 0° in pu.
6. Thus, there are $(n-1)$ unknown bus voltage magnitudes (i.e., $V_2, V_3, \ldots, V_n$), as well as $(n-1)$ bus voltage phase angles (i.e., $\delta_2, \delta_2, \ldots, \delta_n$).

   Thus, if the number of generator buses is n_g, then the number of independent unknowns is $2(n-1) - n_g$.

We now apply the preceding conditions to a general power system, with n-buses and bus 1 as the slack bus, to formulate the power flow equations for all variables found at the

kth iteration for the expressions for real power p and reactive power q at each of the $(n-1)$ buses, using Taylor series expansion and all HOTs neglected, as follows:

$$P_2 = p_2\left(V_2^k, V_3^k, V_4^k, \ldots, V_n^k, \delta_2^k, \delta_3^k, \delta_4^k, \ldots, \delta_n^k\right) + \left(\frac{\partial p_2}{\partial V_2}\right)^k \Delta V_2^k + . + . + \left(\frac{\partial p_2}{\partial \delta_n}\right)^k \Delta \delta_n^k$$

$$\vdots$$

$$P_n = p_n\left(V_2^k, V_3^k, V_4^k, \ldots, V_n^k, \delta_2^k, \delta_3^k, \delta_4^k, \ldots, \delta_n^k\right) + \left(\frac{\partial p_n}{\partial V_2}\right)^k \Delta V_2^k + . + . + \left(\frac{\partial p_n}{\partial \delta_n}\right)^k \Delta \delta_n^k$$

$$Q_2 = q_2\left(V_2^k, V_3^k, V_4^k, \ldots, V_n^k, \delta_2^k, \delta_3^k, \delta_4^k, \ldots, \delta_n^k\right) + \left(\frac{\partial q_2}{\partial V_2}\right)^k \Delta V_2^k + . + . + \left(\frac{\partial q_2}{\partial \delta_n}\right)^k \Delta \delta_n^k$$

$$\vdots$$

$$Q_n = q_n\left(V_2^k, V_3^k, V_4^k, \ldots, V_n^k, \delta_2^k, \delta_3^k, \delta_4^k, \ldots, \delta_n^k\right) + \left(\frac{\partial q_n}{\partial V_2}\right)^k \Delta V_2^k + . + . + \left(\frac{\partial q_n}{\partial \delta_n}\right)^k \Delta \delta_n^k$$

The preceding set of equations can be set up in matrix form at the kth iteration as follows:

$$\begin{bmatrix} P_2 - p_n\left(V_2^k, V_3^k, V_4^k, \ldots, V_n^k, \delta_2^k, \delta_3^k, \delta_4^k, \ldots, \delta_n^k\right) \\ \vdots \\ P_n - p_n\left(V_2^k, V_3^k, V_4^k, \ldots, V_n^k, \delta_2^k, \delta_3^k, \delta_4^k, \ldots, \delta_n^k\right) \\ Q_2 - q_2\left(V_2^k, V_3^k, V_4^k, \ldots, V_n^k, \delta_2^k, \delta_3^k, \delta_4^k, \ldots, \delta_n^k\right) \\ \vdots \\ Q_n - q_n\left(V_2^k, V_3^k, V_4^k, \ldots, V_n^k, \delta_2^k, \delta_3^k, \delta_4^k, \ldots, \delta_n^k\right) \end{bmatrix} = \begin{bmatrix} \frac{\partial p_2}{\partial V_2} \cdots \frac{\partial p_2}{\partial V_n} & \frac{\partial p_2}{\partial \delta_2} \cdots \frac{\partial p_2}{\partial \delta_n} \\ \vdots & \vdots \\ \frac{\partial p_n}{\partial V_2} \cdots \frac{\partial p_n}{\partial V_n} & \frac{\partial p_n}{\partial \delta_2} \cdots \frac{\partial p_n}{\partial \delta_n} \\ \frac{\partial q_2}{\partial V_2} \cdots \frac{\partial q_2}{\partial V_n} & \frac{\partial q_2}{\partial \delta_2} \cdots \frac{\partial q_2}{\partial \delta_n} \\ \vdots & \vdots \\ \frac{\partial q_n}{\partial V_2} \cdots \frac{\partial q_n}{\partial V_n} & \frac{\partial q_n}{\partial \delta_2} \cdots \frac{\partial q_n}{\partial \delta_n} \end{bmatrix}^k \begin{bmatrix} \Delta V_2 \\ \vdots \\ \Delta V_n \\ \Delta \delta_2 \\ \vdots \\ \Delta \delta_n \end{bmatrix}^k \tag{7.29}$$

$$\Delta u^k = J^k \Delta X^k \tag{7.30}$$

where:

Δu^k is the corrective force at the kth iteration
J^k is the Jacobian matrix at the kth iteration
ΔX^k is the error of the system vector of the given power system at the kth iteration

Equation 7.30 is rewritten as follows:

$$\Delta X^k = (J^{-1})^k \Delta u^k \tag{7.31}$$

The updated values of the *system state vector* can then be expressed as

$$X^{k+1} = X^k + \Delta X^k \tag{7.32}$$

7.5 Newton–Raphson Applied to a Two-Bus System

We write the power/load flow equations in polar form for both the real and imaginary power components for n buses as follows:

$$V_k = |V_k|\angle\delta_k;\ V_n = |V_n|\angle\delta_n;\ \text{and}\ Y_{kn} = |Y_{kn}|\angle\theta_{kn} \tag{7.33}$$

Then we call the swing bus number 1, which results in computation to start with bus 2.

Let P_2, Q_2 be the scheduled real and reactive power entering the system at bus 2. Thus, the apparent power at bus 2 is given by

$$S_2 = V_2 I_2^{*} = P_2 + jQ_2 \tag{7.34}$$

$$I_2 = \frac{P_2 - jQ_2}{V_2^{*}}$$

$$I_2 = Y_{21}V_1 + Y_{22}V_2 + .+.Y_{23}V_3 + .+ Y_{2n}V_n \tag{7.35}$$

Then,

$$V_2 = \frac{1}{Y_{22}}\left[\frac{P_2 - jQ_2}{V_2^{*}} - \left(Y_{21}V_1 + Y_{22}V_2 + .+ Y_{23}V_3 + .+ Y_{2n}V_n\right)\right] \tag{7.36}$$

Thus, for a total of N buses, the calculated voltage at any bus k, when P_k and Q_k are given, is obtained as follows:

$$V_k = \frac{1}{Y_{kk}}\left[\frac{P_k - jQ_k}{V_k^{*}} - \sum_{n=1}^{N} Y_{kn}V_n\right] \tag{7.37}$$

The values of the voltages on the right-hand side of Equation 7.37 are the most recently calculated values for the corresponding buses or their estimated values. The special case of this derivation is the Gauss–Seidel method. Thus, at a bus where the voltage magnitude rather than the reactive power is specified, then the real and imaginary components of power and voltage for each iteration are found by first computing a value for the reactive power as follows:

$$P_k - jQ_k = \left(Y_{kk}V_k + \sum_{n=1}^{N} Y_{kn}V_n\right)V_k^{*} \quad n \neq k \tag{7.38}$$

If we now allow $n = $ k, then we have

$$S_k^{*} = V_k^{*}I_k = P_k - jQ_k = V_k^{*}\sum_{n=1}^{N} Y_{kn}V_n \tag{7.39}$$

$$Q_k = -I_m\left\{V_k^{*}\sum_{n=1}^{N} Y_{kn}V_n\right\} \tag{7.40}$$

Q_k is evaluated by using Equation 7.40 for the best previous voltage values at the buses, as indicated earlier, and this value is substituted in Equation 7.38 to find V_k.

Thus, from Equation 7.38 we have

$$P_k - jQ_k = \sum_{n=1}^{N} |V_k V_n Y_{kn}| \angle \theta_{kn} + \delta_n - \delta_k \tag{7.41}$$

yielding

$$P_k = \sum_{n=1}^{N} |V_k V_n Y_{kn}| \cos(\theta_{kn} + \delta_n - \delta_k) \tag{7.42}$$

and

$$Q_k = \sum_{n=1}^{N} |V_k V_n Y_{kn}| sin(\theta_{kn} + \delta_n - \delta_k) \tag{7.43}$$

Finally, the above yields a set of $2n$ non-linear equations to be solved.

7.6 Differentiating Buses

1. *Generator bus:* 15% of the total buses in a given power system are generator buses. One of the generator buses is the slack bus.

   And is defined and quantified by the apparent power at the generator bus in the following equation.

   $$S_{G_i} = P_{G_i} + jQ_{G_i} \tag{7.44}$$

   The power demand by local customers is

   $$S_{D_i} = P_{D_i} + jQ_{D_i} \tag{7.45}$$

   leading to a net outflow of complex power at the ith bus, as follows:

   $$S_i = P_i + jQ_i = S_{G_i} - S_{D_i} \tag{7.46}$$

   This is shown in Figure 7.1.

2. *Load bus:* 85% of the total buses in a given power system, are load buses.

   In the load buses the generated complex power is zero, as given in the following:

   $$S_{G_i} = 0 \tag{7.47}$$

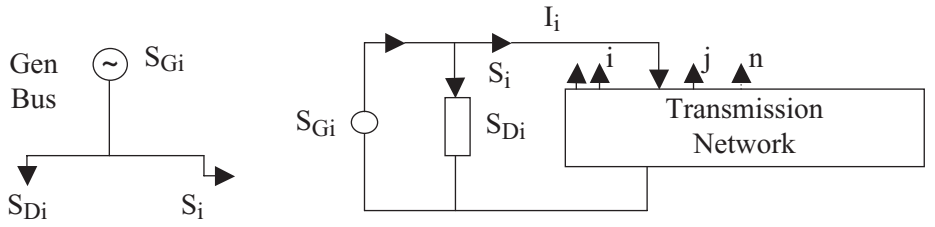

FIGURE 7.1
Generator buses.

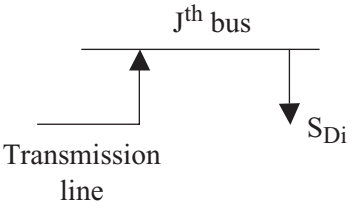

FIGURE 7.2
Load buses.

which leads to

$$S_i = -S_{D_i} \tag{7.48}$$

→ Negative power is drawn from the power system.

These load buses are shown in Figure 7.2.

7.7 Solution Process

Thus, in general terms the steps to be followed in solving the power flow problem in a power system are as follows:

1. Identify all the element values of the bus admittance matrix Y_{bus} (Equation 7.9) based on the engineering data of the electric power system given by the SLD.
2. At each load bus specify the relevant values of the real and reactive powers as in Equation 7.49:

$$S_i = V_i I_i^* \text{ or } S_i^* = V_i^* I_i \tag{7.49}$$

$$S_i = V_i \angle \delta_i \sum_{j=1}^{n} Y_{ij} V_j \angle -\delta_j - \theta_{ij} = V_i \sum_{j=1}^{n} Y_{ij} V_j \angle \delta_i - \delta_j - \theta_{ij} \tag{7.50}$$

$$p_i = V_i \sum_{j=1}^{n} Y_{ij} V_j \cos\left(\delta_i - \delta_j - \theta_{ij}\right) \tag{7.51}$$

$$q_i = V_i \sum_{j=1}^{n} Y_{ij} V_j \sin\left(\delta_i - \delta_j - \theta_{ij}\right) \tag{7.52}$$

3. Identify the declared values of the real power P and imaginary power Q values, thus making these also the P, Q buses.
4. At each generator bus specify the pertinent values of real power P and the magnitude of the bus voltage V. These are called the P and the $|V|$ buses.
5. The slack bus is $n = 1$. At the slack bus, assume a magnitude of $V = 1$ with an angle of 0°. This assumption is the basis for the entire solution process and no deviation is allowed.
6. Next, assume a voltage profile for all the remaining bus voltage phasors (i.e., assume both a magnitude and phase angle at each of these buses). A unity profile is justifiable as an initial assumption, especially if a fast-converging algorithm such as the Newton–Raphson method is employed.
7. Introduce the information from the Y_{bus} and the assumed voltage profile into Equation 7.51 to find P_i at the ith bus and use Equation 7.52 to find Q_i. Where applicable, compare these computed values with the specified ones and determine the difference.
8. Devise a scheme whereby the difference found in step 7 can be used advantageously to correct the element values of the bus voltage vector, so that the computations of step 7 lead to significantly smaller and smaller differences between the calculated and specified values of P and Q that will trigger the *stop iterations* action to preserve computer capabilities (e.g., stopping criterion: 10^{-6} etc., as in Equation 7.26).
9. Repeat the iterations of the preceding steps until the difference is at an acceptably low level, called the *stopping criterion*, as in step 8. The resulting voltage profile of the system then represents the solution process to the power flow equations.
10. Conduct the actual power flow as described in the following example.

Example 7.3: Power Flow in a Two-Bus Power System

A two-bus system is shown in Figure 7.3. The power flow along the transmission line is depicted in the SLD. There is a single generator bus, which is designated the slack bus. Thus, this bus has the following characteristics:

$$\text{Bus 1 (slack bus): } V_1 = 1\angle 0$$

The second bus is a load bus, where the real and imaginary power demands are specified as follows:

$$P_2 = -1.0\,\text{pu and } Q_2 = -1.0\,\text{pu}$$

The reference base for this power system is 100 MVA, and 230 kV at the transmission level.

Find the power flow in the transmission line between bus 1 and bus 2, which is 100 mi. long with the following impedance:

$$z_l = 20 + j80 = 82.5\angle 76°\Omega = \frac{82.5}{529}\angle 76° = 0.156\angle 76°\,\text{pu}$$

and

$$y_{12} = \frac{1}{0.156\angle 76°} = 6.4105\angle -76° = 1.551 - j6.220\,\text{pu}$$

SOLUTION

Step 1: Generate the Y_{bus} as per Equation 7.9.

From the reference base information chosen for the power system, we have

$$Z_B = \frac{230^2}{100} = 529\,\Omega; \quad \text{Y}_\text{B} = \frac{100}{230^2} = 0.00189\,\text{S}$$

The pu values of the shunt-capacitive susceptance associated with the π equivalent circuit of the transmission line shown in Figure 7.3 are

$$y_p = \frac{0.27\times 10^{-3}}{0.00189}\angle 90° = j0.1428\,\text{pu}$$

Thus, the self-admittance of the transmission line at either bus 1 or bus 2 is

$$Y_{11} = Y_{22} = y_{12} + y_p = 1.551 - j6.229 + j0.1428 = 6.272\angle -75.683°$$

Similarly, the transfer impedance between bus 1 and bus 2 is

$$Y_{12} = Y_{21} = -y_{12} = -1.551 + j6.22 = 6.4105\angle 104°$$

Thus, the bus admittance matrix is given by

$$Y_{\text{bus}} = \begin{bmatrix} 6.272\angle -75.683° & 6.4105\angle 104° \\ 6.4105\angle 104° & 6.272\angle -75.683° \end{bmatrix}$$

Step 2: Write the power flow equations at the relevant buses, as in Equations 7.51 and 7.52.

Here, we have already made bus 1 the slack bus; thus,

$$\#\text{ of unknowns: } 2(n-1) = 2;\ \text{for } n = 2 \text{ and } n_g = 0$$

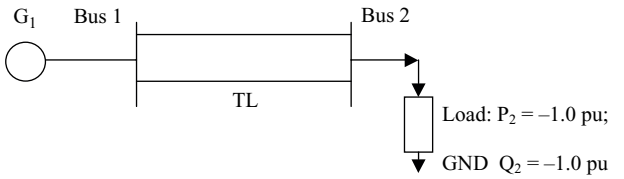

FIGURE 7.3
Two-bus power system power flow analysis in a transmission line.

and bus 2 has declared the real power and imaginary power values given by

$$P_2 = -1 \text{ and } Q_2 = -1$$

With the information provided we have the following bus 2 power flow equation:

$$p_2 = V_2[Y_{21}V_1 \cos(\delta_2 - \delta_1 - \theta_{21}) + Y_{22}V_2 \cos(\delta_2 - \delta_2 - \theta_{22})$$

With the known values of $V_1 = 1$ and $\delta_1 = 0$, we have

$$p_2 = Y_{21}V_2 \cos(\delta_2 - \theta_{21}) + Y_{22}V_2^2 \cos(\theta_{22})$$

$$p_2 = 6.4105V_2 \cos(\delta_2 - 104°) + 1.551V_2^2$$

Similarly,

$$q_2 = Y_{21}V_2 \sin(\delta_2 - \theta_{21}) - Y_{22}V_2^2 \sin(\theta_{22})$$

$$q_2 = 6.4105V_2 \sin(\delta_2 - 104°) + 6.0772V_2^2$$

We now perform the partial derivatives of the preceding equations with respect to V_2 and δ_2 to obtain the Jacobian matrix terms, as follows:

$$\frac{\partial p_2}{\partial \delta_2} = -Y_{21}V_2 \sin(\delta_2 - \theta_{21})$$

$$\frac{\partial p_2}{\partial \delta_2} = -6.4105V_2 \sin(\delta_2 - 104°)$$

$$\frac{\partial p_2}{\partial V_2} = -Y_{21} \cos(\delta_2 - \theta_{21}) + 2Y_{22}V_2 \cos(\theta_{22})$$

$$\frac{\partial p_2}{\partial V_2} = 6.4105 \cos(\delta_2 - 104°) + 3.102V_2$$

$$\frac{\partial q_2}{\partial \delta_2} = Y_{21}V_2 \cos(\delta_2 - \theta_{21})$$

$$\frac{\partial q_2}{\partial \delta_2} = 6.4105V_2 \cos(\delta_2 - 104°)$$

$$\frac{\partial q_2}{\partial V_2} = Y_{21} \sin(\delta_2 - \theta_{21}) - 2Y_{22}V_2 \sin(\theta_{22})$$

$$\frac{\partial q_2}{\partial V_2} = 6.4105 \sin(\delta_2 - 104°) + 12.1544V_2$$

To begin the solution process, we assume the starting solution at iteration to be zero for

$$V_2 = 1\angle 0°$$

yielding the power flow equations at iteration zero as follows:

$$p_2^{\,0} = 0.00016 \;\text{ and }\; q_2^{\,0} = -0.1429$$

and the Jacobian as follows:

$$J^0 = \begin{bmatrix} 6.2201 & 1.5512 \\ -1.5512 & 5.9343 \end{bmatrix}^0$$

With the preceding values and the values of $P_2 = -1.0$ and $Q_2 = -1.0$, we have the corrective force vector and the error in the state vector as follows:

$$\Delta u^0 = \begin{bmatrix} \Delta p_2^{\,0} \\ \Delta q_2^{\,0} \end{bmatrix} = \begin{bmatrix} P_2 - p_2^{\,0} \\ Q_2 - q_2^{\,0} \end{bmatrix} = \begin{bmatrix} -1 - 0.00016 \\ -1 + 0.1429 \end{bmatrix} = \begin{bmatrix} -1.0002 \\ -0.8571 \end{bmatrix}$$

and

$$\Delta X^0 = \begin{bmatrix} \Delta \delta_2^{\,0} \\ \Delta V_2^{\,0} \end{bmatrix} = [J^{-1}]^0 \Delta u^0 = \begin{bmatrix} 0.1509 & 0.0395 \\ -0.0395 & 0.1582 \end{bmatrix} \begin{bmatrix} -1.0002 \\ -0.8571 \end{bmatrix}$$

$$\Delta X^0 = \begin{bmatrix} -10.5883^\circ \\ -0.0962 \end{bmatrix}$$

This leads to new values of the unknown variables as follows:

$$\begin{bmatrix} \Delta \delta_2^{\,1} \\ \Delta V_2^{\,1} \end{bmatrix} = \begin{bmatrix} -10.5883^\circ \\ 0.9038 \,\text{in pu} \end{bmatrix}$$

These are the starting values of the next iteration (*iteration #1*) , which yield

$$p_2^{\,1} = -1.1438$$

and

$$q_2^{\,1} = -0.3042$$

with considerable improvements in the value of p_2 to the declared values of P_2.

We proceed with *iteration #1* to yield

$$\Delta u^1 = \begin{bmatrix} \Delta p_2^{\,1} \\ \Delta q_2^{\,1} \end{bmatrix} = \begin{bmatrix} P_2 - p_2^{\,1} \\ Q_2 - q_2^{\,1} \end{bmatrix} = \begin{bmatrix} -1 + 1.1438 \\ -1 + 0.3042 \end{bmatrix} = \begin{bmatrix} 0.1438 \\ -0.6958 \end{bmatrix}$$

and the new corrective terms are

$$\Delta X^1 = \begin{bmatrix} \Delta \delta_2^{\,1} \\ \Delta V_2^{\,1} \end{bmatrix} = [J^{-1}]^1 \Delta u^1 = \begin{bmatrix} 1.3465^\circ \\ -0.1471 \end{bmatrix}$$

We proceed with *iteration* #2 to yield

$$\Delta u^2 = \begin{bmatrix} \Delta p_2{}^2 \\ \Delta q_2{}^2 \end{bmatrix} = \begin{bmatrix} P_2 - p_2{}^2 \\ Q_2 - q_2{}^2 \end{bmatrix} = \begin{bmatrix} -1 + 1.0261 \\ -1 + 0.9774 \end{bmatrix} = \begin{bmatrix} 0.026118 \\ -0.0226 \end{bmatrix}$$

and the new corrective terms are

$$\Delta X^2 = \begin{bmatrix} \Delta \delta_2{}^2 \\ \Delta V_2{}^2 \end{bmatrix} = [J^{-1}]^2 \Delta u^2 = \begin{bmatrix} 0.3629^\circ \\ -0.01168 \end{bmatrix}$$

We proceed with *iteration #3* to yield

$$\Delta u^3 = \begin{bmatrix} \Delta p_2{}^3 \\ \Delta q_2{}^3 \end{bmatrix} = \begin{bmatrix} P_2 - p_2{}^3 \\ Q_2 - q_2{}^3 \end{bmatrix} = \begin{bmatrix} -1 + 0.99593 \\ -1 + 1.0274 \end{bmatrix} = \begin{bmatrix} -0.00407 \\ 0.02704 \end{bmatrix}$$

We also realize that the difference between the declared and evaluated values of [P_2 and Q_2] and [p_2 and q_2] are getting smaller, respectively,
and the new corrective terms are

$$\Delta X^3 = \begin{bmatrix} \Delta \delta_2{}^3 \\ \Delta V_2{}^3 \end{bmatrix} = [J^{-1}]^3 \Delta u^3 = \begin{bmatrix} 0.0339^\circ \\ 0.009634 \end{bmatrix}$$

The updated values of the unknowns are

$$\begin{bmatrix} \delta_2{}^4 \\ V_2{}^{14} \end{bmatrix} = \begin{bmatrix} -8.9128^\circ \\ 0.75463 \text{ in pu} \end{bmatrix}$$

resulting in the following values of the power flow equations:

$$p_2{}^4 = -0.9985$$

and

$$q_2{}^4 = -0.9950$$

Implying we are much closer to the stopping criterion set in the Newton–Raphson algorithm! Iteration is stopped!
This yields

$$V_2 = |V_2| \angle \delta_2 = 0.75465 \angle -8.9128^\circ \text{ in pu}$$

With these results, the power flow at the slack bus is as follows:

$$P_1 = Y_{11} \cos\theta_{11} + Y_{12} V_2 \cos(\delta_2 + \theta_{12})$$

$$= 1.1220 \text{ pu}$$

$$Q_1 = -Y_{11} \sin\theta_{11} - Y_{12} V_2 \sin(\delta_2 + \theta_{12})$$

$$= 1.2586 \text{ pu}$$

$$S_{G_1} = P_1 + jQ_1 = 1.122 + j1.2586 \text{ in pu}$$

At the load bus, we have from earlier indications

$$S_{D_2} = 1 + j1 \text{ in pu}$$

Thus, the resulting power supplied to the transmission line is

$$S_{G_1} - S_{D_2} = (1.122 + j1.2586) - (1 + j1) \text{ in pu} = 0.122 + j0.2586 \text{ in pu}$$

These copper loss or real power calculations can be confirmed by calculating the current delivered in the transmission line and the resulting copper loss as follows:

$$I_1 = y_{12}(V_1 - V_2) = 6.4105\angle -76° - 0.75465\angle -8.91286° = 1.7944\angle -51.374°$$

With the resistance of the transmission line known as

$$r_1 = 0.156 \cos 76° = 0.03774 \text{ in pu}$$

$$\rightarrow P_{Cu} = I_1^2 r_1 = 1.7944^2 (0.03774) = 0.1215 \text{ pu}$$

$$\rightarrow \cong \text{real part of } (S_{G_1} - S_{D_2}) = 0.122 \text{ in pu}$$

Problems

PROBLEM 7.P.1

A three-bus transmission system is shown in Figure 7.P.1. Bus 1 and bus 3 have generators connected to them as G_1 and G_3.

- G_1: 300 MVA at 15 kV
- G_3: 250 MVA at 15 kV
- Transmission line: 230 kV

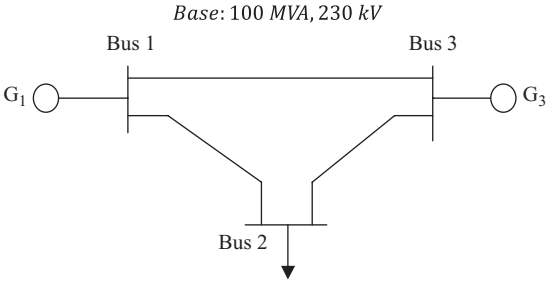

FIGURE P.7.1
Three-bus transmission network.

Appropriate transformers are assumed to be in place to provide the transition from the generating level to the transmission level. Calculate the power flow at the transmission level. The base is chosen as 100 MVA, 230 kVA.

PROBLEM P.7.2

A three-phase synchronous generator, grounded through an impedance Z_n, is shown in Figure P.7.2.

The generator is not supplying load, but because of a fault at the generator terminals, currents I_a, I_b and I_c flow through the phases a, b and c, respectively. Develop and draw the phase sequence networks for the generator in these conditions.

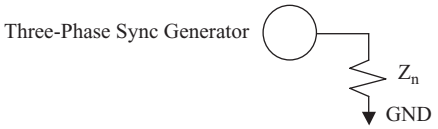

FIGURE P.7.2
Synchronous generator.

PROBLEM P.7.3

For the two-bus system shown in Figure P.7.3, data given is as follows:

$$Y_{11} = Y_{22} = 1.6\angle -80^\circ \text{ pu}$$

and

$$Y_{21} = Y_{12} = 1.9\angle 100^\circ \text{ pu}$$

Find the pu voltage at bus using the Gauss–Seidel method transmission level.

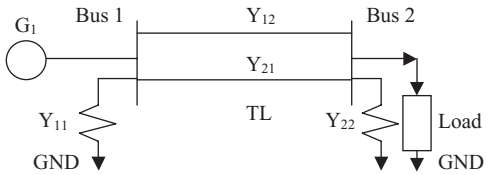

FIGURE P.7.3
Two-bus system with Gauss–Seidel.

PROBLEM P.7.4

For Problem P.7.3, evaluate the power on the swing bus of the network.

PROBLEM P.7.5

Solve the following system of equations using the Newton–Raphson method.

$$10x + 5y = 6$$

$$2x + 9y = 3$$

PROBLEM P.7.6

Repeat Problem P.7.5 using the Gauss–Seidel method.

PROBLEM P.7.7

Evaluate x in the following equation using the Gauss–Seidel method.

$$x + \sin x = 2$$

As a starting value, use $x(0) = 0$.

PROBLEM P.7.8

Repeat Problem P.7.7 using the Newton–Raphson method and compare the number of iterations required to achieve convergence with the two methods.

PROBLEM P.7.9

For the system shown in Figure P.7.9 with three buses, and bus 3 as the reference bus, the bus impedance matrix is given by

$$Z_{\text{bus}} = \begin{bmatrix} 1.33 + j1.33 & 1 + j1 \\ 1 + 1 & 1.5 + j1.5 \end{bmatrix} \times 10^{-2} \text{ pu}$$

Starting with

$$V_1^{(0)} = V_2^{(0)} = 1.05\angle 0°$$

solve V_1 and V_2 using the Gauss–Seidel method (base: 100 MVA, 230 kV).

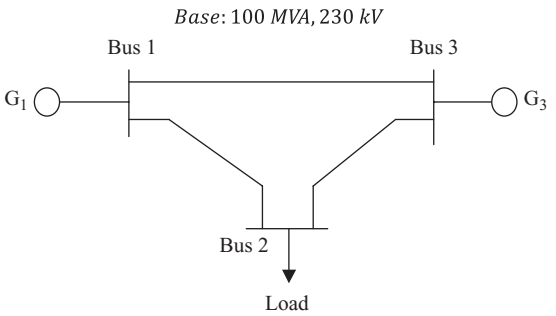

FIGURE P.7.9
Three-bus system.

PROBLEM P.7.10

Repeat Problem P.7.9 using the Newton–Raphson method. Compare the number of iterations it takes to achieve the solution using both methods.

PROBLEM P.7.11

Write a MATLAB code to solve Problem P.7.8 using a PC.

PROBLEM P.7.12

Write a MATLAB code to solve Problem P.7.9 using a PC.

PROBLEM P.7.13

Write a MATLAB code to solve Problem P.7.10 using a PC.

PROBLEM P.7.14

For Problem P.7.9, the bus admittance matrix is given by

$$Y_{\text{bus}} = \begin{bmatrix} 1.6 - j8 & -0.8 + j4 & -0.8 + j4 \\ -0.8 + j4 & 1.6 - j8 & -0.8 + j4 \\ -0.8 + j4 & -0.8 + j4 & 1.6 - j8 \end{bmatrix} \text{pu}$$

Also,

$$V_1 = 1\angle 0° \text{ and } P_2 - jQ_2 = -0.8 + j0.6$$

Find $V_2^{(2)}$ using the Gauss–Seidel method.

PROBLEM P.7.15

Repeat Problem P.7.14 using the Newton–Raphson method.

PROBLEM P.7.16

The transmission line that joins G_1 and G_2 in Figure P.7.16 is of medium length, which permits the line to be modeled by a π-type equivalent circuit. The total series line reactance is 45 Ω, and each capacitor of the π-circuit has an impedance magnitude of 2500 Ω. Line resistance is assumed negligible.

1. Write the equations for the currents injected into the transmission line at each bus in terms of the bus voltages V_1 and V_2 and the line admittance parameters expressed in pu. Assume the reference base for the electric power to be 100 MVA and 230 kV.
2. Find the admittance bus matrix.
3. Discuss the standard steps to follow for the solution to step (a).

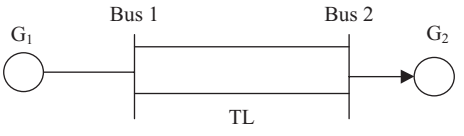

FIGURE P.7.16
Two-bus system with transmission line *TL*.

PROBLEM P.7.17

Consider the system in Figure P.7.17 to be a three-bus DC electric power system. Three transmission links join the buses as shown, and the line resistances are indicated per unit. Show that the power flow equations are described by the following set (base: three-bus DC system):

$$P_1 = 130V_1^2 - 80V_1V_2 - 50V_1V_3$$

$$P_2 = 130V_2^2 - 80V_1V_2 - 50V_2V_3$$

$$P_3 = 100V_3^2 - 50V_2V_3 - 50V_1V_3$$

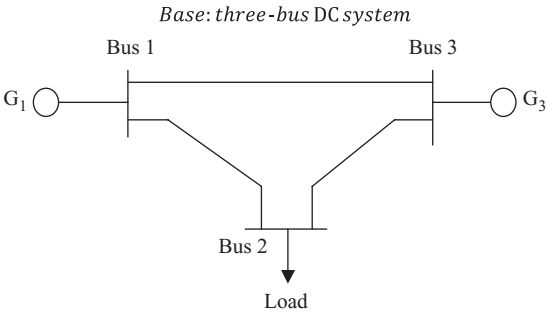

FIGURE P.7.17
DC system.

PROBLEM P.7.18

In the electric power system shown in Figure P.7.18, all pu quantities are related to a reference base of 100 MVA and 230 kV.

Find

1. The bus admittance matrix Y_{bus}
2. The independent variables for this system
3. The power flow equations

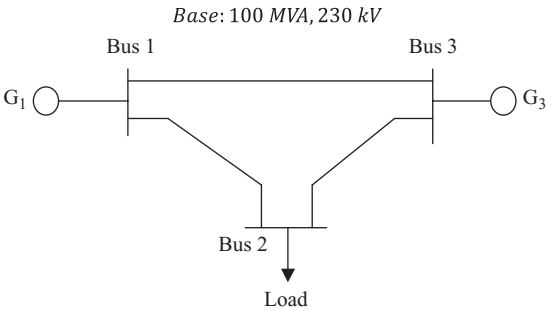

FIGURE P.7.18
100 MVA 230 kV system.

PROBLEM P.7.19

For Problem P.7.18, find the general expressions for the elements of the Jacobian to be used for solving the power flow equations by the Newton–Raphson method.

PROBLEM P.7.20

For the system in Figure P.7.18, the real and reactive powers are specified at a base of 100 MVA and 230 kV.

1. Find the solution to the power flow equations using the Newton–Raphson method, up to three iterations, using MATLAB.
2. Do the same using ETAP©.
3. Find the pu values of all dependent quantities at each bus.
4. Compute the bus-to-bus complex power flows.

Taylor & Francis
Taylor & Francis Group
http://taylorandfrancis.com

8

Control of Power into Networks

The power going into networks is controlled in the following three ways:

1. By using synchronous machines
2. By using capacitor banks
3. By using transformers

Of these three, the first method is comparatively more common.

- Exciter control of reactive power between the generator and the system: This is done by adjusting the terminal voltage by changing the reactive power between the generator and the system. In other words, one can have the over-excited generator shown in Figure 8.1 by supplying imaginary power Q to the system.
- Otherwise, one can have the under-excited generator shown in Figure 8.2 by absorbing imaginary power Q from the system.
- Real power P control: Increasing the real power input to the generator while $|E_g|$ is kept constant will result in the rotor speed increasing, which causes power angle δ to increase, which results in V_t increasing as well as power factor angle θ decreasing. In such conditions, more power is delivered to the network. This means the total value of the apparent power ($S = P + jQ$) needs to be evaluated as follows:

$$V_t = |V_t| \angle 0° \text{ and } E_g = |E_g| \angle \delta$$

$$I_a = \frac{|E_g| \angle \delta - |V_t| \angle 0°}{jX_g}$$

$$I_a^* = \frac{|E_g| \angle -\delta - |V_t| \angle 0°}{-jX_g}$$

$$\therefore P + jQ = V_t I_a^*$$

$$= \frac{V_t \left[|E_g| \angle -\delta - |V_t| \angle 0° \right]}{-jX_g}$$

$$\therefore P + jQ = \frac{|V_t||E_g| \angle 90° - \delta - |V_t|^2 \angle 90°}{X_g}$$

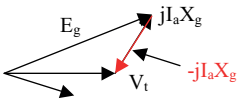

FIGURE 8.1
Over-excited synchronous generator.

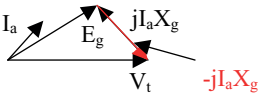

FIGURE 8.2
Under-excited generator.

which yields

$$P = \frac{|V_t||E_g|\cos(90-\delta)}{X_g} = \frac{|V_t||E_g|\sin\delta}{X_g}$$

$$Q = \frac{|V_t||E_g|\sin(90-\delta)}{X_g} - \frac{|V_t|^2}{X_g}$$

$$Q = \frac{|V_t||E_g|\cos\delta - |V_t|^2}{X_g}$$

Thus, when $|E_g|$ and $|V_t|$ are kept constant, the power transferred in a network depends on δ; that is, increasing δ leads to an increase in real power P. When P and $|V_t|$ are constant, δ is decreased and $|E_g|$ is increased by increasing the DC excitation, which in turn implies that the reactive power Q will increase if it is already positive or if it goes from $-Q$ to $+Q$.

In the last case, if $V_t = V_2$ and $E_g = V_1$ and resistance is neglected, then

$$P = \frac{|V_1||V_2|}{X}\sin\delta$$

→ power is transferred from one bus to another with a reactive connection → V_1 leads V_2 by δ.

Similarly,

$$Q = \frac{|V_2||V_1|\cos\delta - |V_2|^2}{X} \rightarrow \text{reactive power received at bus 2}$$

which implies that increases in power angle δ will cause incremental increases in reactive power ΔQ for a small change in δ; this is because sin δ changes widely but cos δ changes by only small amounts with changes in δ when δ lies between 10° and 15°.

The following are some examples of power flow using ETAP© load flow analysis for three-bus and five-bus systems.

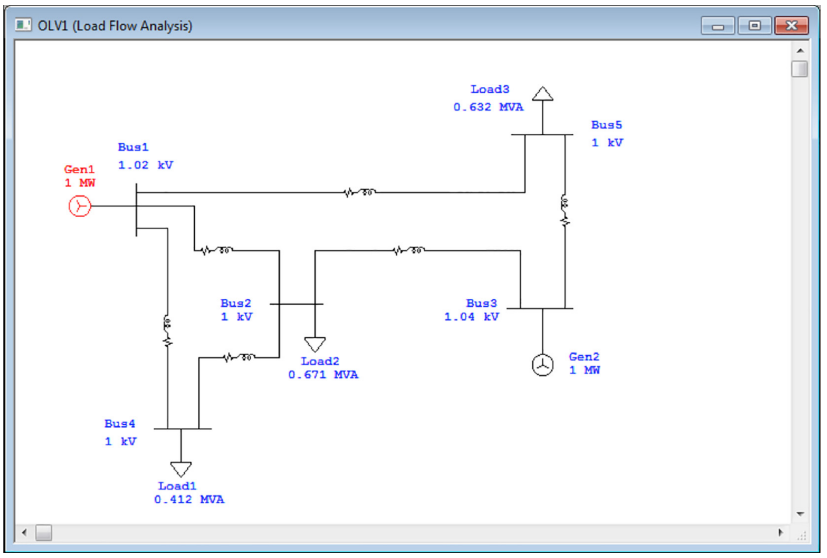

Some examples solved using ETAP. For details visit www.etap.com

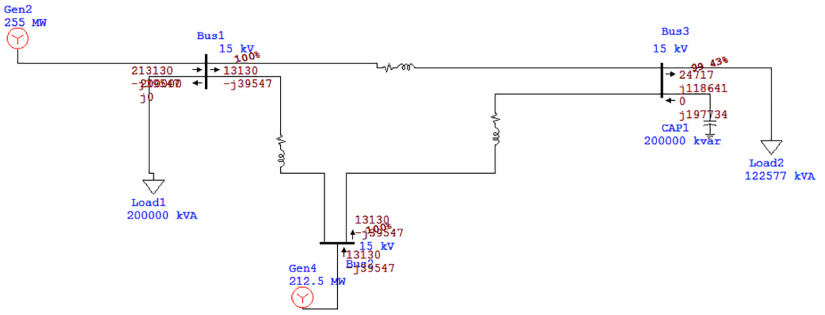

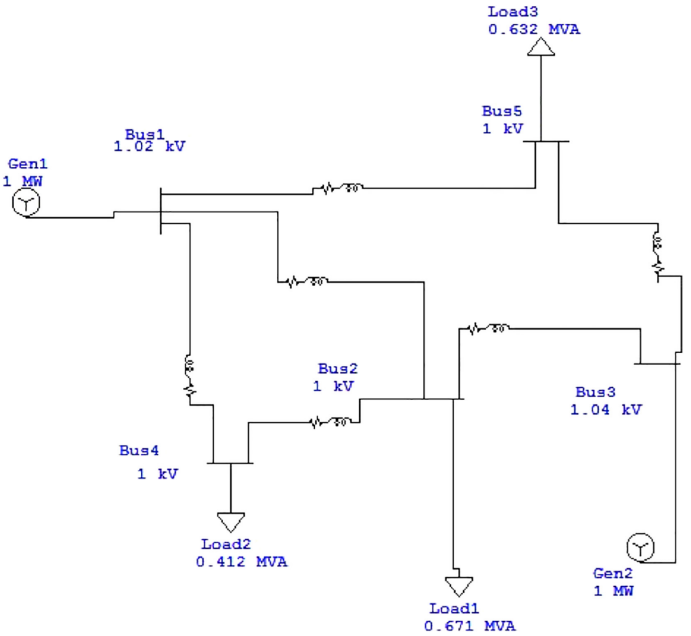

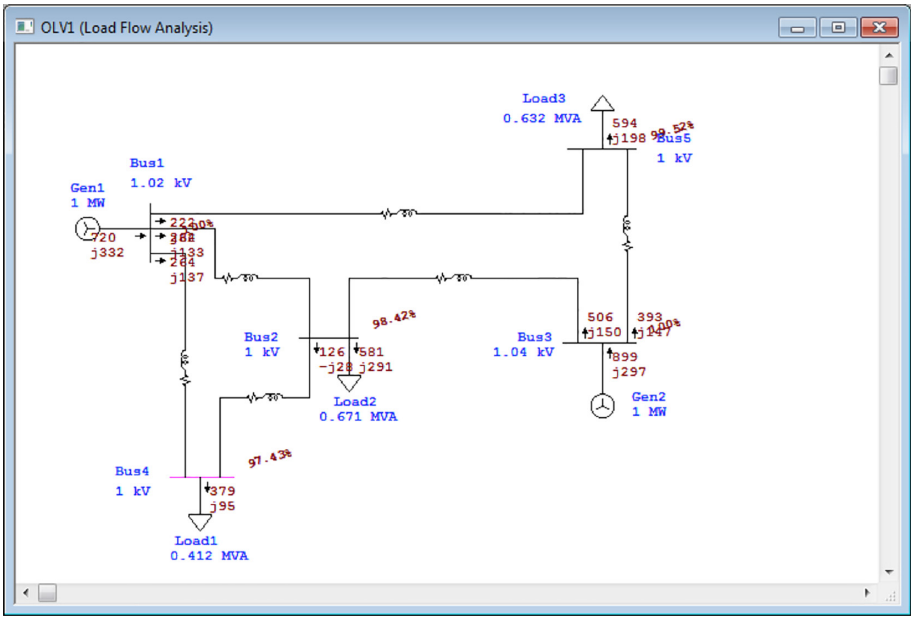
OLV1 (Load Flow Analysis)
Load3
0.632 MVA
594
j198
99.52%
Bus5
1 kV
Bus1
1.02 kV
Gen1
1 MW
720
j332
222
j133
264
j137
Bus2
1 kV
98.42%
126
-j28
581
j291
Load2
0.671 MVA
Bus3
1.04 kV
506
j150
393
j147
899
j297
Gen2
1 MW
Bus4
1 kV
97.43%
379
j95
Load1
0.412 MVA

9

Underground or Belowground Cables

9.1 Introduction

The underground cables need to have sufficient electrical insulation to protect the conductor from the ground or external shield of the cable. In addition, the cable needs to be protected from environmental conditions like mechanical, chemical or other hazardous situations to effect a satisfactory and reliable operation to maintain reliability of delivery of service of electrical power. Many localities which had underground cabling system have chosen to go for overhead cabling system due to flooding and damage caused by such unexpected weather patterns causing inland flooding. However, many localities still prefer the belowground cabling system. The basic components of an underground cable are

1. A conductor that is made of stranded copper or aluminum.
2. Insulation around the conductor in (1). This insulation may be some sort of rubber, such as vulcanized or butyl rubber or polyvinyl chloride (PVC).
3. External protective covering, often a lead alloy sheath over the insulated cable.

A three-phase belowground cable has three conductors inside the sheath. Since the three conductors are much closer to teach other than those of an overhead transmission line and the conductors are almost completely immersed in some kind of dielectrics, the capacitive reactance of the cable is smaller than that of a comparable transmission line. Thus, the use of T- or π-circuit representation for even a short cable may be necessary for analysis.

9.2 Electric Stress in a Single-Core Cable

The insulating material of a cable has a dielectric of a certain strength. Upon the application of a potential to the cable, this capability is exceeded during operation, causing breakdown. Therefore, the cable must be designed so that the maximum electric stress or the electric field strength at the surface of the conductor does not exceed that required to break down the insulation. If the underground cable is otherwise designed with a low line-to-ground voltage gradient, the overall size of the cable becomes very large. On the other hand, if the voltage gradient is made bigger so as to reduce the diameter of the cable, then the dielectric loss may become too large and may lead to excessive heating of the cable. Empirically, it has been found that the optimal ratio of the cable to the radius of the conductor is given by

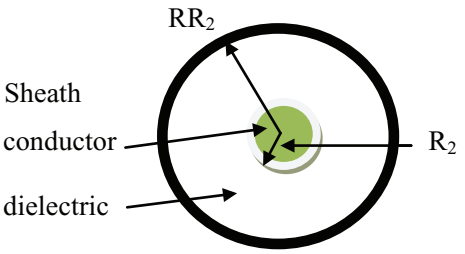

FIGURE 9.1
Underground cable.

$$\frac{R_1}{R_2} = \epsilon = 2.718 \tag{9.1}$$

R_1 and R_2 are illustrated in Figure 9.1. Further, smaller ratios than that in Equation 9.1 will result in unstable operation of the underground cable, as the dielectric will tend to break down. Any ratio exceeding the value of 2.718 will result in undesirable operation of the cable. In summary, for economic reasons it is best to maintain the ratio at 2.718.

9.3 Grading of Underground Cables

The cable in Figure 9.1 is filled with a single dielectric layer, but many cables contain several layers of dielectric. The dielectric materials in such a cable are chosen and distributed so as to minimize the difference between the maximum and minimum electric field strengths in the cable. This process is called *grading*, of which there are two main types:

1. Capacitance grading
2. Intersheath grading

9.3.1 Capacitance Grading

In this type of grading, two or more layers with different values of dielectric constants are used to insulate the cable, as shown in Figure 9.2.

The permittivities of these layers are so chosen that the maximum electric field E with radius r is as shown in Figure 9.3.

For equal maximum field strengths, it is necessary to have

$$\epsilon_1 R_2 = \epsilon_2 R_3 \tag{9.2}$$

Thus, where E_{max} is the maximum allowable electric field, the operating voltage V of the cable is given by

$$V = E_{max}\left(R_3 \ln\frac{R_2}{R_3} + R_2 \ln\frac{R_1}{R_2}\right) \tag{9.3}$$

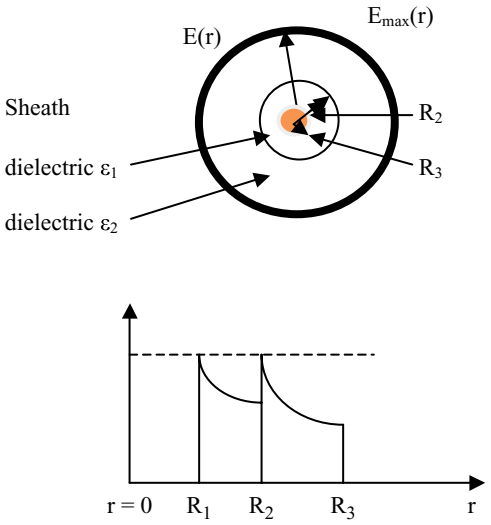

FIGURE 9.2
Capacitance grading.

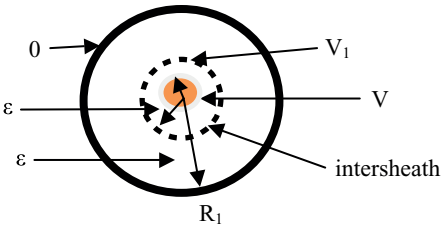

FIGURE 9.3
Electric field as a function of radius *r*.

9.3.2 Intersheath Grading

In intersheath grading, the cable contains several layers of a single dielectric material separated by coaxial metallic sheaths that are inserted into the dielectric and maintained at predetermined voltages suitable to the corresponding dielectric strength of the material. A cable with one such intersheath is shown in the cross-section of Figure 9.4. The radii are so chosen so as to satisfy Equation 9.4:

$$\frac{R_1}{R_2} = \frac{R_2}{R_3} = a \tag{9.4}$$

If the intersheath is kept at voltage V_1, then at the surface of the conductor we have

$$E_{3\max} = \frac{V - V_1}{R_3 \ln\left(\frac{R_2}{R_3}\right)} = \frac{V - V_1}{R_3 \ln a} \tag{9.5}$$

At the surface of the intersheath, the maximum electric field is given by

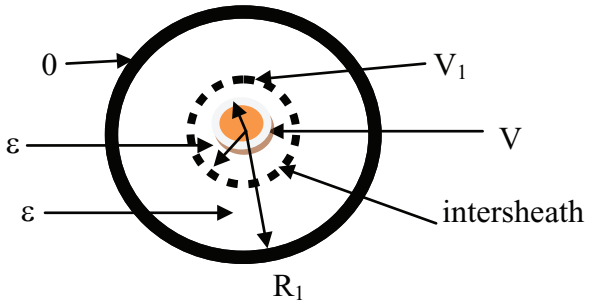

FIGURE 9.4
Cable with intersheath grading.

$$E_{2\max} = \frac{V_1}{R_2 \ln\left(\frac{R_1}{R_2}\right)} = \frac{V_1}{R_2 \ln a} \tag{9.6}$$

Thus, for the maximum electric fields in Equations 9.5 and 9.6 to be equal, the intersheath grading principle at these two surfaces yields

$$V_1 = \left(\frac{a}{1+a}\right)V \tag{9.7}$$

which, using Equations 9.5 and 9.7, further yields

$$E_{3\max} = \frac{V}{R_3 \ln\left(\frac{R_2}{R_3}\right)} = \frac{V}{R_3 \ln a}\left(\frac{a}{1+a}\right) \tag{9.8}$$

Without the intersheath (refer to problems P.9.1 and P.9.4) in solving this equation this results in

$$E_{\max} = \frac{V}{R_3 \ln\left(\frac{R_1}{R_3}\right)} = \frac{V}{R_3 \ln\left(\frac{aR_2}{R_2/a}\right)} = \frac{V}{R_3 \ln a^2} = \frac{V}{2R_3 \ln a} \tag{9.9}$$

Thus, comparing Equations 1.08 and 9.9 yields

$$\frac{E_{\max}\left(\text{with intersheath}\right)}{E_{\max}\left(\text{without intersheath}\right)} = \frac{2}{1+a} \tag{9.10}$$

9.4 Underground Cable Capacitance

We have seen that the capacitance per unit length of a single-conductor cable is given by

$$C = \frac{Q}{V} = \frac{2\pi \in}{\ln\left(\frac{R_1}{R_2}\right)} \quad \text{in farads per meter} \tag{9.11}$$

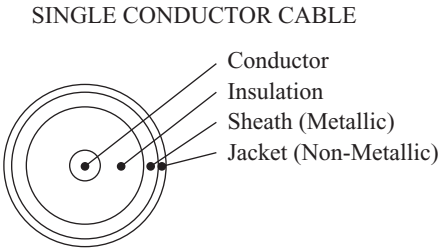

FIGURE 9.5
Equilaterally spaced conductors.

In a three-conductor cable, as shown in Figure 9.5, we assume the conductors are equilaterally spaced.

To find the capacitance per phase, we change the δ-connected capacitances C_2 to their equivalent wye form, as shown in Figure 9.6a, and then obtain the capacitance combinations per phase, as shown in Figure 9.6b and Figure 9.6c, as follows:

$$C_n = C_1 + 3C_2 \tag{9.12}$$

9.5 Underground Cable Inductance

As seen earlier, the inductance per unit length of a single conductor is given by

$$L = \frac{\mu_0}{2\pi} \ln \frac{R_1}{R_2} \quad \text{in Henrys per meter} \tag{9.13}$$

Other expressions leading to the per-phase inductance of a three-conductor cable have been evaluated earlier and can be referred to accordingly.

9.6 Heating and Dielectric Loss

In belowground cables, heat is generated through the I^2R losses in the copper or aluminum conductors and sheath, and dielectric loss occurs in the insulation. The latter is caused due to leakage currents. Thus, a cable has a capacitance that is lossy with a resistance R_i, as shown in Figure 9.7a. The loss in R_i is given by

$$P = \frac{V^2}{R_i} \tag{9.14}$$

In terms of the loss angle δ shown in Figure 9.7b, we have

$$\tan\delta = \frac{I_{R_i}}{I_c} = \frac{V / R_i}{\omega C V} \tag{9.15}$$

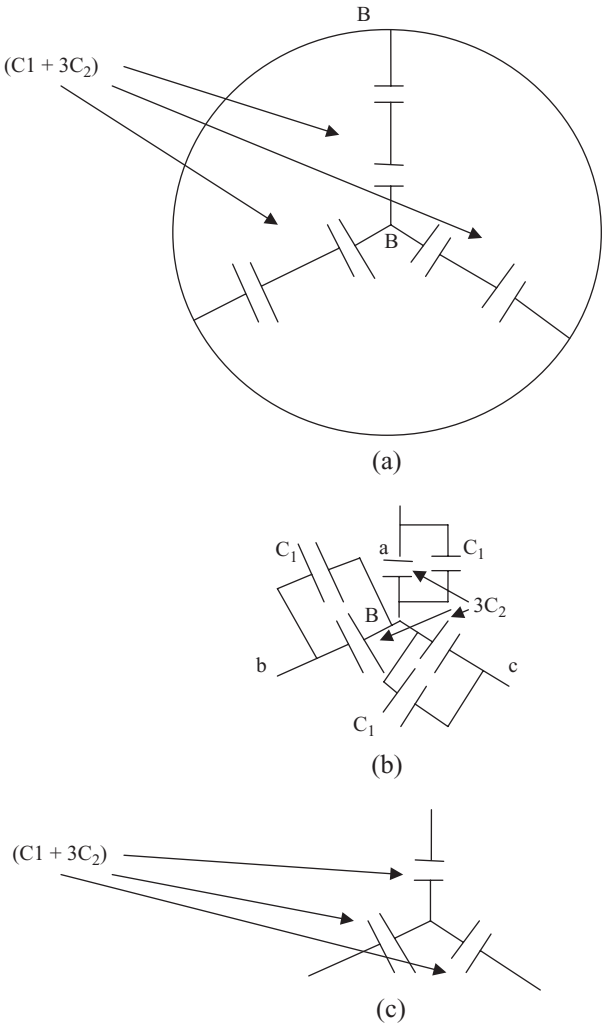

FIGURE 9.6
Capacitance reduction to (C_1+3C_2) as in parts (a), (b) and (c).

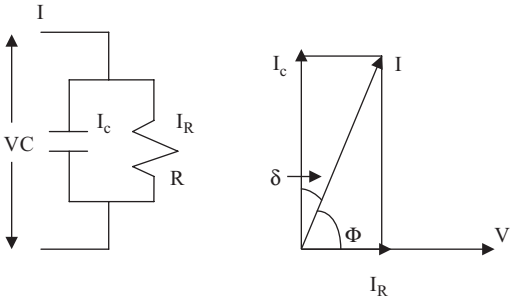

FIGURE 9.7
Heating and dielectric loss in a cable.

Together, Equations 9.14 and 9.15 yield

$$P = \omega C V^2 \tan\delta = \omega C V^2 \delta \quad \forall\, \delta \text{ small} \tag{9.16}$$

9.7 Cable Impedances

These impedances are evaluated using symmetrical component methodology. Generally, most of the formulae are well established and can be found in detail in [1]. The cable constructions are as described in Section 9.2 for different gradings. Some additional configurations are shown in Figure 9.8.

As with overhead lines (Chapter 4), the terms *geometric mean distance* (GMD) and *geometric mean radius* (GMR) are commonly used in underground cables.

9.7.1 Positive- and Negative-Sequence Resistance (r_1 and r_2)

Resistance values for underground cable depend on the following factors:

1. Conductivity of the conductor material or metal
2. Temperature
3. Frequency
4. Proximity to metal surface
5. Sheath material

Besides, resistance values are usually readily available for cable conductors at 60 Hz; these are tabulated in Table 9.1.

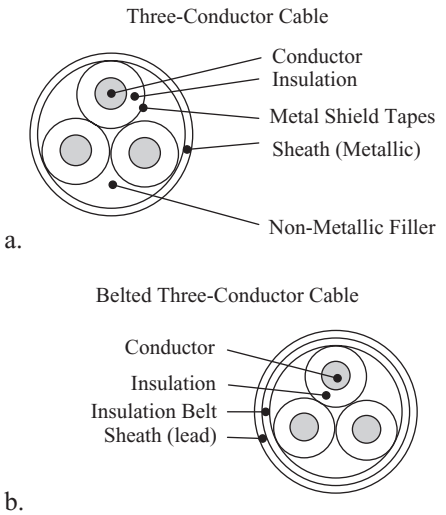

FIGURE 9.8
Different forms of cables.

TABLE 9.1

Skin Effect for X and Related K Factors

X	K	X	K	X	K	X	K
0.0	1.00000	1.0	1.00519	2.0	1.07816	3.0	1.31809
0.1	1.00000	1.1	1.00758	2.1	1.09375	3.1	1.35102
0.2	1.00001	1.2	1.01071	2.2	1.11126	3.2	1.38504
0.3	1.00004	1.3	1.01470	2.3	1.13069	3.3	1.41999
0.4	1.00013	1.4	1.01969	2.4	1.15207	3.4	1.45570
0.5	1.00032	1.5	1.02582	2.5	1.17358	3.5	1.49202
0.6	1.00067	1.6	1.03323	2.6	1.20056	3.6	1.52879
0.7	1.00124	1.7	1.04205	2.7	1.22753	3.7	1.56587
0.8	1.00212	1.8	1.05240	2.8	1.25620	3.8	1.60314
0.9	1.00340	1.9	1.06440	2.9	1.28644	3.9	1.64051

The positive and negative-sequence resistance values for aerial lines are given by

$$r_{t2} = \frac{M + t_2}{M + t_1}(r_{t1}) \tag{9.17}$$

where:

$M = 234.5$ for annealed 100% conductivity copper

$M = 228.1$ for aluminum

Temperatures are in degrees Celsius

In underground cables. the alternating current in the conductor of a single-conductor cable, as shown in Figure 9.8a, induces alternating voltages in the sheaths. When sheaths are continuous and bonded together at their ends so that their currents may flow longitudinally, additional losses develop in the sheaths. The way to represent these stray losses is to consider them as an increase in the resistance of the conductors involved. For single-conductor cables operating in three-phase systems, this increment in resistance can be calculated by the following equation [2]:

$$\text{Incremental } r = \frac{x^2{}_m r_s}{x^2{}_m + r^2{}_s} \tag{9.18}$$

where:

x_m = mutual reactance between conductors and sheath in ohms per phase per mile

$$= 0.2794 \log_{10} \frac{2S}{r_0 + r_i} \text{ for } 60\,\text{c/s}$$

r_s = resistance of the sheath in ohms per phase per mile

S = spacing between conductor centers in inches

r_o = outer radius of the lead sheath in inches

r_i = inner radius of the lead sheath in inches

Note: This correction is only for single-conductor cables and is ignored for three conductors under one sheath.

The total resistance r_a to positive- or negative-sequence current flow in single-conductor cables, including the effect of sheath currents, is given by

$$r_a = r_c + \frac{x^2{}_m r_s}{x^2{}_m + r_s} \tag{9.19}$$

where r_c is the AC resistance of the conductor alone, including the skin effect, at the operating temperature and frequency. Equation 9.19 applies rigorously only when the cables are in equilateral triangular configuration. For further arrangements, the GMD can be used instead of S with sufficiently accurate results for most practical purposes. We also need to use inches for terms in the GMD calculations. The sheath loss in a three-conductor cable is usually negligible, except for very large cables, and then it is important only when making quite accurate calculations. In the largest cables, they amount to only 3% to 5% of the conductor loss.

9.8 Positive- and Negative-Sequence Reactance of Underground Cables

The reactance of single-conductor lead-sheathed underground cables caused by positive- and negative-sequence currents is dependent on the construction of the conductor and the radial separation between the conductor and sheath currents. This phenomenon is described by the following equation:

$$x_1 = x_2 = x_a + x_d + \frac{x^3{}_m}{x^2{}_m r_s{}^2} \frac{\dfrac{\Omega}{\text{phase}}}{\text{mile}} \tag{9.20}$$

x_m and r_s were defined earlier as part of Equation 9.18 for cable conductor resistance.

For 60 c/s, the first and second term of Equation 9.20 can be shown as

$$x_a = 0.2794 \log_{10} \frac{12}{\text{GMR}_{1c}} \tag{9.21}$$

and

$$x_d = 0.2794 \log_{10} \frac{\text{GMD}_{3c}}{12} \tag{9.22}$$

where:

GMR_{1c} = geometric mean radius of one conductor in inches
GMD_{3c} = geometric mean distance among three conductors in inches
GMD = $\sqrt[3]{D_{ab} D_{bc} D_{ca}}$

where:

D_{ab} = distance between centers of conductor a and b
D_{bc} = distance between centers of conductor b and c
D_{ca} = distance between centers of conductor c and a

9.9 Positive- and Negative-Sequence Reactance of Three-Conductor Cables

Three-conductor non-shielded cable has negligible sheath current effects present in it. As a result, the reactance to positive- and negative-sequence currents is a much simpler calculation. It is similar to the equation used for aerial or overhead line impedances, except GMD and GMR are measured in inches, as shown below:

$$x_1 = x_2 = x_a + x_d \tag{9.23}$$

whereas before,

$$x_a = 0.2794 \log_{10} \frac{12}{\text{GMR}_{1c}} \tag{9.24}$$

and

$$x_d = 0.2794 \log_{10} \frac{\text{GMD}_{3c}}{12} \tag{9.25}$$

For sectored, three-conductor cables, as shown in Figure 9.8b, the conductor shape change does change the reactance; however, no accurate data exists to date on this effect. Dr. Donald Simmons who developed the basis for most cable calculations in the 1920s, is still quoted as the authority for the statement that reactance is 5% to 10% less for segmented conductors than for round conductors of the same area and insulation thickness.

For shielded three-conductor cables, the reactance for positive- and negative-sequence currents can be calculated as though the shields were not present, making it similar to that in belted three-conductor cables. The reactance of the circulating currents in the shielding tapes, calculated by the method used for determining sheath effects in single-conductor cables, proves to be negligible.

9.10 Zero-Sequence Resistance and Reactance for Three-Conductor Cables

Zero-sequence currents flowing along the single-phase conductors of a circuit must return either in the ground, in cable sheaths, in neutral wires, or in combinations of the three.

One approach to this problem is to treat the cable, sheath and earth impedances as one entity, where the neutral wire is considered as a separate entity altogether in the calculations, resulting in a combination of these two effects, similar to aerial lines as earlier. These three cases are as follows:

1. The return currents in sheath and ground are in parallel to each other.
2. All return currents exist in the sheath with none in the ground.
3. All return currents exists in the ground with none in the sheath.

We now attempt to find the zero-sequence resistance and reactance for these three cases as follows.

Case 1: Return current in sheath and ground are in parallel to each other

We first consider the impedance of three parallel conductors with the earth conductor as the return circuit, which yields:

$$Z_c = r_c + r_e + j\left(x_a + x_e - 2x_d\right) \tag{9.26}$$

where:

r_e = AC resistance of one conductor in ohms per mile
r_c = AC resistance of the earth return conductor in ohms per mile (values are shown in Table 9.2 for the equivalent depth of the earth return)
x_a = conductor self-reactance in ohms per mile
x_e = reactance of earth return conductor in ohms per mile (=0.8382 $\log_{10} D_e/12$ Ω/mi. for 60 Hz)
x_d = 0.2794 $\log_{10}$ $GMD_{3c}/12$ Ω/mi. and GMD_{3c} is the GMD for the three-conductor spacing in inches

We further consider the impedance of the cable sheath, with the presence of the earth return but ignoring the conductor group.

$$Z_{cs} = 3r_s + r_e + j\left(3x_s + x_e\right) \tag{9.27}$$

where:

r_s = sheath resistance in ohms per mile (= $0.2/(r_o + r_i)(r_o - r_i)$ for lead sheath)
r_i = inside radius of sheath in inches
r_o = outside radius of sheath in inches
x_s = reactance of sheath in ohms per mile (= 0.2794 $\log_{10}$ (24)/$(r_o + r_i)$ Ω/mi. at 60 Hz)

The neutral impedance between conductors and sheath considering the presence of the earth return path common to both sheath and conductors, in zero-sequence terms, is

$$Z_m = r_e + j\left(3x_s + x_e\right) \tag{9.28}$$

TABLE 9.2

Equivalent Depth of Earth Return (D_e) and Earth Impedance (r_e and x_e) at 60 Hz

Earth Resistivity (Ω-m)	Equivalent Depth of Earth Return (D_e) (in.)	Equivalent Depth of Earth Return (D_e) (ft.)	Equivalent Earth Resistance (r_e) (Ω/mi.)	Equivalent Earth Reactance (x_e) (Ω/mi.)
1	3.36×10^3	280	0.286	2.05
5	7.44×10^3	620	0.286	2.34
10	1.06×10^4	880	0.286	2.47
50	2.40×10^4	2,000	0.286	2.76
100	3.36×10^4	2,800	0.286	2.89
500	7.44×10^4	6,200	0.286	3.18
1,000	1.06×10^4	8,800	0.286	3.31
5,000	2.40×10^4	20,000	0.286	3.60
10,000	3.36×10^4	28,000	0.286	3.73

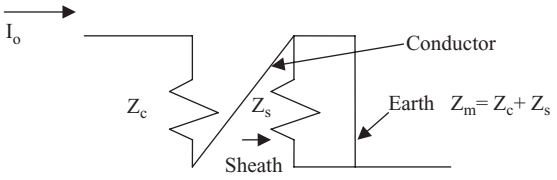

FIGURE 9.9
Case 1 configuration for zero-sequence impedance.

Combining the mutual impedance into a common series element, the total zero-sequence impedance in Figure 9.9b is given by

$$Z_{oa} = (Z_c - Z_m) + \frac{(Z_s - Z_m)Z_m}{Z_s - Z_m + Z_m} = Z_c - \frac{Z^2{}_m}{Z_s} \tag{9.29}$$

Case 2: Solution with sheath current as return path only

In this case, if sheath currents flow in the sheath only, with no current flowing in the ground circuit, then

$$Z_{0a} = (Z_c - Z_m) + (Z_s - Z_m) \qquad \text{(as in Figure 9.9b)} \tag{9.30}$$

$$Z_{0a} = (Z_c + Z_s - 2Z_m)$$

$$Z_{0a} = \left[(r_c + r_e + j(x_a + x_e - 2x_d)\right] + \left[3r_s + r_e + j(3x_s + x_e)\right] - 2\left[r_e + j(3x_s + x_e)\right]$$

Simplifying further yields

$$Z_{0a} = r_c + 3r_s + j\left[x_a - 2x_d - 3x_s\right] \frac{\Omega}{\text{mile}} / \text{phase} \tag{9.31}$$

Case 3: Solution with earth return path only

If the currents in conductors flow only in the ground circuit, with no current in the sheath, as is the case for non-shielded cables, or with closely spaced insulating sleeves, then we have

$$Z_{0a} = (Z_c - Z_m) + Z_m$$

Inserting the values of the components on the right-hand side, we have

$$Z_{0a} = r_c + r_e + j\left[x_a + x_e - 2x_d\right] \frac{\Omega}{\text{mile}} / \text{phase} \tag{9.32}$$

Shielding tapes around the individual cables of three-conductor cables have very little effect on the zero-sequence impedance and can be ignored. Also, the GMRs for three-sector conductors is about 90% of the GMR_{3c} for three-round conductors with the same copper area and insulation thickness.

The neutral wire self-impedance (with earth return) takes the following form:

$$Z_{0g} = 3r_a + r_e + j\left(3x_a + x_e\right) \tag{9.33}$$

where:
r_a = AC resistance of the wire
r_e and x_e are as in Table 9.2
x_a = self-reactance of the wire

The mutual impedance between the cable circuit and the ground wire, both with earth return, is

$$Z_{0ag} = r_e + j\left(x_e - 3x_{\text{dag}}\right) \tag{9.34}$$

where:
r_e and x_e are as in Table 9.2.
$x_{\text{dag}} = 0.2794 \log_{10} \sqrt[3]{d_{ag} d_{bg} d_{cg}}$
d_{ag} = distance between phase a center and ground wire
d_{bg} = distance between phase b center and ground wire
d_{cg} = distance between phase c center and ground wire

Thus, the total zero-sequence impedance with neutral wire takes the following form:

$$Z_0 = Z_{0a} - \frac{Z^2_{0ag}}{z_{0g}} \tag{9.35}$$

where:
Z_{0a} =zero-sequence self-impedance of the cable circuit, including the sheath and earth returns
Z_{0ag} = mutual impedance between the cable circuit and the neutral wire
Z_{0g} =self-impedance of the neutral wire

9.11 Zero-Sequence Resistance and Reactance for Single-Conductor Cables

For the conductor we have

$$Z_c = r_c + r_e + j\left(x_a + x_e - 2x_d\right) \tag{9.36}$$

where:
r_e = AC resistance of one conductor in ohms per mile
r_c = AC resistance of earth return conductor in ohms per mile (values are shown in Table 9.2 for the equivalent depth of the earth return)
x_a = conductor self-reactance in ohms per mile (= $0.2794 \log_{10} 12/\text{GMR}_{1c}$)
x_e = reactance of earth return conductor in ohms per mile (= $0.8382 \log_{10} D_e/12$ Ω/mi. for 60 Hz)
x_d = $0.2794 \log_{10} \text{GMD}_{3c}/12$ Ω/mi. and GMD_{3c} is the GMD for the three-conductor spacing in inches
$\text{GMD}_{3c} = \sqrt[3]{d_{ab} d_{bc} d_{ca}}$
d_{ab} = distance between the centers of conductors a and b, and so on

For the sheath, we have

$$Z_s = r_s + r_e + j\left(x_s + x_e - 2x_d\right) \tag{9.37}$$

where:

r_s = lead sheath resistance in ohms per mile (= $0.2/(r_o + r_i)(r_o - r_i)$ for lead sheath)
r_i = inside radius of sheath in inches
r_o = outside radius of sheath in inches
x_s = reactance of sheath in ohms per mile (= $0.2794 \log_{10}(24)/(r_o + r_i)$ Ω/mi. at 60 Hz)

$$Z_m = r_e + j\left(x_s + x_e - 2x_d\right) \tag{9.38}$$

For parallel paths of ground and sheath current (not including neutral wire):

$$Z_{oa} = \left(Z_c - Z_m\right) + \frac{\left(Z_s - Z_m\right)Z_m}{Z_s - Z_m + Z_m} = Z_c - \frac{Z^2{}_m}{Z_s} \tag{9.39}$$

For sheath return only (ignore neutral wire):

$$Z_{0a} = Z_e + Z_s + 2Z_m$$

$$= r_c + r_s + j\left(x_a - x_s\right)\frac{\Omega}{\text{mile}}/\text{phase} \tag{9.40}$$

For ground return only (ignore neutral wire):

$$Z_{0a} = \left(Z_c - Z_m\right) + Z_m = Z_c \frac{\Omega}{\text{mile}}/\text{phase} \tag{9.41}$$

Additionally, to consider the effects with neutral wires, we need to have

$$Z_0 = Z_{0a} - \frac{Z^2{}_{0ag}}{Z_{0g}} \quad \frac{\Omega}{\text{phase}} \tag{9.42}$$

where Z_{0a} is found above for appropriate return, Z_{0ag} and Z_{0g} are found using the formulas used earlier in the three-conductor cable zero-sequence impedance section.

If no neutral wire exists, we have

$$Z_0 = Z_{0a} \quad \frac{\Omega}{\text{mile}}/\text{phase} \tag{9.43}$$

9.12 Thermal Rating of Distribution Lines

Besides electrical characteristics, the thermal characteristics must be considered in the total design of all distribution lines. In North America (e.g., the United States), temperatures can vary drastically from the north to the south or from east to west. This is made amply clear by the global warming that is being experienced by all parts of the world.

9.12.1 Overhead Lines

The rating of overhead lines is a function of several factors. The conductor metal itself should not be allowed to heat to the point where it will severely anneal and lose its tensile strength. Factors influencing the maximum current the line can carry for this restriction include conductor resistance, ambient temperature, wind speed and solar heating effects. Higher-resistance conductors heat up more for the same current than lower-resistance conductors. Ambient temperature and solar heating have an obvious effect on conductor temperature, and wind will carry away heat, helping keep temperatures down. Annealing is a cumulative effect and does not occur 'all at once' for temperatures encountered in the operation of electrical power lines. Some annealing may be allowed if the loss of strength is within tolerable and manageable limits.

Even if a conductor is not heated to the point where it will anneal, it is usually limited by other restrictions. For example, as any metal is heated, it tends to expand. Current-loaded wires heat up and expand, resulting in an increase sag. This too must be considered, and the conductor must not be heated to the point where its sag will violate required clearances to other utilities or to the ground. One must also consider the ampere rating of devices connected to aerial lines, including slices, connectors, cutouts, and so on, when settling limits for operation.

Finally, ratings are influenced by duration. What may be permissible for 1 h. operation may be allowed for 5 min. without serious consequences. Thermal response is not instantaneous. It has a *thermal time constant*, and this can be utilized to increase ratings for short time periods. The fundamental equation for line ratings is the following heat balance equation:

$$q_c + q_r = q_s + I^2 r \tag{9.44}$$

where:

q_c = convected heat loss in watts per lineal foot of conductor
q_r = related heat loss in watts per lineal foot of conductor
q_s = heat gain from the sun in watts per lineal foot of conductor
I = conductor current in amperes at 60 Hz
r = 60 Hz resistance of the conductor in ohms per foot

We now find I as follows:

$$I = \sqrt{\frac{q_c + q_r - q_s}{r}} \tag{9.45}$$

This leads to the convected heat loss as follows:

$$q_c = \begin{cases} \left[1.01 + 0.3711\left(\dfrac{D\rho_f V}{\mu f}\right)^{0.52}\right] k_f\left(t_c - t_a\right); \forall \dfrac{D_o \rho_f V}{\mu f} = 0.1 \text{ to } 1000 \\ \text{OR} \\ \left[0.1695\left(\dfrac{D\rho_f V}{\mu f}\right)^{0.6}\right] k_f\left(t_c - t_a\right); \forall \dfrac{D_o \rho_f V}{\mu f} = 1000 \text{ to } 18{,}000 \end{cases} \tag{9.46}$$

where:

D = conductor diameter in inches
D_o = conductor diameter in feet
ρ_f = density of air in pounds per cubed feet
V = wind speed in feet per hour
μf = absolute conductivity of air in pounds per kilo foot-hour or as kilo foot-second (kfs)
kf = thermal conductivity of air in watts per square foot degrees Celsius
t_c = conductor temperature, average in degrees Celsius
t_a = ambient temperature in degrees Celsius

If $V = 0$, use the natural convection heat loss equation at sea level:

$$q_c = 0.072\ D^{0.75}(t_c - t_a)^{1.25}\ \text{watts per linear foot of conductor} \tag{9.47}$$

At higher altitudes:

$$q_c = 0.0283\ D^{0.75}(t_c - t_a)^{1.25}\ \text{watts per linear foot of conductor} \tag{9.47}$$

ρf, μf and kf are taken from tables of air properties (Table 9.3). Use the values at temperature t_f, where

$$t_f = \frac{(t_c + t_a)}{2} \tag{9.48}$$

Table 9.3 displays the viscosity, density and thermal conductivity. All values are from [2–4].

9.12.1.1 Radiated Heat Loss

$$q_r = 0.138 D\varepsilon\left[\left(\frac{K_c}{100}\right)^4 - \left(\frac{K_a}{100}\right)^4\right]\ \text{watts per foot of conductor} \tag{9.49}$$

where:

D = conductor diameter in inches
ε = emissivity factor = 0.23 for new wire
= 0.91 for black wire
= 0.75 for general EverSource Company
(erstwhile North East Utilities, Connecticut) use
K_c = temperature of conductor in degrees Kelvin
K_a = ambient temperature in degrees Kelvin

Note: degrees Kelvin = degrees Celsius + 273

TABLE 9.3

Viscosity, Density and Thermal Conductivity of Air

Temp °F	Temp °C	Temp °K	(°K/100)^4	Absolute Viscosity (lb./ft. hr.) [3]	Density Air [4] (lb/ft.^{2}) ρ_f Sea level	5,000 ft.	10,000 ft.	15,000 ft.	Thermal Conductivity of Air [5] (W/ft.^{2} °C) K_f
32	0	273	55.55	0.0415	0.0807	0.0671	0.0555	0.0447	0.00739
41	5	278	59.73	0.0421	0.0793	0.0660	0.0545	0.0439	0.00750
50	10	283	64.14	0.0427	0.0779	0.0648	0.0535	0.0431	0.00762
59	15	288	68.80	0.0433	0.0765	0.0636	0.0526	0.0424	0.00773
68	20	293	73.70	0.0439	0.0752	0.0626	0.0517	0.0417	0.00784
77	25	298	78.86	0.0444	0.0740	0.0616	0.0508	0.0411	0.00795
86	30	303	84.29	0.0450	0.0728	0.0606	0.0500	0.0404	0.00807
96	35	308	89.99	0.0456	0.0716	0.0596	0.0492	0.0397	0.00818
104	40	313	95.98	0.0461	0.0704	0.0586	0.0484	0.0391	0.00830
113	45	318	102.26	0.0467	0.0693	0.0577	0.0476	0.0385	0.00841
122	50	323	108.85	0.0473	0.0683	0.0568	0.0469	0.0379	0.00852
131	55	328	115.74	0.0478	0.0672	0.0559	0.0462	0.0373	0.00864
140	60	333	122.96	0.0484	0.0661	0.0550	0.0454	0.0367	0.00875
149	65	338	130.52	0.0489	0.0652	0.0542	0.0448	0.0363	0.00886
158	70	343	138.41	0.0494	0.0643	0.0535	0.0442	0.0358	0.00898
167	75	348	146.66	0.0500	0.0634	0.0527	0.0436	0.0354	0.00909
176	80	353	155.27	0.0505	0.0627	0.0522	0.0431	0.03947	0.00921
185	85	358	164.26	0.0510	0.0616	0.0513	0.0423	0.0347	0.00932
194	90	363	173.63	0.0515	0.0608	0.0506	0.0418	0.0343	0.00943
203	95	368	183.40	0.0521	0.0599	0.0498	0.0412	0.0338	0.00953
212	100	373	193.57	0.0526	0.0591	0.0492	0.0406	0.0333	0.00966

9.12.1.2 Solar Heat Gain

$$q_s = 5.59 \times D \text{ for summer general EverSource Company use} \tag{9.50}$$

$$q_s = 2.41 \times D \text{ for winter general EverSource Company use} \tag{9.51}$$

There are very complete formulae for solar heat gain, but for practicality, they have been reduced to the preceding formulae. See [3] for more information.

Using a normal maximum temperature $t_c = 100°C$ and 3 ft./s wind speed, it is expected conductors will not seriously anneal over their expected life cycle. Although annealing starts to occur well below 100°C, considering the daily variation in loads, the odds are that the annealing will not be serious enough to deteriorate the condition of the conductor severely. In all cases, the emergency rating is calculated using a conductor temperature t_c of 140°C.

To account for the sag, sag curves are calculated by wire temperatures for the conductor at every temperature needing consideration. The line must be designed so the sag at 140°C is acceptable. A sag curve is a catenary curve for the conductor at a given temperature, drawn to a required and appropriate scale. Transient ratings are developed from formulae taking into account the thermal time constant of the conductor. These time constants range from 5 to 15 min. In one time constant, the cable will reach 67% of the ultimate temperature it will attain for the given loading. Usually, an infinite number of time constants are required, but the changes after three are very small. Formulae for calculating ratings on a transient basis are left for the interested reader to seek out for themselves.

9.12.1.3 Cables

Calculation of the ampere rating of cables is usually based on the work of Neher and McGrath [4]. Further information can be obtained from [5] for the material adopted herein.

The calculation of the temperature rise of cable systems under steady-state conditions only, which includes the effect of operation under a repetitive load cycle, as opposed to transient temperature rises due to the sudden application of large loads, is a relatively easy procedure. It involves only the application of the thermal equivalents of Ohm's and Kirchhoff's laws to a relatively simple thermal circuit. In general, all thermal resistances are developed on the basis of the per-conductor heat flow through each of them. It is convenient to utilize an effective thermal resistance for the earth portion of the thermal circuit, which includes the effect of the loading cycle and the mutual heating effect of the other cables in the system. For reasonable simplicity, all cables in a system under analysis are considered to carry the same load currents and operate under the same load cycle.

The temperature rise of the conductor of a cable above ambient temperature may be considered to be composed of a temperature rise due to its own losses (ΔT_c) and the rise produced by the dielectric loss (ΔT_d). The self-losses include current-produced losses (I^2R), sheath losses and conduit losses, the latter also being current related. Dielectric losses are present at all times the cable is energized.

The above-ambient temperature rise of the conductor is found as follows:

$$T_c - T_a = \Delta T_c + \Delta T_d \tag{9.52}$$

where:
T_c = conductor temperature
T_a = ambient temperature

The change in conductor temperature due to current-produced losses is found as follows:

$$\Delta T_c = T_c - \left(T_a + \Delta T_d\right) \tag{9.53}$$

where:
ΔT_c = (heat power loss) × (thermal resistance to the heat power)

$$\Delta T_c = I^2 R dc\left(1 + Y_c\right)\left(\overline{R'_{ca}}\right) \tag{9.54}$$

where:
I = conductor current in kilo-amperes
Rdc = DC resistance of conductor in micro-ohms per foot
Y_c = increment in the resistance ratio due to the losses originating in the conductor with components Y_{cs} due to the skin effect and Y_{cp} due to the proximity effect
$\overline{R'_{ca}}$ = effective thermal resistance of the thermal circuit

$$= \overline{R_i} + q_s\overline{R_{se}} + q_e\overline{R}_e \tag{9.55}$$

where:
$\overline{R_i}$ = thermal resistance of insulation in thermal ohm-feet
q_s = ratio of sum of losses in conductor and sheath to losses in conductors
$\overline{R_{se}}$ = thermal resistance total between n sheath and diameter D_c around the cable
q_e = ratio of the sum of losses in the conductors, sheath and conduit to the losses in the conductors
$\overline{R'_e}$ = thermal resistance effective between diameter D_e around the cable and ambient earth, including the effects of the loss factor and mutual heating by other cables, calculated for the load factor of cable loading

From Equations 9.53 through 9.55 we find current I as follows:

$$I = \sqrt{\frac{\Delta T_c}{R_{dc}\left(1 + Y_c\right)R'_{ca}}} = \sqrt{\frac{T_c - \left(T_a + \Delta T_d\right)}{R_{dc}\left(1 + Y_c\right)R'_{ca}}}\ \text{kA} \tag{9.56}$$

where:
T_c = conductor temperature
T_a = ambient temperature
ΔT_d = temperature rise due to dielectric loss

$$\Delta T_d = W_d\overline{R'_{da}}$$
$$= W_d\left(\frac{\overline{R}_i}{2} + \overline{R}_{se} + \overline{R}_{eu}\right)$$

The heat loss due to dielectric losses incurs a thermal resistance of half the insulation itself on the average and all the thermal resistance of everything else. The heat rise due to dielectric losses is the product of the loss times the sum of all these thermal resistances.

$$\bar{R}_{se} = \bar{R}_j + \bar{R}_{sd} + \bar{R}_d$$

where:

$\bar{R}_j$ = jacket thermal resistance
$\bar{R}_d$ = duct wall thermal resistance
$\bar{R}_{sd}$ = thermal resistance between cable surface and surrounding duct or conduit wall
$\bar{R}_{eu}$ = thermal resistance of earth at unity load factor (dielectric losses are present at all times)

Terms such as $\bar{R}_j$ and $\bar{R}_d$ are found from the general formula for the thermal resistance of thin cylindrical sections. For quick calculations, $\bar{R}_j$ and $\bar{R}_d$ are often ignored and set equal to zero, as these values are small relative to $\bar{R}_{sd}$.

$$\bar{R} = 0.0104\bar{\rho}n^1\left(\frac{t}{D-t}\right)\text{thermal-ohm-feet} \tag{9.57}$$

where:

$\bar{\rho}$ = thermal resistivity of the material in degrees Celsius-centimeter per watt (Table 9.4)
t = thickness of cylinder
D = outside diameter of cylinder
n^1 = number of heat-producing conductors contained within the cylinder

q_s and $\bar{R}_{sd}$ are available from tables or the cable manufacturer. W_d is available from tables or the cable manufacturer and is expressed in watts per conductor foot. The reader is encouraged to read reference [4] for more details behind these factors.

The earth thermal resistance terms are defined by the following equation for direct buried cables:

$$\bar{R}'_e = 0.012\bar{\rho}_e n^1\left\{\log_{10}\left(\frac{D_x}{D_e}\right) + (L_F)\log_{10}\left[\left(\frac{4L}{D_x}\right)F\right]\right\} \quad \text{thermal-ohm-feet} \tag{9.58}$$

TABLE 9.4

Thermal Resistivities

Material	Thermal Resistivity ($\bar{\rho}$)
Paper insulation solid	700
Varnished cambric	600
Other paper	500–550
Rubber, rubber-like	500
Jute and textiles	500
Fiber duct	480
Polyethylene	450
Transite	200
Somastic	100
Concrete	85

where:

$\bar{\rho}_e$ = earth thermal resistivity (=90°C cm/W, unless known to be different)
n^1 = number of heat-producing conductors within the surrounding earth portion at different diameters D_e
D_x = diameter in inches at which portion of system commences (outer edge of duct bank)
L = depth of cable below earth's surface in inches
L_F = loss factor ($= 0.3(I_f + 0.7(I_f)^2$ per unit, where I_f = daily load factor)
F = factor accounting for the mutual heating of other cables in the cable system

$$F = \left(\frac{d'_{12}}{d_{12}}\right)\left(\frac{d'_{13}}{d_{13}}\right).....\left(\frac{d'_{1N}}{d_{1N}}\right) N-1 \text{ terms}$$

F = 1 if $N=1$
N = number of cables interacting
d_{1N} = distance from cable 1 to cable N
d'_{1N} = distance from cable 1 to image of cable N reflected aboveground (here, the principle of reflection will be used, as in the development of expression for the capacitance of a multi-cable system, as seen in Chapter 4)

For ducts in concrete, the following equation applies.

$$\overline{R'_e} = 0.012\bar{\rho}_e n^1 \left\{\log_{10}\left(\frac{D_x}{D_e}\right) + (L_F)\log_{10}\left[\left(\frac{4L}{D_x}\right)F\right]\right\} + 0.012(\bar{\rho}_e - \bar{\rho}_c)n^1 N(L_F)G_b \qquad (9.60)$$

where terms are as defined previously, and in addition:

$\bar{\rho}_c$ = concrete thermal resistivity (=85° cm/W unless known to be different)
G_b = a geometric factor found from Figure 9.10 as a function of L_b/P and the ratio of the long dimension to the short dimension of the duct bank, where:
L_b = depth to center of concrete enclosure
P = perimeter of duck bank in inches
q_e = sum of losses in conductor, sheath and conduit loss in conductor
q_e = $[(1+Y_c)+Y_a+Y_p]/(1+Y_c)$
$1+Y_c$ = ratio of conductor losses
Y_s = increment in ratio to account for sheath loss
Y_p = increment in ratio to account for conduit loss
q_e = $[(1+Y_c)+Y_s]/(1+Y_c)+Y_p/(1+Y_c) = q_s + Y_p/(1+Y_s)$
q_s can be found from tables
Y_p = 0 for non-magnetic ducts or conduits

OR

$$Y_p = \frac{1.54s - 0.115D_p}{R_{dc}} \text{ for three-conductor cable} \qquad (9.61)$$

OR

$$Y_p = \frac{0.89s - 0.115D_p}{R_{dc}} \text{ for single-conductor cable in close triangular formation} \qquad (9.62)$$

OR

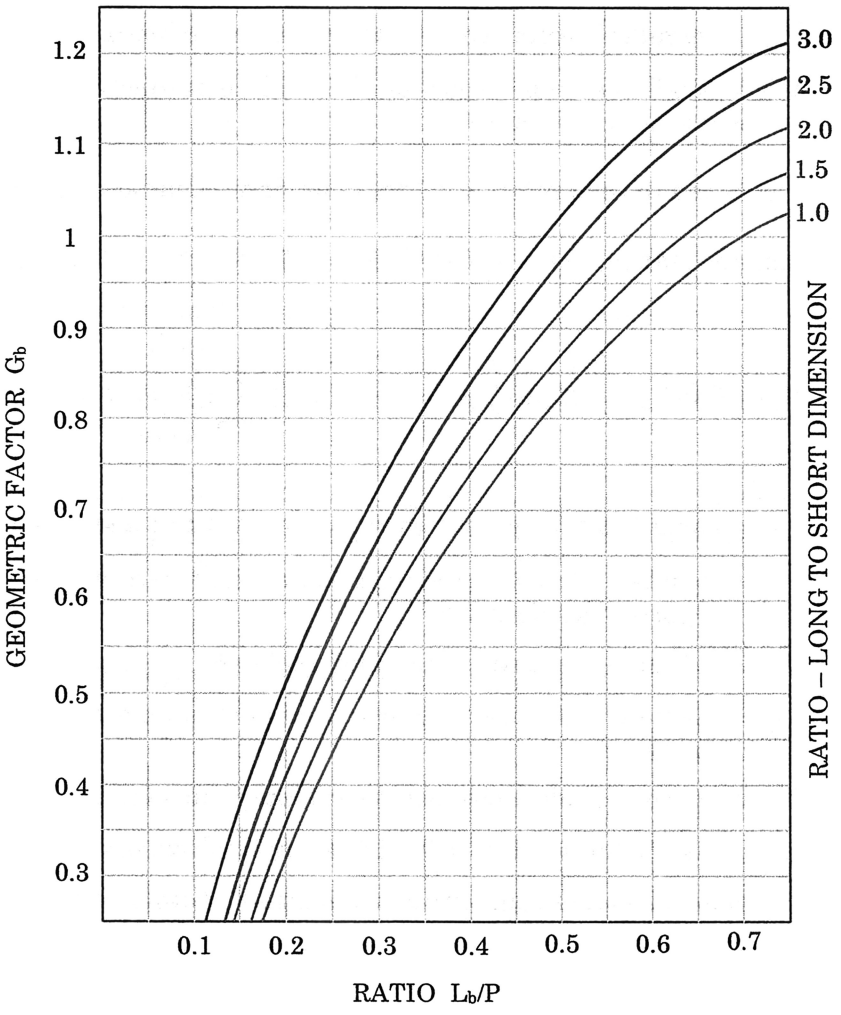

FIGURE 9.10
Geometric factor vs. ratio L_b/P.

$$Y_p = \frac{.34s - 0.175D_p}{R_{dc}} \quad \text{for single-conductor cable, cradled} \tag{9.63}$$

where:
D_p = inner diameter of duct wall in inches
S = axial (center line) spacing between adjacent cables in inches
s = distance between effective current center of the conductor and the axis of the cable

Tables are available for many common configurations of cables in duct banks, using the formulae presented here as their basis. Cases not covered here but left for the reader to investigate include cables in air, cables in conduit in air, other external heat sources and transient ratings ([3,4]). As a very quick approximation, loading guides have been developed for various duct banks where the ampacity of cables relative to a 2×2 duct bank are given (Figure 9.11).

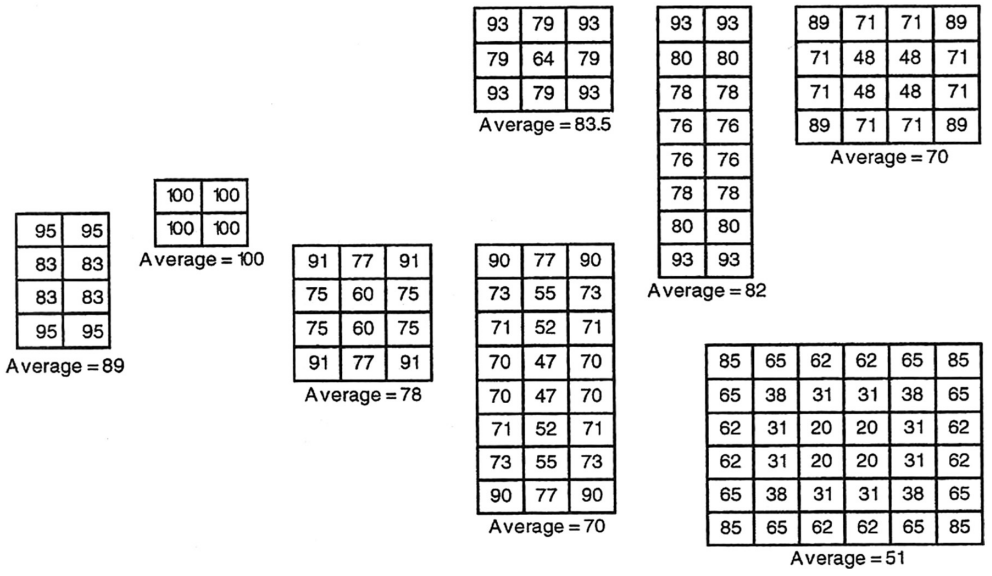

FIGURE 9.11
Effect of cable position in duct banks.

9.12.1.4 Effect of Cable Position in Duct Banks

When several equally loaded cables are placed in the same duct bank, the maximum permissible loading is the root mean square peak load of all cables. If all cables actually carried this load, the operating temperature of those in interior ducts would exceed the safe operating temperature of the insulation. Cables in outer ducts would not reach this value; overloading or underloading would always occur. To equalize the operating temperature of cables in the various locations at a value corresponding to the safe maximum temperature, the load must be multiplied by a position factor. This will decrease the load for the inner ducts and increase it for the outer ducts. The root mean square of the loads remains unchanged.

For unequally loaded cables, the same load position adjustment should be made.

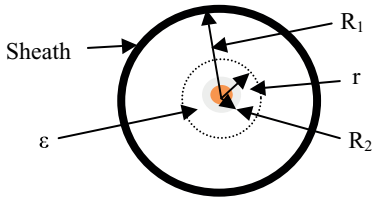

FIGURE P.9.1
Electric field strength of a cable.

Problems

PROBLEM P.9.1

Evaluate the maximum and minimum electric field strengths in the cable shown in Figure P.9.1.

PROBLEM P.9.2

Derive Equation 9.1.

PROBLEM P.9.3

A 13.2 kV single-conductor cable has an outside diameter of 10 cm. Find the conductor radius and the electric field strength that must be withstood by the insulating material in the most economical (optimal ratio) configuration.

PROBLEM P.9.4

For the cable shown in Figure P.9.4, find the condition under which the maximum values of the electric fields in the two regions are equal.

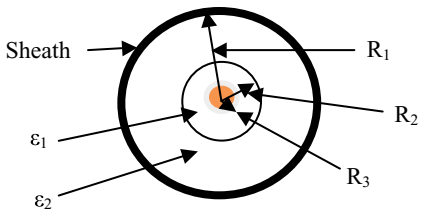

FIGURE P.9.4
Graded capacitance cable.

PROBLEM P.9.5

Sketch the electric field distribution in the cable of Figure P.9.4 if the following equation is implemented.

$$\in_1 R_1 = \in_2 R_2$$

PROBLEM P.9.6

For the cable shown in Figure P.9.4, let $R_1 = 2.5$ cm, $R_3 = 0.92$ cm and $R_2 = 1.75$ cm. Find

1. The maximum electric field for an operating voltage of 13.2 kV with capacitance grading
2. The maximum electric field for an operating voltage of 13.2 kV without capacitance grading

PROBLEM P.9.7

A cable has intersheath grading that satisfies Equation 9.4. The cable radii in reference to Figure 9.4 has $R_3 = 0.92$ cm and $R_1 = 2.5$ cm.

1. Determine the location of the intersheath.
2. Calculate the ratio of the maximum electric field strengths with intersheath.
3. Calculate the ratio of maximum electric field strengths without intersheath.

PROBLEM P.9.8

In Problem P.9.7, if the cable is designed to operate nominally at 13.2 kV without any grading, determine the maximum voltage at which the cable may be operated with appropriate intersheath grading.

PROBLEM P.9.9

Radially flowing leakage currents (dashed lined arrows in Figure P.9.9) are often present in underground cables. The leakage current is essentially limited by the insulation resistance of the cable. Derive an expression for the insulation resistance of a cable of length l m and having a dielectric resistivity of ρ Ω-m.

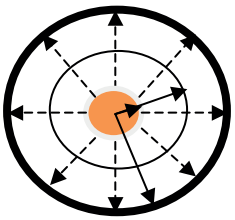

FIGURE P.9.9
Leakage currents in a cable.

PROBLEM P.9.10

In a test of a three-conductor cable, the three conductors are first bunched together, and the capacitance between the bunched conductors and sheath is found to be C_A. Then, two of the conductors are bunched with the sheath, and the capacitance between these and the third conductor is found to be C_B. Find

1. C_1 of Figure 9.5
2. C_2 of Figure 9.5

PROBLEM P.9.11

The capacitances per kilometer of a three-wire cable are 0.90 μF between the three-bunched conductors and the sheath, and 0.40 μF between the conductor and the other two connected to the sheath.

1. Find the line-to-ground capacitance of a 20 km length of this cable.
2. Find the line-to-ground capacitance of a 100 km length of this cable.

PROBLEM P.9.12

A single-core cable, consisting of a 1 cm-diameter cable inside a 2.5 cm-diameter sheath, is 10 km long and operates at 13.2 kV and 60 Hz. The relative permittivity of the dielectric is 5, and the open-circuit power factor of the cable is 0.08.

Find the capacitance of the cable and the charging current through the capacitor.

PROBLEM P.9.13

For the cable in Problem P.9.12, find the resistance and the dielectric loss.

PROBLEM P.9.14

For a cable as shown in Figure 9.2, $R_3 = 0.5$ cm, $R_1 = 2.5$ cm, $\varepsilon_1 = 2.5\varepsilon_0$ and $\varepsilon_2 = 4\varepsilon_0$. The electrical stresses in the inner and outer dielectrics are not to exceed 60 kV/cm and 50 kV/cm, respectively. What is the maximum permissible operating voltage for the cable?

References

1. Central Station Engineers of the Westinghouse Electric Corporation, *Westinghouse Electrical Transmission and Distribution Reference Book*, 1964, Chapter 4.
2. Hilsernath, J. and J. H. Touloukian, "The Viscosity, Thermal 5th Conductivity and Prandtl Numberfor Air and other Gases", 1948, *ASME Transactions*, Vol. 76, 1954, pp. 967–081.
3. Madison, R. D. (ed.), *Fan Engineering: An Engineer's Handbook*. Buffalo Forge Company, New York, 1949.
4. McAdams, W. H., *Heat Transmission*, 3rd edition. McGraw-Hill, New York, 1954.
5. Bartok, G. J et. al., "Fundamentals of Power Systems Analysis", Prepared by Engineers of the Northeast Utilities System, 1979, 1982, 1998, March, 25, 2008.

10

Symmetrical Three-Phase Faults

10.1 Symmetrical Three-Phase Faults

As discussed earlier, the flow of power can happen under fault-free conditions in the network. But if a fault does occur, then the current flowing in the network after the fault occurs depends on the following conditions and resources:

1. Internal EMFs or voltage sources of all synchronous machines, such as generators, in the network. This current has three distinct components: the current flowing immediately after the fault (subtransient), the current flowing a few cycles after the fault (transient) and the sustained (steady-state) value. All these differ significantly because of the effect of the armature flux and the inherent R–L circuit characteristic of the machine to a voltage source.
2. Impedances in the network between the synchronous machines and the fault.

We will try to understand the considerations in item (1) for a synchronous machine under fault, as seen in Figure 10.1 and as follows.

Analyzing the KVL for the circuit in Figure 10.1 we have

$$V = V_m \sin(\omega t + \alpha) = Ri + L\frac{di}{dt} \tag{10.1}$$

If at time $t = 0$ switch s is closed, then the magnitude of the voltage in Equation 10.1 is

$$i = \frac{V_{\max}}{|Z|}\left\{\sin(\omega t + \alpha - \theta) - e^{-\frac{Rt}{L}}\sin(\alpha - \theta)\right\} \tag{10.2}$$

where:

$$Z = \sqrt{R^2 + (\omega L)^2}\,;\ \text{and}\ \ \theta = \tan^{-1}\left(\frac{\omega L}{R}\right) \tag{10.3}$$

The first term inside the braces in Equation 10.2 varies sinusoidally over time, and the second term has an exponential decay, as shown in Figure 10.2.

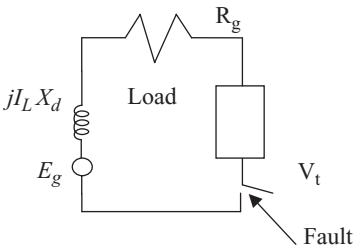

FIGURE 10.1
Synchronous machine under fault.

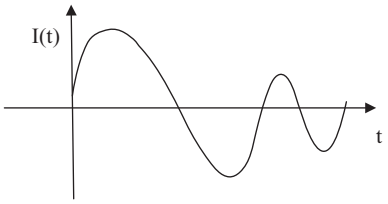

FIGURE 10.2
Current flowing in the synchronous machine after a fault occurs.

10.2 Symmetrical Three-Phase Fault Currents

Now consider a three-phase condition of the same synchronous machine in which a short circuit (SC) occurs; we will now try to find the shapes of these currents in all three phases as time changes, noting that the phase voltages in the three different phases E_a, E_b and E_c are displaced by 120° and when the SC occurs, over time it occurs at different amplitude points on the waves of each phase, as shown in Figure 10.3.

This implies that the DC transient component is different in each phase. If this DC component is eliminated, then the resulting plot from Figures 10.2 and 10.3 changes for each phase, as shown in Figure 10.4.

Referring to Figure 10.4 (as we also note in Figure 12.2), we can see it has the three regions as indicated by the different markings:

c: subtransient

b: transient

a: steady state

Thus, when a fault occurs, the flux across the air gap of the machine is much larger at the instant the SC occurs than it is a few cycles later. This reduction from point *c* to point *b* and then to point *a* is due to the armature current and is called the *armature reaction*. Thus, *oa* is the maximum value of the sustained SC current, and the corresponding RMS value is $0.707 \times oa = |I_g|$, and the corresponding reactance is given by

$$X_g = \frac{|E_g|}{|I_g|} - \text{synchronous reactance} = X_d \tag{10.4}$$

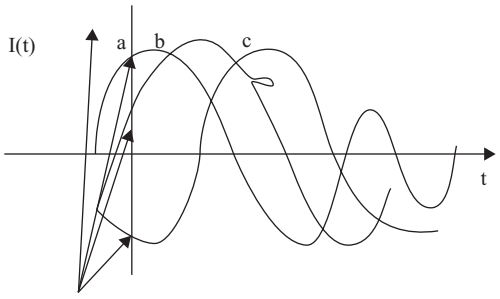

FIGURE 10.3
Failure points in each phase of the synchronous machine.

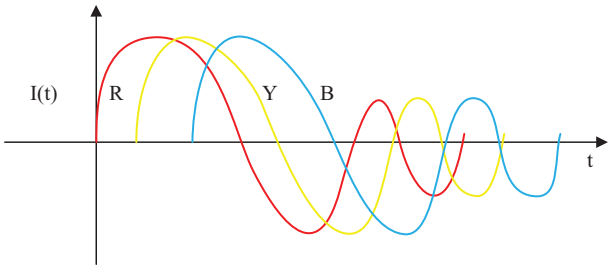

FIGURE 10.4
Short-circuit current in time after the fault.

Equation 10.4 also represents the direct-axis synchronous reactance X_d, as mentioned in Chapter 3 on generalized machines.

Over section *ob* is the transient current and $|I'_g|$ and the RMS value of that is $0.707 \times ob$. This results in another definition, as follows:

$$X'_d = \frac{|E_g|}{|I'_g|} - \text{transient reactance} \tag{10.5}$$

Over section *oc* is the subtransient current and $|I_g''|$ and the RMS value of that is $0.707 \times oc$, which results in another definition, as follows:

$$X''_d = \frac{|E_g|}{|I''_g|} - \text{subtransient reactance} \tag{10.6}$$

Example 10.1

The network shown in Figure 10.5 has two generators connected to a bus that is in turn connected to a transformer.

$$G_1 : 50\,\text{MVA}, 13.8\,\text{kV}; X''_g = 25\%$$

$$G_2 : 50\,\text{MVA}, 13.8\,\text{kV}; X''_g = 25\%$$

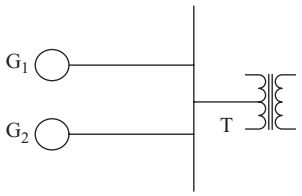

FIGURE 10.5
Two generators and a transformer connected to a bus.

$$T: 75\,\text{MVA}, 13.8\frac{\text{kV}}{69}\text{kV}\Delta / Y; X_1 = 10\%$$

Data given: Before a fault occurs, the voltage on the high-voltage side of transformer T is 66 kV. Transformer T is unloaded and there is no circulating current between the generators. Find the subtransient current in each generator when an SC occurs on the high-voltage side of the transformer.

SOLUTION

We choose a new base as 75 MVA, 69 kV, which results in the new subtransient reactances of generator G_1 and G_2 as follows:

$$G_1 : X_d'' = 0.25 \cdot \frac{75000}{50000} = 0.375\,\text{pu}$$

$$E_{g1} = \frac{66}{69} = 0.957\,\text{pu}$$

$$G_2 : X_d'' = 0.25 \cdot \frac{75000}{25000} = 0.75\,\text{pu}$$

$$E_{g2} = \frac{66}{69} = 0.957\,\text{pu}$$

$$T : X = 0.1\,\text{pu}$$

This yields the overall reactance diagram before fault given in Figure 10.6.

Say a three-phase fault at point P is simulated by closing switch s, resulting in a reduced reactance diagram at fault, as in Figure 10.7.

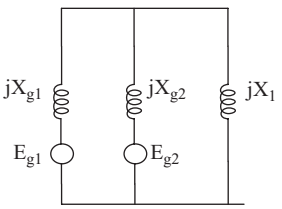

FIGURE 10.6
Reactance diagram of the network before fault.

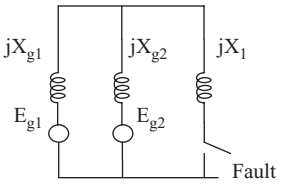

FIGURE 10.7
Reduced reactance diagram at fault.

The subtransient fault current in the circuit of Figure 10.7 is given by

$$I'' = \frac{E_g}{j0.35} = \frac{0.957}{j0.35} = -j2.735$$

The voltage on the δ side of the transformer T is given by

$$(-j2.735)(j0.10 = j0.2735)\,\text{pu}$$

Thus, the subtransient current on the primary side of the transformer is

$$I_1'' = \frac{0.957 - j0.2735}{j0.375} = -j1.823\,\text{pu} = 5720\,\text{A}$$

$$I_2'' = \frac{0.957 - j0.2735}{j0.75} = -j0.912\,\text{pu} = 2810\,\text{A}$$

10.3 Internal Voltages of Loaded Machines under Transient Conditions

Steady-state conditions are shown in Figure 10.8 and written as:

$$\text{Generator}: E_g = V_t + jI_L X_s \tag{10.7}$$

$$\text{Motor}: E_m = V_t - jI_m X_s \tag{10.8}$$

Transient conditions are shown in in Figure 10.9.

$$\text{Generator}: E_g' = V_t + jI_L X_d' \tag{10.9}$$

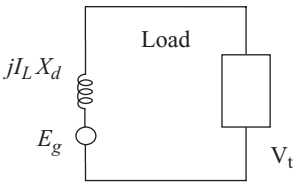

FIGURE 10.8
Steady-state circuit of a loaded machine.

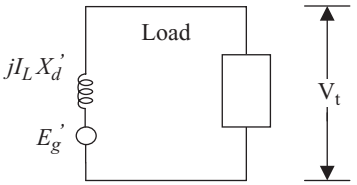

FIGURE 10.9
Transient circuit of a loaded machine.

$$\text{Motor}: E_m' = V_t - jI_m X_d' \tag{10.10}$$

Subtransient conditions are shown in Figure 10.10.

$$\text{Generator}: E_g'' = V_t + jI_L X_d'' \tag{10.11}$$

$$\text{Motor}: E_m' = V_t - jI_m X_d'' \tag{10.12}$$

10.4 Bus Impedance Matrix Equivalent Network in Fault Calculations

Using the concept presented in Section 10.3, in Figure 10.11 the reactances are replaced by subtransient reactances in series with the generator EMFs. Also, the fault occurs at bus 4 between points *A* and *B*. We can now simulate the fault by connecting V_f and $-V_f$ in series, as shown in Figure 10.11, and replacing the reactances with the corresponding admittances. V_f represents the fault voltage created at bus 4 between points *A* and *B*, as the sum of V_f and $-V_f$ in series simulates an equivalent SC.

The SC creates a fault current I_f and incremental voltages at all buses, including $-V_f$, between points *A* and *B*, as shown in the following node equations in matrix form, with perturbation indicated by the Δ quantities.

$$\begin{bmatrix} 0 \\ 0 \\ 0 \\ -I_f'' \end{bmatrix} = j \begin{bmatrix} -12.33 & 0 & 4.0 & 5.0 \\ 0 & -10.83 & 2.5 & 5.0 \\ 4 & 2.5 & -17.83 & 8.0 \\ 5 & 5 & 8 & -18 \end{bmatrix} \begin{bmatrix} V_1^{\Delta} \\ V_2^{\Delta} \\ V_3^{\Delta} \\ -V_f \end{bmatrix} \tag{10.13}$$

where Δ implies the voltages only due to the insertion of $-V_f$ in the overall system. This gives the incremental voltage matrix as follows:

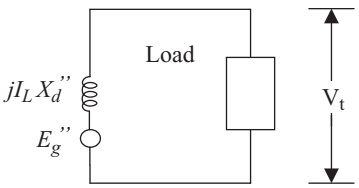

FIGURE 10.10
Subtransient circuit of a loaded machine.

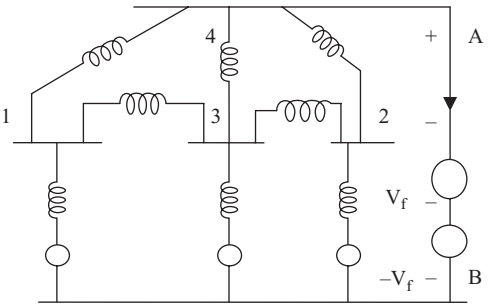

FIGURE 10.11
Equivalent network in fault calculations.

$$\begin{bmatrix} V_1^{\Delta} \\ V_2^{\Delta} \\ V_3^{\Delta} \\ -V_f \end{bmatrix} = Z_{\text{bus}} \begin{bmatrix} 0 \\ 0 \\ 0 \\ -I_f'' \end{bmatrix} \tag{10.14}$$

and

$$I_f'' = \frac{V_f}{Z_{44}} \tag{10.15}$$

and

$$V_1^{\Delta} = -I_f'' Z_{14} = -\frac{Z_{14}}{Z_{44}} V_f \tag{10.16}$$

or in general,

$$V_i^{\Delta} = -I_f'' Z_{i4} = -\frac{Z_{i4}}{Z_{44}} V_f ; \forall i = 1,2,3 \tag{10.17}$$

We now apply superposition theorem as follows to generate new voltages at all buses after the fault occurs.

$$V_1 = V_f + V_1^{\Delta} \tag{10.18}$$

$$V_2 = V_f + V_2^{\Delta} \tag{10.19}$$

$$V_3 = V_f + V_3^{\Delta} \tag{10.20}$$

$$V_4 = V_f - V_f = 0 \tag{10.21}$$

Thus, in general, for a fault on bus k and neglecting pre-fault currents, the fault current is given by

$$I_f = \frac{V_f}{Z_{kk}} \tag{10.22}$$

and the post-fault voltage at bus n is

$$V_n = V_f - \frac{Z_{nk}}{Z_{kk}} V_f \tag{10.23}$$

Example 10.2

A 25 MVA, 13.8 kV generator in which $X_d'' = 15\%$ is connected through a transformer to a bus that supplies four identical motors, as shown in Figure 10.12.

The X_d'' reactance of each motor is 20% on a base of 5 MVA, 6.9 kV. The transformer is rated at 25 MVA, 13.6 kV/6.9 kV with $X_1 = 10\%$. The bus voltages at the motors is 6.9 kV when a fault occurs at point *P*. For the fault specified, find

1. Subtransient current I_f'' in the fault
2. The transient current in breaker *A*
3. The symmetrical SC interrupting current in the fault and in breaker *A*

Data given:

$$G_1 : 25\,\text{MVA}, 13.8\,\text{kV};\ X_d'' = 0.15$$

$$T_1 : 25\,\text{MVA}, \frac{13.8}{6.9}\,\text{kV};\ X_1 = 0.10$$

$$M_s : \text{base} - 5\,\text{MVA}, 6.9\,\text{kV};\ X_d'' = 0.2$$

SOLUTION

We can find the equivalent circuit using the bus impedance matrix method, as shown in Figure 10.13.

Thus, we have two buses that constitute the two nodes:

- Node 1 on the low-voltage side of the transformer
- Node 2 on the high-voltage side of the transformer

To generate the circuit breaker ratings, we need the motor reactance to be multiplied by 1.5, implying the X_d'' of the motor is 1.5 pu.

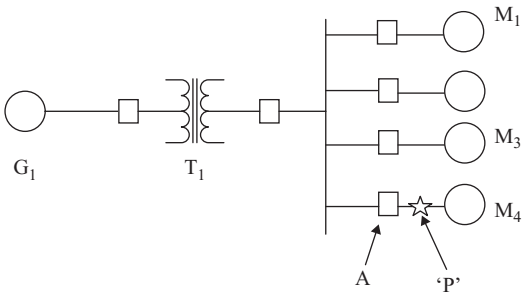

FIGURE 10.12
Network for Example 10.2

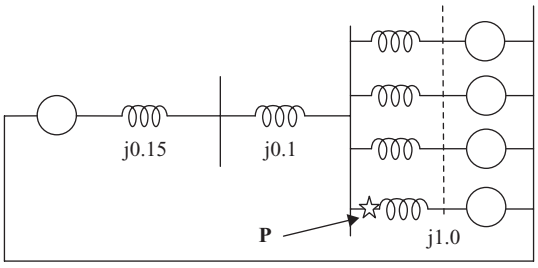

FIGURE 10.13
Bus impedance matrix equivalent circuit.

An equivalent circuit with a fault condition at point *P* is generated as in Figure 10.14. With further analysis using the methods illustrated earlier for bus impedance equivalency under fault conditions, as seen in Section 10.4, we have

$$Y_{11} = \frac{1}{j0.1} + \frac{1}{j\frac{1.5}{4}} = -j10 + \left(-j2.67\right) = -j12.67$$

$$Y_{12} = j10$$

$$Y_{22} = -j10 + \frac{1}{j0.15} = -j10 - j6.67 = -j16.67$$

This yields the following node admittance matrix:

$$Y_{\text{bus}} = \begin{bmatrix} -j12.67 & j10.0 \\ j10.0 & -j16.67 \end{bmatrix}$$

$$Z_{\text{bus}} = Y_{\text{bus}}^{-1} = j\begin{bmatrix} 0.150 & 0.090 \\ 0.090 & 0.114 \end{bmatrix}$$

We now assess the fault conditions as follows.

Switch S_1 is closed and switch S_2 is opened to simulate the fault at bus 1, yielding the following SC interrupting current in a three-phase fault at node 1.

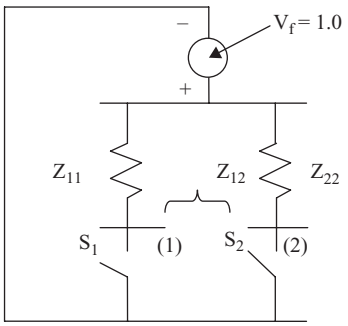

FIGURE 10.14
Fault equivalent circuit.

$$I_{sc} = \frac{1.0}{j0.15} = -j6.67\,\text{pu}$$

Further, the voltage on bus 2 with the fault on bus 1 is given by

$$V_2 = 1.0 - I_{sc}Z_{21} = 1.0 - \left(-j6.67\right)\left(j0.09\right) = 0.4$$

$$\because Y_{12} = j10 \Rightarrow y_{12} = -j10$$

This means the current into the fault from the transformer is

$$I_f = \left(0.4 - 0.0\right)\left(-j10\right) = -j4.0\,\text{pu}$$

With switch S_2 closed and S_1 open, this yields

$$I_{sc} = \frac{1.0}{j0.114} = -j8.77\,\text{pu}$$

Problems

PROBLEM P.10.1

A three-phase, wye-connected load is connected across a three-phase, balanced supply system. Obtain a set of equations relating the symmetrical components of the line and phase voltages.

PROBLEM P.10.2

A three-phase synchronous generator, grounded through an impedance Z_n is shown in Figure P.10.2.

The generator is not supplying load, but because of a fault at the generator terminals, currents I_a, I_b and I_c flow through phases a, b and c, respectively. Develop and draw the phase sequence networks for the generator in these conditions.

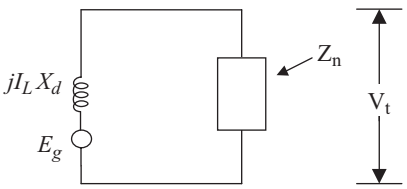

FIGURE P.10.2
Synchronous generator.

PROBLEM P.10.3

A three-phase SC fault occurs at point F in the system shown in Figure P.10.3. Calculate the fault current.

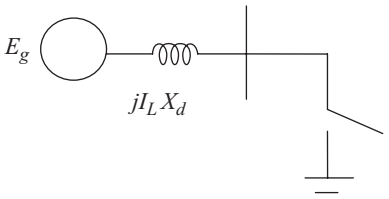

FIGURE P.10.3
SC fault at point F.

PROBLEM P.10.4

Figure P.10.4 shows the SLD for a single phase of a system in which a generator supplies a load through a step-up transformer, a transmission line and a step-down transformer. Calculate the pu current. The transformers are assumed to be ideal.

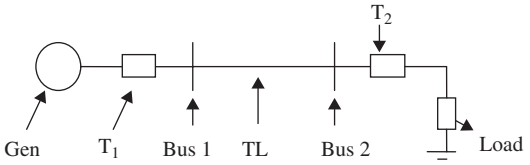

FIGURE P.10.4
SLD for a single-phase system.

PROBLEM P.10.5

A line-to-ground fault occurs in phase *a* of the generator in Figure P.10.5, which was operating without load. Derive a sequence network representation of this condition and determine the current in phase *a*.

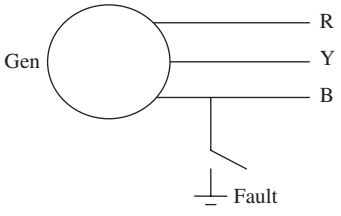

FIGURE P.10.5
A line-to-ground fault in phase *a* of a generator.

PROBLEM P.10.6

Develop the sequence network for an unloaded generator with a double line-to-ground fault as shown in Figure P.10.6.

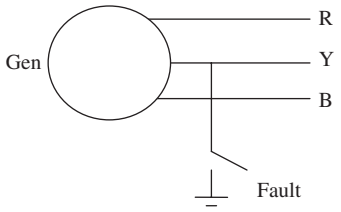

FIGURE P.10.6
Double line-to-ground fault on a generator.

PROBLEM P.10.7

The positive-, negative- and zero-sequence reactances of a 20 MVA, 13.2 kV synchronous generator are 0.3 pu, 0.2 pu and 0.1 pu, respectively. The generator is solidly grounded and is not loaded. A line-to-ground fault occurs in phase *a*. Neglecting the resistances, find the fault current.

PROBLEM P.10.8

A line-to-ground fault occurs at the terminals of the unloaded generator in Problem P.10.7. Calculate the fault current.

PROBLEM P.10.9

The generator in Problem P.10.7 is initially unloaded. A double line-to-ground fault occurs at the generator terminals. Calculate the fault current and the line voltages at the generator terminals.

PROBLEM P.10.10

Calculate the line-to-line voltages for the generator in Problem P.10.8, which has a line-to-line fault, as mentioned therein.

PROBLEM P.10.11

Find the voltages V_a, V_b and V_c for the generator in Problem P.10.7.

PROBLEM P.10.12

A three-phase SC fault occurs at point *F* in the system shown in Figure P.10.12.

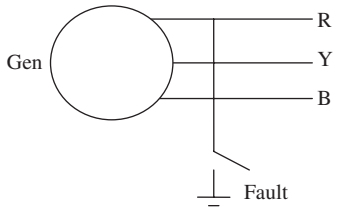

FIGURE P.10.12
A three-phase SC at F.

The generator is loaded to 80% of its capacity at the time of the fault, and the receiving end power factor is unity. Find the RMS pu current in one phase at point *F* after the occurrence of the fault.

PROBLEM P.10.13

The pu reactances of a synchronous generator are $X_d = 1.1$, $X_d'' = 0.24$ and $X_d'' = 0.15$, respectively. The generator is operating without load at 5% above rated voltage when a three-phase SC occurs at its terminals.

1. What is the pu subtransient fault current in the generator?
2. If the generator is rated at 500 MVA and 20 kV, find the subtransient current in kilo-amperes in the generator.

PROBLEM P.10.14

A synchronous generator with a subtransient reactance of 0.15 pu and operating at 5% above its rated voltage supplies a synchronous motor with a 0.20 pu subtransient reactance. The motor is connected to the generator by a transmission line and a transformer with a total reactance of 0.305 pu. A sudden three-phase SC occurs at the generator terminals. Find the pu subtransient fault current.

Taylor & Francis
Taylor & Francis Group
http://taylorandfrancis.com

11

Symmetrical Component Analysis in Fault Calculations

11.1 Symmetrical Components

The method of symmetrical components is a powerful mathematical abstraction that enables one to interpret the behavior of and find solutions for three-phase electrical systems, as long as their responses can be considered linear.

This is a very important constraint that makes sure that the independent response of the system (networks, transformers, loads, etc.) can be obtained at any point of interest as the superposition of the responses to the positive-, negative- and zero-sequence excitations.

In power transformers, the response is not always linear, as is the case when saturation affects parameters. In such conditions, actual system behavior can only be estimated with conventional tools, such as symmetrical components, and non-linear analysis methods are available for most general cases.

These are generated using three distinct components called *sequence components*:

1. Positive-sequence components with a phase sequence given by *abc*:

$$V_{a1},\quad V_{b1},\quad V_{c1} \tag{11.1}$$

2. Negative-sequence components with a phase sequence given by *acb*:

$$V_{a2},\quad V_{b2},\quad V_{c2} \tag{11.2}$$

3. Zero-sequence components with no phase difference:

$$V_{a0},\quad V_{b0},\quad V_{c0} \tag{11.3}$$

In this instance, we need to define the *a* operator. An *a* operator advances a phasor by 120°. Thus, a^2 advances a phasor by 240° and a^3 advances a phasor by 360°, as shown in Figure 11.1.

Thus, a relationship between the different phase sequence components of a given phase sequence is given by

$$\text{Positive sequence} \rightarrow V_{b1} = a^2 V_{a1};\ V_{c1} = a V_{a1} \tag{11.4}$$

$$\text{Negative sequence} \rightarrow V_{b2} = a V_{a2};\ V_{c2} = a^2 V_{a2} \tag{11.5}$$

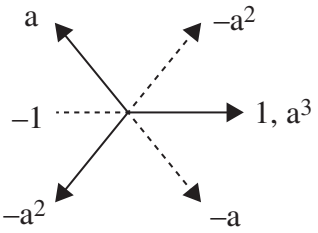

FIGURE 11.1
Phasor diagram of an *a* operator.

$$\text{Zero sequence} \rightarrow V_{b0} = V_{a0};\ V_{c0} = V_{a0} \tag{11.6}$$

which can be written in general matrix form for a set of unbalanced phase voltages as follows:

$$\begin{bmatrix} V_a \\ V_b \\ V_c \end{bmatrix} = \begin{bmatrix} 1 & 1 & 1 \\ 1 & a^2 & a \\ 1 & a & a^2 \end{bmatrix} \begin{bmatrix} V_{a0} \\ V_{a1} \\ V_{a2} \end{bmatrix} \tag{11.7}$$

$$\Rightarrow V_p = TV_s$$

$\rightarrow$ Phase voltage vector

= Transformation matrix × symmetrical sequence voltage vector

$$\begin{bmatrix} V_{a0} \\ V_{a1} \\ V_{a2} \end{bmatrix} = \frac{1}{3} \begin{bmatrix} 1 & 1 & 1 \\ 1 & a & a^2 \\ 1 & a^2 & a \end{bmatrix} \begin{bmatrix} V_a \\ V_b \\ V_c \end{bmatrix} \tag{11.8}$$

Thus, the complex power in a circuit, as shown in Figure 11.2, is given by

$$S = VI^*$$

$$= VIe^{j(\varphi-\theta)}$$

$$= VIe^{j\alpha} = VI\cos\alpha + jVI\sin\alpha$$

$$S = P + jQ \tag{11.9}$$

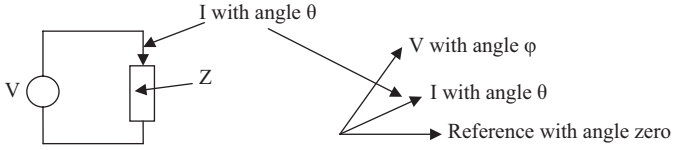

FIGURE 11.2
Complex power in a circuit with load *Z*.

If the circuit is a three-phase circuit with unbalanced phase voltages and corresponding phase currents given by

$$\begin{bmatrix} V_a \\ V_b \\ V_c \end{bmatrix}; \begin{bmatrix} I_a \\ I_b \\ I_c \end{bmatrix} \tag{11.10}$$

then the real and reactive power in the three-phase system is given by

$$S = V_a I_a^* + V_b I_b^* + V_c I_c^*$$

$$= [V_a \ V_b \ V_c] \begin{bmatrix} I_a \\ I_b \\ I_c \end{bmatrix}^* = V_p{}^T I_p^* \tag{11.11}$$

We also know from matrix algebra that

$$I_p^* = T^* I_s^* \ \text{ and } \ V_p = T V_s \tag{11.12}$$

where:

$$I_s^* = \begin{bmatrix} I_1 \\ I_2 \\ I_0 \end{bmatrix}$$

Then,

$$S = [TV_s]^T \left[T^* I_s{}^* \right] = V_s{}^T T^T T^* I_s{}^*$$

with

$$T^T = \begin{bmatrix} 1 & a^2 & a \\ 1 & a & a^2 \\ 1 & 1 & 1 \end{bmatrix}; T^* = \begin{bmatrix} 1 & 1 & 1 \\ a & a^2 & 1 \\ a^2 & a & 1 \end{bmatrix}$$

Then,

$$T^T T^* = 3 \begin{bmatrix} 1 & 0 & 0 \\ 0 & 1 & 0 \\ 0 & 0 & 1 \end{bmatrix} = 3I \tag{11.13}$$

and

$$S = 3V_s{}^T U I_s{}^* = 3 \begin{bmatrix} V_a & V_a & V_a \end{bmatrix} \begin{bmatrix} 1 & 0 & 0 \\ 0 & 1 & 0 \\ 0 & 0 & 1 \end{bmatrix} \begin{bmatrix} I_1{}^* \\ I_2{}^* \\ I_0{}^* \end{bmatrix} \tag{11.14}$$

11.2 Representation of All Elements of SLD Using Sequential Components

11.2.1 Inductance

Equally spaced transmission lines are represented as follows:

$$\text{Positive sequence} \rightarrow Z_1 = j\frac{\omega\mu}{2\pi}\ln\frac{D}{r'} = Z_2 \rightarrow \text{negative sequence} \quad \frac{\Omega}{\text{m}} \tag{11.15}$$

$$\text{Zero sequence} \rightarrow Z_0 = j\frac{\omega\mu}{2\pi}\ln\frac{(D_n)^6}{D^2 r'(r_n')^3} \quad \frac{\Omega}{\text{m}} \tag{11.16}$$

where:

$$\mu = 4\pi\cdot\frac{10^{-7}H}{m};\ D_n = D_{an} = D_{bn} = D_{cn} \text{ and } D = D_{ab} = D_{bc} = D_{ac}; \tag{11.17}$$

11.2.2 Capacitance

$$\text{Positive sequence} \rightarrow Y_1 = j\frac{2\pi\in\omega}{\ln\frac{D}{r}} = Y_2 \rightarrow \text{negative sequence} \quad \frac{\text{S}}{\text{m}} \tag{11.18}$$

$$\text{Zero sequence} \rightarrow Y_0 = j\frac{2\pi\in\omega}{\ln\frac{(D)^4}{27r^4}} \quad \frac{\text{S}}{\text{m}} \tag{11.19}$$

where:

$$\in = 8.654\cdot\frac{10^{-12}F}{\text{m}} \tag{11.20}$$

Here we can also use

$$\begin{bmatrix} V_a \\ V_b \\ V_c \end{bmatrix} = \begin{bmatrix} 1 & 1 & 1 \\ a^2 & a & 1 \\ a & a^2 & 1 \end{bmatrix}\begin{bmatrix} V_1 \\ V_2 \\ V_0 \end{bmatrix} \tag{11.21}$$

and

$$T = \begin{bmatrix} 1 & 1 & 1 \\ a^2 & a & 1 \\ a & a^2 & 1 \end{bmatrix} \tag{11.22}$$

11.2.3 Sequential Impedances of a Transformer

Here we use a Y/Δ-connected three-phase transformer with the neutral on the primary grounded via a neutral grounding impedance Z_n. Also, the equivalent impedance Z_e of the transformer is a representation of both the primary and secondary windings of the

transformer under consideration and the excitation current in the transformer $I_\Phi = 0$. The equivalent circuit of a transformer with sequential impedances is shown in Figure 11.3.

Then,

$$\begin{bmatrix} \Delta V_a \\ \Delta V_b \\ \Delta V_c \end{bmatrix} = \begin{bmatrix} Z_e + Z_n & Z_n & Z_n \\ Z_n & Z_e + Z_n & Z_n \\ Z_n & Z_n & Z_e + Z_n \end{bmatrix} \begin{bmatrix} I_a \\ I_b \\ I_c \end{bmatrix}$$

where:

$$Z = \begin{bmatrix} Z_e + Z_n & Z_n & Z_n \\ Z_n & Z_e + Z_n & Z_n \\ Z_n & Z_n & Z_e + Z_n \end{bmatrix} \tag{11.23}$$

Then,

$$Z_s = T^{-1} Z_p T$$

$$= \begin{bmatrix} Z_1 & 0 & 0 \\ 0 & Z_2 & 0 \\ 0 & 0 & Z_3 \end{bmatrix} = \begin{bmatrix} Z_e & 0 & 0 \\ 0 & Z_e & 0 \\ 0 & 0 & Z_e + 3Z_n \end{bmatrix} \tag{11.24}$$

The equivalent circuit for zero-sequence impedance is shown in Figure 11.4.
If Z_n is removed, then the equivalent circuit transforms as shown in Figure 11.5.

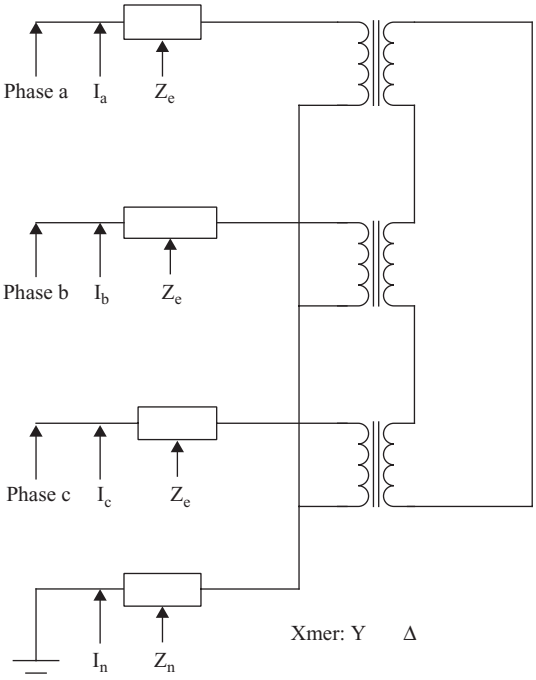

FIGURE 11.3
Equivalent circuit of a transformer with sequential impedances.

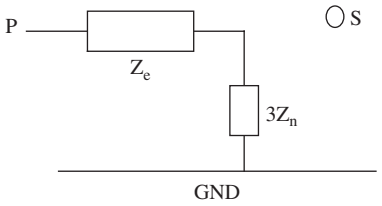

FIGURE 11.4
Equivalent circuit for the zero-sequence impedances.

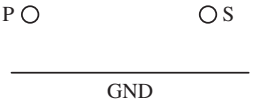

FIGURE 11.5
Equivalent circuit for the zero-sequence impedances without Z_n.

11.2.4 Generator Balanced and Unbalanced Equations and Equivalent Circuits with Sequential Components

The induced EMF of the generator is given by

$$E_p = V_p + Z_n I_p \tag{11.25}$$

where Z_n is a diagonal matrix under balanced conditions.
Thus,

$$V_p = E_p - Z_n I_p \tag{11.26}$$

Further,

$$E_p = \begin{bmatrix} E_a \\ E_b \\ E_c \end{bmatrix} = \begin{bmatrix} E_a \\ a^2 E_a \\ aE_c \end{bmatrix} \rightarrow \begin{bmatrix} V_1 \\ V_2 \\ V_0 \end{bmatrix} = \begin{bmatrix} E_a \\ 0 \\ 0 \end{bmatrix} - \begin{bmatrix} Z_n & 0 & 0 \\ 0 & Z_n & 0 \\ 0 & 0 & Z_n \end{bmatrix} \begin{bmatrix} I_1 \\ I_2 \\ I_0 \end{bmatrix} \tag{11.27}$$

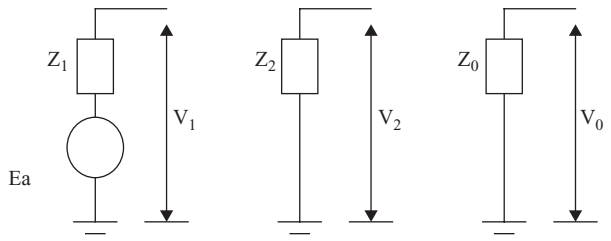

FIGURE 11.6
Phase sequence circuit for generators balanced/unbalanced.

(as shown in Figure 11.6) and

$$V_p = TV_s \quad \text{and} \quad I_p = TI_s \tag{11.28}$$

$$TV_s = E_p - Z_n TI_s \rightarrow V_s = T^{-1}E_p - T^{-1}Z_n TI_s \tag{11.29}$$

$$\therefore E_s = T^{-1}E_p = \begin{bmatrix} E_a \\ 0 \\ 0 \end{bmatrix} \tag{11.30}$$

and

$$Z_s = \begin{bmatrix} Z_1 & 0 & 0 \\ 0 & Z_2 & 0 \\ 0 & 0 & Z_0 \end{bmatrix} \tag{11.31}$$

where:

$$Z_1 = jX_d \quad \text{or} \quad jX'_d \quad \text{or} \quad jX''_d \tag{11.32}$$

$$Z_2 \cong jX''_d \tag{11.33}$$

and

$$Z_0 = jX_e = Z_e + 3Z_n \tag{11.34}$$

The equivalent phase sequence circuits for the EMFs are shown in Figure 11.7.

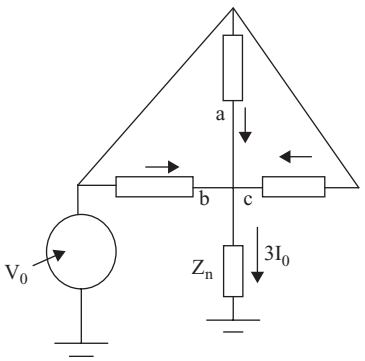

FIGURE 11.7
Sequential circuits of EMFs for balanced Z_n.

11.3 Balanced and Unbalanced Fault Analysis Using a Two-Bus Electric Power System SLD

We will use the SLD shown in Figure 11.8 to carry out the fault analysis for several fault conditions:

1. Three-phase fault to ground
2. Single line-to-ground fault
3. Double line-to-ground fault
4. Line-to-line fault

The SLD shows two generators, two transformers, two buses and a transmission line, as in Figure 11.8. The fault analysis is done between points *A* and *B*.

The different parts of the SLD are specified as follows:

$$\text{Generator } G_1 : 50\text{ MVA}, 20\text{ kV}; x_d'' = 14\%; x_l = 5\%$$

$$\text{Generator } G_2 : 70\,\text{MVA}, 12\,\text{kV}; x_d'' = 20\%; x_l = 6\%$$

$$\text{Transformer } T_1 : 50\,\text{MVA}, \frac{20}{69}\,\text{kV}; X_e = 8\%$$

$$\text{Transformer } T_2 : 70\,\text{MVA}, \frac{12}{69}\,\text{kV}; X_e = 10\%$$

$$\text{Transmission line } TL : 69\,\text{kV}; X_{TL_1} = X_{TL_2} = j10\,\Omega; X_{TL_0} = j35\,\Omega$$

$$\text{Reference base: } 50\,\text{MVA}, 20\,\text{kV}$$

Since kV rating for all components remains at the same base from end to end in this SLD, only the corrections need be done for all pu values of reactances on the MVA base change value to 50 MVA for the second generator and transformer and the transmission line. Thus, we have

$$\text{Generator } G_2: x_d'' = 20\%\left(\frac{50}{70}\right) = 0.144\,\text{pu};\quad x_l = 6\%\left(\frac{50}{70}\right) = 0.0432\,\text{pu}$$

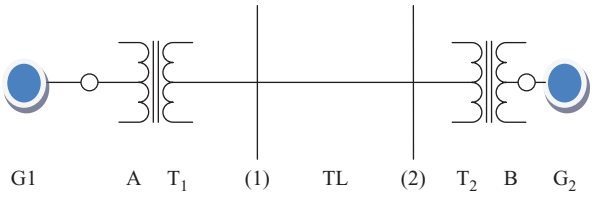

FIGURE 11.8
Two-bus electric power system for fault analysis.

$$\text{Transformer } T_2 : X_e = 10\%\left(\frac{50}{70}\right) = 0.072\,\text{pu}$$

$$\text{Transmission line } TL : 69\,\text{kV};\ Z_{\text{base}} = \frac{69^2}{50} = 95.22\,\Omega$$

$$X_{TL_1} = X_{TL_2} = \frac{j10}{95.22} = j0.105\,\text{pu};\ X_{TL_0} = \frac{j35}{95.22} = j0.3675\,\text{pu}$$

The fault occurs at bus 2. We can now draw all the phase sequence circuits of this SLD in Figure 11.8 by following the analysis in Section 11.2, as shown in Figure 11.9a–c for the positive-, negative- and zero-sequence circuits, respectively.

Using the preceding circuits, we will now analyze the different kinds of faults:

1. Three-phase fault to ground

   A three-phase fault to ground is shown in Figure 11.10; the fault occurs at bus 2.

   The boundary conditions that are applicable to this kind of fault are as follows:

$$V_a = V_b = V_c = 0 \tag{11.35}$$

and

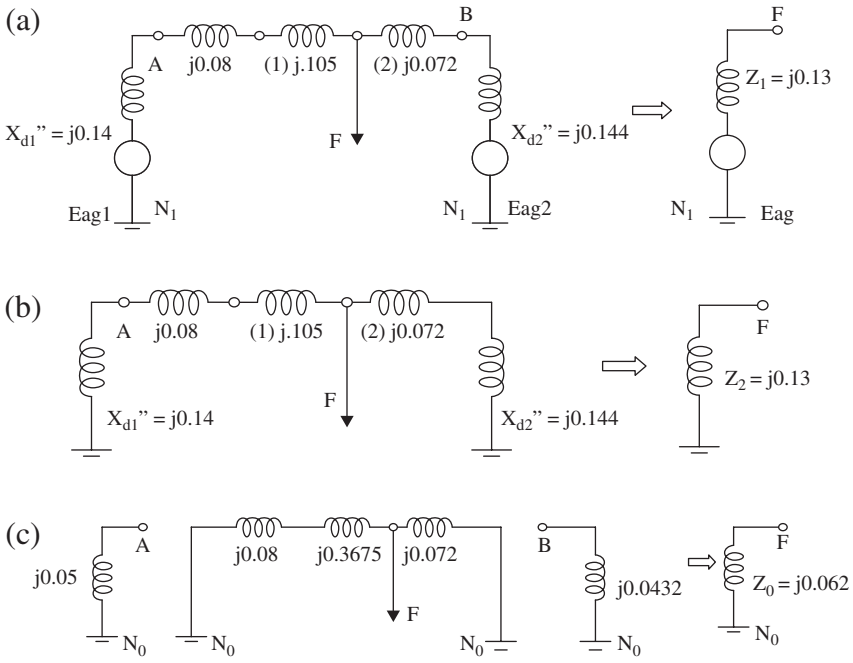

FIGURE 11.9

(a) Positive-sequence circuit of the SLD in Figure 11.8 (all values in pu). (b) Negative-sequence circuit of the SLD in Figure 11.8 (all values pu). (c) Zero-sequence circuit of the SLD in Figure 11.8 (all values in pu).

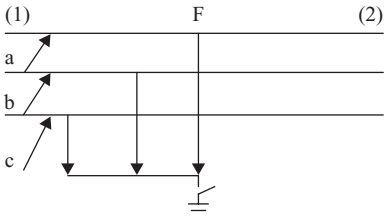

FIGURE 11.10
Three-phase to ground fault.

$$I_a + I_b + I_c = 0 \tag{11.36}$$

$$I_b = a^2 I_a;\ \ I_c = aI_a \tag{11.37}$$

$$I_0 = \frac{1}{3}\left(I_a + I_b + I_c\right) = 0 \text{ at fault } F \tag{11.38}$$

$$I_2 = \frac{1}{3}\left(I_a + a^2 I_b + aI_c\right) = 0$$

$$I_2 = \frac{1}{3}\left(I_a + aI_a + a^2 I_a\right) = 0 \tag{11.39}$$

and

$$I_1 = \frac{1}{3}\left(I_a + aI_b + a^2 I_c\right) = I_2 = \frac{1}{3}\left(I_a + a^3 I_a + a^3 I_a\right) = I_a \tag{11.40}$$

and

$$V_1 = 0; V_2 = 0 \quad \text{and} \quad V_0 = 0 \tag{11.41}$$

$$\rightarrow I_{aF} = I_1,\ \ I_{bF} = a^2 I_a \ \text{ and } \ I_{cF} = aI_a \tag{11.42}$$

$\rightarrow$ No interconnections of sequential circuits

2. Single line-to-ground fault

   The fault is as shown in Figure 11.11.

   We now have new boundary conditions, as follows:

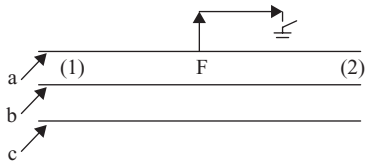

FIGURE 11.11
Single line-to-ground fault on line *a* and fault at bus 2.

$$I_{aF} \neq 0 \quad \text{and} \quad I_{bF} = I_{cF} = 0 \tag{11.43}$$

and

$$V_{aF} = 0 \tag{11.44}$$

The two boundary conditions from Equations 11.43 and 11.44 result in an intuitive interconnection of the sequential circuits, yielding:

$$I_{1F} = \frac{1}{3}\left(I_{aF} + aI_{bF} + a^2 I_{cF}\right) = \frac{1}{3} I_{aF} \tag{11.45}$$

$$I_{2F} = \frac{1}{3}\left(I_{aF} + aI_{bF} + a^2 I_{cF}\right) = \frac{1}{3} I_{aF} \tag{11.46}$$

$$I_{0F} = \frac{1}{3}\left(I_{aF} + aI_{bF} + a^2 I_{cF}\right) = \frac{1}{3} I_{aF} \tag{11.47}$$

This implies all sequential circuits should be connected in series, as shown in Figure 11.12 with the KVL at fault, as in Equation 11.48:

$$V_{aF} = V_{1F} + V_{2F} + V_{0F} = 0 \tag{11.48}$$

and

$$I_{0F} = I_{1F} = I_{2F}$$

$$= \frac{1\angle 0}{Z_1 + Z_2 + Z_0} = \frac{1\angle 0}{j0.13 + j0.13 + j0.0621}$$

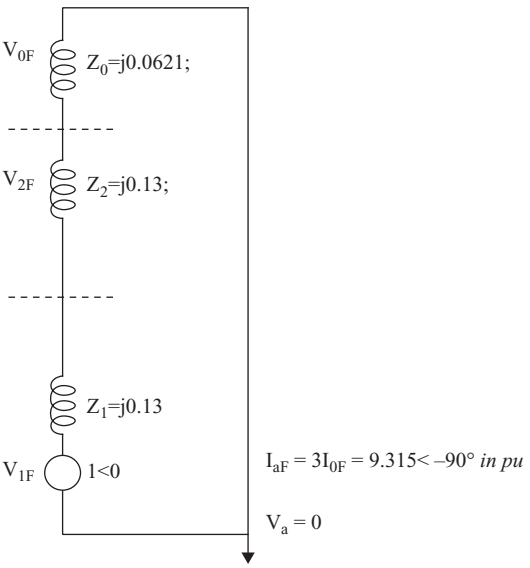

FIGURE 11.12
All sequential circuits connected in series for a single line-to-ground fault.

3. Double line-to-ground fault

The double line-to-ground fault is as shown in Figure 11.13, with faults on lines *b* and *c* at bus 2.

The boundary conditions here are as follows:

$$V_{bF} = V_{cF} = 0 \tag{11.49}$$

and

$$I_{aF} = 0 \tag{11.50}$$

Equations 11.49 and 11.50 yield the following relation in matrix form:

$$\begin{bmatrix} V_1 \\ V_2 \\ V_0 \end{bmatrix} = \frac{1}{3}\begin{bmatrix} 1 & a & a^2 \\ 1 & a^2 & a \\ 1 & 1 & 1 \end{bmatrix}\begin{bmatrix} V_a \\ V_b \\ V_c \end{bmatrix} = \frac{1}{3}\begin{bmatrix} 1 & a & a^2 \\ 1 & a^2 & a \\ 1 & 1 & 1 \end{bmatrix}\begin{bmatrix} V_{aF} \\ 0 \\ 0 \end{bmatrix} \tag{11.51}$$

$$\rightarrow V_{1F} = V_{2F} = V_{0F} = \frac{1}{3}V_{aF} \tag{11.52}$$

and

$$I_{1F} + I_{2F} + I_{0F} = I_{aF} = 0 \tag{11.53}$$

This implies that the sequential circuits are connected in parallel, as shown in Figure 11.14.

$$V_{1F} = V_{2F} = V_{0F} \tag{11.54}$$

We can use the preceding equations to find first I_{1F} and then I_{2F} and I_{0F} by division.

4. Line-to-line fault

The fault is as shown in Figure 11.15 between lines *b* and *c* at bus 2.

In the line-to-line fault situation, the boundary conditions are as follows:

$$I_{aF} = 0 \rightarrow I_{bF} = -I_{cF} \tag{11.55}$$

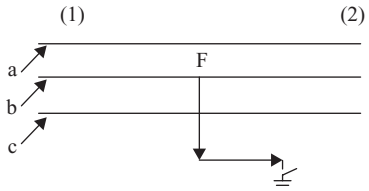

FIGURE 11.13
Double line-to-ground fault on lines *b* and *c* at bus 2.

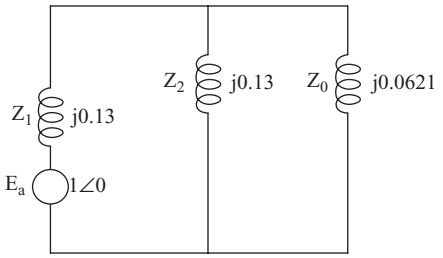

FIGURE 11.14
Double line-to-ground fault sequential circuit connection in parallel.

and

$$V_{bF} = V_{cF} \tag{11.56}$$

Thus,

$$I_{1F} = \frac{1}{3}\left(I_{aF} + aI_{bF} + a^2 I_{cF}\right) = \frac{1}{3}\left(a - a^2\right)I_{bF} \tag{11.57}$$

$$I_{2F} = -\frac{1}{3}\left(a - a^2\right)I_{bF} = \frac{1}{3}\left(I_{aF} + a^2 I_{bF} + aI_{cF}\right) \tag{11.58}$$

$$I_{0F} = \frac{1}{3}\left(I_{aF} + I_{bF} + I_{cF}\right) = 0 \tag{11.59}$$

$$\rightarrow I_{1F} = -I_{2F}; \quad \text{and} \quad I_{0F} = 0 \tag{11.60}$$

→ The positive-sequence circuit is in series with the negative-sequence circuit and the zero-sequence circuit is isolated, as shown in Figure 11.16.

$$I_{1F} = -I_{2F} = \frac{1\angle 0}{Z_1 + Z_2} \tag{11.61}$$

$$I_{bF} = a^2 I_{1F} + aI_{2F} \tag{11.62}$$

and

$$I_{2F} = -I_{bF} \tag{11.63}$$

as well as

$$V_{1F} = V_{2F} = -Z_2 I_{2F} \tag{11.64}$$

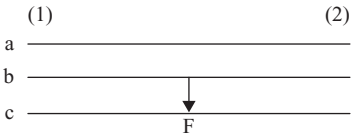

FIGURE 11.15
Line-to-line fault between lines *b* and *c* at bus 2.

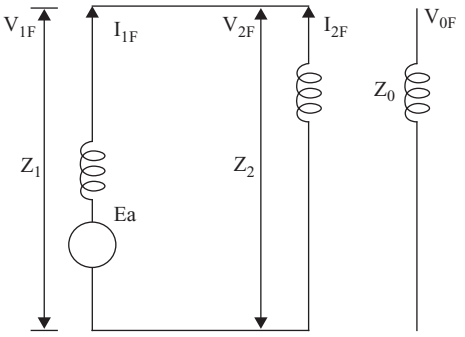

FIGURE 11.16
Line-to-line fault sequential circuits for fault at bus 2.

Problems

PROBLEM P.11.1

For the problem discussed in Section 11.3:

1. Find the positive-, negative- and zero-sequence circuits for the given SLD with a new base of 70 MVA, 69 kV.
2. Solve
   a. The single line-to-ground fault on line *a*
   b. The double line-to-ground fault on lines *a* and *b*
   c. The triple line-to-ground fault on lines *a*, *b* and *c*
   d. The fault between lines *a* and *b* only

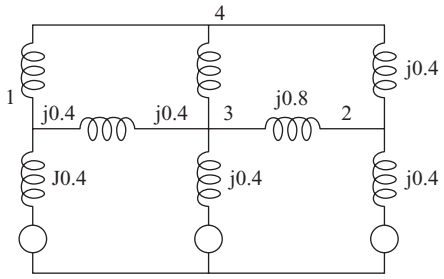

FIGURE 11.P.1
SLD of a four-bus system.

PROBLEM 11.P.2

For the SLD circuit in Figure 11.P.1, find the Z-matrix, then the Y-matrix. A fault occurs at point *F* at bus 4. Find

1. The single line-to-ground fault on line *a*
2. The double line-to-ground fault on lines *a* and *b*
3. The triple line-to-ground fault on lines *a*, *b* and *c*
4. The fault between lines *a* and *b* only

Taylor & Francis
Taylor & Francis Group
http://taylorandfrancis.com

12

Power System Stability

12.1 Different Kinds of Power System Stability

There are three different kinds of power system stability:

1. Steady-state stability

   Steady-state stability describes how generators respond to increased load demands or specifically to relatively small disturbances in the power system.

2. Transient stability

   Transient stability is focused on the first few seconds after a specific severe condition/fault occurs as the severity and suddenness of the disturbance. Specifically, transient conditions exist for the first two or three cycles of the system; that is, if it is a 60 Hz power signal, this condition can occur for about 50–60 ms after the severe condition/fault occurs. It is concerned with maintaining synchronism among all generators when the power system is suddenly subjected to severe disturbances, such as

   - Faults caused by lightning strikes
   - Sudden removal from the transmission network of a generator or a tie line
   - Any severe shock to the system caused by a switching operation

3. Subtransient stability

   Subtransient stability is focused on less than a first few seconds after a specific severe condition/fault occurs as the severity and suddenness of the disturbance. Specifically, subtransient conditions exist for the first half to one cycle of the system; that is, if it is a 60 Hz power signal, this condition can occur for about 0–10 ms after the severe condition/fault occurs. It is concerned with maintaining synchronism among all generators when the power system is suddenly subjected to severe disturbances, such as

   - Faults caused by lightning strikes
   - Sudden removal from the transmission network of a generator or a tie line
   - Any severe shock to the system caused by a switching operation

These severe conditions cause the rotor of the synchronous generator machine to oscillate or swing about its axis like a pendulum. This is shown in Figure 12.1.

This initial oscillation is also called the *first swing* analysis in transient stability studies of the power system in its entirety. During the brief initial period following a severe disturbance, the synchronous machine or the generator undergoes its first transient overshoot

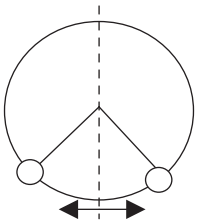

FIGURE 12.1
First pendulum-like swing of a generator after a severe disturbance.

or swing. If the generator gets through its dynamic rotational motions without losing synchronism, then it is said to be *transient stable*. In addition, dynamic stability describes the behavior of a system when the transients that continue after the successful first swing go for an extended period of time. This dynamic stability is also illustrated in the overall shape of the voltage or current curve in the time domain, as in Figure 12.2. These transient conditions also lead to what is called the *security* of a power system.

The security of a power system is also described as the likelihood of encountering severe shocks and the frequency of such occurrences. If the available reserve capacity in the form of idle generators and the availability of lines to nearby power systems is successfully shared, then the power system is rendered secure in its successful operation of providing power at different points in the geographical proximity of the entire system, either as a local area network (LAN), wide area network (WAN) or metropolitan area network (MAN). Subsequently, reliability is the extent to which an electric power system has sufficient capacity to meet the changing needs of its customers along the given transmission network. In this stability analysis study, we will consider two cases:

Case 1: Transient stability of a single generator connected to an infinite bus
Case 2: Transient stability of a multi-machine case

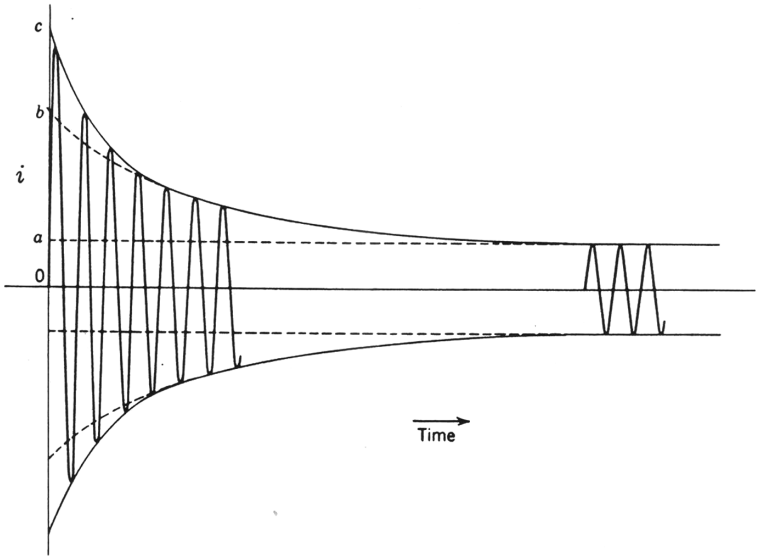

FIGURE 12.2
Dynamic stability in the time domain of the generator.

12.2 Case 1: Single-Generator System

Figure 12.3 illustrates a single generator and its energy source, which is the input to its prime mover (PM) and is connected to an infinite bus via a set of transmission lines. We will study the generator shaft dynamics that will illustrate the *swing equation*.

We will define some terms for this analysis as follows (also shown in Figure 12.3):

1. T_m: Mechanical energy input.
2. P_e: Electric power at the infinite bus.
3. Infinite bus G_∞ is a second generator of enormous capacity compared to generator G. Passive loads are connected to this infinite bus that draw from it real and reactive power.
4. Generator G is connected to the infinite bus by means of two parallel transmission lines.

We can now describe the differential equation of the dynamics of this system as follows:

$$T_m = J\alpha_m + T_D + T_e \tag{12.1}$$

where:

T_m is the mechanical torque
J is the moment of inertia
α_m is the mechanical acceleration
T_D is the external disturbance torque
T_e is the electrical torque produced by generator G

In the absence of the external disturbance torque, Equation 12.1 reduces to

$$T_m = J\alpha_m + T_e \tag{12.2}$$

The disturbance torque included in Equation 12.1 can easily be added later to the eventual analysis as a corrective factor, using the principle of superposition.

Equation 12.2 is multiplied on both sides by the synchronous speed of generator ω_s to yield the mechanical power–equivalent expression as follows:

$$P_m = \omega_s T_m = J\omega_s\alpha_m + \omega_s T_e \tag{12.3}$$

The second term on the right-hand side of Equation 12.3 is the electrical power $P_e = \omega_s T_e$, generated by the synchronous generator G with q number of phases, as shown in Equation 12.4:

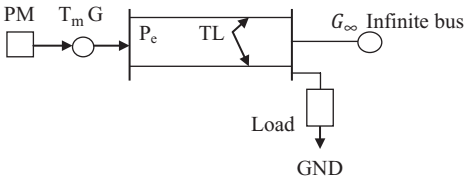

FIGURE 12.3
A synchronous generator and its energy source connected to an infinite bus via transmission lines.

$$P_m = \omega_s T_m = J\omega_s \alpha_m + q\frac{E_f V}{X}\sin\delta = J\omega_s \alpha_m + P_e \tag{12.4}$$

Thus,

$$J\omega_s \alpha_m = P_m - P_e \tag{12.5}$$

Mechanical power P_m is also given by the mechanical angular velocity of the PM, as both the shaft of the PM and the synchronous generator are connected together.

$$P_m = \omega_m T_m = \omega_s T_m \tag{12.6}$$

In Equation 12.4 we introduced another new term, δ, which is the power angle of the power system. We will now try to rewrite Equation 12.4 by relating angular acceleration α_m to power angle δ as follows.

Let θ be the angle of the field pole of generator *G* relative to the stationary reference line when the generator is operating at synchronous speed, as illustrated in Figure 12.4.

The generator rotates at a synchronous speed of ω_s, generating constant power, and θ and δ are measured in electrical radians, where:

$$\theta = \omega t + \delta \tag{12.7}$$

$$\omega = 2\pi f = \frac{p}{2}\omega_s \tag{12.8}$$

where *p* is the number of poles of the generator.

We now differentiate Equation 12.7 with respect to time, yielding

$$\dot{\theta} = \frac{d\theta}{dt} = \omega + \dot{\delta} \tag{12.9}$$

By using Equation 12.8, we can now convert Equation 12.9 to mechanical angular velocity as follows:

$$\frac{2}{p}\dot{\theta} = \frac{2}{p}\omega + \frac{2}{p}\dot{\delta} \tag{12.10}$$

yielding

$$\dot{\theta}_m = \omega_s + \dot{\delta}_m \tag{12.11}$$

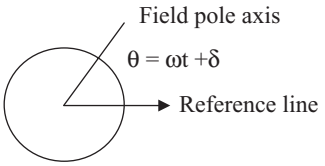

FIGURE 12.4
Generator field pole axis and power angle δ.

Thus, angular mechanical acceleration is given by

$$\alpha_m = \dot{\omega}_m = \frac{2}{p}\ddot{\delta} \tag{12.12}$$

where power angle δ is in electrical radians. Placing Equation 12.12 into Equation 12.5 yields a comprehensive form for the dynamics of the generator shaft in the absence of disturbance torque, as follows:

$$J\omega_s \frac{2}{p}\ddot{\delta} = P_m - P_e \tag{12.13}$$

where $J\omega_s$ is the angular momentum of the rotor structure and has different values for different machines.

On multiplying Equation 12.13 by $2\omega_s/2\omega_s$, we have

$$\frac{2\frac{1}{2}J\omega_s^2}{\frac{p}{2}\omega_s}\ddot{\delta} = P_m - P_e \tag{12.14}$$

$$\frac{\frac{1}{2}J\omega_s^2}{\pi f}\ddot{\delta} = P_m - P_e \tag{12.15}$$

If we divide Equation 12.15 by base power S_B of the generator, we can convert all quantities into pu values for all power involved as follows:

$$\frac{1}{\pi f}\frac{\frac{1}{2}J\omega_s^2}{S_B}\ddot{\delta} = P_m / S_B - P_e / S_B \tag{12.16}$$

where the numerator of the left-hand side of Equation 12.15 ($\frac{1}{2}J\omega_s^2$) is the rotor-stored kinetic energy at synchronous speed in megajoules (MJ), defined as follows:

$$H \triangleq \frac{\frac{1}{2}J\omega_s^2}{S_B} = \text{pu inertia constant of the generator} \tag{12.17}$$

This yields the final form of the differential equation that is used to study the transient stability of the power system in Figure 12.3 as a part of the swing equation:

$$\ddot{\delta} = \frac{\pi f}{H}\left(\text{pu } P_m - \text{pu } P_e\right) \tag{12.18}$$

Some reference curves for inertia H are shown in Figure 12.5.

We can rewrite Equation 12.18 in terms of reference power S_r, yielding

$$\frac{1}{\pi f}\frac{\frac{1}{2}J\omega_s^2}{S_R}\ddot{\delta} = P_m/S_R - P_e/S_R \tag{12.19}$$

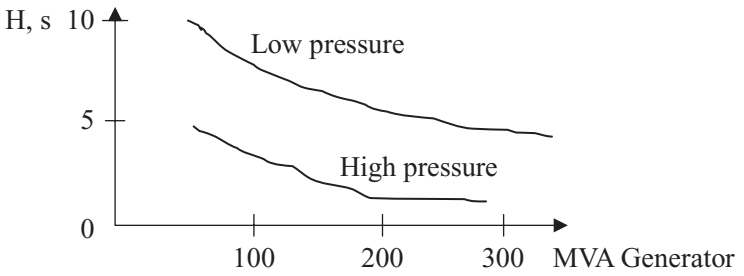

FIGURE 12.5
Inertia H parameter for large turbogenerators.

Multiplying Equation 12.19 by S_B/S_B yields

$$\frac{1}{\pi f}\left(\frac{\frac{1}{2}J\omega_s^2}{S_B}\right)\left(\frac{S_B}{S_R}\right)\ddot{\delta} = P_m/S_R - P_e/S_R \tag{12.20}$$

Using the definition of H in Equation 12.17 in Equation 12.20 yields

$$\frac{1}{\pi f}H\left(\frac{S_B}{S_R}\right)\ddot{\delta} = \frac{P_m}{S_R} - \frac{P_e}{S_R} \tag{12.21}$$

which can be further modified as follows:

$$\ddot{\delta} = \frac{\pi f}{H'}(P_m - P_e)\text{in pu} \tag{12.22}$$

using S_r as the base, where:

$$H' \triangleq H\frac{S_B}{S_R} \tag{12.23}$$

Equation 12.23 is very useful in multi-machine power systems.

12.3 Fault-Driven Changes to the Transmission Network

The different faults discussed in Chapter 11 can have a significant effect on the working of a power system, especially as follows.

1. Faults can have an effect on the electrical power (i.e., P_e) during the pre-fault condition and the post-fault condition of the power system. For a system to be reliable, all faults need to be removed as soon as possible and not sustained for a long time. Any removal of fault conditions will lead to the components of the system being rearranged/removed, thus changing the respective SLDs. To put it into a real-time perspective, when the system is in a stable condition of operation, the

mechanical power and electrical power are equal, and the result is that the right-hand side of Equations 12.18 and 12.22 set the value of the swing equation to zero and there are no changes to the values of the power angles in the system. In comparison, when the system is in 'shock'—as when lightning strikes, causing a line-to-ground fault—the transmission network undergoes a change in configuration that directly affects the electrical power P_e. As a result of the fault, the reactance associated with the generator field voltage E_f and terminal voltage V can change, as in Equation 12.4, while the mechanical power P_m remains constant due to the large rotor mass, a result of which is an unbalance in energy that causes the generator to accelerate for a condition as:

If the power angle increases as a result of the decrease in the electrical power,

$$\Rightarrow \delta \uparrow \text{ if } P_e \downarrow$$

This is a general condition that can change the dynamics of the rotor. If this change in power angle δ is sufficiently large during the first swing, the generator can lose synchronism and be shut down.

$$\Rightarrow \text{The machine is in } \textit{transient instability}.$$

otherwise if machine regains synchronism $\Longrightarrow$ *it is "transient stable"*

2. The at-fault condition is the most undesirable state for a power system and every effort is made by system operators to not sustain this condition for a long enough time to detrimentally affect the working conditions of the entire power system. Every effort is made to remove the fault condition as expeditiously as possible to increase reliability and continuous and uninterrupted electrical power to customers. The time needed to remove the fault is defined as the *critical time*, which plays an important role in the stable operation of the power system.
3. Once a fault is removed from a power system, the system moves to the post-fault condition. The physical representations, especially in terms of reactances, recreate a newer Z_{bus} or Y_{bus} that can lead to different power flow conditions in the revised network.

We will try to illustrate these conditions using the two-bus example with specific SLD component values, as in Example 12.1 and shown in Figure 12.5.

Example 12.1

The different components are specified as follows:

$$\text{Infinite bus: } 1\angle 0^\circ \text{ pu}$$

$$\text{Generator } G_1 : E_f = 1.3\angle\delta_0 \text{ pu and } x_s' = 0.25$$

$$\text{Transformer } T : x_l = 0.083$$

$$\text{Transmission lines } TL : x_{TL} = 0.5, \text{ both lines with suitable circuit breakers}$$

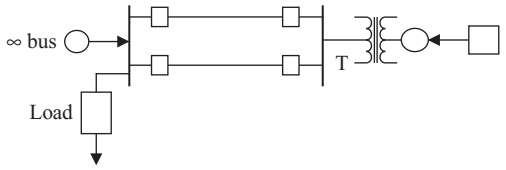

FIGURE 12.6
Two-bus system with two transmission lines.

At the pre-fault condition, when the system is stable, the SLD of the network is as shown in Figure 12.6, with the corresponding impedances of the SLD components and any power sources in pu.

Subsequently, an admittance diagram of the SLD with parameters as admittances can be drawn as in Figure 12.7 of the two-bus system with pre-fault conditions (Figure 12.8).

We can now write down the equations for the pre-fault conditions as follows:

$$\text{Synchronous generator: } P_e = \frac{E_f V}{x}\sin\delta \tag{12.24}$$

where:

V is the voltage of the ∞ bus

x is the reactance between E_f and V

$$x = \frac{0.5}{2} + 0.333 = 0.583\,\text{in pu} \tag{12.25}$$

which yields the electrical power of the synchronous generator:

$$P_e = \frac{E_f V}{x}\sin\delta = \frac{(1.3)(1)}{0.583}\sin\delta = 2.23\sin\delta \tag{12.26}$$

Assuming that the mechanical power from the PM is given by

$$P_m = 1.15\,\text{pu} \tag{12.27}$$

$$\rightarrow \text{for equilibrium } \delta_0 = \sin^{-1}\left(\frac{1.15}{2.23}\right) = 31^\circ \tag{12.28}$$

Equations 12.26 through 12.28 serve as the initial pre-fault condition, which can also be obtained using the node elimination method, as seen in the previous chapter. As an

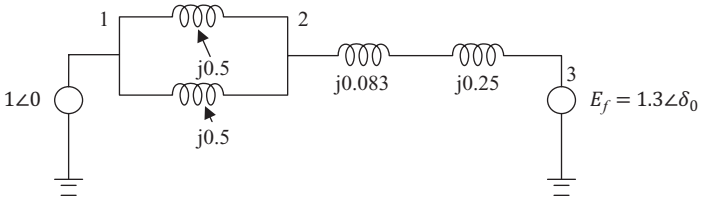

FIGURE 12.7
Reactance diagram of the SLD of the two-bus system pre-fault condition.

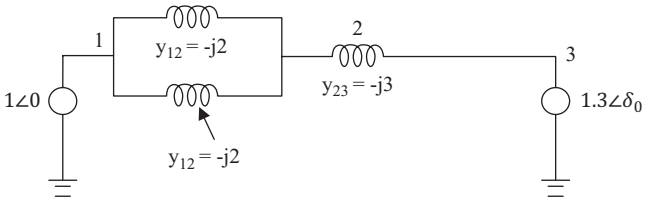

FIGURE 12.8
Admittance diagram of the SLD of the two-bus system pre-fault condition.

exercise, the reader is personally challenged to try it out and verify the result. Thus, power angle δ_0 given by Equation 12.28 serves as the starting value from which any stability considerations can be initiated if a fault were to exist. Let us now analyze a situation in which a fault occurs on the lower TL at a distance of one-third from bus 1. This fault situation changes the reactance diagram as shown in Figure 12.9.

This can be rearranged and solved for a reduced circuit, as shown in Figure 12.10.

Further, using Thevenin's equivalent for the circuit to the left of the dotted line *ab*, we have

$$V_{TH} = \frac{0.333}{0.333+0.5}1 = 0.4; \quad x_{TH} = \frac{(0.5)(0.333)}{0.833} = 0.2 \tag{12.29}$$

Using Equation 12.29, we have a new reactance diagram of the SLD after the fault, as shown in Figure 12.11 with a 0.4 pu EMF and a reactance of *j*0.2 representing the circuit to the left of the dashed line *ab* in Figure 12.10 as follows:

Resulting in a new expression for the electrical power at fault conditions to be:

$$P'_e = \frac{E_f V_{TH}}{x'}\sin\delta = \frac{(1.3)(0.4)}{0.533}\sin\delta = 0.976\sin\delta \tag{12.30}$$

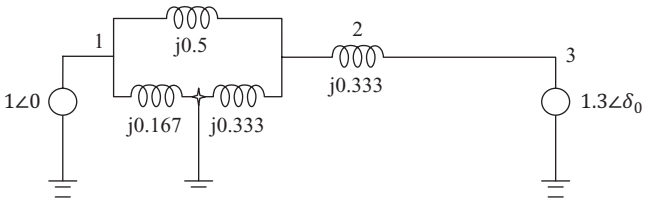

FIGURE 12.9
Reactance diagram of the fault-altered SLD.

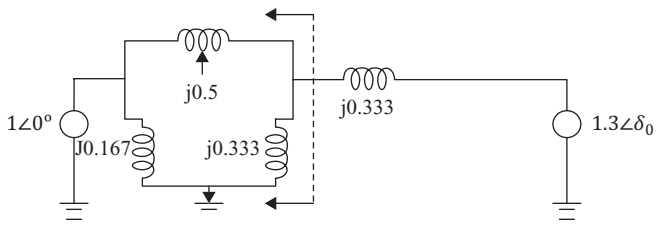

FIGURE 12.10
Reduced circuit after fault occurs.

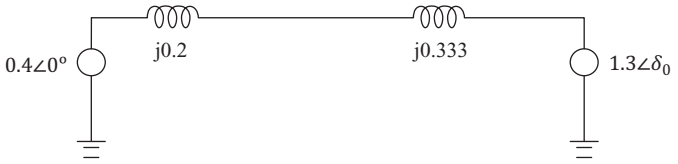

FIGURE 12.11
Resulting SLD.

→ Reduction in maximum power capability of the power system under fault

However, this fault condition cannot be sustained for a very long time, otherwise it will lead to detrimental conditions for the power network. In real-time conditions, the fault is removed by operating the corresponding circuit breakers that tie TL 2 from the network, resulting in a revised diagram as shown in Figure 12.12 for the post-fault conditions of the SLD.

The resulting new post-fault electrical power of the SLD is

$$P_e'' = \frac{E_f V}{x''}\sin\delta = \frac{(1.3)(1)}{0.833}\sin\delta = 1.56\sin\delta \tag{12.31}$$

→ Increase in the maximum power capability of the power system

in the post-fault condition but smaller than in the pre-fault condition

In addition, it is imperative to note that all these powers are sinusoidal in nature and can be easily plotted for comparison, as shown in Figure 12.13.

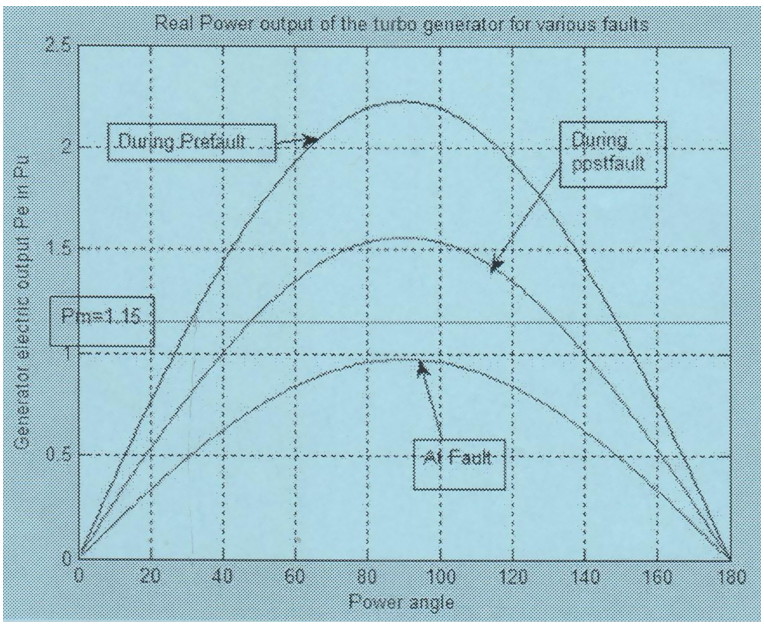

FIGURE 12.12
Post-fault, pre-fault and at-fault electrical power curves for the two-bus power network.

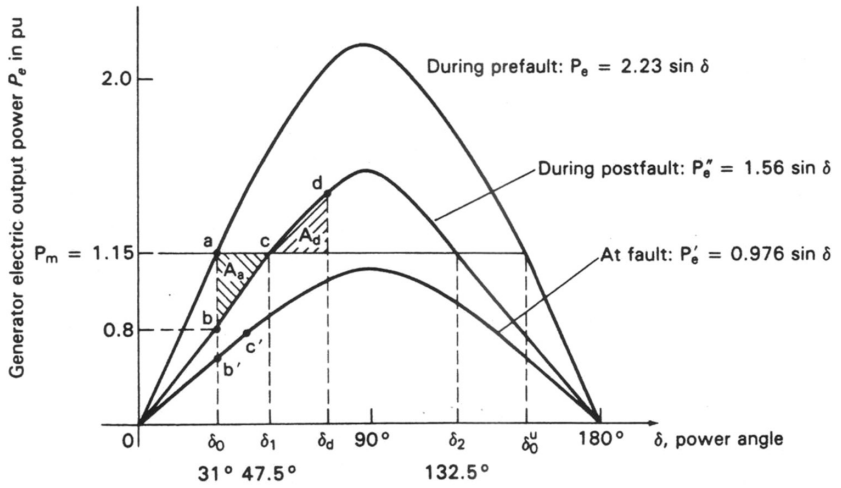

FIGURE 12.13
Pre-fault, at-fault and post-fault electrical power curves.

Figure 12.13 shows that the electrical power swings from a maximum value of 2.23 in the pre-fault condition to a maximum value of 0.997 in the fault condition and then swinging back to the maximum value of 1.56 in the post-fault condition. As a result, the power angle that was at a start value of 31° at pre-fault will 'swing' to different values depending on the transient stability conditions experienced by the rotor and the corresponding dynamics. This dynamic of the rotor is called the swing equation, as given by Equation 12.22. This change in the power angle can be solved by using a computer, where the *critical clearing* (CC) *time* between at-fault and post-fault is of great relevance and decides the transient stability quantification. This is also the time it takes for the power angle to change from δ_0 to δ_{cc} in response to the accelerating torque following the fault occurrence. This time is called critical clearing time: t_{cc} and its actual value is not known since a closed-form solution is not available to the non-linear differential Equation 12.22 during the fault period. There are different forms of solutions provided by the Runge–Kutta procedure for solving such a second-order non-linear differential equation. The solution is provided stepwise as follows.

Create state equations at fault with the power angle δ and the disturbance angular velocity ω_d as given by

$$\dot{\delta} = \frac{d\delta}{dt} = \omega_d \tag{12.32}$$

$$\ddot{\delta} = \frac{d\omega_d}{dt} = \frac{\pi f}{H}\left(P_m - P_e'\right) \tag{12.33}$$

The disturbance angular velocity is also the deviation from the synchronous speed caused by the accelerating torque following the fault. Thus, considering the starting value of the power angle before the fault (pre-fault) in the previous example, we have

$$\delta_0^{\circ} = 0.541 \text{ rad} = 31^{\circ} \tag{12.34}$$

and

$$\dot{\delta}^{\circ} = \omega^{\circ}{}_d = 0 \text{ rad/s} \tag{12.35}$$

12.4 Runge–Kutta Algorithm

With the starting values as indicated in Equations 12.34 and 12.35, the Runge–Kutta algorithm is given for incremental values as follows:

$$\Delta\delta^{o} = \frac{1}{6}\left(k_1{}^{o} + 2k^{o}{}_2 + 2k^{o}{}_3 + k^{o}{}_4\right) \tag{12.36}$$

$$\Delta\omega^{o}{}_d = \frac{1}{6}\left(l^{o}{}_1 + 2l^{o}{}_2 + 2l^{o}{}_3 + l^{o}{}_4\right) \tag{12.37}$$

where the four auxiliary k and l quantities are given by and evaluated for assumed incremental time ΔT as follows:

$$k^{o}{}_1 = (\Delta T)\Delta\omega_d{}^{o} \tag{12.38}$$

$$l^{o}{}_1 = (\Delta T)\frac{\pi f}{H}(P_m - P_e') \tag{12.39}$$

For the example we have been looking at so far, we have Equation 12.39 as follows:

$$l^{o}{}_1 = (\Delta T)\frac{\pi f}{H}(P_m - P_e') = (\Delta T)62.83(1.15 - 0.976\sin\delta) \tag{12.40}$$

Since the right-hand side of Equations 12.38 and 12.40 are known, both unknowns

$$k_1{}^{o} \text{ and } l_1{}^{o}$$

can be easily evaluated for the starting values at the first iteration and used to find the succeeding values as follows:

$$k_2{}^{o} = (\Delta T)\left(\omega_d{}^{o} + \frac{1}{2}l_1{}^{o}\right) \tag{12.41}$$

$$l_2{}^{o} = (\Delta T)62.83\left[1.15 - 0.976\left(\delta^{o} + \frac{1}{2}k_1{}^{o}\right)\right] \tag{12.42}$$

and

$$k_3{}^{o} = (\Delta T)\left(\omega_d{}^{o} + \frac{1}{2}l_2{}^{o}\right) \tag{12.43}$$

$$l_3{}^{o} = (\Delta T)62.83\left[1.15 - 0.976\left(\delta^{o} + \frac{1}{2}k_2{}^{o}\right)\right] \tag{12.44}$$

and further,

$$k_4{}^{o} = (\Delta T)\left(\omega_d{}^{o} + \frac{1}{2}l_3{}^{o}\right) \tag{12.45}$$

$$l_4^{\circ} = (\Delta T)62.83\left[1.15 - 0.976\left(\delta^{\circ} + \frac{1}{2}k_3^{\circ}\right)\right] \tag{12.46}$$

Using the values of the constants in Equations 12.38 through 12.46 in Equations 12.36 and 12.37 yields the updated values of the state variables, which are given as

$$\delta^1 = \delta^{\circ} + \Delta\delta^{\circ} \tag{12.47}$$

$$\omega_d{}^1 = \omega_d{}^{\circ} + \Delta\omega_d{}^{\circ} \tag{12.48}$$

with the updated time given by

$$t^1 = t^0 + \Delta T \tag{12.49}$$

The solution to the swing equation using the Runge–Kutta algorithm is an iterative process that is continued till the contributions to the state variables at the kth iteration (i.e., $\Delta\delta^k$ and $\Delta\omega_d{}^k$) fall within the acceptable stopping criteria set in the algorithm (i.e., 10^{-6}).

12.5 Transient Stability Assessment via the Equal Area Method

The three conditions of the network—pre-fault, at fault and post-fault—provide considerable information about transient stability, especially when the network is at fault and how quickly it moves to the post-fault state after the fault has been removed and at what time. In other words, the replacement of P_e with P_e'' in swing Equation 12.22 as follows will yield a better picture of the power angle dynamics.

$$\ddot{\delta} = \frac{\pi f}{H'}(P_m - P_e'') \text{ in pu} \tag{12.50}$$

For the example under consideration, $H = 3$ s. Using the appropriate value of P_e'' from Equation 12.31 and with the same value of the mechanical PM power as $P_m = 1.15$, the swing equation for a 60 Hz source yields

$$\delta + 98\ \sin\delta - 72\ddot{.}25 = 0 \tag{12.51}$$

Equation 12.51 is non-linear and has a closed-form solution that is very difficult to achieve. Also, it is imperative to note that if the fault in Equation 12.5 is a sustained short circuit at the generator bus, then the post-fault electrical power P_e'' would be the same as the at-fault electrical power of P_e' (which we know is zero), which results in a parabolic change in the power angle δ with time. This is evident from the double integration of the power angle δ, which yields

$$\delta = \delta_0 + 36.13t^2 \tag{12.52}$$

with δ_0 as the pre-fault power angle value, as calculated in Equation 12.34.

For the network to recover from the at-fault condition to the post-fault condition, it will depend on the fault-clearing time. If the fault is cleared instantaneously, then at time 0^+ after the fault the value of the electrical power is given by

$$1.56\sin 31° = 0.8 \tag{12.53}$$

The rotor inertia prevents instantaneous changes in the power angle!

The net result is a positive value for the quantity:

$$\left(P_m - P_e''\right) = \left(1.15 - 0.8\right) = 0.35 \tag{12.54}$$

The pre-fault, at-fault and post-fault values of electrical power are plotted again in Figure 12.14.

In Figure 12.14, there are two equilibrium points of interest associated with the post-fault power P_e'' given by the two power angles.

$$\delta_1 = \sin^{-1}\left(\frac{1.15}{1.56}\right) = 47.5° \text{ or } 0.829\,\text{rad} \tag{12.55}$$

and

$$\delta_2 = 180° - 47.5° = 132.5° \tag{12.56}$$

In Figure 12.14, there are several points that need to be described.

a: Intersection of the P_m line with the pre-fault electrical power P_e sinusoidal curve

b: Intersection of the post-fault electrical power P_e'' with the vertical line *a-b-b′*-δ_0, where $\delta_0 = 31°$

b′: Intersection of the at-fault electrical power P_e' with the vertical line *a-b-b′*- δ_0, where $\delta_0 = 31°$

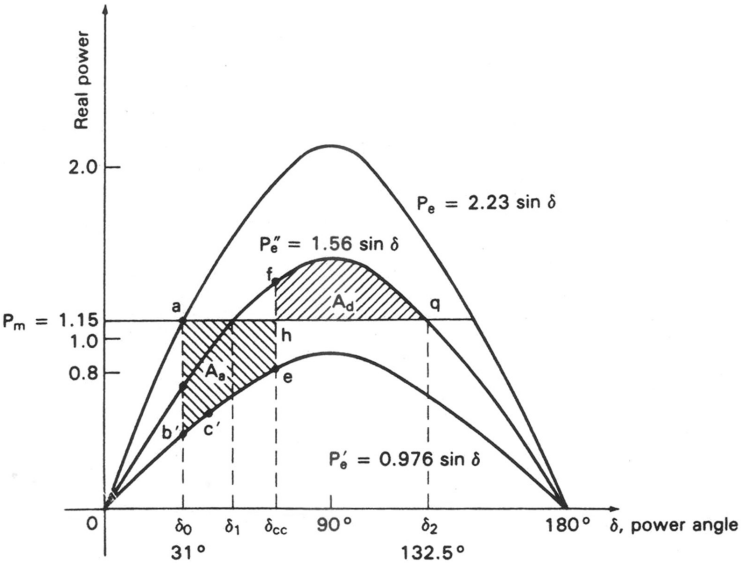

FIGURE 12.14
Pre-fault, at-fault and post-fault electrical power curves with hatched areas of interest to verify equal area method.

c: Intersection of the mechanical input power line P_m with the post-fault electrical power P_e'' sinusoidal curve

c′: An arbitrary point along the at-fault electrical power sinusoid curve after point *b′*

d: Point at which the deceleration halts the motion of the rotor along the post-fault power curve that signifies the power angle δ_d

The two hatched areas signify a transient stability condition if they are equal; thus, it is the *equal area* solution method. When the generator is switched from pre-fault to post-fault, an accelerating torque acts on the generator shaft that brings about a change in the power angle, which increases from 30° at point *b* to 47.5° at point *c* along the post-fault electrical power curve. The hatched area *abc* is called the *accelerating area*, A_a. Beyond that, the generator shaft continues to move along this post-fault curve but now at a decelerating motion to the point *d* at a power angle of δ_d. The second hatched area *cdd* is called the *decelerating area*, A_d. When $A_a = A_d$, the generator achieves transient stability. As the swing equation does not have a first derivative term $\dot{\delta} = \frac{d\delta}{dt} = \omega_d$, there is no damping action and the rotor continues its swinging action; however, due to the moment of inertia of the generator, this swing would die down to achieve its dynamic stable condition. This change needs to be measured and can be done as follows by understanding that the difference in angular velocity ω_d is the difference between the mechanical angular velocity ω_m of the generator and the synchronous angular velocity ω_s of the network.

$$\dot{\delta} = \frac{d\delta}{dt} = \omega_d = \omega_m - \omega_s \tag{12.57}$$

We now perform some mathematical differential manipulations, as follows:

$$\frac{d}{dt}(\dot{\delta})^2 = 2\dot{\delta}\ddot{\delta} = 2\frac{d\delta}{dt}\ddot{\delta} \tag{12.58}$$

which can be rewritten as

$$d\left(\omega_d{}^2\right) = 2\ddot{\delta}d\delta \tag{12.59}$$

We can now integrate both sides of Equation 12.59, and inserting Equation 12.22 we have

$$\frac{H}{\omega}\int_{\omega_{db}}^{\omega_{dd}} d\left(\omega_d{}^2\right) = \int_{\delta_0}^{\delta_d}\left(P_m - P_e''\right)d\delta \tag{12.60}$$

or

$$\frac{H}{\omega}\left[\omega_{dd}{}^2 - \omega_{db}{}^2\right] = \int_{\delta_0}^{\delta_d}\left(P_m - P_e''\right)d\delta \tag{12.61}$$

where:

ω_{dd} is the difference speed corresponding to operation point *d*

ω_{db} is the difference speed corresponding to point *b*

Since the speed of the generator rotor is synchronous at point *a* on the pre-fault curve, and the speed at point *b* is also synchronous, as the rotor inertia prevents a speed change immediately on switching to clear the fault, the value of ω_d at this instant is zero; that is,

$$\omega_{db} = 0 \tag{12.62}$$

In addition, if there is sufficient reserve power capacity in the post-fault electrical power P_e'', then it is possible for the decelerating action (A_d) to produce an opposing effect that completely negates the accelerating action (A_a) that occurs during operating along section *ac*. This results in $\omega_{dd} = 0$, which means the left-hand side of Equation 12.61 is zero and the rotor of the generator is transient stable, which yields

$$0 = \int_{\delta_0}^{\delta_1} \left(P_m - P_e''\right) d\delta + \int_{\delta_1}^{\delta_d} \left(P_m - P_e''\right) d\delta \tag{12.63}$$

Also, as post-fault power $P_e'' > P_m$, the mechanical power input, we rewrite the second term of Equation 12.63 over the interval δ_1–δ_d as follows:

$$0 = \int_{\delta_0}^{\delta_1} \left(P_m - P_e''\right) d\delta - \int_{\delta_1}^{\delta_d} \left(P_e'' - P_m\right) d\delta \tag{12.64}$$

$$\rightarrow 0 = A_a - A_d \rightarrow \text{accelerating area } A_a = \text{decelerating area } A_d \tag{12.65}$$

$$\rightarrow \text{Transient stability of the rotor using the equal area method}$$

This can be numerically verified and is left for the reader as an exercise in the problems to follow for this chapter.

12.6 Effect of Finite Fault-Clearing Time on Transient Stability

The transient stability of the previous section was analyzed assuming that the transition from the fault condition to the post-fault state occurs with no time delay; that is, the fault has been removed immediately without any time delay by isolating the faulted parts of the circuit using appropriate circuit breakers. This indicates that the dynamics of the rotor were allowed to move directly from the pre-fault electrical power sinusoidal curve P_e to the post-fault electrical power sinusoidal curve P_e'' of the generator rotor along the section of the line *ab*. This is the ideal action that needs to be taken to not allow the fault to sustain for too long (i.e., instantaneously). This is not practically possible as there are no fast-reacting circuit breakers available with zero switching time capability, which means that the changeover from pre-fault to post-fault takes place through the intermediate step of transiting through the at-fault condition after curve P_e'. The operation is shown with its path in Figure 12.15.

The operation moves from point *a* to point *b′* on the at-fault curve P_e'. From here on, with the finite fault-clearing time under consideration, the operation moves along P_e' through the points *bc′* until the fault is cleared at *c′*, at which time the operating point moves up to the line *bc* along an ordinate line at *c′*, and then the expression for the electric power in the swing equation moves to the post-fault curve P_e''.

In Figure 12.15, it can be seen that the accelerating area A_a is much greater than the decelerating area A_d, causing the equal-area criterion to fail and the rotor to move about

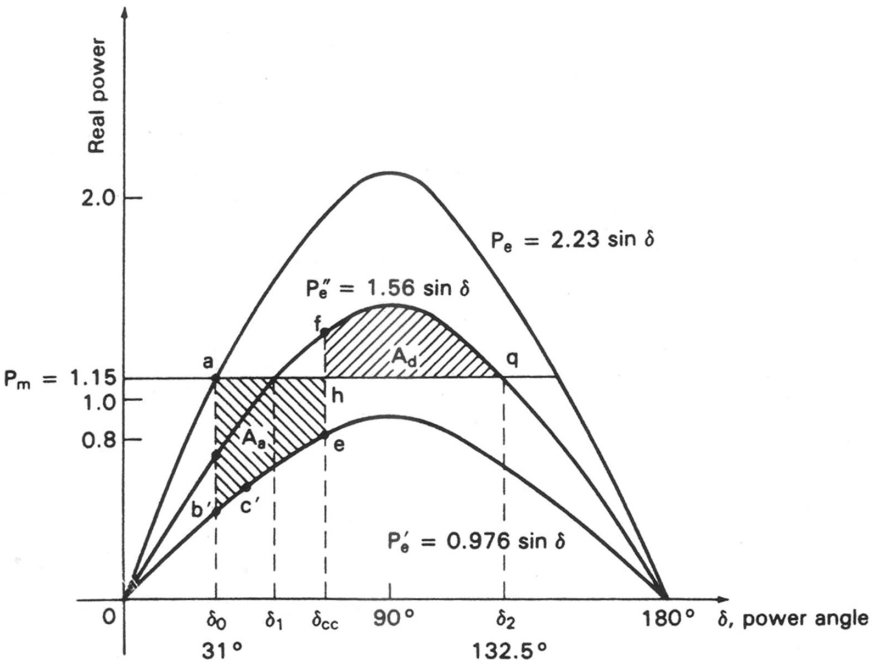

FIGURE 12.15
Pre-fault, at-fault and post-fault electric power sinusoidal curves to show the effect of finite fault-clearing time on transient stability.

its axis until the two areas either equate to each other, causing transient stability, or swing beyond control and lose synchronism with the infinite bus. This transition is decided by the critical clearing time t_{cc}. Its effect can be seen in problem to be attempted at the end of the chapter.

12.7 Case 2: Two-Machine System

For two machines, Equation 12.18 can be written as

$$\text{Machine 1: } M_1\ddot{\delta}_1 = P_{m_1} - P_{e_1} \tag{12.66}$$

$$\text{Machine 2: } M_2\ddot{\delta}_2 = P_{m_2} - P_{e_2} \tag{12.67}$$

If the relative power angle between two rotors is denoted as

$$\delta = \delta_1 - \delta_2 \tag{12.68}$$

then Equations 12.66 and 12.67 can be combined together for the two machines as follows:

$$M\ddot{\delta} = P_m - P_e \tag{12.69}$$

where:

$$M = \frac{M_1 M_2}{M_1 + M_2};\ P_m = \frac{M_2 P_{m_1} - M_1 P_{m_2}}{M_1 + M_2};\ P_e = \frac{M_2 P_{e_1} - M_1 P_{e_2}}{M_1 + M_2} \tag{12.70}$$

The solution derived earlier in Section 12.5 is used to find the conditions of stability for the two-machine case.

Problems

PROBLEM P.12.1

A 100 MVA hydroelectric generator has the inertia constant H, as given in Equation 12.18 for electrical degrees instead of radians, and a value of 4.0 MJ/MVA. The latter unit can be shown to be equivalent to the unit H in Equation 12.18.

a. How much energy is stored in the rotor at synchronous speed?
b. If the input to the generator suddenly increases by 20 MVA, what acceleration is imparted to the rotor?

PROBLEM P.12.2

a. Find the value of H in Problem P.12.1 at a 200 MVA base.
b. Find the energy stored at the 200 MVA base.

PROBLEM P.12.3

In a short transmission line of impedance $R + jX$, the sending end and receiving end voltages are equal for a certain lagging power factor load.

a. Find the ratio of X:R so that maximum power is transmitted over the line under steady-state conditions.
b. Draw the corresponding phasor diagram to illustrate the steady-state condition.

PROBLEM P.12.4

A 500 MW synchronous generator operates at a power angle of 8°. Calculate the increase in synchronous generator shaft power without the loss of steady-state stability.

PROBLEM P.12.5

The sending end and receiving end voltages of a transmission line at a 100 MW load are equal at 115 kV. The per phase line impedance is $(4 + j7)$ Ω. Find the maximum steady-state power that can be transmitted over the line.

PROBLEM P.12.6

Find the maximum additional load that can be suddenly taken on by the transmission line of Problem P.12.5 without losing stability.

PROBLEM P.12.7

The kinetic energy stored in the rotor of a 50 MVA, six-pole, 60 c/s machine is 200 MJ. The input to the machine is 25 MW at a developed power of 22.5 MW. Find the accelerating power and the related acceleration of the power angle (i.e., $\ddot{\delta}$).

PROBLEM P.12.8

If the acceleration of the machine in Problem P.12.7 remains the same for 10 cycles, what is the power angle at the end of the 10 cycles?

PROBLEM P.12.9

The generator in Problem P.12.7 has an internal voltage of 1.2 pu and is connected to an infinite bus operating at a voltage of 1.0 pu through a reactance of 0.3 pu. A three-phase short circuit occurs on the line. Circuit breakers operate and the new reactance between the generator and the infinite bus changes to a reactance value of 0.4 pu. Find the critical clearing angle.

PROBLEM P.12.10

In a plant, two synchronous generators swing together. The inertia constants of the machines are H_1 and H_2, with MVA ratings S_1 and S_2, the per-unit power inputs to the two units are P_{m1} and P_{m2}, respectively, and the electrical powers developed are P_{e1} and P_{e2}, respectively.

Obtain an equivalent swing equation for the two-machine system in terms of inertia constants referred to a common base, the per-unit synchronous frequency ω_s in radians per second, the per-unit electrical frequency in radians per second and the given values of the per-unit power values.

PROBLEM P.12.11

The swing equation for a 60 c/s synchronous machine during a fault lasting 0.05 s in pu values is given by

$$\ddot{\delta} = \frac{5\pi}{3} \quad \forall \quad 0 \le t \le 0.05\,\text{s}$$

The initial power angle was 0.418 rad. When the fault was cleared, the developed electrical power became 2.46 sinδ in pu.

a. Find the maximum power angle
b. Find out whether the machine remained stable

PROBLEM P.12.12

Calculate the critical clearing time in cycles for the machine in Problem P.12.11.

PROBLEM P.12.13

Use MATLAB® numerical methods to solve Problem P.12.11.

PROBLEM P.12.14

Use MATLAB numerical methods to solve Problem P.12.12.

PROBLEM P.12.15

As shown in Figure P.12.15, generator *G* is connected to an infinite bus by two transmission lines with reactances of *j*0.8 and *j*0.4 pu for the top and bottom transmission lines, respectively. The other parameters are as follows:

$$\text{Generator G: } E_1 = 1.25\angle\delta$$

$$\text{Infinite bus: } V_1 = 1\angle 0°$$

$$\text{Transformer: } x_1 = 0.1\,\text{pu}$$

A fault occurs at the midpoint of the top transmission line.

a. Find the value of the equivalent reactance that joins the excitation voltage of *G* to the infinite bus.
b. Find the expression for the electric power of the generator *G* at fault P_e'.
b. The breakers operate and remove the top transmission line from the circuit. Find the electric fault at post-fault P_e''.

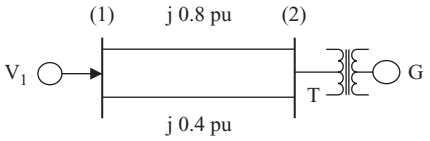

FIGURE P.12.15
SLD of system with two transmission lines connected to bus 1 and bus 2.

PROBLEM P.12.16

Redo Problem P.12.15 if the fault occurs on the bottom transmission line one-third of the distance from bus 2.

PROBLEM P.12.17

The generator in Problem P.12.15 is a two-pole turbogenerator with an *H* parameter of 3 s. The mechanical input power to the system is given by 1.2 pu. The P_e is given by

$$P_e = 1.87\sin\delta\,\text{pu}$$

Subsequently, a fault occurs on one of the transmission lines and the at-fault and post-fault electrical powers are

$$P_e' = 1.04\sin\delta\,\text{pu}$$

$$P_e'' = 1.56\sin\delta\,\text{pu}$$

a. Find the pre-fault steady-state power angle for both the stable and unstable points of operation for the given turbine power input.
b. Switching occurs immediately from pre-fault to post-fault. Will the decelerating torque cause stability or instability?
c. Use the equal area concept to show whether or not the turbogenerator is transient stable.
d. Use the numerical Runge–Kutta method to evaluate the transient-stable equations and plot the performance.
e. Find the suitable critical clearing time for the switching to take place to maintain instability and transient stability, respectively.

PROBLEM P.12.18

Repeat Problem P.12.17 with the following quantities:

$$\text{Mechanical power input } P_m = 0.8 \text{ pu}$$

$$\text{Pre-fault electrical power } P_e = 1.87 \text{ pu}$$

$$\text{Post-fault electrical power } P_e'' = 1.04 \text{ pu}$$

$$\text{At-fault electrical power } P_e' = 1.56 \text{ pu}$$

PROBLEM P.12.19

Investigate the effect of the damping action generated by the short-circuited rotor pole winding embedded in the pole faces. Perform this for the following values of damping power:

a. 0.01 pu
b. 0.1 pu

Use a value of fault-clearing time less than but close to the critical clearing time t_{cc}.

PROBLEM P.12.20

Use the Runge–Kutta numerical method to verify the results in Problem P.12.19.

PROBLEM P.12.21

The system in Figure P.12.21 is the translational equivalent of the rotational situation in a turbogenerator. Hence, M denotes the mass of the object, K is a spring constant, and D represents a viscous friction coefficient.

a. Assuming the mass is at rest, write the ordinary differential equation (ODE) that describes the motion of the mass with time for an applied force F.
b. If D is negligible and K is a constant, explain the behavior of the mass when any force is applied. Is this situation analogous to that described in the initial part of this chapter?

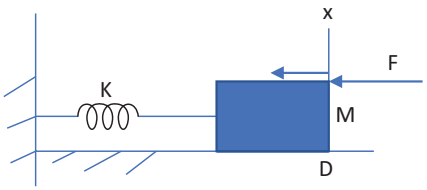

FIGURE P.12.21
Mass-Spring-Damper system.

c. Repeat part (a) on the assumption that the linear spring is replaced by one with a resisting force that sinusoidally varies with displacement.
d. Discuss how you would generally seek a solution to the ODE found in part (a).
e. Use MATLAB to solve the equation in (d).

PROBLEM P.12.22

Although *H* is expressed as MJ/MVA, it carries the unit of seconds as an equivalent term. Assuming that a turbogenerator is operating at synchronous speed under no-load conditions, find the time it takes for the rotor to reach zero speed when a counter-torque of rated value is applied to the spinning rotor. What significance can be assigned to *H* from this analysis?

13

Test Cases

Case 1: Load Flow Analysis Using the Newton–Raphson Method

Problem Statement

A three-base electric power system is depicted in Figure 13.1. It is composed of a slack bus and a load bus with transmission links that can be represented solely by their line reactance, as shown in the Figure 13.1. The drain of real and reactive power at each bus is expressed on a pu basis using the base reference quantities 100 MVA and 230 kV.

Both the real power and the magnitude of the bus voltages are specified at bus 2. For simplicity, the transmission network is considered lossless.

1. Find the Y_{bus}.
2. Identify the independent variables for this system.
3. Write the power flow equations expressed solely in terms of the independent variables and the specified system parameters.
4. Use the Newton–Raphson method to find the solutions to the power flow equations up to three iterations (modify the MATLAB® routine developed earlier).
5. Compute the bus-to-bus complex power.
6. Develop your MATLAB programs.

Solution

$$Z_{base} = \frac{230^2}{100} = 529\,\Omega$$

$$z_{12} = j75.57\,\Omega = j0.14285\,\text{pu}$$

$$y_{12} = -j7\,\text{pu}$$

Similarly,

$$y_{13} = -j8\,\text{pu}$$

$$y_{23} = -j10\,\text{pu}$$

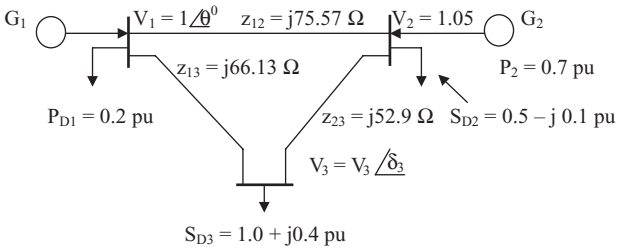

FIGURE 13.1
Three-bus electric power system.

1. $$Y_{\text{bus}} = \begin{bmatrix} -j15 & j7 & j8 \\ j7 & -j17 & j10 \\ j8 & j10 & -j18 \end{bmatrix}.$$

2. The independent variables are δ_2, V_3 and δ_3.
3. Using power flow equations for the dependent variables declared in Figure 13.1 (P_2, P_3 and Q_3), we have

$$P_2 = V_2 Y_{21} V_1 \cos(\delta_2 - \delta_1 - \theta_{21})$$

$$+V_2 Y_{22} V_2 \cos(\delta_2 - \delta_2 - \theta_{22})$$

$$+V_2 Y_{23} V_3 \cos(\delta_2 - \delta_3 - \theta_{23})$$

$$= 7.35\cos(\delta_2 - 90°) + 10.5\cos(\delta_2 - \delta_3 - 90°)$$

$$P_3 = V_3 Y_{31} V_1 \cos(\delta_3 - \delta_1 - \theta_{31})$$

$$+V_3 Y_{32} V_2 \cos(\delta_3 - \delta_2 - \theta_{32})$$

$$+V_2 Y_{33} V_3 \cos(\delta_3 - \delta_3 - \theta_{33})$$

$$= V_3.8.1\cos(\delta_3 - 90°) + V_3.10.(1.05)\cos(\delta_3 - \delta_2 - 90°) + V_3.18V_3\cos(-90^0)$$

and

$$Q_3 = V_3 Y_{31} V_1 \sin(\delta_3 - \delta_1 - \theta_{31})$$

$$+V_3 Y_{32} V_2 \sin(\delta_3 - \delta_2 - \theta_{32})$$

$$+V_2 Y_{33} V_3 \sin(\delta_3 - \delta_3 - \theta_{33})$$

$$= V_3.8.1\sin(\delta_3 - 90°) + V_3.10.(1.05)\sin(\delta_3 - \delta_2 - 90°) + V_3.18V_3\sin(-90°)$$

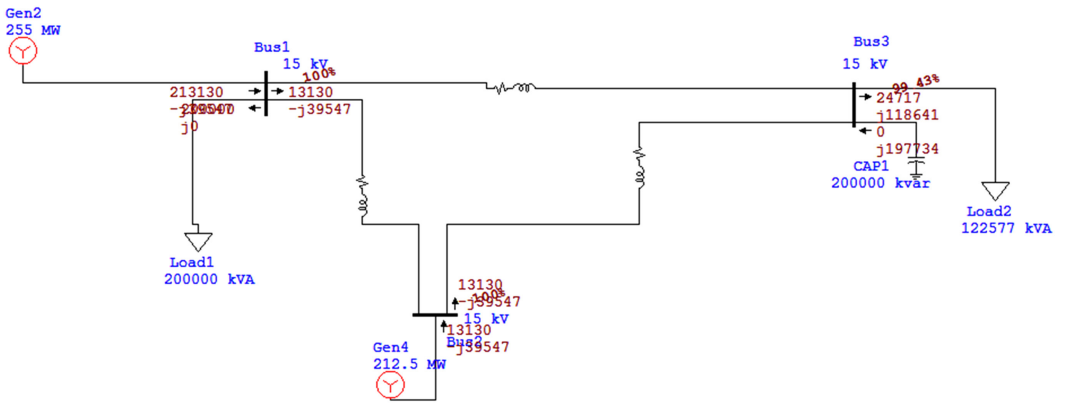

FIGURE 13.2
Three-bus SLD using ETAP power flow analysis.

4. Using the Newton–Raphson method and suitable MATLAB code, at the end of the third iteration we have

$$V_1 = 1.0;\ \delta_1 = 0$$

$$V_2 = 1.05;\ \delta_2 = 0.0111\,\text{rad}$$

$$V_3 = 1.0041;\ \delta_3 = -0.0475\,\text{rad}$$

A suitable MATLAB code provided by one of my students who took my ECE-572 power systems analysis course (Mr. Sead Alihodzic from spring 2009) is provided for reference in Appendix C. No guarantee is provided for the success of this code by the author. A similar attempt using ETAP is provided in the body of the text. A sample output is shown in Figure 13.2.

Case 2: Power System Stability Using the Runge–Kutta Algorithm

Problem Statement

A fault occurs at a point located along the lower transmission line at a distance one-third from bus 1, as in the pre-fault network shown in Figure 13.3. Using the swing equation in conjunction with the Runge–Kutta, method evaluate all the aspects of this power system's stability in terms of transient and steady-state conditions depending on the *critical clearing time*: T_{cc}.

Select the following parameters for the computer-based solution:

1. $T_{cc} = 0.2$ s and $\Delta T = 0.01$ s
2. The power equation $P_e' \sin\delta$ is given in the following equation:

$$\frac{d\omega_d}{dt} = \frac{\pi f}{H}\left(P_m - P_e'\right)$$

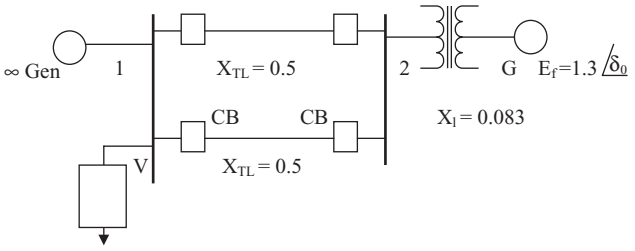

FIGURE 13.3
Pre-fault transmission network.

After the first 20 iterations, use the post-fault power

$$P_e'' = 1.56 \sin\delta$$

Find the transient and steady-state conditions for system stability and plot the same.

Solution

This problem is solved using the sample code and results shown in Appendix 3. No guarantee is provided for the use of the code and the results given in Appendix 3.

Appendix A: Electrical Circuits

1) Single Phase Circuits

R-L Circuit

As illustrated in Figure A.1 we have a resistance in series with an inductor.

The applied voltage 'V' from a single phase ac source is connected to the series combination of an inductor 'L' and a resistor 'R'. V is given by:

$$V = V_m \mathrm{Sin}(\omega t) \tag{A.1}$$

where V_m is the maximum value of the sinusoidal voltage applied from a source at an angular velocity 'ω' = 2πf; where f is the frequency of the alternating signal. The rms value of the voltage applied to this circuit is given by:

$$V_{rms} = \frac{V_m}{\sqrt{2}} \tag{A.2}$$

The impedance of this series circuit is given by:

$$Z = R + jX_L \tag{A.3}$$

where $X_L = 2\pi fL$, and the impedance angle $\theta = \tan^{-1}(X_L/R)$ and power factor of the circuit is given by pf = cos θ. Leading to the evaluation of I as:

$$I = \frac{V}{Z} = |I| \text{ with an angle}(-\theta) \tag{A.4}$$

as shown in Figure A.2. The voltage phasor diagram of this circuit is shown in Figure A.2 with the voltage phasor as the reference phasor. Such a circuit is called a lagging circuit as the current vector lags the voltage vector by the angle θ and the power factor is called a lagging power factor. Thus all inductive circuits are called 'lagging circuits'. If the circuit has a pure inductance in it without any resistance then the current vector will lag the voltage vector by 90°. This aspect will be consistently illustrated and used in the material covered under the scope of this book.

R-C Circuit

As illustrated in Figure A.3 we have a resistance in series with a capacitor.

The applied voltage 'V' from a single phase ac source is connected to the series combination of a capacitor 'C' and a resistor 'R'. V is given by:

$$V = V_m \mathrm{Sin}(\omega t) \tag{A.5}$$

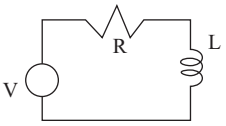

FIGURE A.1
Voltage source V with R and L in series.

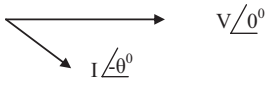

FIGURE A.2
Voltage phasor diagram of circuit in Figure A.1.

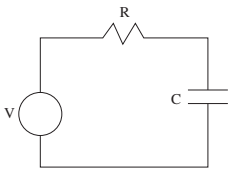

FIGURE A.3
Voltage supplied to an R-C circuit.

where V_m is the maximum value of the sinusoidal voltage applied from a source at an angular velocity '$\omega = 2\pi f$; where f is the frequency of the alternating signal. The rms value of the voltage of the applied to this circuit is given by:

$$V_{rms} = \frac{V_m}{\sqrt{2}} \tag{A.6}$$

The impedance of this series circuit is given by:

$$Z = R - jX_C \tag{A.7}$$

where $X_L = 2\pi fL$; and the impedance angle $\theta = \tan^{-1}(X_C/R)$ and power factor of the circuit is given by $pf = \cos\theta$.

Yielding the evaluation of I as:

$$I = \frac{V}{Z} = |I| \text{with an angle}(\theta) \tag{A.8}$$

as shown in Figure A.4.

The voltage phasor diagram of this circuit is shown in Figure A.4 with the voltage phasor as the reference phasor. Such a circuit is called a leading circuit as the current vector leads the voltage vector by the angle θ and the power factor is called a leading power factor. Thus all capacitive circuits are called 'leading circuits'. If the circuit has a pure capacitor in it without any resistance then the current vector will lead the voltage vector by 90°. This aspect will be consistently illustrated and used in the material covered under the scope of this book.

A purely resistive circuit has no inductance or capacitance involved thus leading to a condition of the current phasor in phase with the reference voltage which results in a

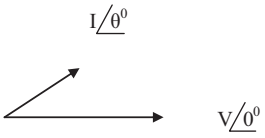

FIGURE A.4
Voltage phasor diagram of circuit in Figure A.3.

unique condition when the power factor is unity as cosine (0°) = 1 as shown in Figure A.5. Where θ, the impedance angle, in this purely resistive circuit is zero, the two phasors are said to be co-linear. Such a condition can occur in power system analysis when the load is purely resistive as in the base board heating of a residential or industrial space.

Thus all purely resistive circuits are called unity power factor (upf) circuits.

Eventually, circuits can be set-up as an RLC circuit with resistor, inductor and capacitor connected in series. The nature of the pf of the circuit will be determined by which component of the circuit, either the inductor or capacitor, is predominant.

Three-Phase Circuits

In three-phase circuits, either resistive, inductive or capacitive circuits are connected in a three-phase physical connection as shown in Figure A.6 as a purely resistive circuit.

The three line-line voltages are denoted by:

$$V_{ab} = V_m \sin(\omega t) \tag{A.9}$$

$$V_{bc} = V_m \sin(\omega t + 120°) \tag{A.10}$$

$$V_{ca} = V_m \sin(\omega t + 240°) \tag{A.11}$$

The three phasors in Equations (A.9) to (A.11) are shown in Figure A.7

Figure A.7 shows a three-phase circuit in the 'Wye' configuration with a source and load connected in each phase with a conductor which is usually the conductor say as a transmission line.

FIGURE A.5
Pure resistive circuit.

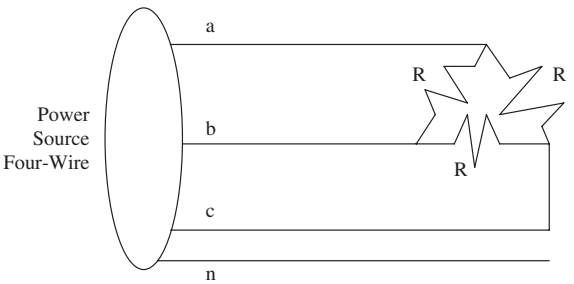

FIGURE A.6
Purely resistive circuit connected in a three-phase delta condition to a three-phase source, four-wire power source.

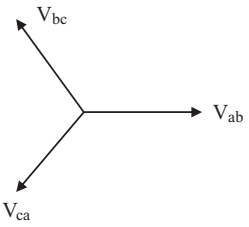

FIGURE A.7
Three-phase diagram of voltages in Figure A.6 Voltage and currents in Balanced three-phase circuits.

Generally, the phase sequence is the starting point for all three-phase connections. Say the phase sequence is 'abc' corresponding to Red-Yellow-Blue (RYB), where phase A leads Phase B by 120° and phase B leads phase C by 120°, respectively. Thus for a Y connection, we have the voltage vectors for quantities in Figure A.7 as:

$$V_{ao} = E_{a'o} - I_{an}Z_g; \quad I_{an} = \frac{V_{an}}{Z_R} = \frac{E_{a'o}}{Z_g + Z_R} \tag{A.12}$$

$$V_{bo} = E_{b'o} - I_{bn}Z_g; \quad I_{bn} = \frac{V_n}{Z_R} = \frac{E_{b'o}}{Z_g + Z_R} \tag{A.13}$$

$$V_{co} = E_{co} - I_{cn}Z_g; \quad I_{cn} = \frac{V_{cn}}{Z_R} = \frac{E_{c'o}}{Z_g + Z_R} \tag{A.14}$$

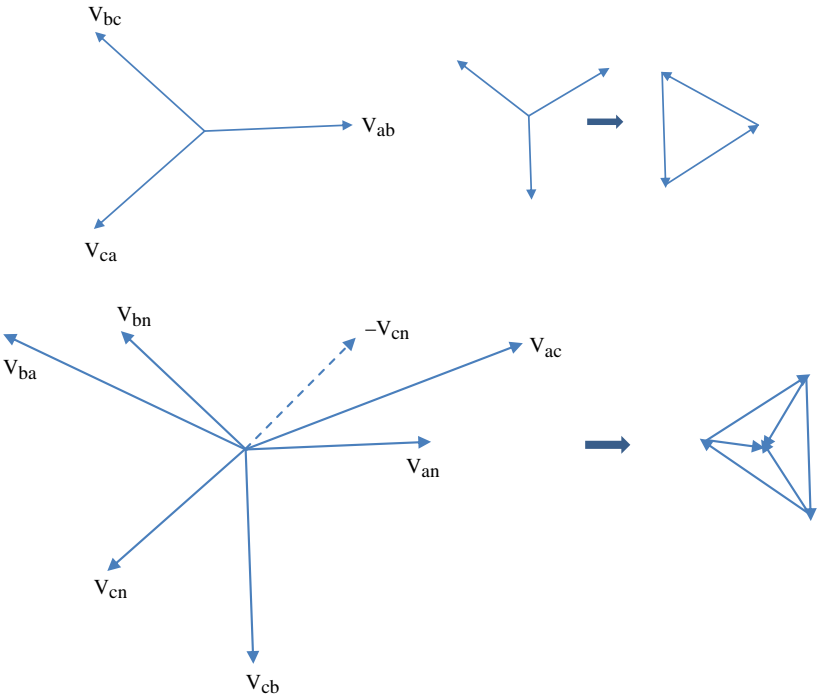

FIGURE A.8
Line-to-line voltage and phase voltage phasor diagrams to generate equivalent three phase delta and wye connections.

$$V_{ab} = V_{an} + V_{nb} = V_{an} - V_{bn} \tag{A.15}$$

$$|V_{ab}| = 2|V_{an}|\cos 30° = \sqrt{3}\,|V_{an}| \tag{A.16}$$

⟶ Line-to-line voltage is $\sqrt{3}$ times phase voltage
In a delta connection

$$|I_{ab}| = \frac{1}{\sqrt{3}}|I_a| \rightarrow |I_a| = \sqrt{3}\,|I_{ab}| \tag{A.17}$$

⟶ Line current is $\sqrt{3}$ times phase current.
Power in Balanced three-phase circuits
Y:

$$V_p = |Van| = |Vbn| = |Vcn| \text{ and } I_p == |Van| == |Ibn| = |Icn| \tag{A.18}$$

$$P = 3V_p Ip\cos\theta_p = \sqrt{}3V_L I_L \cos\theta_p \tag{A.19}$$

$$V_p = \frac{V_L}{\sqrt{3}} \quad \text{and } I_p = I_L \tag{A.20}$$

$$Q = 3V_p Ip\sin\theta_p = \sqrt{}3V_L I_L \sin\theta_p \tag{A.21}$$

$$|S| = \sqrt{}3V_L I_L \tag{A.22}$$

Δ - Delta:

$$I_p = \frac{I_L}{\sqrt{3}} \quad \text{and } V_p = V_L \tag{A.23}$$

$$P = 3V_p Ip\cos\theta_p = \sqrt{}3V_L I_L \cos\theta_p \tag{A.24}$$

$$Q = 3V_p Ip\sin\theta_p = \sqrt{}3V_L I_L \sin\theta_p \tag{A.25}$$

Per-Unit (pu) quantities or % quantities

$$\text{pu quantity} = \frac{\text{actual quantity}}{\text{base quantity}} \tag{A.26}$$

$$\%\text{ quantity} = \frac{\text{actual quantity}}{\text{base quantity}} \times 100 \tag{A.27}$$

Single Phase

$$\text{Base current, } I = \frac{\text{base kVA}_{1\varnothing}}{\text{base voltage, kV}_{LN}} \tag{A.28}$$

$$\text{Base impedance, } Z = \frac{\text{base voltage, } V_{LN}}{\text{base current, A}} \tag{A.29}$$

$$\text{Base impedance, } Z = \frac{(\text{base voltage, kV}_{LN})^2 \times 1000}{\text{base kVA}_{1\varnothing}} \tag{A.30}$$

$$\text{Base impedance, } Z = \frac{(\text{base voltage, kV}_{LN})^2}{\text{base MVA}_{1\varnothing}} \tag{A.31}$$

$$\text{Base power } kW_{1\varnothing} = \text{base kVA}_{1\varnothing} \text{ for unity power factor} \tag{A.32}$$

$$\text{Base power MW}_{1\varnothing} = \text{base MVA}_{1\varnothing} \text{ for unity power factor} \tag{A.33}$$

$$\text{pu impedance of a circuit element} = \frac{\text{actual impedance in ohms}}{\text{base impedance in ohms}} \tag{A.34}$$

Three-Phase circuits

$$\text{Base current, } I = \frac{\text{base kVA}_{3\varnothing}}{\sqrt{3}\ \text{base voltage, kV}_{LL}} \tag{A.35}$$

$$\text{Base impedance, } Z = \frac{(\text{base voltage, } \text{kV}_{LL}/\sqrt{3})^2 \times 1000}{\text{base kVA}_{3\varnothing}/3} \tag{A.36}$$

$$\text{Base impedance, } Z = \frac{(\text{base voltage, } \text{kV}_{LL})^2 \times 1000}{\text{base kVA}_{3\varnothing}} \tag{A.37}$$

$$\text{Base impedance, } Z = \frac{(\text{base voltage, kV}_{LL})^2}{\text{base MVA}_{3\varnothing}} \tag{A.38}$$

CHANGING THE BASE OF PU QUANTITIES

pu impedance of a circuit element

$$= \frac{(\text{actual impedance in ohms}) \times (\text{base kVA})}{(\text{base voltage, kV})^2 \times 1000} \tag{A.39}$$

Thus

$$puZ_{\text{new}} = puZ_{\text{given}} \left(\frac{\text{base kV}_{\text{given}}}{\text{base kV}_{\text{new}}} \right)^2 \left(\frac{\text{base kVA}_{\text{new}}}{\text{base kVA}_{\text{given}}} \right) \tag{A.40}$$

Example A.1

A portion of a power system consists of two generators in parallel, as shown in Figure A.9, connected to a step-up transformer that links them with a 230 kV transmission line. The detailed ratings relevant to this example are provided for all the components as follows:

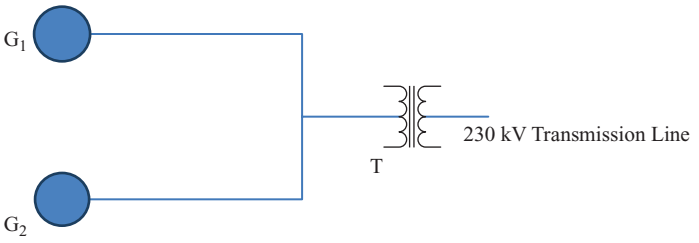

FIGURE A.9
SLD of Two generators connected to a transmission line via a transformer.

Generator G_1: 10 MVA, with a 12% reactance
Generator G_2: 5 MVA, with an 8% reactance
Transformer T: 15 MVA, with a 6% reactance
Transmission line: Z = (4 + j60) ohms, 230 kV

where the percent reactances are computed on the basis of the individual ratings respectively. Find the reactances and the impedance in percent with 15 MVA as the new base value.

SOLUTION

One needs to observe that in all the components in this example the voltage is the same. Thus, the given and new voltage base is the same. Using Equation (A.38) to obtain the pu values for all the components in the circuit, we have:

Percent reactance of Generator G_1= 12(15/10) = 18%
Percent reactance of Generator G_2 = 8 (15/5) = 24%
Percent reactance of Transformer = 6(15/15) = 6%

Now we proceed to evaluate for the transmission line as follows:

$$\text{Percent impedance } Z = (4 + j60)\left(15\times10^6\right)/\left(230\times10^3\right)^2 \times 100$$

$$= \left(0.113 + j\ 1.7\right)\ \%$$

Example A.2

This example illustrates a four-bus electric power system as in Figure A. This example will also be illustrated using the latest ETAP® version of the Software provided by OTI, CA.

1. Find the base impedance of the Generator G_1 and determine the ohmic value of the transient reactance.
2. Find the base impedance of Transformer T_4 at bus 4, referred to as the low-voltage side of the transformer, and evaluate the ohmic value of the leakage reactance on the LV side, referred to as the HV side.

Generator G_1: 50 MVA, 13.8 kV with a 20% transient reactance
Generator G_2: 30 MVA, 13.8 kV with a 25% transient reactance
Transmission line TL_1: 69 kV, 30 miles long
Transmission line TL_2: 69 kV, 20 miles long
Transmission line TL_3: 69 kV, 15 miles long
Synchronous Machine SM_1: 30 MVA, 13.8 kV, Transient Reactance of 25%

Synchronous Machine SM_2: 20 MVA, 13.8 kV, Transient Reactance of 25%
Transformer T_1: 50 MVA, with a 5% equivalent reactance, Delta/Wye, 13.8/69 kV
Transformer T_2: 30 MVA, with a 10% equivalent reactance, Wye/Delta, 69/13.8 kV
Transformer T_3: 30 MVA, with a 5% equivalent reactance, Wye/Delta, 69/13.8 kV
Transformer T_4: 20 MVA, with an 8% equivalent reactance, Wye/Delta, 69/6.9 kV
The above components are configured in Figure A.10.

SOLUTION

1. Base Impedance of Generator G_1

2. $$Z_{BG} = \frac{(13.8)^2}{50} = 3.81\Omega$$

3. Therefore,

4. $$X'_G = (puX')Z_{BG} = \left(\frac{20}{100}\right)(3.81) = 0.762\Omega$$

5. On examining the circuit OLD, one realizes that the LV rating of Transformer T_4 is 6.9 Kv. Hence, base impedance of T_4 on the LV side is given by:

6. $$Z_{BL} = \frac{(6.9)^2}{20} = 2.381\Omega$$

7. Thus

8. $$X_{eqLV} = (puX_{eq})Z_{BL} = (0.08)(2.381) = 0.19\Omega$$

9. Knowing the turns ratio of the transformer T_4 as 'a' = 10 = 69/6.9, we have

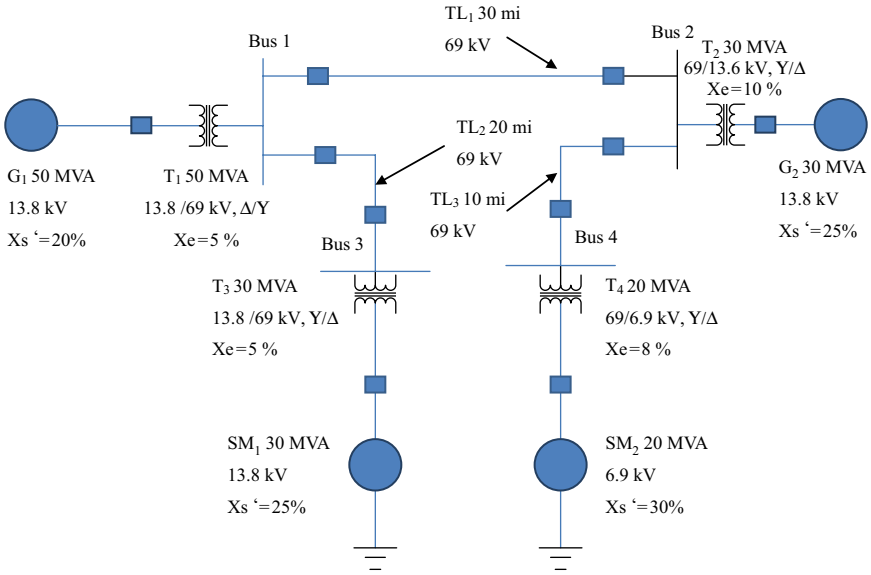

FIGURE A.10
SLD of a Four-bus Electric Power System.

10. $$X_{eqHV} = a^2 X_{eqLV} = \left(\frac{69}{6.9}\right)^2 (0.19) = 19\Omega$$

Example A.3

Referring to Example A.2 and the SLD as in Figure A.9 with all component details mentioned there, determine the pu values of the reactances of Generators G_1 and Transformer T_4. Use a reference base of: 100 MVA at 69 kV.

SOLUTION

In this case and referring to Figure A.9, the reference voltage selection of 69 kV is the transmission line voltage. With this we can proceed with the evaluation of the pu values of the reactances posed in the problem statement as follows:

Generator G_1: If we examine the SLD in Figure A.9, this generator is on the LV side of Transformer T_1 so the reference voltage to be used for the conversion of the transient reactance of G_1 is 13.8 kV. Thus, using Equation (A.38), we have:

$$pu\ X'_{sr} = \left(\frac{20}{100}\right)\left(\frac{13.8}{13.8}\right)^2\left(\frac{100}{50}\right) = 0.4$$

It is imperative to note here that the above pu value is larger than the original or old value by a factor of 2. To recover the original or old value of this reactance, it is necessary to work with the reference base impedance on the LV side of G_1.

Thus

$$Z_{BL} = \frac{(13.8)^2}{100} = 1.9\Omega$$

$$\text{Which yields; } X'_s = (0.4)Z_{BL} = 0.762\Omega\text{; as before}$$

Which further yields pu value of equivalent reactance of T_4 as

$$\text{pu } X_e = \left(\frac{8}{100}\right)\left(\frac{69}{69}\right)^2\left(\frac{100}{20}\right) = 0.4$$

as above.

Taylor & Francis
Taylor & Francis Group
http://taylorandfrancis.com

Appendix B: Joint Information Vibrant Active Network (JIVAN)

I. Project Context

Introduction

The focus of this project was to form a Joint Information Vibrant Active Network (JIVAN) designed to avoid future blackouts. In the Indian language 'JIVAN' means life. Our objective is to instill new life into the existing United States Power Grid Interconnect System.

The Grid Interconnect System has seen two major changes since it was developed. First, deregulation led to the separation of generation, transmission and distribution into separate and distinct businesses. The number of companies that must plan, design, implement and manage the system had increased dramatically, making the operating environment more complex. Second, the fear of terrorism has heightened concerns about the systems' vulnerabilities. This new threat has raised the possibility that the infrastructure could be physically or virtually attacked, leading to more frequent and widespread blackouts.

There are presently three interconnections in the United States: The Eastern Interconnection, the Western Interconnection and the ERCOT Interconnection (mainly consisting of Texas). These are divided into 10 NERC Regions. Figure B.1 shows a boundary map of these 10 regions. The North American Electric Reliability Council (NERC) is responsible for establishing the planning, engineering and operating standards for all power companies in the United States. All regions must meet the minimum criteria set by NERC.

Intellectual Merit

JIVAN was intended to create a new information architecture that will improve the collection, processing and decision-making information systems in the power industry. This will involve the development of new software and hardware components focused on improving the reliability of the entire network. To this end, the intention was to develop a rich platform, both in the research and the instruction domain. The objective of the research was to create a rapid response, self-healing network that can meet the challenges that face the industry.

The latter will enable end users like students in engineering, information systems and technology programs to incorporate their research findings into their educational experience. It will better prepare them for entry-level positions within the power industry. In addition, it will enhance the power industry as a career choice for many undergraduate students that may view it as a less than desirable career choice.

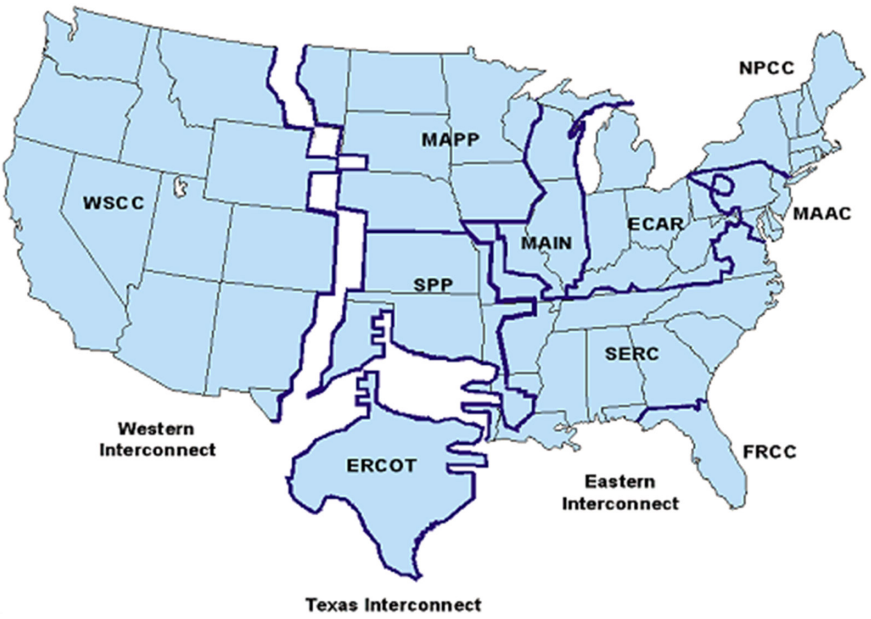

FIGURE B.1
Map of the 10 NERC regions and their boundaries. From JIVAN.

Recently, the Electrical and Computer Engineering Department and the Electronics Engineering Technology Department at the University of Hartford underwent successful ABET accreditations of their respective programs. The Computer Engineering Program was evaluated for the first time. This project will enable both programs to further strengthen their respective educational offerings and research opportunities. This project would lead to the development of several new courses in the areas of industrial automation and controls and information systems. The key technologies that will play a role in this project and, once approved, will become part of the new course curriculum are: n-tier software architectures, web-centric application development, distributed intelligent software agents, voice over IP networks and multi-tier SCADA (supervisory control and data acquisition) systems. SCADA systems are core systems for distribution network and facility management.

Broader Impacts

Real Life Situation – Blackout of August 14, 2003

On August 14, 2003, significant portions of the Northeast and Midwest experienced a major power blackout that took days to restore. Figure B.2 shows the generating plants that were affected by the blackout. The Electric System Working Group, officially assigned to investigate, found that the initial event that led to the cascading blackout occurred in Ohio. The blackout was initiated when three high-voltage transmission lines operated by FirstEnergy Corporation short-circuited and went out of service after they came into contact with trees that were too close to the lines. The root cause of most blackouts is either inadequate capacity or instability within the supply and demand nodes of the network. The blackout on August 14, 2003 was caused by

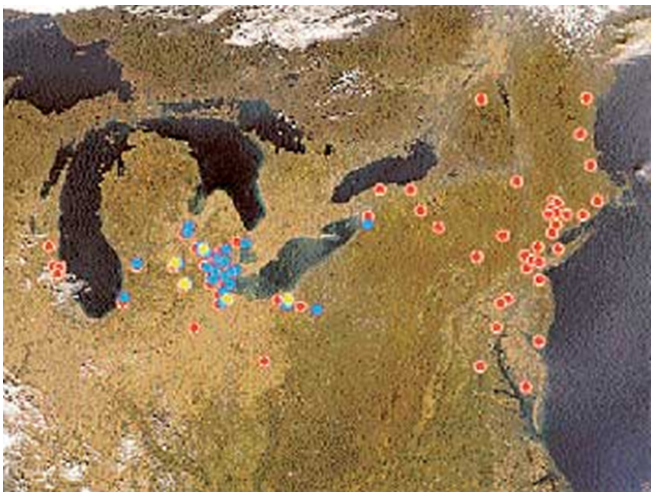

FIGURE B.2
Power generation plants affected by August 14, 2003 blackout. From JIVAN.

a cascading series of disruptions that were not compensated quickly enough. When voltage level or frequency variations become excessive, control systems that supervise segments of the grid are programmed to disconnect those segments of the power infrastructure they are assigned to manage and protect. Figure B.3 shows how over the last five years two measures of electric grid stability have increased making the system more likely to fail.

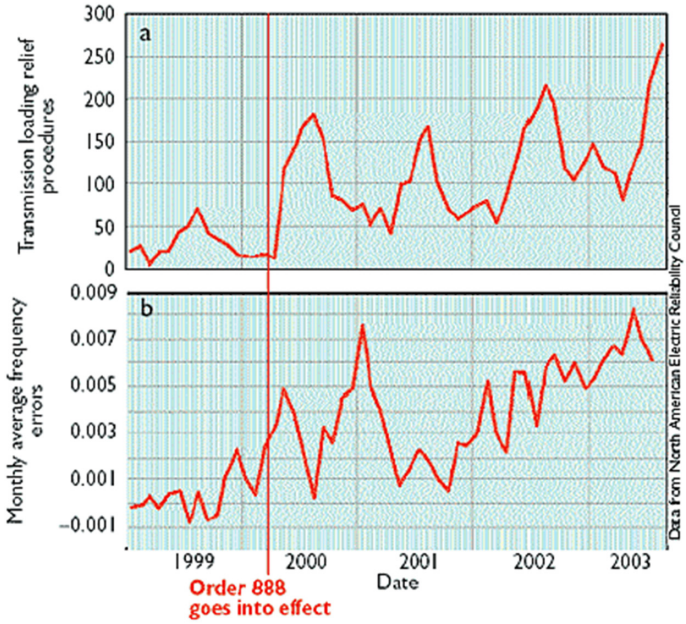

FIGURE B.3
Increasing instability of the electric power grid from 1999 to 2003. From JIVAN.

A 'root cause analysis' of the August 14, 2003 blackout by the Electric System Working Group identified several areas that need attention to prevent future occurrences:

- Lack of Communication – failure to identify emergency conditions; and expeditiously act on this information.
- Lack of operator training and execution of emergency procedures.
- Outdated infrastructure and system architecture.
- Inadequate vegetation management.
- Failure to operate within secure and safe limits.
- Inadequate regional-scale visibility over the power system.

The Security Working Group was asked to examine the blackout from a purely security perspective, and they concluded that

- No evidence indicated that individuals or organizations were responsible for, or contributed to the power outage.
- No reports indicated that there were any specific terrorist plans or plans against the energy infrastructure.
- However, there was threat-information, which suggested Al-Qaeda.
- Numerous worms and viruses affected the Internet and Internet-connected systems and networks. This, however, did not affect the generation and transmission of the power delivery system.
- There was a failure to use modern dynamic mapping and data sharing systems.
- Increasing numbers of internal and external links directly to SCADA control systems increases cyber-related vulnerabilities in the future.

The purpose of the JIVAN project was to conduct and incorporate applied research into programs in engineering, technology and computer science. The practical and hands-on application of new information system components, industrial controls and high-speed data networks will create a solid learning ground for students. It will increase the visibility of career opportunities within the power industry and further encourage women and minorities to enter the technology field.

Why the 'Blackout 2003' Issue Is Important.

Electrical power is an essential element of the day-to-day lives of all individuals and is critical to the industrial economy of the United States. It's safe and efficient delivery is vital to all. State-of-the-art technology is now available in information systems that make it possible to create a safe and reliable electric utility grid. This requires a highly intelligent and distributed system that is capable of making good decisions in a matter of milliseconds. The new electric grid will jointly coordinate the activities of both the Power System and the Control System in a vibrant and active manner. Figure B.4 shows the new JIVAN architecture we propose. JIVAN will also offer the electric power industry attractive rates of return for their investment in the JIVAN architecture.

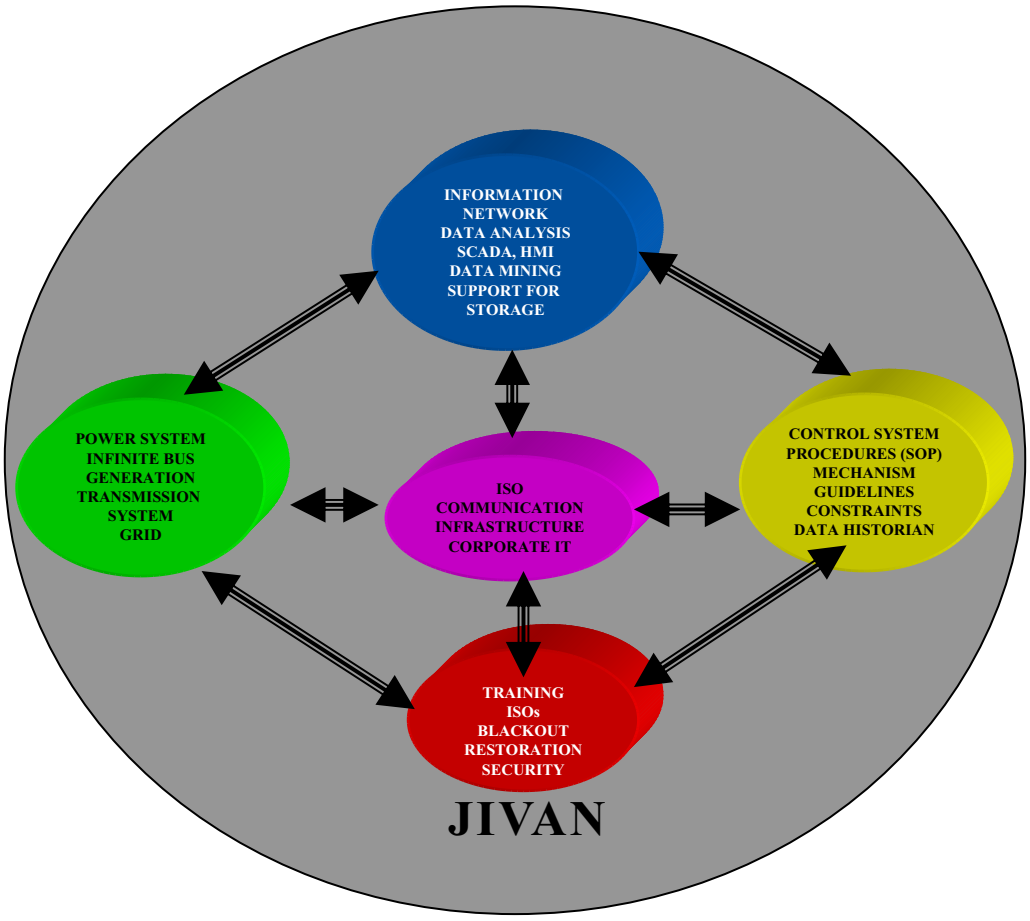

FIGURE B.4
Interaction between different components of the JIVAN system as shown by the arrows.

II. Program Activities

Description

JIVAN is composed of a distributed network of information systems, power systems and control systems connected by a broadband data network. It contains seven major elements as shown in Figure B.4:

- Redundant Broadband Data Network.
- Distributed Intelligent Software Agents.
- Information Systems (decision support, data warehouses and mining).
- Human-Machine Interfaces.
- Multi-tiered SCADA Control Systems.
- Power Delivery System.
- Education and Training Systems.

Blackout 2003

As discussed in the prequel, the two salient reasons for the failure were: lack of communication and lack of key information in real-time. In most highly-dynamic systems, the latter leads to the former. To alleviate this, our research framework will be based on the following elements.

What is needed in the Research domain?

A multi-tier SCADA system will be built one layer over the other. We will use one SCADA system to control small areas (1,2,3,…,12 in the picture). Next, we use a higher layer SCADA system (for example: Layer2-1/Layer2-3/…) to control the bundle of smaller areas and their respective SCADA systems. Descending levels of authority are assigned by the closeness to the top of Figure B.5.

In such a SCADA system, if two layers send a control signal for a particular operation, the signal from the higher layer overrides the signal from the lower layer. This ensures that the higher layers have authority over the lower layers. Another feature is the ability of the system to predict conditions after certain periods of time based on current conditions. This enables the system to predict future situations with enough time to take corrective action.. For large-scale applications, the core of the solution is the Real Time Application Platform (RTAP). It is based on open industry standards for hardware, software, communications and applications, and provides customers with many advantages such as state-of-the-art technology, interconnectivity, compatibility and multi-sourcing of hardware platforms.

JIVAN will ensure that there is sufficient information exchange between sub-systems, an essential element for successful operation. We believe that such a system can be implemented using present WAN and Internet technologies as the communications backbone. The information system components will be written in Java programming language and in a way that is compatible with n-tier application architectures.

The next area of concern is the actual control of the power system delivery system itself. The focus of the project will largely be on hardware and embedded systems at this point. The hardware will consist of control and data collection circuits built on a single chassis. This will require careful design and simulation of prototype digital sub-systems, which can later be designed and optimized for lower cost using tools like VHDL/Verilog.

Human Machine Interface (HMI) and SCADA

The HMI plays a critical role in the process of building a SCADA-based system. There are many factors to be considered during its design:

- Ease of use.
- Simplicity.
- A large number of features needed.
- Different modes of operation needed.

The activity is described in Figure B.6. For a SCADA system to be used on a large geographic scale, it needs a wide area network (WAN). The Internet will be a large component of the data network backbone. The communications protocol will be based on TCP/IP. This

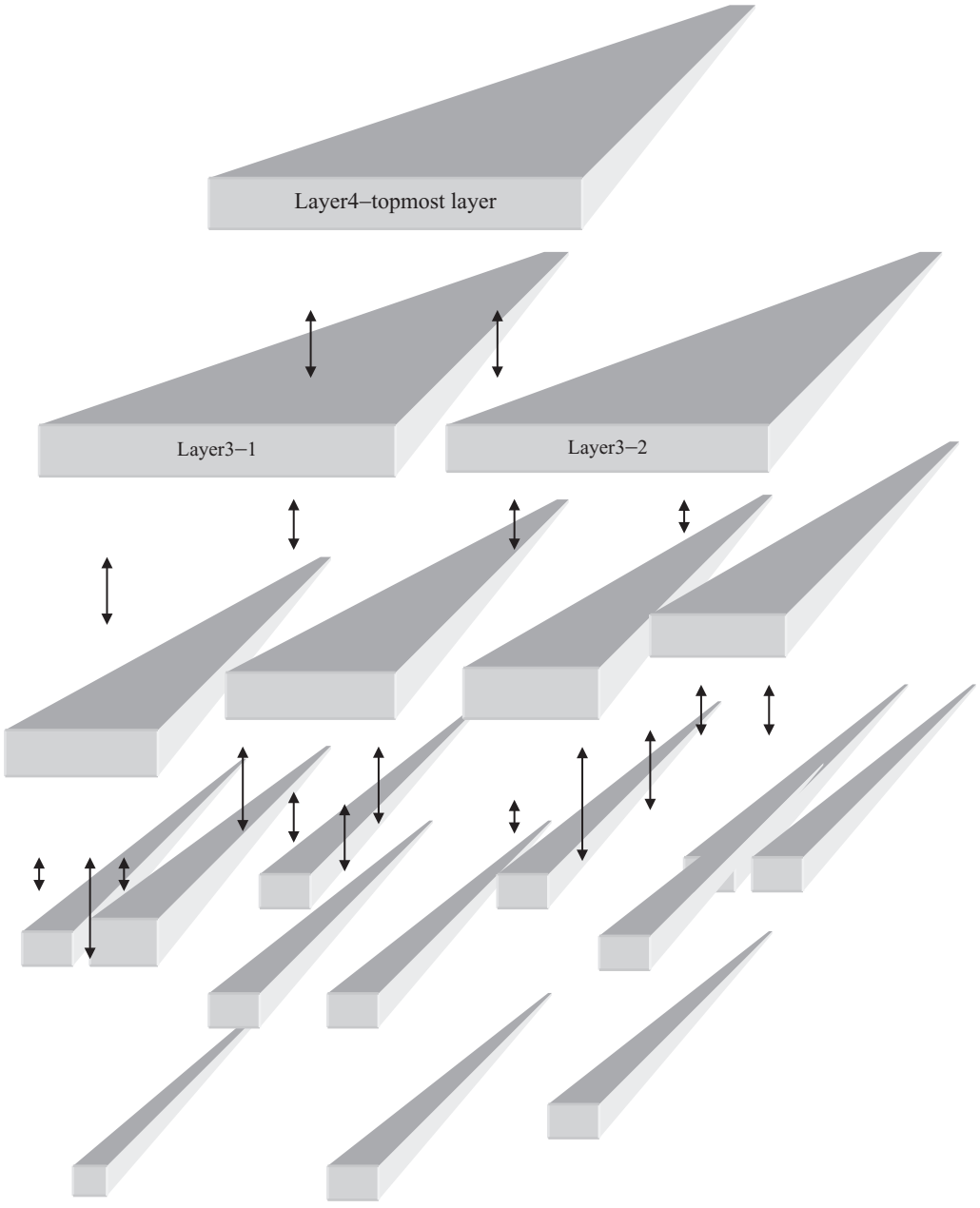

FIGURE B.5
Distributed levels of SCADA authority. From JIVAN.

will allow us to use a web-based server and client software with browsers as the primary HMI. The HMI will have the following requirements:

- It will have a real-time display of data including graphics and animation.
- The software will run in a web-browser.

- It can be embedded with audio/video media and voice over IP.
- It can interface to the SCADA systems using thin client interfaces like the PDAs/mobile phones.
- It must give users access to the system from anywhere in the world.
- It must add to the overall security level, which is a critical aspect of the system.
- It will lower the overall cost due to the availability of web-browsers and related tools.

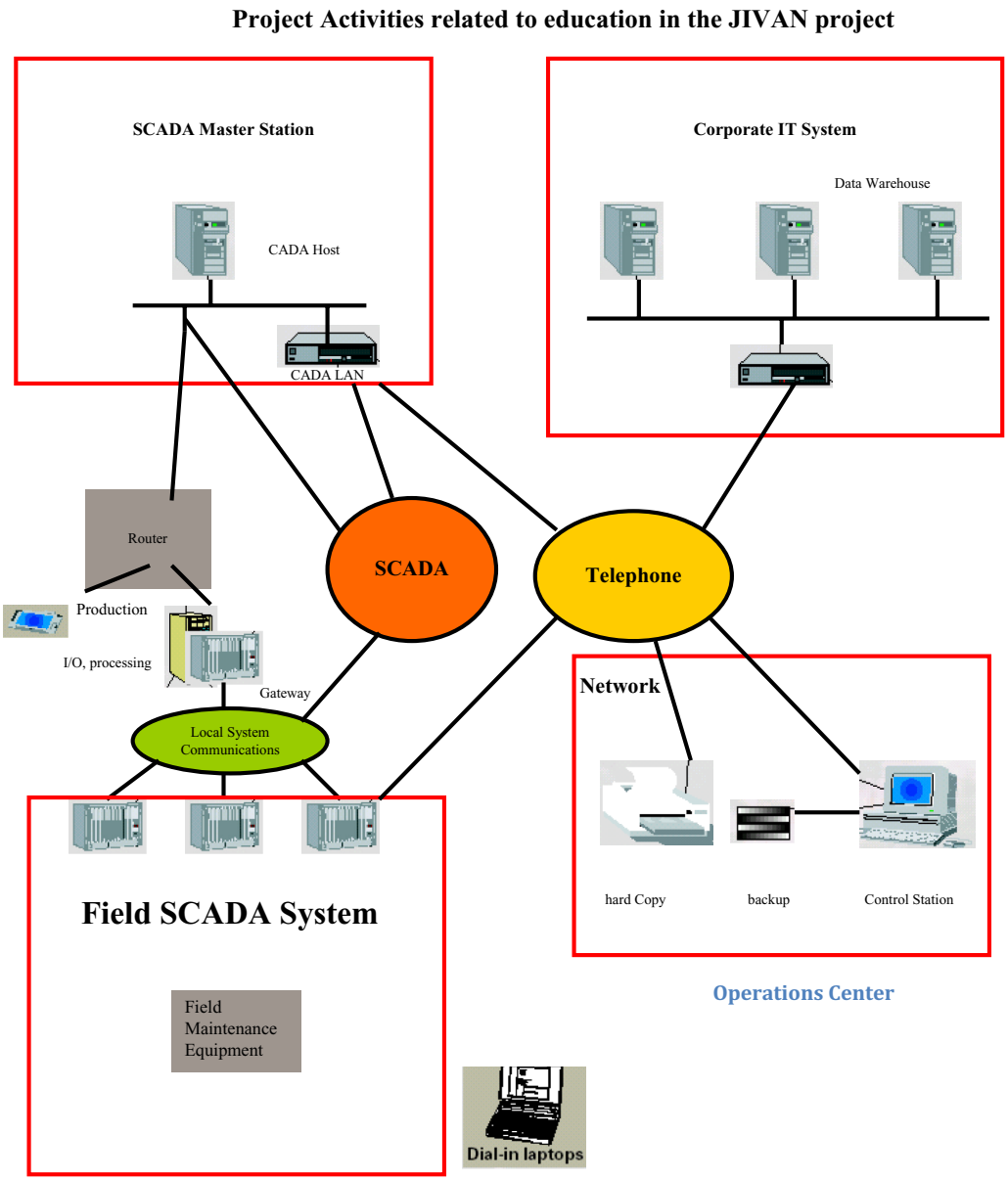

FIGURE B.6
SCADA and HMI system and the corporate WAN. From JIVAN.

MATLAB® CODE & INSTRUCTIONS

Readme.txt

April 22, 2009
Sead Alihodzic

ECE 572 computer Assignment # 2
/
**********/

1. This zip file contains 7 files:

   - newreppf.m
   - powerflow.m
   - bldybus.m
   - busdata3.m
   - linedata3.m
   - pol2rect.m
   - Readme.txt

2. To RUN this program keep all the files in the same Matlab directory.

3. First run the main program "newreppf.m" to obtain solution by the Newton-Raphson Method.

4. Second run the "powerflow.m" only after executing "newreppf.m", to evaluate Dependent quantities (P1,Q1, and Q3) and Bus-to-Bus complex power (Si) flow.

   4.1 Run "Iij" to evaluate bus-to-bus current flow.
   4.2 Run "Sij" to evaluate bus- to-bus complex power flow.
   4.3 Run "Ii" to evaluate net injected current at each bus.
   4.4 Run "Si" to evaluate net injected complex power at each bus.
   4.5 Run "Pi" to evaluate net injected real power at each bus.
   4.6 Run "Qi" to evaluate net injected reactive power at each bus.

5. Bus 1 is the slack bus, Bus 2 is a load bus (PQ), and Bus 3 is a voltage controlled Bus (PV).

/
**********/

```
% //////////////////////////////////////////////////////////////////////
% April 22, 2009
% Sead Alihodzic
% ECE 572 - Computer Assignment# 2
% //////////////////////////////////////////////////////////////////////

% ************************************************************************
% ********************** Bus Data of 3 Bus System.. ********************
% ************************************************************************

function busdata = busdata3()
 %         | Bus | Type |  Vpu  | delta |  PG  |  QG  |  PL  |   QL   | Qmin | Qmax |
 busdata = [  1     1      1.0      0       0      0      0       0        0       O;
              2     2      1.0      0     0.0    0.0   -2.5     0.8      0       0;
              3     3      1.1      0     2.0     0     0.0     0.0      0       0];

% ************************************************************************
```

```
% ////////////////////////////////////////////////////////////////////////
% April 22, 2009
% Sead Alihodzic
% ECE 572 - Computer Assignment# 2
% ////////////////////////////////////////////////////////////////////////

% ************************************************************************
% ************** Admittance And Impedance Bus Formation****************
% ************************************************************************

function ybus = bldybus() % Returns ybus

linedata = linedata3();  % Call "linedata3.m" for LINE DATA Input...
fb = linedata(:,1);      % From bus number...
tb = linedata(:,2);      % To bus number...
b = linedata(:,5);       % Ground Admittance, B/2...
b = i*b;                 % Make B imaginary...

nbus = max(max(fb),max(tb));      % no. of buses...
nbranch = length(fb);             % no. of branches...
ybus = zeros(nbus,nbus);          % Initialise YBus...

 % Formation of the Off Diagonal Elements...
for k=1:nbranch
    ybus(fb(k),tb(k)) = ybus(fb(k),tb(k)) - b(k);
    ybus(tb(k),fb(k)) = ybus(fb(k),tb(k));
end

% Formation of Diagonal Elements....
for m =1:nbus
    for n =1:nbranch
        if fb(n) == m
           ybus(m,m) = ybus(m,m) + b(n);

       elseif tb(n) == m
           ybus(m,m) = ybus(m,m) + b(n);
       end
    end
end
%ybus;                    % Bus Admittance Matrix
%zbus = inv(ybus);        % Bus Impedance Matrix
```

```
% ////////////////////////////////////////////////////////////////////////
% April 22, 2009
% Sead Alihodzic
% ECE 572 - Computer Assignment# 2
% ////////////////////////////////////////////////////////////////////////

% ************************************************************************
% ********************** Line Data of 3 Bus System.. ********************
% ************************************************************************

function linedata = linedata3()

 %          |   From  | To    |   R      |   X       |      B/2   |  X'mer     |
 %          |   Bus   | Bus   |   Pu     |   pu      |      pu    |  TAP (a)   |
linedata  = [ 1         2       0.0000     0.0000       -10.0           0
              1         3       0.0000     0.0000       -15.0           0
              2         3       0.0000     0.0000       -12.0           O];

% ************************************************************************
```

```
% ////////////////////////////////////////////////////////////////////////
% April 22, 2009
% Sead Alihodzic
% ECE - 572  Computer Assignment # 2
% ////////////////////////////////////////////////////////////////////////

% **************************************************************************
% *************** Newton-Raphson Power Flow Analysis*******************
% ********************** Bus 1 is a Slack Bus************************
% **************************************************************************

% Data provided for this system for the power flow solutions is located and
% upated via LINE DATA (linedata3.m) and BUS DATA (busdata3.m) files.
% This program is capable to provide solution to the system with N number
% of buses only after upating LINE DATA and BUS DATA information.

% **************************************************************************
format short
disp('--------------------------------------');
disp(' Ybus Admittance Matrix ');
disp('--------------------------------------');
Y = bldybus()             % Call bldybus.m to get Bus Admittance Matrix..

busdata = busdata3();     % Call busdata3.m to get busdata..
bus= busdata(:,1);        % Bus Number..
type= busdata(:,2);       % Type of Bus 1-Slack, 2-PV, 3-PQ..
V = busdata(:,3);         % Specified Voltage(p.u) ..
del = busdata(:,4);       % Voltage Angle(degrees)..
Pg = busdata(:,5);        % PG(p.u)..
Qg = busdata(:,6);        % QG(p.u)..
Pl = busdata(:,7);        % PL(p.u)..
Ql = busdata(:,8);        % QL(p.u)..
Qmin = busdata(:,9);      % Minimum Reactive Power Limit..
Qmax = busdata(:,10);     % Maximum Reactive Power Limit..
nbus = max(bus);          % To get no. of buses..
P = Pg+ Pl;               % Pi = PGi + PLi..
Q = Ql;                   % Qi = QGi + QLi = QLi..
% **************************************************************************
G = real(Y);       % Conductance.. (For this problem G = 0)...

disp('--------------------------------------');
disp('              Susceptance             ');
disp('--------------------------------------');
B = imag(Y)      % Susceptance..

% **************************************************************************
Tol = 5; % Keep tolerence at high value.

disp('////////////////////////////////////////////');
disp('                  START ITERATION           ');
Iter = 0
```

```
disp('//////////////////////////////////////////');
Psp = P;
Qsp = Q;

% ********************************************************************

% ********************************************************************
pv = find(type == 3 | type == 1); % Index of PV Buses..
pq = find(type == 2); % Index of PQ Buses..

npv = length(pv); % Number of PV buses..
npq = length(pq); % Number of PQ buses..
% ********************************************************************

while (Tol > 10e-5)     %  Iteration starting ..
    format long
    P = zeros(nbus,1);
    Q = zeros(nbus,1);

    % Calculate P and Q
    for i = 1:nbus
        for k = 1:nbus
          P(i} = P(i} + V(i}* V(k}* (G(i,k}*cos(del(i)-del(k)) + B(i,k)*sin(del(i)-del↙
(k)));
          Q(i) = Q(i) + V(i)*  V(k}* (G(i,k}*sin(del(i}-del(k}}  - B(i,k}*cos(del(i}-del↙
(k)));
        end
    end

    % Calculate change from specified value
    dPa = Psp-P;
    dQa = Qsp-Q;

    disp('------------------------------------------ ');
    fprintf('Calculated P and Q (ITERATION =%2g} ',Iter};
    dP = dPa(2:nbus)     % Calcualted P(i)
    dQ = dQa(2)          % Calculated Q(i)

    disp('------------------------------------------');
    fprintf('Mismatch Vector (M) (ITERATION =%2g) ',Iter);
    M = [ dP; dQ]       % Mismatch Vector

    % Jacobian
    % Jl - Derivative of Real Power Injections with Angles..
    Jl = zeros(nbus-1,nbus-1);
    for i = 1:(nbus-1)
        m = i+1;
        for k = 1:(nbus-1)
            n = k+1;
            if n == m
```

```
       for n = 1:nbus
          J1(i,k) = J1(i,k) + V(m)* V(n)* (-G(m,n)*sin(del(m)-del(n)) + B(m,n)↙
*cos(del(m)-del(n)));
         end
         J1(i,k) = J1(i,k) - V(m)^2*B(m,m);
     else
         J1(i,k) = V(m)* V(n)* (G(m,n)*sin(del(m)-del(n)) - B(m,n)*cos(del(m)-del↙
(n)));
     end
   end
end

% J2 - Derivative of Real Power Injections with V..
J2 = zeros(nbus-1,npq);
for i = 1:(nbus-1)
    m = i+1;
    for k = 1:npq
        n = pq(k);
        if n == m
            for n = 1:nbus
                J2(i,k) = J2(i,k) + V(n)* (G(m,n)*cos(del(m)-del(n)) + B(m,n)*sin(del↙
(m)-del(n)));
            end
            J2(i,k) = J2(i,k) + V(m)*G(m,m);
        else
            J2(i,k) = V(m)* (G(m,n)*cos(del(m)-del(n)) + B(m,n)*sin(del(m)-del(n)));
          end
       end
   end

   % J3 - Derivative of Reactive Power Injections with Angles..
   J3 = zeros(npq,nbus-1);
   for i = 1:npq
      m = pq (i);
      for k = 1:(nbus-1)
          n = k+1;
          if n == m
              for n = 1:nbus
                 J3(i,k) = J3(i,k) + V(m)* V(n)* (G(m,n)*cos(del(m)-del(n)) + B(m,n)↙
*sin(del(m)-del(n)));
               end
          J3(i,k) = J3(i,k) - V(m) ^2*G(m,m);
       else
         J3(i,k) = V(m)* V(n)* (-G(m,n)*cos(del(m)-del(n)) - B(m,n)*sin(del(m)-del↙
(n)));
       end
   end
end

% J4 - Derivative of Reactive Power Injections with V..
J4 = zeros(npq,npq);
```

```
     for i = 1:npq
         m = pq(i);
         for k = 1:npq
            n = pq (k);
          if n == m
              for n = 1:nbus
                 J4(i,k) = J4(i,k) + V(n)* (G(m,n)*sin(del(m)-del(n)) -
                 B(m,n)*cos(del(m)-del(n)));
              end
              J4 (i, k) = J4(i,k) - V(m)*B(m,m);
          else
              J4 (i, k) = V(m)* (G(m,n)*sin(del(m)-del(n)) -
              B(m,n)*cos(del(m)-del(n)));
          end
       end
   end

   disp('-----------------------------------------');
   fprintf(' Jacobian Matrix (ITERATION =%2g)',Iter);
   J = [ J1 J2; J3 J4]     % Jacobian Matrix

   disp('-----------------------------------------');
   fprintf(' Inverse of Jacobian Matrix (ITERATION =%2g)',Iter);
   J_inv = inv(J)

   disp('-----------------------------------------');
   fprintf('Correction (State) Vector (ITERATION =%2g)',Iter);
   X = J_inv * M          % Correction (State) Vector

   dTh = X(1:nbus-1);
   dV = X(nbus:end);
   del(2:nbus) = dTh + del(2:nbus);
   k = 1;
   for i = 2:nbus
       if type(i) == 2
          V(i) = dV(k) + V(i);
          k = k+1;
       end
   end
   disp('////////////////////////////////////////////////');
   Iter = Iter + 1
   disp('////////////////////////////////////////////////');
   Tol = max(abs(M));
end

Iter; % Number of Iterations took..
V; % Bus Voltage Magnitudes in p.u...
Del= 180/pi*del; % Bus Voltage Angles in Degree...
disp('-------------------------------');
disp('|   BUS   |     V     |  Angle  | ');
disp('|   No    |     pu    |  Degree | ');
```

```
disp('-----------------------------------');
for m= 1:nbus
    fprintf('%4g', m); fprintf('    %8.4f', V(m)); fprintf('    %8.4f',
    Del(m) ); fprintf↙
('\n');
end
disp('-----------------------------');
```

```
% ////////////////////////////////////////////////////////////////////
% April 22, 2009
% Sead Alihodzic
% ECE 572 - Computer Assignment#2
% ////////////////////////////////////////////////////////////////////

% ********************************************************************
%  ****************** Polar to Rectangular Conversion******************
% ********************************************************************

% ********************************************************************
% [ RECT]= RECT2POL(RHO, THETA)
% RECT   - Complex matrix or number, RECT = A + jB, A = Real, B = Imaginary
% RHO    - Magnitude
% THETA  - Angle in radians
% ********************************************************************

function rect = pol2rect(rho,theta)
rect = rho.*cos(theta) + j*rho.*sin(theta);
```

```
% ////////////////////////////////////////////////////////////////////////
% April 22, 2009
% Sead Alihodzic
% ECE 572 - Computer Assignment# 2
% ////////////////////////////////////////////////////////////////////////

% **********************************************************************
%         Evaluation of Dependent Quantities @ Generator Buses
%                                and
%            Bus-to-Bus Complex Power Flow(p.u) calculations ...
% **********************************************************************

Y = bldybus();           % Call Ybus program (ybus..
nbus = length(Y);        % No. of buses...
Vm = pol2rect(V,del);    % Converting polar to rectangular form..
Iij = zeros(nbus,nbus);
Sij = zeros(nbus,nbus);

% Line Current Flows..
% Evaluation of bus m_to-bus_n current flow.
  for m = 1:nbus
     for n = 1:nbus
        if m ~= n
           Iij(m,n) = -(Vm(m) - Vm(n))*Y(m,n); % Y(m,n) =  -y(m,n)..
        end
     end
  end
  Iij = sparse(Iij);
  Iijm = abs(Iij);
  Iija = angle(Iij);

% Load Flows..
% Evaluation of bus_m-to-bus_n complex power flow, inlcuding real and
% reactive powers.
for m= 1:nbus
    for n = 1:nbus
       if m ~= n
          Sij(m,n) = Vm(m)*conj (Iij(m,n));
       end
   end
end
Sij = sparse(Sij);
Pij = sparse(real(Sij));
Qij = sparse(imag(Sij));

% Net injected current (Ii) at Bus N...
Ii= zeros(nbus,1);
for i = 1:nbus
    for k= 1:nbus;
          Ii(i) = Ii(i) + Iij(i,k);
    end
```

```
end

% Net injected complex power (Si) at Bus N...
Si = zeros(nbus,1);
for i = 1:nbus
    for k= 1:nbus
       Si(i) = Vm(i)*conj(Ii(i));
    end
end

% Net injected real (Pi) and reactive (Qi) power at Bus N...
Pi = real(Si);
Qi = imag(Si);
```

MATLAB® SOLUTIONS

```
>> % Sead Alihodzic
>> % ECE 572 Computer Assignment# 2
>> % Due Date: April 23, 2009
>> % ************************************************************************
>> %
>> % MATLAB SOLUTION FOR 3-BUS POWER FLOW SYSTEM
>> %
>> % ************************************************************************
>> %
>> % ************************************************************************
>> % NEWTON-RAPHSON POWER FLOW ANALYSIS
>> % ************************************************************************
>> % ************************************************************************
>> %
>> % Solution by the Newton-Raphson Method
>> % M-File: newreppf.m
>> % ************************************************************************
>> %
>> % Run the main program "newreppf.m" to obtain a solution for this problem
>> % using the Newton-Raphson method.
>> %
>> % Start Execution !!!
>> %
--------------------------------
Ybus Admittance Matrix
--------------------------------

Y =
     0  –25.0000i         0  +10.0000i         0  +15.0000i
     0  +10.0000i         0  –22.0000i         0  +12.0000i
     0  +15.0000i         0  +12.0000i         0  –27.0000i

---------------------------------------
           Susceptance
---------------------------------------
B =

–25       10       15
 10      –22       12
 15       12      –27

//////////////////////////////////////////////
              START ITERATION
Iter =
0
//////////////////////////////////////////////
----------------------------------------------
```

```
Calculated P and Q (ITERATION= 0)
dP =

  -2.500000000000000
   2.000000000000000

dQ =

   2.000000000000001

-------------------------------------------
Mismatch Vector (M) (ITERATION = 0)
M =

  -2.500000000000000
   2.000000000000000
   2.000000000000001

-------------------------------------------
  Jacobian Matrix (ITERATION = 0)
J =

   23.200000000000003     -13.200000000000001                      0
  -13.200000000000001      29.700000000000003                      0
                    0                       0     20.799999999999997

-------------------------------------------
  Inverse of Jacobian Matrix (ITERATION = 0)
J_inv =

    0.057692307692308       0.025641025641026                      0
    0.025641025641026       0.045066045066045                      0
                    0                       0      0.048076923076923

-------------------------------------------
  Correction (State) Vector (ITERATION = 0)
X =

   -0.092948717948718
    0.026029526029526
    0.096153846153846

///////////////////////////////////////////

Iter =

     1

///////////////////////////////////////////
-------------------------------------------
Calculated P and Q (ITERATION = 1)
```

```
dP =

    0.234859456750145
   -0.146903627450576

dQ =

   -0.353010373618180

--------------------------------
Mismatch Vector (M) (ITERATION = 1)
M =

    0.234859456750145
   -0.146903627450576
   -0.353010373618180

--------------------------------
  Jacobian Matrix (ITERATION = 1)
J =

  25.281161224014959  -14.366939591136045  -2.494959504403641
 -14.366939591136045   30.861350232870560   1.566810125422052
  -2.734859456750145    1.717464945174173  25.167253728159096

--------------------------------
  Inverse of Jacobian Matrix (ITERATION = 1)
J_inv =

   0.054181004055075    0.025010716987912   0.003814177241644
   0.025010716987912    0.044060943390452  -0.000263612639286
   0.004180925053340   -0.000288960008448   0.040166638564741

--------------------------------
  Correction (State) Vector (ITERATION = 1)
X =

    0.007704311994770
   -0.000505651011954
   -0.013154861026556

//////////////////////////////////////////////

Iter =

     2

//////////////////////////////////////////////
--------------------------------
Calculated P and Q (ITERATION = 2)
dP =
```

```
    0.002339762854513
   -0.001359601714512

dQ =

   -0.004869028562674

----------------------------------------
Mismatch Vector (M) (ITERATION = 2)
M =

 0.002339762854513
-0.001359601714512
-0.004869028562674

----------------------------------------
  Jacobian Matrix (ITERATION = 2)
J =

     24.998640610745625      -14.207975587128688       -2.310565196476524
    -14.207975587128688       30.702601266288504        1.459153158144105
     -2.502339762854513        1.580261389415346       24.569163067815392

----------------------------------------
  Inverse of Jacobian Matrix (ITERATION = 2)
J_inv =

     0.054628401356023         0.025092187646134         0.003647219802174
     0.025092187646134         0.044195864178931        -0.000265023244667
     0.003949935344290        -0.000287019905009         0.041089938080071

----------------------------------------
  Correction (State) Vector (ITERATION = 2)
X =

   1.0e-003 *

    0.075943705558575
   -0.000088598371060
   -0.190435937399123

//////////////////////////////////////////////

Iter =

     3

//////////////////////////////////////////////
----------------------------------------
Calculated P and Q (ITERATION = 3)
```

```
dP =

  1.0e-006 *

   0.326830577712656
  -0.185389377627132

dQ =

  -9.034618801972982e-007

----------------------------------------
Mismatch Vector (M) (ITERATION = 3)
M =

   1.0e-006 *

    0.326830577712656
   -0.185389377627132
   -0.903461880197298

----------------------------------------
  Jacobian Matrix (ITERATION = 3)
J =

   24.994434888909893   -14.205597327115433   -2.308811034693959
  -14.205597327115433    30.700223043583797    1.458155678276132
   -2.500000326830578     1.578903434487180   24.560608351061155

----------------------------------------
  Inverse of Jacobian Matrix (ITERATION = 3)
J_inv =

    0.054635432609203     0.025093366877135    0.003646198539320
    0.025093366877135     0.044197883030774   -0.000265121762152
    0.003948134950419    -0.000287076110634    0.041103790458724

----------------------------------------
  Correction (State) Vector (ITERATION = 3)
X =

  1.0e-007 *

   0.099102849474188
   0.002469889714127
  -0.357921157228595

//////////////////////////////////////////////

Iter =
```

```
         4

//////////////////////////////////////////
--------------------------------------
|  Bus   |    V         |  Angle     |
|  No    |    pu        |  Degree    |
--------------------------------------
    1          1.0000        0.0000
    2          1.0828       -4.8798
    3          1.1000        1.4624
--------------------------------------
>> % ********************************************************************
>> % The 3rd iteration has found independent variables solutions to this
>> % power flow problem using Newton-Raphson method. The error tolerance of
>> % 0.00001 was met after three iterations.
>> % We have found solution for the three unknown independent variables:
>> %    1. Voltage Magnitude at Bus-2 = 1.0828 p.u.
>> %    2. Voltage Angle at Bus-2 (delta 2) = -4.87981 degrees.
>> %    3. Voltage Angle at Bus-3 (delta 3) = 1.4624 degrees.
>> %
>> % Using these values we can evaluate unknown dependent variables at
>> % generator buses (P1,Q1, and Q3). We can also evaluate Bus-to-Bus Complex
>> % power flow. Solution for these evaluations is computed using
>> % "powerflow.m" file.
>> %
>> % In the next step we will find solutions for dependent variables and
>> % and Bus-to-Bus complex power flows.
>> % ********************************************************************
>> % ********************************************************************
```

```
>> % ********************************************************************
>> %                    EVALUATION OF DEPENDENT QUANTITIES
>> % ********************************************************************
>> %
>> % Run program "powerflow.m", only after executing "newreppf.m", to obtain
>> % solutions for unknown dependent quantities (P1, Q1, and Q3) and
>> % bus-to-bus complex power flow.
>> %
>> % Start Execution!!!
>> % ********************************************************************
>> %                           BUS TO BUS CURRENT FLOW
>> % --------------------------------------------------------------------
>> Iij

 Iij =

    (2, 1)   -0.921096754976192 - 0.788837214298970i
    (3, 1)    0.421096754976188 - 1.494625716364361i
    (1, 2)    0.921096754976192 + 0.788837214298970i
    (3, 2)    1.442193509952381 - 0.249095915932725i
    (1, 3)   -0.421096754976188 + 1.494625716364361i
    (2, 3)   -1.442193509952381 + 0.249095915932725i

>> % --------------------------------------------------------------------
>> %                         BUS TO BUS COMPLEX POWER FLOW
>> % --------------------------------------------------------------------
>> Sij

  Sij =

    (2, 1)    -0.921096754976192 + 0.935905552568033i
    (3, 1)     0.421096754976188 + 1.655374283635638i
    (1, 2)     0.921096754976192 - 0.788837214298970i
    (3, 2)     1.578903245023816 + 0.314403127191595i
    (1, 3)    -0.421096754976188 + 1.494625716364361i
    (2, 3)    -1.578903245023816 - 0.135905552568001i

>> % --------------------------------------------------------------------
>> %                       NET INJECTED CURRENT AT EACH BUS
>> % --------------------------------------------------------------------
>> Ii

Ii =

   0.500000000000004 + 2.283462930663331i
  -2.363290264928573 - 0.539741298366245i
   1.863290264928570 - 1.743721632297085i

>> % --------------------------------------------------------------------
>> %                    NET INJECTED COMPLEX POWER AT EACH BUS
>> % --------------------------------------------------------------------
>> Si
```

```
Si =

   0.500000000000004 -  2.283462930663331i
  -2.500000000000008 +  0.800000000000032i
   2.000000000000004 +  1.969777410827233i

>> % -------------------------------------------------------------------
>> %          NET INJECTED REAL & REACTIVE POWER AT EACH BUS
>> % -------------------------------------------------------------------
>> Pi

Pi =

   0.500000000000004
  -2.500006000000008
   2.000000000000004

>> Qi

Qi =

  -2.283462930663331
   0.800000000000032
   1.969777410827233

>> % ********************************************************************
>> % NOTE: Output results are in form of 3x1 vector matrix. For exapmle:
>> % Ii=I1
>> %    I2
>> %    I3
>> % ********************************************************************
>> % ********************************************************************
```

SAMPLE OUTPUTS

FOR TCC=0.21 and 0.22 s

```
INDUCTANCE OF UPPER TRANSMISSION LINE=.5
INDUCTANCE OF LOWER TRANSMISSION LINE=.5
REACTANCE OF TRANSFORMER=.083
TRANSIENT REACTANCE OF GENERATOR=.25
ON WHICH TRANMISSION LINE FAULT OCCURS? LOWER(L) OR UPPER(U):L
AT WHAT DISTANCE (FRACTION) THE FAULT OCCURS FROM INFINITE
BUS=1/3
ENTER Ef=1.3
ENTER Vt=1
CRITICAL CLEARING TIME=.21
TIME INCREMENT=.01
FREQUENCY=60
MECHANICAL INPUT POWER=l.15
NUMBER OF ITERATION IN CRITICAL CLOSING TIME=21
NO OF ITERATION FOR POST FAULT=200
INPUT INTIAL POWER ANGLE (RADIANS)=.541
INPUT INTIAL DIFFERENCE VELOCITY (Wd)=0

 ------------------------------------------------------------------------
----------------------RESULTS---------------------------------------
------------------------------------------------------------------------

 ------------------------------------------------------------------------
*****Expression for Electric power*****
********* Pre-Fault ****************
------------------------------------------------------------------------

 Pe_pre =

 1300/583 *sin(delta)


 ------------------------------------------------------------------------
*****Expression for Electric power*****
********* During-Fault *************
------------------------------------------------------------------------

 Pe_during =

40/41*sin(delta)
```

*****Expression for Electric power*****
********* **Post-Fault** **********

Pe_post =

1300/833*sin(delta)

****** **RUNGE KUTTA ITERATIONS** *********

********** **During Fault** **********

Time	Delta	Omega
0	0.5410	0.0000
0.01	0.5430	0.4065
0.02	0.5491	0.8109
0.03	0.5592	1.2111
0.04	0.5733	1.6049
0.05	0.5913	1.9906
0.06	0.6131	2.3660
0.07	0.6386	2.7297
0.08	0.6677	3.0799
0.09	0.7001	3.4153
0.1	0.7359	3.7348
0.11	0.7748	4.0372
0.12	0.8166	4.3220
0.13	0.8612	4.5887
0.14	0.9083	4.8371
0.15	0.9578	5.0673
0.16	1.0096	5.2796
0.17	1.0634	5.4748
0.18	1.1190	5.6536
0.19	1.1764	5.8173
0.2	1.2353	5.9674

********** **Post Fault** **********

Time	Delta	Omega
0.21	1.2957	6.1054
0.22	1.3556	5.8768

0.23	1.4132	5.6359	
0.24	1.4683	5.3863	
0.25	1.5209	5.1312	
0.26	1.5709	4.8736	
0.27	1.6184	4.6160	
0.28	1.6633	4.3605	
0.29	1.7056	4.1089	
0.3	1.7455	3.8627	
0.31	1.7829	3.6231	
0.32	1.8179	3.3909	
0.33	1.8507	3.1668	
0.34	1.8813	2.9513	
0.35	1.9098	2.7447	
0.36	1.9362	2.5469	
0.37	1.9607	2.3581	
0.38	1.9834	2.1781	
0.39	2.0043	2.0066	
0.4	2.0236	1.8434	
0.41	2.0412	1.6881	
0.42	2.0574	1.5403	
0.43	2.0721	1.3996	
0.44	2.0854	1.2654	
0.45	2.0974	1.1374	
0.46	2.1081	1.0149	
0.47	2.1177	0.8976	
0.48	2.1261	0.7848	
0.49	2.1334	0.6761	
0.5	2.1397	0.5709	
0.51	2.1448	0.4688	
0.52	2.1490	0.3691	
0.53	2.1522	0.2714	
0.54	2.1545	0.1752	
0.55	2.1557	0.0799	
0.56	2.1561	-0.0149	
0.57	2.1554	-0.1098	
0.58	2.1539	-0.2054	
0.59	2.1513	-0.3020	
0.6	2.1478	-0.4002	
0.61	2.1433	-0.5006	
0.62	2.1378	-0.6037	
0.63	2.1312	-0.7099	
0.64	2.1236	-0.8199	
0.65	2.1148	-0.9340	
0.66	2.1049	-1.0529	
0.67	2.0937	-1.1771	
0.68	2.0813	-1.3070	
0.69	2.0676	-1.4432	

0.7	2.0524	-1.5861	
0.71	2.0358	-1.7362	
0.72	2.0177	-1.8939	
0.73	1.9979	-2.0597	
0.74	1.9765	-2.2338	
0.75	1.9532	-2.4166	
0.76	1.9281	-2.6082	
0.77	1.9010	-2.8088	
0.78	1.8719	-3.0182	
0.79	1.8406	-3.2365	
0.8	1.8072	-3.4631	
0.81	1.7714	-3.6977	
0.82	1.7332	-3.9395	
0.83	1.6925	-4.1876	
0.84	1.6494	-4.4406	
0.85	1.6037	-4.6969	
0.86	1.5555	-4.9548	
0.87	1.5046	-5.2119	
0.88	1.4512	-5.4656	
0.89	1.3953	-5.7128	
0.9	1.3370	-5.9503	
0.91	1.2764	-6.1742	
0.92	1.2136	-6.3805	
0.93	1.1488	-6.5649	
0.94	1.0824	-6.7230	
0.95	1.0145	-6.8501	
0.96	0.9455	-6.9418	
0.97	0.8758	-6.9936	
0.98	0.8058	-7.0016	
0.99	0.7359	-6.9621	
1	0.6667	-6.8720	
1.01	0.5986	-6.7290	
1.02	0.5323	-6.5316	
1.03	0.4682	-6.2791	
1.04	0.4069	-5.9717	
1.05	0.3489	-5.6107	
1.06	0.2949	-5.1980	
1.07	0.2451	-4.7365	
1.08	0.2003	-4.2301	
1.09	0.1607	-3.6831	
1.1	0.1267	-3.1005	
1.11	0.0988	-2.4878	
1.12	0.0771	-1.8508	
1.13	0.0618	-1.1957	
1.14	0.0532	-0.5289	
1.15	0.0512	0.1430	

‖	1.16	0.0560	0.8135
‖	1.17	0.0675	1.4761
‖	1.18	0.0855	2.1243
‖	1.19	0.1099	2.7517
‖	1.2	0.1405	3.3523
‖	1.21	0.1768	3.9205
‖	1.22	0.2187	4.4508
‖	1.23	0.2657	4.9385
‖	1.24	0.3174	5.3796
‖	1.25	0.3731	5.7707
‖	1.26	0.4326	6.1091
‖	1.27	0.4951	6.3933
‖	1.28	0.5603	6.6223
‖	1.29	0.6274	6.7964
‖	1.3	0.6960	6.9166
‖	1.31	0.7656	6.9849
‖	1.32	0.8356	7.0038
‖	1.33	0.9055	6.9767
‖	1.34	0.9749	6.9074
‖	1.35	1.0435	6.8001
‖	1.36	1.1108	6.6593
‖	1.37	1.1766	6.4895
‖	1.38	1.2405	6.2952
‖	1.39	1.3024	6.0809
‖	1.4	1.3621	5.8507
‖	1.41	1.4194	5.6087
‖	1.42	1.4743	5.3583
‖	1.43	1.5266	5.1028
‖	1.44	1.5763	4.8451
‖	1.45	1.6235	4.5876
‖	1.46	1.6681	4.3324
‖	1.47	1.7101	4.0814
‖	1.48	1.7497	3.8359
‖	1.49	1.7869	3.5970
‖	1.5	1.8217	3.3657
‖	1.51	1.8542	3.1426
‖	1.52	1.8846	2.9281
‖	1.53	1.9128	2.7224
‖	1.54	1.9390	2.5256
‖	1.55	1.9633	2.3378
‖	1.56	1.9858	2.1587
‖	1.57	2.0065	1.9882
‖	1.58	2.0256	1.8259
‖	1.59	2.0431	1.6714
‖	1.6	2.0591	1.5244
‖	1.61	2.0736	1.3844

‖	1.62	2.0868	1.2510
‖	1.63	2.0986	1.1236
‖	1.64	2.1093	1.0017
‖	1.65	2.1181	0.8849
‖	1.66	2.1270	0.7726
‖	1.67	2.1342	0.6643
‖	1.68	2.1403	0.5595
‖	1.69	2.1454	0.4576
‖	1.7	2.1494	0.3582
‖	1.71	2.1525	0.2607
‖	1.72	2.1547	0.1646
‖	1.73	2.1558	0.0694
‖	1.74	2.1560	-0.0254
‖	1.75	2.1553	-0.1204
‖	1.76	2.1536	-0.2160
‖	1.77	2.1510	-0.3128
‖	1.78	2.1474	-0.4112
‖	1.79	2.1428	-0.5119
‖	1.8	2.1371	-0.6153
‖	1.81	2.1304	-0.7219
‖	1.82	2.1227	-0.8323
‖	1.83	2.1138	-0.9469
‖	1.84	2.1037	-1.0664
‖	1.85	2.0924	-1.1911
‖	1.86	2.0799	-1.3217
‖	1.87	2.0660	-1.4586
‖	1.88	2.0507	-1.6023
‖	1.89	2.0339	-1.7533
‖	1.9	2.0156	-1.9119
‖	1.91	1.9956	-2.0786
‖	1.92	1.9740	-2.2536
‖	1.93	1.9505	-2.4374
‖	1.94	1.9252	-2.6300
‖	1.95	1.8979	-2.8315
‖	1.96	1.8686	-3.0420
‖	1.97	1.8370	-3.2611
‖	1.98	1.8033	-3.4887
‖	1.99	1.7672	-3.7242
‖	2	1.7288	-3.9667
‖	2.01	1.6879	-4.2154
‖	2.02	1.6445	-4.4688
‖	2.03	1.5985	-4.7255
‖	2.04	1.5500	-4.9834
‖	2.05	1.4988	-5.2402
‖	2.06	1.4452	-5.4933
‖	2.07	1.3890	-5.7397

```
||   2.08   ||  1.3304  ||  -5.9758  ||
||   2.09   ||  1.2695  ||  -6.1980  ||
||    2.1   ||  1.2065  ||  -6.4021  ||
||   2.11   ||  1.1416  ||  -6.5838  ||
||   2.12   ||  1.0749  ||  -6.7387  ||
||   2.13   ||  1.0069  ||  -6.8621  ||
||   2.14   ||  0.9378  ||  -6.9496  ||
||   2.15   ||  0.8680  ||  -6.9967  ||
||   2.16   ||  0.7980  ||  -6.9996  ||
||   2.17   ||  0.7282  ||  -6.9546  ||
||   2.18   ||  0.6591  ||  -6.8588  ||
||   2.19   ||  0.5912  ||  -6.7099  ||
||    2.2   ||  0.5251  ||  -6.5064  ||
||   2.21   ||  0.4613  ||  -6.2478  ||
 ------------------------------------------------
>>
```

For Critical time is 0.21, the variation of Power angle during the fault and post fault period gave the graph:

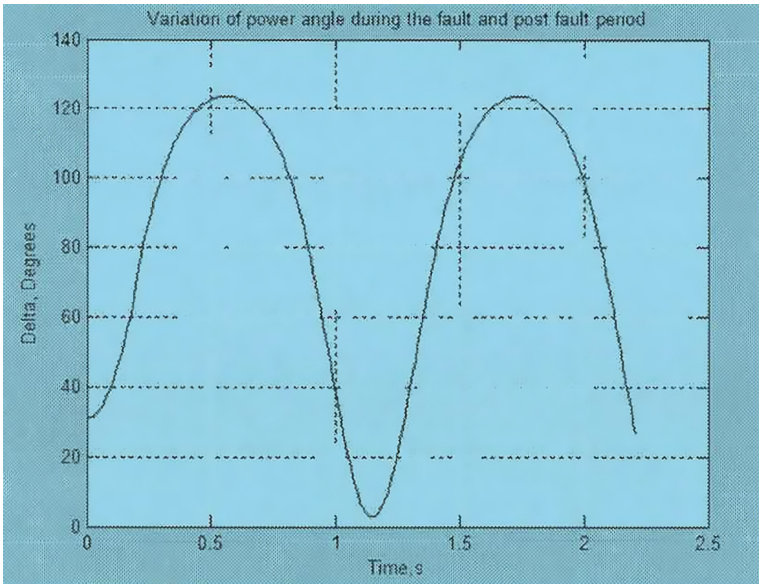

FIGURE C.1
Power angle variation during fault and post fault conditions.

When Critical closing time changed to 0.22 seconds, i.e. only increase of 0.01 seconds, the graph we obtained is below and goes into transient unstable.

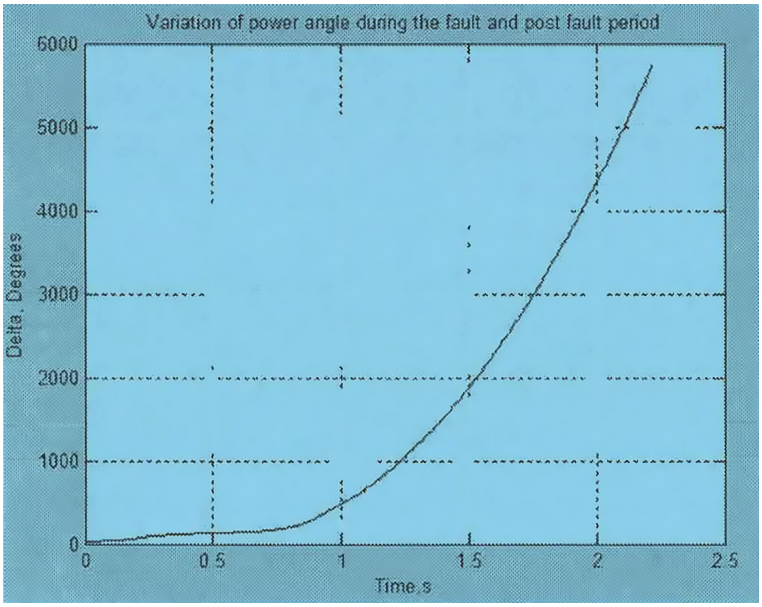

FIGURE C.2
Variation of the power angle during fault and post fault conditions.

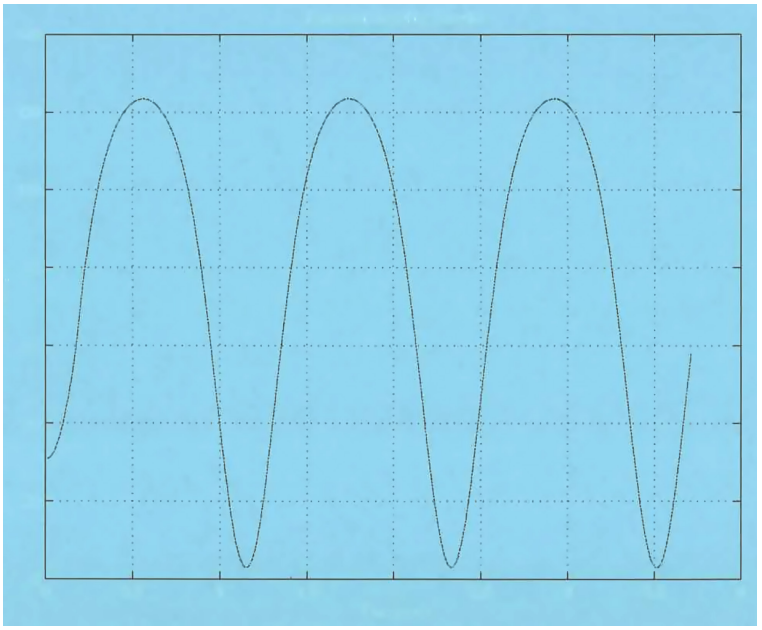

FIGURE C.3
Transient Stability for fault clearing time less than critical clearing time T_{cc}

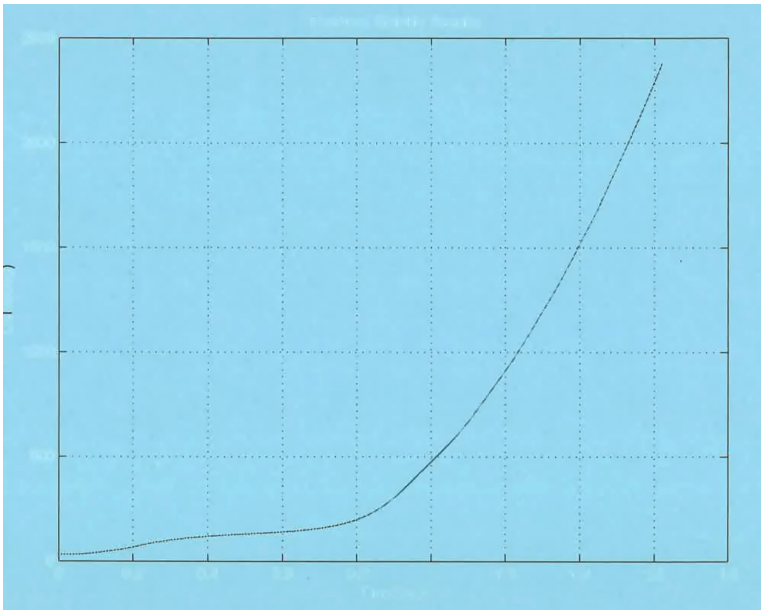

FIGURE C.4
Transient Stability results for fault clearing time exceeding threshold T_{cc}.

Also program can plot the Generator electric output power Pe in Pu for different power angles during pre-fault, fault and post fault conditions for the given system.

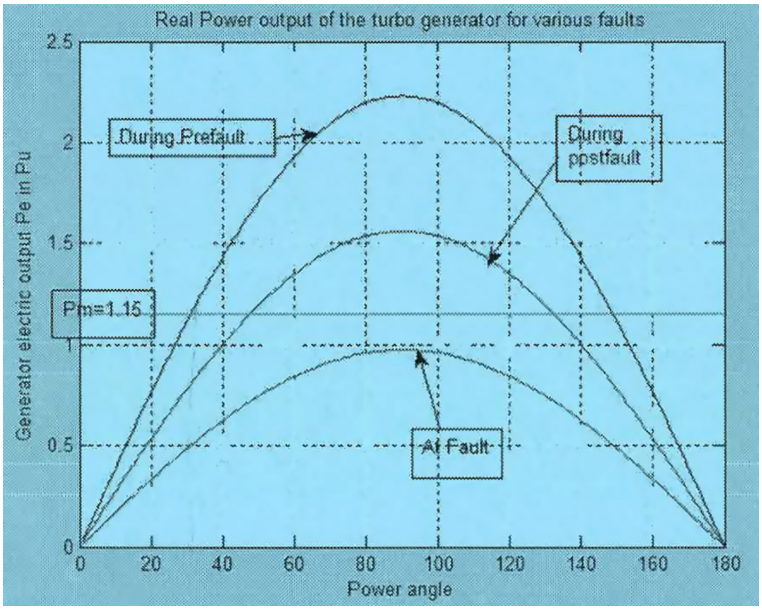

FIGURE C.5
Generator Power for different fault conditions.

Taylor & Francis
Taylor & Francis Group
http://taylorandfrancis.com

Bibliography

Bergen, A. R., *Power Systems Analysis*. Prentice Hall, Upper Saddle River, NJ, 1986.

Buckmaster, David, Hopkinson, Phil, Shertukde, Hemchandra, "Transformers used with Alternative Energy Sources—Wind & Solar", Technical Presentation, April 11, 2011.

C57.116: IEEE Guide for Transformers Directly Connected to Generators, 1989.

Elgerd, O. I., *Electric Energy Systems Theory*, 2nd edition. McGraw-Hill, New York, 1982.

Fitzgerald, A. E., C. Kingsley, Jr., and S. D. Umans, *Electric Machinery*, 4th edition. McGraw-Hill, New York, 1983.

Nasar, Syed A., *Electric Power Systems, Schaum's Outline Series*. McGraw-Hill, New York, 1990.

Shertukde, Hemchandra M., *Distributed Photovoltaic Grid Transformers*. CRC Press, Boca Raton, FL, 2014.

Shertukde, Hemchandra M., *Transformers: Theory, Design and Practice with Practical Applications: New and Improved Look at Transformers with Emphasis on Partial Discharge, Core Designs Using Finite Element Analysis and 18-Slot Designs*. VDM Verlag Dr Mueller, 2010.

Stevens, S. D., Jr., *Elements of Power Systems Analysis*, 4th edition. McGraw-Hill, New York, 1982.

Taylor & Francis
Taylor & Francis Group
http://taylorandfrancis.com

Index

N

O

P

R

S